Universidad Nacional Autónoma de México
Maestría y Doctorado en Ciencias Bioquímicas

Papel del estradiol en la regulación de la marca H3K27me3 y del patrón de expresión génica en células derivadas de glioblastomas humanos.

T E S I S

que para optar por el grado de

Maestra en Ciencias

PRESENTA:
Aylin del Moral Morales

TUTOR PRINCIPAL:
Dr. Ignacio Camacho Arroyo
Facultad de Química

MIEMBROS DEL COMITÉ TUTOR
Dr. Ernesto Soto Reyes Solís
Universidad Autónoma Metropolitana - Unidad Cuajimalpa
Dr. Samuel Canizalez Quinteros
Instituto Nacional de Medicina Genómica

Ciudad de México, Agosto de 2020

Universidad Nacional Autónoma de México
UNAM
Biblioteca Central
Dirección General de Bibliotecas de la UNAM

UNAM – Dirección General de Bibliotecas
Tesis Digitales
Restricciones de uso

DERECHOS RESERVADOS ©
PROHIBIDA SU REPRODUCCIÓN TOTAL O PARCIAL

Todo el material contenido en esta tesis esta protegido por la Ley Federal del Derecho de Autor (LFDA) de los Estados Unidos Mexicanos (México).

El uso de imágenes, fragmentos de videos, y demás material que sea objeto de protección de los derechos de autor, será exclusivamente para fines educativos e informativos y deberá citar la fuente donde la obtuvo mencionando el autor o autores. Cualquier uso distinto como el lucro, reproducción, edición o modificación, será perseguido y sancionado por el respectivo titular de los Derechos de Autor.

Agradecimientos

Esta tesis se realizó en la Unidad de Investigación en Reproducción Humana, Instituto Nacional de Perinatología-Facultad De Química, Universidad Nacional Autónoma De México bajo la dirección del Dr. Ignacio Camacho Arroyo.

A los miembros del comité tutor, Dr. Ernesto Soto Reyes Solís y Dr. Samuel Canizales Quinteros por su asesoría en este proyecto.

Al Consejo Nacional de Ciencia y Tecnología (CONACYT) por otorgar la beca número 894530 para estudios de posgrado.

Al Programa de Apoyo a los Estudios de Posgrado (PAEP) por el apoyo económico otorgado para la realización de una estancia corta en el Instituto Curie, Francia.

Al Dr. Raphaël Margueron y la Dra. Laia Richart Gines por su asesoría y apoyo durante mi estancia en su laboratorio.

Índice general

1. Resumen **1**

2. Introducción **3**

3. Antecedentes **5**

3.1. Gliomas 5

3.1.1. Generalidades 5

3.1.2. Glioblastomas 7

3.1.3. Subtipos de Glioblastomas 8

3.1.4. Hormonas sexuales y Glioblastomas 9

3.2. EZH2 y H3K27me3 10

3.2.1. Epigenética 10

3.2.2. El complejo represor Polycomb 13

3.2.3. Mecanismo de acción de EZH2 16

3.2.4. Papel EZH2 y H3K27me3 en cáncer 19

3.2.5. Alteraciones epigenéticas en Glioblastomas 21

3.2.6. EZH2 en Glioblastomas 23

3.3. Estradiol (E2) 25

3.3.1. Generalidades 25

3.3.2. Mecanismo genómico del estradiol 25

3.3.3. Mecanismo no genómico del estradiol 27

3.3.4. Estradiol y Glioblastomas 28

3.3.5. Estradiol y EZH2 29

4. Justificación **31**

5. Planteamiento del problema **32**

6. Hipótesis **33**

7. Objetivos **34**

7.1. Objetivo general 34

7.2. Objetivos particulares 34

8. Metodología **35**

8.1. Cultivo Celular y tratamientos hormonales 35

8.2. Extracción de RNA y RT-qPCR 35

8.2.1. Oligonucleótidos 36

8.3. Extracción de proteínas y Western Blot 37

8.4. Inmunofluorescencia 38

8.5. Predicción de elementos de respuesta a estrógenos 38

8.6. Silenciamiento de EZH2 38

8.7. Ensayos de proliferación celular 39

8.8. Ensayos de migración 39

8.9. Ensayos de invasión 40

8.10. Análisis de datos de secuenciación masiva de RNA (TCGA y GTEx) 40

8.11. Análisis estadístico 41

9. Resultados **42**

9.1. EZH2 se expresa de forma basal en líneas celulares derivadas de GBMs humanos 42

9.2. E2 no incrementa la expresión de EZH2 en GBM humanos 44

9.3. El silenciamiento de EZH2 inhibe la proliferación, invasión y migración inducida por E2 48

9.4. EZH2 y ERs en biopsias de GBM 49

10. Discusión **58**

11. Conclusiones **64**

12. Perspectivas **65**

13. Bibliografía **66**

14. ANEXOS **81**

14.1. Figuras suplementarias 81

14.2. Artículos relacionados con el proyecto publicados en revistas indizadas. . . 82

14.2.1. Zamora-Sánchez, C. J., Del Moral-Morales, A., Hernández-Vega, A. M., Hansberg-Pastor, V., Salido-Guadarrama, I., Rodríguez-Dorantes, M., & Camacho-Arroyo, I. (2018). Allopregnanolone Alters the Gene Expression Profile of Human Glioblastoma Cells. *International journal of molecular sciences*, 19(3), 864. 83

14.2.2. Rodríguez-Castelán, J., Del Moral-Morales, A., Piña-Medina, A. G., Zepeda-Pérez, D., Castillo-Romano, M., Méndez-Tepepa, M., Espindola-Lozano, M., Camacho-Arroyo, I., & Cuevas-Romero, E. (2019). Hypothyroidism induces uterine hyperplasia and inflammation related to sex hormone receptors expression in virgin rabbits. *Life sciences*, 230, 111–120. 99

14.2.3. Del Moral-Morales, A., González-Orozco, J. C., Capetillo-Velázquez, J. M., Piña-Medina, A. G., & Camacho-Arroyo, I. (2020). The Role of mPRδ and mPRε in Human Glioblastoma Cells: Expression, Hormonal Regulation, and Possible Clinical Outcome. *Hormones & cancer*, 11(2), 117–127. . 109

14.2.4. González-Orozco, J. C., Moral-Morales, A. D., & Camacho-Arroyo, I. (2020). Progesterone through Progesterone Receptor B Isoform Promotes Rodent Embryonic Oligodendrogenesis. *Cells*, 9(4), E960. 120

1. Resumen

Los glioblastomas (GBM) son los tumores primarios más frecuentes y agresivos del sistema nervioso central (SNC). Debido a que tienen una incidencia diferencial en hombres respecto a mujeres (en proporción 3:2), ha sido de gran interés el estudio del rol que las hormonas sexuales tales como el estradiol, la progesterona y la testosterona tienen en el surgimiento y la progresión de los GBM. Trabajos anteriores han demostrado que el estradiol (E2) incrementa la proliferación, invasión y migración de células derivadas de GBM humanos; sin embargo, los mecanismos mediante los cuales el E2 ejerce su efecto sobre los GBM no han sido totalmente dilucidados.

Previamente ha sido demostrado que el E2 regula la expresión de la enzima Homóloga del Enhancer de Zeste 2 (EZH2) en cáncer de mama. EZH2 es el núcleo catalítico del complejo represor de Polycomb 2 (PRC2) y cataliza la mono, di y trimetilación de la histona 3 en la lisina 27 (H3K27me1/me2/me3). H3K27me3 es una marca epigenética asociada a heterocromatina facultativa y represión transcripcional de genes tejido-específico, tales como aquellos involucrados en el desarrollo embrionario y la diferenciación celular. EZH2 está sobre-expresado en varios tipos de cáncer, incluidos los GBMs y varios estudios funcionales han sugerido que la expresión de EZH2 está correlacionada con un aumento en la proliferación, migración e invasión de células derivadas de GBM, mismos procesos que son regulados por el E2. Sin embargo, no se ha investigado si existe una relación directa entre EZH2 y E2 en GBMs.

En este trabajo, se determinó la expresión basal de EZH2 en tres líneas celulares derivadas de GBMs humanos (U251, U87 y D54) mediante RT-qPCR, Western Blot e Inmunofluorescencia, y se encontró que las tres líneas expresan EZH2 de forma basal y en cantidades mayores que astrocitos humanos procedentes de un tejido sano. La línea U251 mostró el nivel más alto y la U87 el más bajo tanto a nivel de mRNA como de proteína. También observamos que el E2 induce la expresión de EZH2 (a nivel de mRNA) en la línea U87 después de 12 horas de tratamiento. Sin embargo, no se observaron cambios significativos en las células U251 ni D54. A nivel de la proteína no se observaron cambios significativos inducidos por el E2 a ninguno de los tiempos evaluados.

Para evaluar la posible mediación de EZH2 en los efectos inducidos por E2 en células derivadas de GBM, se silenció la expresión de EZH2 en la línea celular U251 y se evaluó la proliferación, migración e invasión de las células después de ser tratadas con E2. Se observó que al silenciar EZH2, se inhibe el aumento en la proliferación, migración e invasión celulares inducido por el E2.

Los resultados sugieren que el E2 induce la proliferación, invasión y migración de líneas celulares derivadas de GBM y que estos efectos podrían estar mediados por la enzima EZH2, posiblemente a través de la represión epigenética que ejerce sobre sus genes diana.

2. Introducción

Los astrocitomas son tumores del Sistema Nervioso Central (SNC) que se generan por la malignización de células gliales, progenitoras gliales, o células troncales neurales transformadas. La OMS clasifica estos tumores en cuatro grados de acuerdo con sus características histopatológicas, donde el grado IV o glioblastoma (GBM) es el más agresivo y frecuente [Louis et al., 2016]. Los GBMs se caracterizan por ser altamente invasivos y de rápido crecimiento, por lo que los pacientes tienen baja expectativa de vida (12 a 16 meses posteriores al diagnóstico). Desafortunadamente, las terapias disponibles actualmente (cirugía, quimioterapia y radioterapia) no resultan efectivas, ya que la tasa de supervivencia a 5 años es menor al 5 % [Hamza and Gilbert, 2014, Ostrom et al., 2018].

En tiempos recientes ha cobrado relevancia el papel que las hormonas sexuales; tales como la progesterona, el estradiol y la testosterona; desempeñan en la incidencia y progresión de los GBMs [González-Arenas et al., 2012, Germán-Castelán et al., 2014, Rodríguez-Lozano et al., 2019]. En particular, se ha reportado que la concentración de estradiol (E2) es elevada en biopsias de pacientes con GBM con respecto a gliomas de menor grado [Dueñas Jiménez et al., 2014], además de que el E2 promueve la proliferación, invasión y migración de células derivadas de GBM humanos [González-Arenas et al., 2012, Wan et al., 2018], por lo que esta hormona y sus mecanismos de acción son de gran interés para el estudio de los GBMs.

En cáncer de mama, ha sido demostrado que el E2, por medio de su receptor intracelular, regula directamente la expresión del Homólogo del Enhancer de Zeste 2 (EZH2) [Bhan et al., 2014]. Esta enzima forma parte de un complejo miembro del Grupo Polycomb (PcG), que es un conjunto de represores transcripcionales que modifican la cromatina, controlan la progresión del ciclo celular y participan en el mantenimiento de la diferenciación celular [Sauvageau and Sauvageau, 2010]. Este grupo está representado por los complejos represores de Polycomb 1 y 2 (PRC1 y PRC2). PRC2 es el complejo encargado de mono, di y trimetilar a la lisina 27 de la histona 3 (H3K27me1/2/3) [Yin et al., 2016]. La marca H3K27me3 está asociada a promotores de genes que se encuentran en heterocromatina facultativa [Margueron and Reinberg, 2011], y es leída por PRC1 el cual se

une a la cromatina impidiendo que se lleve a cabo la transcripción. La composición de ambos complejos es variable, sin embargo, PRC2 tiene tres componentes constantes: EZH2 que funge como metiltransferasa debido a que posee un dominio catalítico SET; EED que contiene dominios WD40 que sirven para identificar marcas adyacentes en histonas (metilaciones, acetilaciones, etc.) así como para anclar el complejo a la cromatina; y SUZ12 que es una desacetilasa de histonas [Wiles and Selker, 2017]. PRC2 es requerido para mantener la identidad y diferenciación celular mediante la represión de genes tejido-específico e inhibidores de la proliferación [Sauvageau and Sauvageau, 2010].

Se ha visto que EZH2 se encuentra desregulado en diversos tipos de cáncer [Scelfo et al., 2015], entre ellos los tumores cerebrales. En GBMs, la sobre-expresión de este gen está directamente relacionada con la malignidad del tumor [Zhang et al., 2015a] y se ha relacionado con un mal pronóstico de vida. Por otra parte, EZH2 es requerido para el mantenimiento y renovación de las células troncales de glioma (GSC), las cuales se piensa que son responsables de la resistencia a fármacos y de la reincidencia del tumor [Louis et al., 2016]. Lamentablemente, aún no se sabe mucho acerca de los factores que están implicados en la regulación de la expresión del gen EZH2 y de la localización de la marca H3K27me3.

Dado que EZH2 se encuentra sobre-expresado en biopsias de GBMs y que el E2 participa en diversos procesos importantes para el desarrollo y progresión de estos tumores, es probable que este gen se exprese en líneas celulares derivadas de este tipo de tumores y que su expresión sea regulada por hormonas sexuales, lo cual se verá reflejado en cambios en la expresión génica de genes asociados a la represión transcripcional mediada por Polycomb.

3. Antecedentes

3.1. Gliomas

3.1.1. Generalidades

La palabra cáncer se refiere a un conjunto de enfermedades caracterizadas por proliferación celular excesiva como resultado de la alteración de procesos involucrados en la regulación del ciclo celular, muerte y diferenciación de las células [Chow, 2010, Hanahan and Weinberg, 2011]. De acuerdo con la Organización Mundial de la Salud (OMS), el cáncer es una de las principales causas de muerte en el mundo ya que tan sólo en 2018 se registraron alrededor de 18 millones de nuevos casos y 9.6 millones de defunciones relacionadas a algún tipo de cáncer [Ferlay et al., 2019].

Los gliomas son los tumores primarios más frecuentes del SNC con una incidencia de 6.6 por cada 100,000 individuos en Estados Unidos [Ostrom et al., 2018]. Aún no es claro el linaje celular a partir del cual se originan, sin embargo, debido a las características de los tumores se cree que proceden de células del SNC tales como las células troncales cancerosas, las células progenitoras oligodendrocíticas (OPCs) o los astrocitos [Zong et al., 2015]. Los gliomas se encuentran entre los cánceres con peor pronóstico, y se clasifican de acuerdo con sus características histológicas, inmunohistoquímicas y moleculares en astrocitomas, oligodendrogliomas y oligoastrocitomas [Furnari et al., 2007].

Los astrocitomas, los gliomas más comunes [Ostrom et al., 2018], son tumores que poseen características histopatológicas similares a las de los astrocitos y son clasificados por la OMS en cuatro grados de malignidad que se asignan de acuerdo con características histológicas y alteraciones genéticas [Louis et al., 2016] y que a continuación se describen:

Los astrocitomas de grado I (también conocidos como pilocíticos) son neoplasias benignas, delimitadas, de lento crecimiento que se presentan preferencialmente en niños y

adultos jóvenes [Weller et al., 2015]. Al ser tumores con bordes muy definidos y poco infiltrantes, el tratamiento usual es la remoción quirúrgica y la supervivencia a 5 años es superior al 90 % [Ostrom et al., 2018]. La principal característica estos tumores son mutaciones en genes que codifican para diversas proteínas involucradas en la activación de la vía de cinasas activadas por mitógenos (MAPK), a tal grado de que se les conoce como "enfermedad de una sola vía" [Reifenberger et al., 2017].

Los astrocitomas de grado II, también conocidos como difusos, son los astrocitomas más comunes en adultos jóvenes. Se caracterizan por difusión infiltrante hacia el parénquima cerebral y su tendencia a la recurrencia y progresión maligna [Weller et al., 2015]. Actualmente, son divididos en dos grupos de acuerdo con su perfil molecular, los que presentan un genotipo astrocítico están caracterizados por mutación en el gen supresor de tumores TP53, mientras que los de origen oligodendrocítico presentan co-deleción de los brazos cromosómicos 1p y 19q. Ambos genotipos poseen mutaciones en el gen de la enzima isocitrato deshidrogenasa (IDH1), la cual forma parte del ciclo de Krebs y podría representar la alteración que da inicio al tumor. También es característico de este tipo de tumores la mutación en los genes HIST1H3B o H3F3A (codificantes para la histona H3), la cual consiste en la sustitución de la lisina 27 por metionina (H3K27M) [Louis et al., 2016, Reifenberger et al., 2017]. Ha sido demostrado que dicha modificación inhibe al Complejo Represor de Polycomb 2 provocando una disminución global de la marca H3K27me3 [Mohammad et al., 2017].

Los astrocitomas de grado III o anaplásicos usualmente se presentan en adultos de entre 40 y 60 años. Histológicamente se caracterizan por atipia nuclear, aumento en el tamaño celular y alta actividad proliferativa, además de células multinucleadas con anormalidades en la mitosis y positivas a la proteína acídica fibrilar glial (GFAP). Comúnmente presentan mutaciones en los genes IDH y TP53 [Zhao et al., 2007, Weller et al., 2015].

Los astrocitomas de grado IV, llamados también GBMs, son los astrocitomas más frecuentes y también los más agresivos ya que la expectativa de vida de los pacientes raramente excede los 14 meses posteriores al diagnóstico. Comúnmente se presentan en adultos entre las edades de 45 a 70 años [Kim et al., 1991]. Se localizan principalmente en la corteza cerebral [Sarkar et al., 2009], son altamente anaplásicos y están compuestos de células con diversas morfologías. Alrededor de la mitad de los astrocitomas diagnosticados son clasificados como GBMs [Reifenberger et al., 2017], sin embargo, las estrategias disponibles para su tratamiento (cirugía, quimioterapia y radioterapia) no resultan efectivas, ya que aumentan sólo unos meses la esperanza de vida de los pacientes [Hamza and Gilbert, 2014].

3.1.2. Glioblastomas

Los GBMs o astrocitomas grado IV, son los tumores malignos más frecuentes del SNC, representan del 60 al 75 % de los astrocitomas y tienen una incidencia de 3.21 por cada 100,000 habitantes en Estados Unidos. Pueden presentarse a cualquier edad, sin embargo, la mayoría de los pacientes son adultos entre 45 y 75 años, además de que estos tumores son más frecuentes en varones que en mujeres a razón de 3:2 [Ostrom et al., 2018].

La historia clínica de los pacientes con GBM es corta (menos de 3 meses en más de 50 % de los pacientes), los síntomas incluyen dolor de cabeza, náuseas y vómito ocasionados por el aumento en la presión intracraneal. En algunos pacientes se pueden presentar episodios epilépticos y/o cambios en el comportamiento [Kleihues et al., 2002]. Algunos síntomas menos frecuentes son demencia, problemas con la memoria, el aprendizaje, la concentración y problemas motores, éstos últimos varían de acuerdo con la localización del tumor [Louis et al., 2016].

Existen dos tipos de GBM: los primarios; son los que se generan de novo, es decir, sin evidencia de un tumor previo de menor malignidad, representan aproximadamente el 80-90 % de los casos, mientras que los secundarios son aquellos que surgen por la progresión de astrocitomas de menor malignidad [Furnari et al., 2007]. Los GBMs primarios y secundarios son morfológicamente indistinguibles entre ellos. Sin embargo, se presentan en distintos rangos de edad y poseen mutaciones específicas que permite identificarlos.

Los GBMs primarios generalmente se presentan personas mayores de 50 años [Louis et al., 2016] y se caracterizan por la amplificación y sobre-expresión del receptor del factor de crecimiento epidérmico (EGFR) junto con la deleción del locus INK4a/ARF que codifica para las proteínas p16 y p14 que pueden arrestar el ciclo celular en la fase G1 y G2, además de mutaciones en el gen que codifica para la fosfatidilinositol 3,4,5-trisfosfato 3-fosfatasa (PTEN), amplificación del gen MDM2 y pérdida de heterocigosidad en el cromosoma 10 [Ivanchuk et al., 2001].

Los GBM secundarios se presentan principalmente en pacientes jóvenes y se derivan de astrocitomas grado II (difusos) o de grado III (anaplásicos), presentan diversas mutaciones en TP53, la sobre-expresión del factor de crecimiento derivado de plaquetas (PDGF) y de su receptor, así como mutaciones en el gen IDH, además de pérdida alélica de los cromosomas 19q y 10q [Godard et al., 2003].

Los pacientes con GBM tienen una sobrevida corta y generalmente fallecen dentro del primer año posterior al diagnóstico [Louis et al., 2016]. Estos tumores son resistentes a la radioterapia y a la quimioterapia y debido a su alta capacidad para infiltrarse, en especial al

parénquima cerebral, no es posible realizar resección quirúrgica total, por lo que hay una alta tasa de recurrencia de los tumores [Hadjipanayis and Van Meir, 2009].

3.1.3. Subtipos de Glioblastomas

En 2010 Verhaak y colaboradores clasificaron a los GBMs en cuatro categorías basadas en la genómica de los tumores y en patrones de expresión génica [Verhaak et al., 2010]. Los cuatros subtipos son los siguientes:

Clásico

Este subtipo está caracterizado por pérdida o mutación de PTEN, pérdida del gen CDKN2A que codifica para el inhibidor 2A de cinasa dependiente de ciclina (p16), amplificación, mutación o sobreexpresión de EGFR y pérdida del cromosoma 10. Además de tener completa función de IDH y p53. Es frecuente la activación de las vías Notch y Hedgehog.

Mesenquimal

Entre las marcas bioquímicas que lo caracterizan se encuentra la pérdida o mutación de los genes NF1 (regulador negativo de la vía de ras), TP53 y PTEN, además de la sobreexpresión de diversos genes involucrados en las vías activadas por el factor de necrosis tumoral (TNF).

Neural

Este subtipo se caracteriza por ser similar a las células neurales, presenta amplificación o sobreexpresión de EGFR, y expresión de diversos marcadores neurales tales como componente de neurofilamento (NEFL), un receptor de ácido gamma-aminobutírico (GABRA1), una proteína de vesículas sinápticas (SYT1) y un canal K-Cl (SLC12A5). Cabe mencionar que ha surgido controversia sobre este subtipo debido a que un estudio a nivel transcriptómico sugiere que las muestras del estudio de Veerhak y colaboradores estaban contaminadas con células no tumorales, por lo que el subtipo neural es inexistente [Wang et al., 2017].

Proneural

Se caracteriza por ser IDH mutante y por tener pérdida o mutación de TP53, CDKN2A, PTEN y amplificación o sobreexpresión del factor de crecimiento derivado de plaquetas (PDGFRA).

3.1.4. Hormonas sexuales y Glioblastomas

Los GBMs son más frecuentes en hombres que en mujeres con una relación 3:2 [Ostrom et al., 2018], lo cual sugiere que las hormonas sexuales pueden tener un papel importante en la progresión de estos tumores. Además, debido a que se ha detectado la expresión de los receptores a hormonas sexuales en astrocitomas, la terapia hormonal ha sido propuesta como una alternativa terapéutica [Atif et al., 2015].

Diversos estudios han demostrado que la progesterona (P4) y la testosterona (T) promueven la proliferación, invasión y migración de células derivadas de GBMs humanos [Germán-Castelán et al., 2014, Piña-Medina et al., 2016, Rodríguez-Lozano et al., 2019]. También se ha reportado que la alopregnanolona, un metabolito de la P4 induce la expresión de genes relacionados con la reparación de daño al DNA, invasión, migración y transporte de moléculas [Zamora-Sánchez et al., 2018].

Se ha demostrado que el estradiol (E2) induce proliferación, angiogénesis y resistencia a la terapia en células derivadas de GBMs humanos [González-Arenas et al., 2012, Lappano et al., 2014]. Se sabe que el tratamiento con E2 aumenta la expresión del receptor intracelular a P4 en GBM [Hansberg-Pastor et al., 2017] y se ha reportado que tanto la P4 como el E2 pueden regular la transcripción de diferentes RNAs no codificantes, que entre otras cosas regulan la expresión de genes involucrados en procesos de proliferación, ciclo celular, resistencia a la terapia invasión y migración, además de que pueden modular la actividad del complejo represor de Polycomb 2 (PRC2), el cual está encargado de la regulación de la expresión de genes tejido-específicos [Smits et al., 2010, Finlay-Schultz et al., 2015, Tao et al., 2015].

3.2. EZH2 y H3K27me3

3.2.1. Epigenética

El término *epigenética* significa "por encima de la genética" y fue acuñado originalmente por Conrad Waddington en los años 50s para referirse a cambios en el fenotipo celular que son heredables e independientes de alteraciones en la secuencia de DNA [Berger et al., 2009]. Waddigton observó que los embriones de mosca de fruta pueden presentar diferencias en la estructura del tórax y alas como respuesta a cambios en la temperatura de incubación o a estímulos químicos. El siguiente paso en su experimento fue seleccionar y criar entre sí a los animales que mostraban la nueva característica. Expuestos al mismo estímulo ambiental, estos dieron lugar a una progenie con mayor proporción de adultos que muestran el nuevo fenotipo. Después de un número relativamente pequeño de generaciones, descubrió que podía reproducir a los animales y obtener una herencia sólida, incluso sin aplicar el estímulo ambiental. Llamó a este proceso asimilación genética y concluyó que dichos fenotipos no dependían de la aparición de una mutación en la secuencia de DNA, sino de la activación de alelos pre-existentes, por lo tanto, creó el término epigenética y la describió como el estudio de las interacciones de los genes con su entorno que dan vida al fenotipo [Noble, 2015].

Actualmente la epigenética se describe como la ciencia que estudia los cambios en la expresión de genes que no involucran modificaciones en la secuencia de DNA [Berdasco and Esteller, 2019]. Este término es usado generalmente para describir eventos relacionados con la estructura de la cromatina (**Figura 1**), los cuales incluyen la modificación covalente de DNA e histonas, el cambio en la posición de los nucleosomas, así como la actividad de RNAs largos no codificantes (lncRNAs), entre otros [Dawson and Kouzarides, 2012].

La cromatina es el complejo macromolecular de DNA e histonas que provee de un andamiaje para el empaquetamiento del material genético dentro de la célula. El DNA se encuentra compactado dentro del núcleo gracias a su interacción con las histonas, que poseen carga positiva debido a que son ricas en residuos de lisina y arginina. Los eucariontes poseen cinco tipos de histonas: H1, H2A, H2B, H3 y H4. Las histonas H2A, H2B, H3 y H4 forman un octámero compuesto por dos dímeros H2A-H2B y un tetrámero H3-H4; alrededor del cual se enrolla el DNA formando una estructura denominada nucleosoma, que es la unidad funcional de la cromatina. La histona H1 se conoce como "linker" ya que forma asas de cromatina entre nucleosoma y nucleosoma, lo que facilita la compactación del material genético [Felsenfeld and Groudine, 2003, Turner, 2005].

El estudio de los nucleosomas ha demostrado que todos sus componentes pueden ser

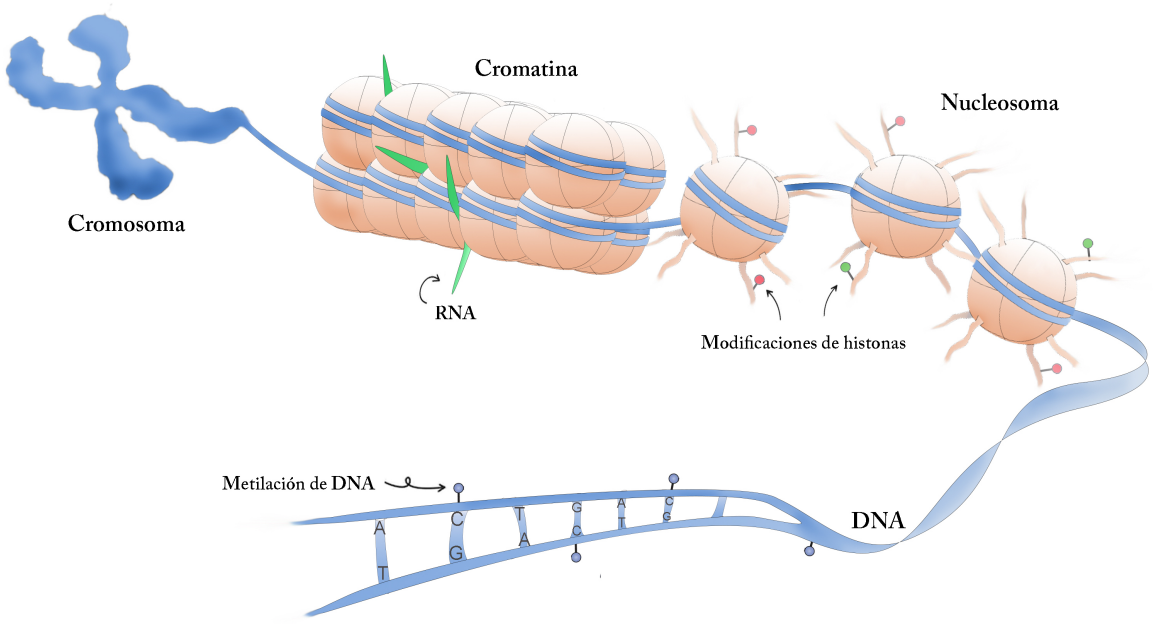

Figura 1: Representación de la estructura de la cromatina. La unidad fundamental es el nucleosoma, compuesto por DNA e histonas. Los extremos amino terminales de las histonas sobresalen, lo que los hace accesibles a los complejos que regulan las marcas epigenéticas. EL DNA puede ser metilado también, marca que ha sido asociada a represión transcripcional.

modificados covalentemente, lo que altera la organización y función de la cromatina. En términos generales, la cromatina se divide en dos grandes tipos: heterocromatina, la cual está altamente compactada y contiene principalmente genes inactivos y eucromatina, que se encuentra relativamente relajada y contiene la mayor parte de los genes activos. A su vez, la heterocromatina se divide en facultativa y constitutiva. La primera contiene genes cuya expresión se encuentra reprimida, pero puede reactivarse bajo las circunstancias adecuadas, mientras que la segunda es más compacta y tiene funciones principalmente estructurales [Liu et al., 2020].

El estado de la cromatina es dinámico y puede ser regulado mediante la modificación covalente de los extremos amino-terminal de las histonas que sobresalen del nucleosoma y son accesibles a enzimas que los modifican químicamente mediante un sistema de complejos escritores, lectores y borradores (**Figura 2**) [Felsenfeld and Groudine, 2003]. Estas modificaciones conforman una especie de código que funciona en conjunto con la secuencia del DNA para determinar el estado de la cromatina, así como establecer y estabilizar los patrones de expresión génica [Esteller, 2011].

Los residuos modificados son las lisinas que pueden ser acetiladas (ac) metiladas (me) o ubiquitinadas (ub), las argininas pueden ser metiladas y las serinas son fosforiladas, entre otros (ver **Tabla 1**) [Dawson and Kouzarides, 2012]. Las modificaciones postraduccionales

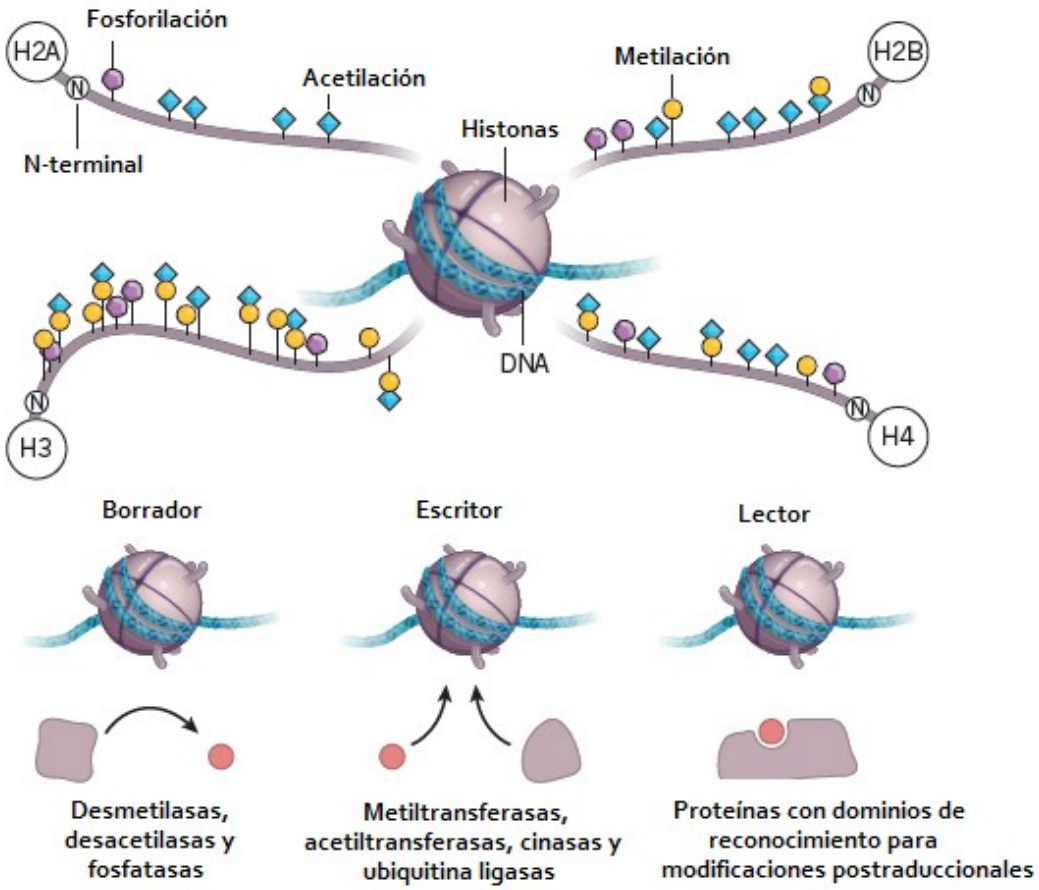

Figura 2: Modificaciones postraduccionales de histonas. La compactación del DNA está regulada por las marcas postraduccionales de las histonas. Los escritores catalizan la inserción de estas marcas. Los borradores son enzimas que remueven las marcas y los lectores son proteínas con dominios de reconocimiento para modificaciones de histonas. Imagen modificada de Helin y Dhanak, 2013.

de histonas se regulan de forma dinámica, ciertas modificaciones pueden afectar a otras y muchas están positiva o negativamente relacionadas. La acetilación es la única marca que por sí misma tiene una función, ya que al neutralizar la carga de los aminoácidos positivamente cargados (lisina y arginina) disminuye la interacción del nucleosoma con el DNA (negativamente cargado por los grupos fosfato) favoreciendo un estado de cromatina relajado, característico de la eucromatina y los genes transcripcionalmente activos. El resto de las marcas dependen del sistema de escritores y lectores para llevar a cabo su función [Felsenfeld and Groudine, 2003].

Para identificar las modificaciones postraduccionales, éstas reciben un código que inicia con el nombre de la histona, el residuo que es modificado, la posición que este ocupa en la secuencia de aminoácidos, el tipo de modificación y el número en caso de que puedan ser varias. Por ejemplo, la acetilación del residuo 4 de lisina en la histona 3 se abrevia H3K4ac y la trimetilación de la lisina 27 de la histona 3 es H3K27me3.

Tabla 1: Modificaciones postraduccionales de histonas

Modificación postraduccional	Residuo	Nomenclatura	Función atribuída
Acetilación	Lisinas	K_ac	Activación transcripcional
Metilación	Lisinas	K_me1, K_me2, K_me3	Activación o represión transcripcional dependiendo del residuo
	Argininas	R_me1, R_me2s, R_me2a	Activación transcripcional
Fosforilación	Serinas	S_ph	Activación transcripcional, reparación de daño al DNA, Ciclo celular
	Treoninas	T_ph	
	Tirosinas	Y_ph	
Ubiquitinación	Lisinas	K_ub	Poliubiquitinación: Reparación de daño al DNA Monoubiuqitinación: represión transcripcional
Sumoilación	Lisinas	K_su	Desconocido
ADP ribosilación	Lisinas	K_ar	Reparación de daño al DNA
Citrulinación	Argininas	R_ci	Apoptosis celular
Biotinilación	Lisinas	K_bio	Represión transcripcional

3.2.2. El complejo represor Polycomb

Las proteínas que forman parte del Grupo Polycomb (PcG) son modificadores postraduccionales de histonas y su acción generalmente está asociada a represión de la expresión de genes tejido-específicos. Este grupo está conformado por los complejos represores de Polycomb 1 y 2 (PRC1 y PRC2). PRC2 es el complejo que actúa como escritor ya que está encargado de mono, di y trimetilar a la lisina 27 de la histona 3

(H3K27me3) [Margueron and Reinberg, 2011]. Esta marca está asociada a promotores de genes silenciados y a heterocromatina facultativa. La H3K27me3 es reconocida por PRC1 (lector) que se une a la cromatina, monoubiquitina a la lisina 119 de la histona H2A (H2AK119ub), e impide que se lleve a cabo la transcripción al bloquear el reclutamiento de la RNA polimerasa II [Wiles and Selker, 2017].

La composición multiproteica de ambos complejos es variable, aunque, algunos elementos se mantienen constantes. El núcleo catalítico de PRC2 (**Figura 3**) se compone del homólogo de Enhancer de Zeste (EZH). En humanos existen dos homólogos del enhancer de Zeste (codificados por genes independientes y denominados EZH1 y EZH2), sin embargo, ha sido reportado que EZH2 tiene mayor actividad catalítica que EZH1 [Margueron and Reinberg, 2011]. EZH1 se expresa principalmente en tejidos diferenciados y células que no se encuentran en división, mientras que EZH2 es poco detectable en tejidos adultos normales, pero está altamente expresado en células troncales y progenitoras.

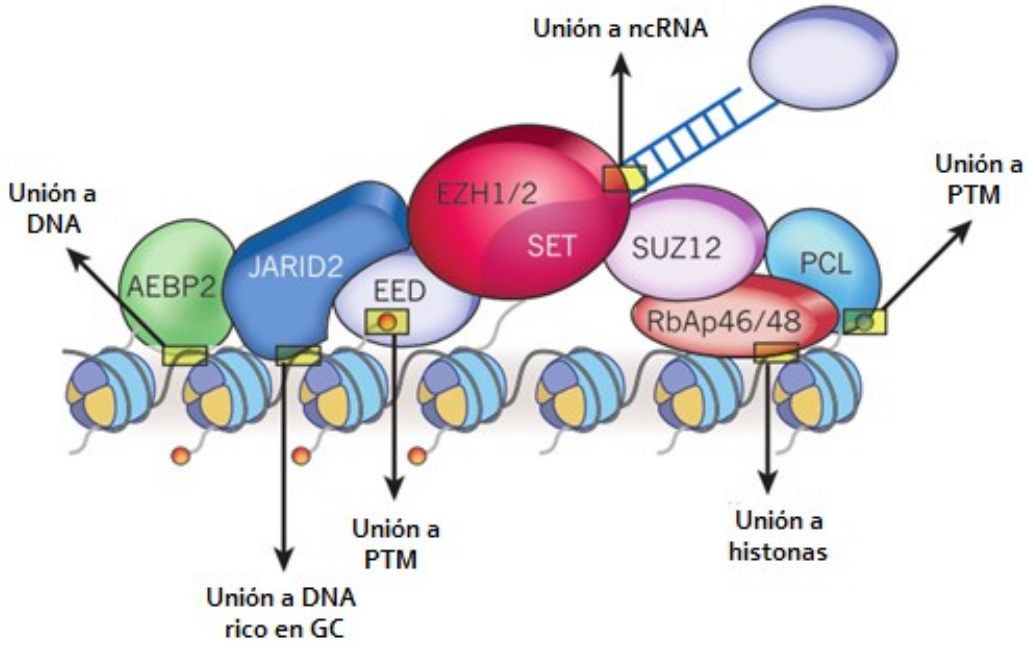

Figura 3: Complejo Represor de Polycomb 2. Este complejo tiene tres componentes principales; enhancer de Zeste 2 (EZH2)), Desarrollo de Ectodermo Embrionario (EED) y Supresor de Zeste 12 (SUZ12). Los otros: jumonji, dominio interactivo de sitios ricos en GC 2 (JARID2), proteína de unión potenciadora de adipocitos (AEBP2) y las proteínas Polycomb-like (PCL) son variables y funcionan como anclaje y reconocimiento de otras marcas epigenéticas. Modificado de Margueron et al., 2011).

Se ha reportado que EZH1 tiene los mismos blancos que EZH2 y puede formar el complejo PRC2. Sin embargo, el complejo PRC2-EZH1 tiene diferente actividad que PRC2-EZH2. EZH1 se expresa tanto en células en división activa como en tejidos diferenciados, mientras que EZH2 se expresa mayoritariamente en células troncales [Margueron and Reinberg, 2011]. Por lo tanto, se ha sugerido que EZH2 se expresa en

niveles altos en células capaces de diferenciarse y participa activamente en la diferenciación celular, estableciendo los patrones de metilación de H3K27 que silencian genes tejido-específicos y otorgan identidad a la célula. Por otra parte, la subunidad EZH1 se encarga de mantener la represión de genes establecida por EZH2 y por lo tanto protege la identidad celular de los tejidos diferenciados [Margueron et al., 2008].

Los otros componentes constantes del complejo PRC2 son el factor de desarrollo ectodérmico embrionario (EED) y el supresor de zeste (SUZ12). EED contiene dominios WD40 que reconocen la marca H3K27me3 y se cree que participa en la expansión de la marca. SUZ12 modula la actividad de PRC2 mediante el dominio VEFS, aunque su papel exacto aún no está definido. De igual forma se ha reportado que eliminar a cualquiera de los genes que codifican para los tres componentes principales de PRC2, el complejo no puede formarse y se pierde la marca H3K27me3 [Margueron and Reinberg, 2011, Mohammad et al., 2017, Scelfo et al., 2015].

Por otra parte, los demás componentes variables de PRC2 funcionan como puntos de anclaje para el complejo. Por ejemplo, Jarid2, proteína miembro de la familia Jumonji de desmetilasas de histonas, que, a pesar de carecer de actividad catalítica, posee un dominio de unión a regiones de DNA ricas en GC reclutando a EZH2 al promotor de diversos genes. Otra subinidad de PRC2, RbAp46/48, se une a las histonas H3 y H4, mientras que las proteínas PCL reconocen otras modificaciones postraduccionales de las histonas [Trošelj et al., 2016].

Las funciones de PRC2 han sido estudiadas en dos direcciones, una es su rol en el desarrollo, la otra su implicación en la proliferación celular y la tumorigénesis. El incremento en la actividad de EZH2 está asociado a un pronóstico negativo en diversos tumores, mientras que la deleción de EZH2 en embriones de ratón resulta letal o produce defectos en el desarrollo [Scelfo et al., 2015]. EZH2 está involucrado en procesos como embriogénesis, inactivación del cromosoma X, modificación de la cromatina, desarrollo de células troncales y progresión tumoral [Lu et al., 2016]. Entre los blancos mejor conocidos de EZH2 se encuentran los genes Hox, que son un conjunto de 39 genes que codifican para factores de transcripción. Éstos definen los patrones de desarrollo en las extremidades de los vertebrados, controlan la identidad celular del eje anteroposterior del plano corporal y están conservados en todos los animales con simetría bilateral [Comet et al., 2016, Lappin et al., 2006].

Además de los genes Hox, se ha reportado que PRC2 reprime la expresión de diversos genes involucrados en la regulación del ciclo celular, entre ellos el ejemplo más importante es la inhibición del locus INK4a/ARF. Este locus codifica para las proteínas p15, p16, and p19ARF, las cuales son represoras de la transición de la fase G1 a la fase S del ciclo celular. PRC2 regula también la reparación del DNA, la sobre-expresión de EZH2 genera una dramática disminución en la expresión de RAD51 que es una proteína requerida para la

recombinación homóloga y reparación de rupturas de doble cadena. La represión de la expresión de este gen mediada por Polycomb tiene como consecuencia el decremento en el número de loci de DNA reparados, aumento de aneuploidías y reducción en las tasas de supervivencia de células expuestas a estrés genotóxico [Sauvageau and Sauvageau, 2010].

El papel de EZH2 en la diferenciación de ESCs está ampliamente estudiado. Mediante ensayos genómicos se ha descubierto que los complejos Polycomb reprimen varios genes que codifican para reguladores importantes del desarrollo y señalización en ESCs [Zhao et al., 2007]. Es característico de ESC que en los promotores de los genes tejido-específicos exista una bivalencia de marcas, es decir coexista la H3K27me3 que es asociada a represión junto con la H3K4me3, marca regulada por el complejo Trithorax y que se asocia a cromatina transcripcionalmente activa. Este estado se conoce como "listo para el arranque" ya que los genes pueden ser activados rápidamente, lo que es fundamental en la diferenciación celular al permitir que los genes que darán la identidad y linaje a la célula se expresen o repriman según sea el caso [Sauvageau and Sauvageau, 2010].

Debido a que las proteínas que pertenecen a Polycomb reprimen locus asociados a progresión del ciclo celular, replicación y reparación del DNA, se ha sugerido que cambios en la expresión de PRC2 podrían romper el equilibrio entre la represión y activación transcripcional, alterar la homeostasis celular, y provocar diversas patologías, entre ellas el cáncer. Se ha observado que la expresión de EZH2 se encuentra desregulada en diversos tipos de cáncer, entre ellos los tumores cerebrales [Scelfo et al., 2015].

Así pues, PRC2 es importante para la célula ya que ayuda a mantener la identidad celular al conservar reprimidos a los genes que se silencian durante el desarrollo embrionario [Wiles and Selker, 2017]. Se ha sugerido que en un ambiente estable y controlado este complejo no es requerido para preservar la diferenciación celular, es decir en una célula totalmente diferenciada que se encuentra en homeostasis, PRC2 no es indispensable para mantener su patrón de expresión génica. Sin embargo, cuando las células se ven expuestas a cambios en el medio extracelular se vuelve importante su papel para mantener el patrón de expresión génica que da identidad a la célula [Scelfo et al., 2015, Comet et al., 2016].

3.2.3. Mecanismo de acción de EZH2

La estructura de la proteína EZH2 está conservada evolutivamente entre especies, desde organismos unicelulares eucariotas hasta plantas, este grado de homología sugiere que tiene un rol importante en la biología celular [Wiles and Selker, 2017]. EZH2 se compone de cinco dominios, tal como se muestra en la **Figura 4**. SANT (Siglas de: proteína de conmutación defectuosa 3 (Swi3), adaptador 2 (Ada2), correpresor del receptor nuclear (NCoR), factor de transcripción IIIB) es el dominio responsable de la localización subcelular de EZH2 en

el núcleo y es importante para el remodelado de la cromatina al promover la unión a los extremos terminales de las histonas [Yan et al., 2017]. El dominio SET es el que le confiere la actividad enzimática de histona metiltransferasa (KMT), el dominio recibe este nombre por las siglas de Suv(var)3-9, Enhancer-of-zeste y Trithorax [Margueron and Reinberg, 2011], los tres son proteínas con actividad de KMT, y tienen en común este dominio catalítico altamente conservado [Katoh, 2016].

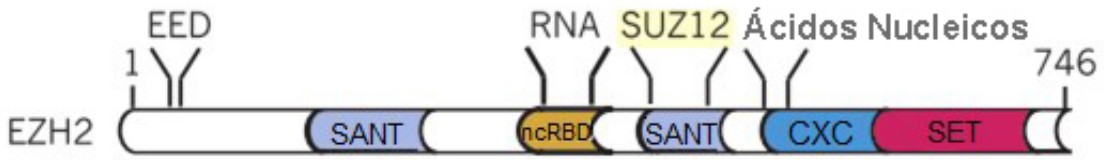

Figura 4: Dominios caracterizados de la proteína EZH2. Los dominios de EZH2 caracterizados con funciones potenciales están indicados. CXC es un dominio de unión a DNA rico en cisteína; ncRBD, dominio de unión a RNA no codificante; SANT, dominio de unión de SWI3, ADA2, N-CoR y TFIIIB; SET, Su (var) 3-9, enhancer de zeste, trithorax. Modificado de Margueron et al., Nature (2011).

Una vez reclutado, EZH2 puede mono, di, y trimetilar a la lisina 27 en la histona H3. Al ser una KMT, la acción de EZH2 es dependiente de la disponibilidad de S-adenosil metionina (SAM), molécula donadora de grupos metilo. H3K27me3 es reconocida por PRC1, este complejo se une a la cromatina y monoubiquitina la lisina 119 de la histona H2A (H2AK119ub) e impide que la RNA polimerasa II se una a los promotores, además de que compacta la cromatina [Lu et al., 2016].

La secuencia del dominio SET de EZH2 es similar a la de otras proteínas con actividad de KMT. Este dominio consiste en un sitio catalítico formado principalmente por estructuras de hoja β-plegada y contiene dos secuencias de aminoácidos altamente conservadas: HXCXPN y ELXFDY. El dominio CXC o post-SET contiene residuos de lisina esenciales para la actividad de KMT [Dillon et al., 2005]. En estudios de cristalografía se ha encontrado que EZH2 en solitario no puede unirse al cofactor SAM ni al residuo de lisina ya que el dominio SET se encuentra muy abierto, por lo que se sugiere que es necesaria la unión de SUZ12 y EED para que el dominio catalítico adquiera la conformación necesaria para albergar el cofactor junto al nitrógeno correspondiente a la lisina que será metilada [Wu et al., 2013]. También se ha descrito que el complejo PRC2 reconoce elementos como la histona conectora H1, además de discriminar entre mononucleosomas y oligonucleosomas artificiales, teniendo mayor actividad cuando se une a éstos últimos [Martin et al., 2006].

El mecanismo exacto por el cual PRC2 es reclutado hacia los promotores de los genes que son silenciados mediante H3K27me3 no se conoce. En *Drosophila* se ha descrito que PRC2 y PRC1 pueden ser reclutados a través de secuencias de DNA de respuesta a Polycomb (PRE) que son reconocidos por Pho, una proteína con dominios de unión a DNA que pertenece a

PcG. YY1 es un factor de transcripción presente en vertebrados y tiene 90 % de homología con Pho, sin embargo, no existe evidencia suficiente para afirmar que recluta a PRC2 o PRC1 de forma similar a como actúa Pho en *Drosophila* [Kassis and Brown, 2013].

EZH2 puede unirse a diversos RNA largos no codificantes (lncRNA) mediante el dominio de unión a RNA no codificante (lncRBD), además de que el mismo dominio podría estar involucrado en el reclutamiento del complejo a sitios transcripcionalmente activos mediante la unión a mRNAs nacientes [Holoch and Margueron, 2017]. Se estima que cerca de 3,000 RNAs pueden unirse al complejo y regular su actividad. Algunos de los más sobresalientes son el lncRNA HOTAIR, cuya expresión está relacionada con el silenciamiento del locus HOXD en fibroblastos humanos procedentes de extremidades distales posteriores [Rinn et al., 2007]. Además, TUG1, un lncRNA inducido por daño a DNA, recluta a PRC2 para inhibir genes que regulan mitosis, formación del huso mitótico y progresión del ciclo celular [Khalil et al., 2009]. Adicionalmente, PRC2 puede unirse a una gran variedad de RNAs nacientes, lo que inhibe su actividad e impide el silenciamiento de genes que se encuentran transcripcionalmente activos [Kaneko et al., 2013, Davidovich et al., 2013].

Por otra parte, ha sido sugerido que la metilación del DNA es una marca que impide la unión del complejo PRC2 (Holoch and Margueron, 2017). En una gran variedad de líneas celulares la pérdida de metilación del DNA causada por la inhibición de las enzimas DNA metiltransferasas resulta en una acumulación de H3K27me en regiones previamente marcadas por 5-metilcitosina [Lindroth et al., 2008, Wiles and Selker, 2017]. Estos estudios son consistentes con datos que muestran que las islas CpG no metiladas pueden reclutar a PRC2 [Jermann et al., 2014]. Además de la metilación del DNA, se ha reportado que la metilación de H3K27 es inhibida por la presencia de marcas características de cromatina activa, tales como H3K36me3 y H3K27ac [Schmitges et al., 2011]. Por el contrario, la unión de EED a H3K27me3 estimula la actividad enzimática de EZH2, promoviendo la trimetilación de H3K27 en los nucleosomas vecinos lo cual contribuye en gran medida a la propagación de la marca a lo largo de amplios dominios de cromatina [Lee et al., 2018]. Estos hechos indican que Polycomb responde al ambiente de la cromatina y depende de este para establecer los dominios de H3K27me3.

EZH2 y STAT3

La actividad catalítica de EZH2 puede ser regulada por la fosforilación de varios residuos. Se ha reportado que la activación de la vía de AKT/PI3K promueve la fosforilación de EZH2 en el residuo Ser21, lo que disminuye su actividad de metiltransferasa de histonas e impide que PRC2 se una a la cromatina, ocasionando pérdida de la trimetilación de H3K27 y des-represión de los genes blanco [Cha et al., 2005, Ott

et al., 2012]. Por ejemplo, en la línea celular MCF-7 derivada de cáncer de mama, ha sido descrito que la expresión de el gen anti-apoptótico BCL2 se encuentra reprimida por la presencia de la marca H3K27me3 en su promotor. Sin embargo, el tratamiento con E2 activa la vía de AKT, lo que provoca que EZH2 se fosforile en el residuo Ser21 (pSer21) inhibiendo la trimetilación de H3K27. Esto permite la unión del receptor a estrógenos alfa (ERα) a los elementos de respuesta a estrógenos (EREs) que se encuentran en el promotor de BCL2 lo que finalmente activa la expresión este gen [Svotelis et al., 2011].

Además de inhibir la metilación de H3K27, la fosforilación de Ser21 incrementa la afinidad de EZH2 por varios sustratos no-histónicos, un ejemplo es el activador de transcripción inducido por señales 3 (STAT3) [Trošelj et al., 2016]. Se ha demostrado que EZH2 al fosforilarse en la Ser21 por medio de la activación de la vía de señalización AKT/PI3K, metila a STAT3 e incrementa su actividad transcripcional **(Figura 5)** [Chang et al., 2017]. Este proceso fue descrito por Kim y colaboradores en células troncales de glioma (GSC) [Kim et al., 2013], en cáncer de próstata [Majumdar et al., 2019] y recientemente ha sido reportada en *Xenopus laevis* [Loreti et al., 2020].

STAT3 es uno de los factores de transcripción oncogénicos más estudiados en los últimos años, que se ha asociado a diversos procesos tales como iniciación del cáncer, progresión, metástasis, resistencia a quimioterapia y evasión del sistema inmune. Se ha propuesto que STAT3 puede ser el punto de convergencia de varias vías de señalización involucradas en diversos procesos neoplásicos como el receptor del factor de crecimiento epidérmico (EGFR), el receptor al factor de crecimiento derivado de plaquetas (PDGFR) y la familia de cinasas Janus (JAK) [Qu et al., 2019].

3.2.4. Papel EZH2 y H3K27me3 en cáncer

La importancia de H3K27me3 en el mantenimiento a largo plazo de los patrones de expresión génica apropiados se ha demostrado por la amplia variedad de mutaciones en los miembros del complejo PRC2 y de su sustrato H3K27 en cáncer. Las regiones del genoma que poseen la marca H3K27me3 varían entre diferentes etapas del desarrollo, tipos celulares y en tejidos normales con respecto a los patológicos [Wiles and Selker, 2017]. Se ha reportado que EZH2 se encuentra mutado en varios tipos de cáncer como melanoma, linfoma, cáncer de mama y de próstata [Sørensen and Ørntoft, 2010, Margueron and Reinberg, 2011]. Además, en cáncer de próstata resistente a la castración y tumores paratiroideos se ha detectado sobre-expresión de EZH2 y amplificación del número de copias del gen.

La activación aberrante de EZH2 promueve procesos neoplásicos tales como la transición epitelio-mesénquima (con la subsecuente invasión y metástasis), incremento en

la proliferación, el mantenimiento de inflamación crónica y establecimiento de tolerancia a la respuesta inmune [Katoh, 2016]. La promoción del crecimiento tumoral mediante las proteínas del complejo Polycomb está asociada frecuentemente a su habilidad para reprimir el locus Ink4a/Arf, un supresor de tumores y regulador negativo de la progresión del ciclo celular [Scelfo et al., 2015, Yin et al., 2016]. Además, EZH2 está relacionado con la resistencia a la quimioterapia y promueve la angiogénesis, la invasión, proliferación y migración de diversas células tumorales [Yan et al., 2017].

Han sido descritos diversos mecanismos transcripcionales y postranscripcionales mediante los cuales la expresión de EZH2 es regulada en distintos tipos de cáncer. Varios factores de transcripción inducen la expresión de esta KMT, por ejemplo, la oncoproteína c-Myc incrementa la expresión de EZH2, así como otros factores de transcripción conocidos como SOX4, NF-Y, STAT3, ETS y E2F. Se ha reportado también que una gran cantidad de miRNAS regulan directamente la expresión de EZH2 en cáncer, tales como

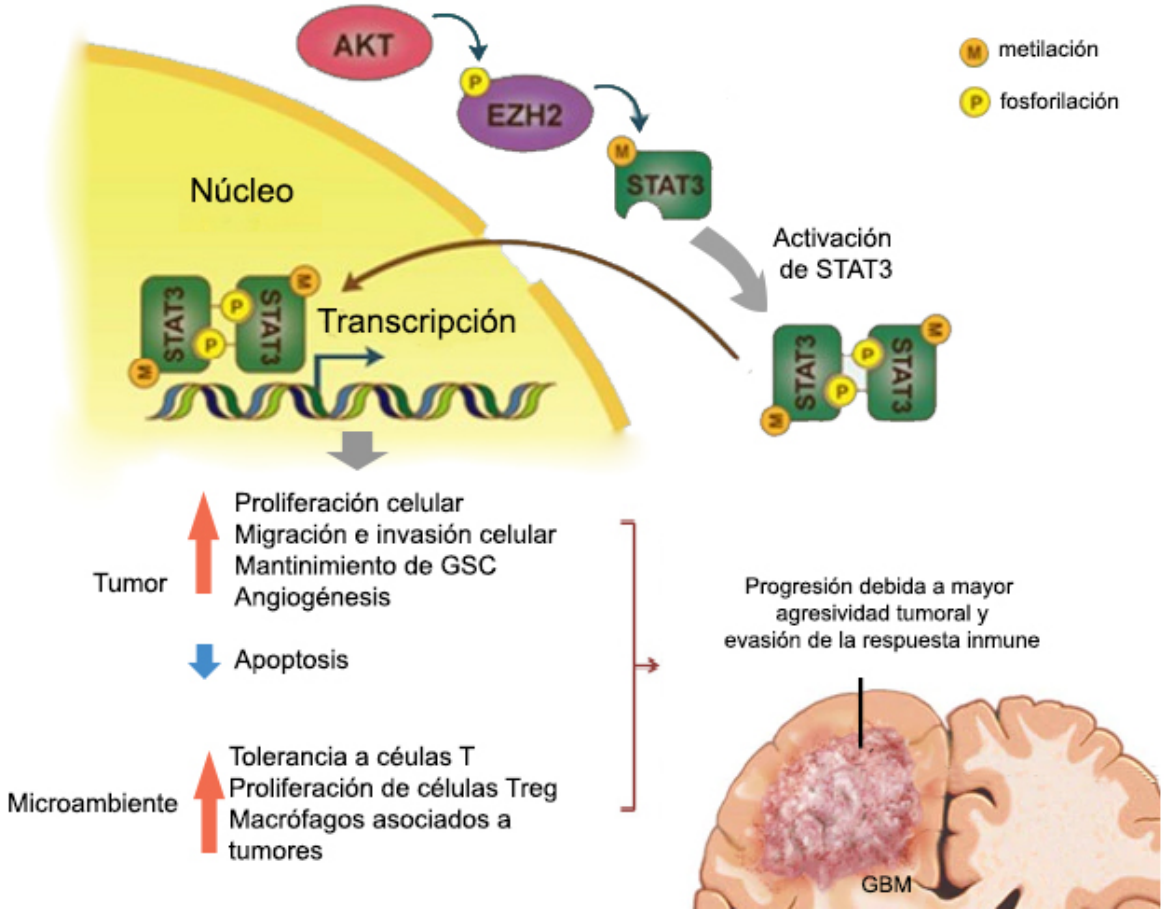

Figura 5: Mecanismo de activación de STAT3 mediado por EZH2 en glioblastomas. P y M representan fosforilación y metilación, respectivamente. GSC: Células troncales de glioma. GBM: Glioblastoma. Modificado de Chang et al., 2017.

miR-26, miR-32, miR-101, miR-137, miR-138 y miR-506 [Lu et al., 2016]. A nivel de proteína existen también distintas modificaciones postraduccionales que modifican la actividad de EZH2. Por ejemplo, en cáncer de mama, la fosforilación en la Ser2 mediada por Akt disminuye los niveles de H3K27me3 y promueve el desarrollo del tumor mediante los blancos no-histona de EZH2 presentes en el citoplasma, tales como STAT3 que es un factor de trascripción involucrado en la respuesta celular a interleucinas y factores de crecimiento [Kim et al., 2013].

En adición a las mutaciones o alteraciones que provocan ganancia de función, también se han descubierto mutaciones que conducen a pérdida de la actividad de EZH2. Esto en tumores malignos originados a partir de células mieloides, la mayoría de estas mutaciones localizadas en el dominio catalítico SET lo que promueve el desarrollo de leucemia, y demuestra que el papel de esta KMT en el desarrollo del cáncer es más complejo de lo que se piensa. Hay algunos estudios donde se ha asociado la pérdida en los niveles de H3K27me3 a un mal pronóstico en diferentes tipos de cáncer, incluidos de mama, ovario y pulmonar [Scelfo et al., 2015, Trošelj et al., 2016].

La inhibición de EZH2 en los tumores donde se ha demostrado un aumento de H3K27me3 podría ser una estrategia atractiva para el tratamiento del cáncer; en diversos estudios se ha reportado que el knockdown, knockout o inhibición de EZH2 reduce la proliferación de líneas celulares derivadas de varios tipos de cáncer como leucemia, linfoma, cáncer de próstata, entre otros [Scelfo et al., 2015, Comet et al., 2016]. En los últimos años se han desarrollado y probado gran diversidad de fármacos inhibidores de EZH2, todos con moderado éxito en el tratamiento de leucemias [Yan et al., 2017]. Sin embargo, es importante tener en cuenta que existen reportes que indican que la inhibición prolongada de EZH2 en GBM causa un profundo cambio en la célula, induciendo proliferación, mecanismos de reparación de daño a DNA y activación de genes relacionados con pluripotencialidad que resultan en la alteración de la identidad celular y la progresión tumoral [de Vries et al., 2015].

Por lo tanto, el papel de EZH2 como oncogén o supresor de tumores está determinado por el contexto celular, el tipo de cáncer y la identidad de la célula que da origen a la transformación. De igual forma, este doble rol que tiene EZH2 sugiere que el papel de esta enzima en el cáncer es complejo por lo que requiere de un estudio cuidadoso y detallado que permita conocer sus mecanismos de acción a fin de entender cómo afecta al desarrollo tumoral.

3.2.5. Alteraciones epigenéticas en Glioblastomas

El estudio de los GBM ha revelado perfiles epigenéticos característicos que permiten su clasificación en distintos subtipos moleculares que han sido integrados en la clasificación

de Tumores del Sistema Nervioso 2016 de la OMS [Louis et al., 2016]. Mutaciones en reguladores epigenéticos como IDH1 o IDH2 y en los genes de la histona H3 (H3F3A o HIST1H3B) son biomarcadores clave que han enfatizado la relevancia de las alteraciones epigenéticas en la evolución de los gliomas [Gusyatiner and Hegi, 2018].

En GBMs, son frecuentes las mutaciones en los genes IDH1 o IDH2 que codifican para la enzima isocitrato deshidrogenasa que forma parte del ciclo de Krebs. Los gliomas con mutaciones en los genes IDH1 o IDH2 (IDHmt) tienen un perfil de metilación del DNA completamente diferente al de aquellos tumores que contienen el gen silvestre (IDHwt) y se les ha denominado Glioma con fenotipo metilador de islas CpG (G-CIMP por sus siglas en inglés). Los tumores IDHmt adquieren actividad enzimática para convertir el α-cetoglutarato a D-2-hidroxiglutarato (2-HG). El 2-HG es inhibidor de una gran variedad de enzimas desmetilasas de histonas dependientes de α-cetoglutarato, así como las enzimas oxigenasas de DNA, por lo que el G-CIMP se caracteriza por la hipermetilación local de CpGs. En adultos mayores, alrededor de la mitad de los casos de GBM son IDHwt [Reifenberger et al., 2017].

La temozolomida es el agente alquilante más utilizado en el tratamiento de los GBMs [Hamza and Gilbert, 2014]. Este fármaco induce el aducto 6-O-metilguanosina (O6-meG) en el DNA el cual provoca rupturas de doble cadena y promueve la muerte celular. Este efecto puede ser revertido mediante diferentes sistemas de reparación del DNA. Uno de los principales marcadores asociados a la resistencia a temozolomida es el gen que codifica para la O-6-Metilguanina-DNA Metiltransferasa (MGMT), esta enzima puede restaurar la integridad de las bases O6-meG al transferir el grupo metilo a una cisteína en su sitio catalítico [Johannessen and Bjerkvig, 2012]. Por lo tanto, los niveles de expresión de MGMT corresponden a la capacidad celular de reparación de O6-meG. La metilación del promotor de MGMT ocurre en menos de la mitad de GBM IDHwt y es considerada como un buen pronóstico ante la terapia con temozolomida [Reifenberger et al., 2017].

En gliomas pediátricos se ha sugerido que una mutación en la histona H3.3 (H3F3A) que sustituye la lisina 27 por metionina (H3K27M) es importante en el desarrollo de estos tumores ya que reduce bloquea la actividad de PRC2, así como los niveles globales de H3K27me3 y contribuye al desarrollo tumoral, por lo que bajo este contexto EZH2 actúa como supresor de tumores [Mohammad et al., 2017]. Sin embargo, en GBMs de adultos no son comunes las mutaciones en H3F3A, además de que las mutaciones en IDH1 y H3F3A son mutuamente excluyentes y presentan diferentes patrones de metilación del DNA [Kondo et al., 2014].

3.2.6. EZH2 en Glioblastomas

El papel de EZH2 ha sido ampliamente estudiado en gliomas, ha sido descrito que en biopsias de GBM, la sobre-expresión de este gen está directamente involucrada en la malignidad del tumor y una menor esperanza de vida [Zhang et al., 2015a]. EZH2 participa en la regulación de genes involucrados en la invasión y migración de células derivadas de GBM como el receptor tipo tirosina-cinasa AXL [Ott et al., 2012, Yen et al., 2017]. También se ha visto que influye en la proliferación ya que el silenciamiento de EZH2 provocó un arresto en la fase G1 del ciclo celular y disminuyó el volumen de tumores formados por células derivadas de GBM después de su implantación en ratones desnudos [Yin et al., 2016].

En las células derivadas de GBMs humanos resistentes a temozolomida, se ha descrito que EZH2 se encuentra sobre-expresado en comparación con las células que son sensibles a este fármaco. Además de que el knockdown de EZH2 disminuyó la expresión de varios transportadores ABC involucrados en la resistencia de los tumores a la quimioterapia [Fan et al., 2014].

Los lncRNA también participan en la regulación de vías de señalización en GBM [Han et al., 2012]. HOTAIR es un lncRNA que se une a EZH2 mediante el dominio ncRBD y recluta a PRC2 hacia los genes HOX que están involucrados en el desarrollo embrionario y la diferenciación celular [Marsh et al., 2014]. HOTAIR se encuentra sobre-expresado en GBM, causando progresión acelerada del ciclo celular, además de que es un indicador de pobre pronóstico para el paciente [Zhang et al., 2015b].

Por otro lado, varios miRNAs están involucrados en la regulación de la actividad de EZH2, la expresión de varios de miRNAs se encuentra desregulada en GBM, un ejemplo es miR-708 cuya expresión en líneas celulares de GBM está disminuida en comparación con tejido normal, la sobrexpresión de este miRNA reduce la expresión de EZH2 e inhibe la proliferación e invasión de líneas celulares de GBMs humanos. De manera similar, miR-138 inhibe la expresión de EZH2 tanto en biopsias de GBM como en líneas celulares derivadas de estos tumores [Yin et al., 2016].

Recientemente se ha sugerido que las células troncales de glioma (GSC) son en parte responsables de la resistencia de los GBM a la remoción quirúrgica y la resistencia a la quimioterapia ya que son capaces de autorrenovarse, diferenciarse y generar nuevos tumores similares al de origen [Singh et al., 2004]. EZH2 es requerido para el mantenimiento y renovación de las células troncales de glioma [Yin et al., 2016], en GSC obtenidas de biopsias de pacientes y tratadas con el inhibidor farmacológico de EZH2, 3-Deazaneplanocin A (DZNep), disminuyó significativamente la proliferación y autorrenovación de éstas [Suvà et al., 2009] lo que apunta a que efectivamente Polycomb

podría tener un papel relevante en el mantenimiento de las GSC.

Aunado a esto, ha sido demostrado que STAT3 se encuentra activo en más de 50 % de los GBM y que está sobre-activado en comparación con el tejido normal, además de que hay una correlación positiva entre el grado del tumor y el grado de activación [Chang et al., 2017]. Esto es interesante debido a que EZH2 puede metilar a STAT3 lo que incrementa su actividad, como ya se mencionó anteriormente.

Interesantemente, se tienen evidencias de que las hormonas sexuales pueden regular la expresión de EZH2 en diferentes tipos celulares, sobre todo en tumores sensibles a hormonas como el cáncer de mama y de próstata [Shi et al., 2007, Tamm-Rosenstein et al., 2013, Bhan et al., 2014, Tao et al., 2015]. Estos datos sugieren que E2 podría regular la actividad y/o expresión de EZH2 en GBM ya que son tumores que han demostrado ser sensibles a tratamientos hormonales, además de que se caracterizan por una alta expresión de EZH2 y de los receptores intracelulares a hormonas esteroides, en especial el receptor intracelular a estrógenos [González-Arenas et al., 2012].

3.3. Estradiol (E2)

3.3.1. Generalidades

El estradiol (E2) es una hormona sexual esteroide que se sintetiza principalmente en los ovarios a partir de la testosterona por la enzima aromatasa, aunque puede ser sintetizado también en las glándulas adrenales, en tejido adiposo y en cerebro [Brown, 2006]. El E2 puede ser sintetizado a partir del colesterol, que al entrar a la célula es translocado a la mitocondria y convertido a pregnenolona, la cual se transporta al retículo endoplásmico liso donde se metaboliza a E2 [Miller, 2013, Rossetti et al., 2016].

El E2 es considerado un neuroesteroide, lo que significa que puede ser sintetizado de novo en tejidos neurales, donde regula la plasticidad sináptica, la diferenciación sexual del cerebro, el comportamiento reproductivo y el aprendizaje [Rossetti et al., 2016]. La síntesis local de estrógenos en el cerebro es un proceso dinámico y regulado que varía se acuerdo a la edad, el sexo, el estado fisiológico y difiere entre regiones cerebrales [Mani and O'Malley, 2002]. La enzima aromatasa (CYP19A1) además de las gónadas, se expresa en diversas regiones del cerebro relacionadas con la reproducción, como la amígdala y el hipotálamo [Azcoitia et al., 2011], principalmente en neuronas y astrocitos. Los receptores a estrógenos se expresan en células normales de glía de ratas, así como en cultivos de astrocitos de rata [Kabat et al., 2010] y ha sido demostrado que el E2 modula la diferenciación neuronal, al influenciar la migración celular, supervivencia y plasticidad sináptica [Giretti and Simoncini, 2008].

Se conocen dos mecanismos de acción para el E2, el clásico (o genómico), y el no clásico (o no genómico). El mecanismo clásico involucra la interacción de la hormona con su receptor intracelular, el cual es un factor de transcripción activado por ligando, que puede unirse a elementos de respuesta a estrógenos activando la transcripción de genes blanco [Heldring et al., 2007]. Los efectos rápidos o no genómicos del E2 están mediados por receptores membranales. A continuación se describen ambos mecanismos de acción:

3.3.2. Mecanismo genómico del estradiol

Este mecanismo está mediado por los receptores intracelulares a estrógenos (ER) [Melmed and Conn, 2007]. Se han descrito dos tipos de ER los cuales son transcritos de diferentes genes; ERα identificado en 1986 y ERβ identificado en 1996 [Kabat et al., 2010]. En ausencia de ligando, el ER se encuentra inactivo y asociado a diversas proteínas chaperonas [Mani and O'Malley, 2002]. Ambos receptores se pueden unir a E2, lo cual ocasiona un cambio conformacional en el receptor, este se disocia de las proteínas

chaperonas y forma heterodímeros o dímeros que son translocados al núcleo, donde funciona como factor de transcripción al unirse a regiones con elementos de respuesta a estrógenos (ERE) **(Figura 6)** [Schwartz et al., 2016]. Los ERE son secuencias altamente conservadas compuestas por dos medios sitos hexaméricos separados por tres bases. ERα y ERβ se unen a los mismos ERE, sin embargo, ERα se une con al menos el doble de afinidad que ERβ [Gruber et al., 2004].

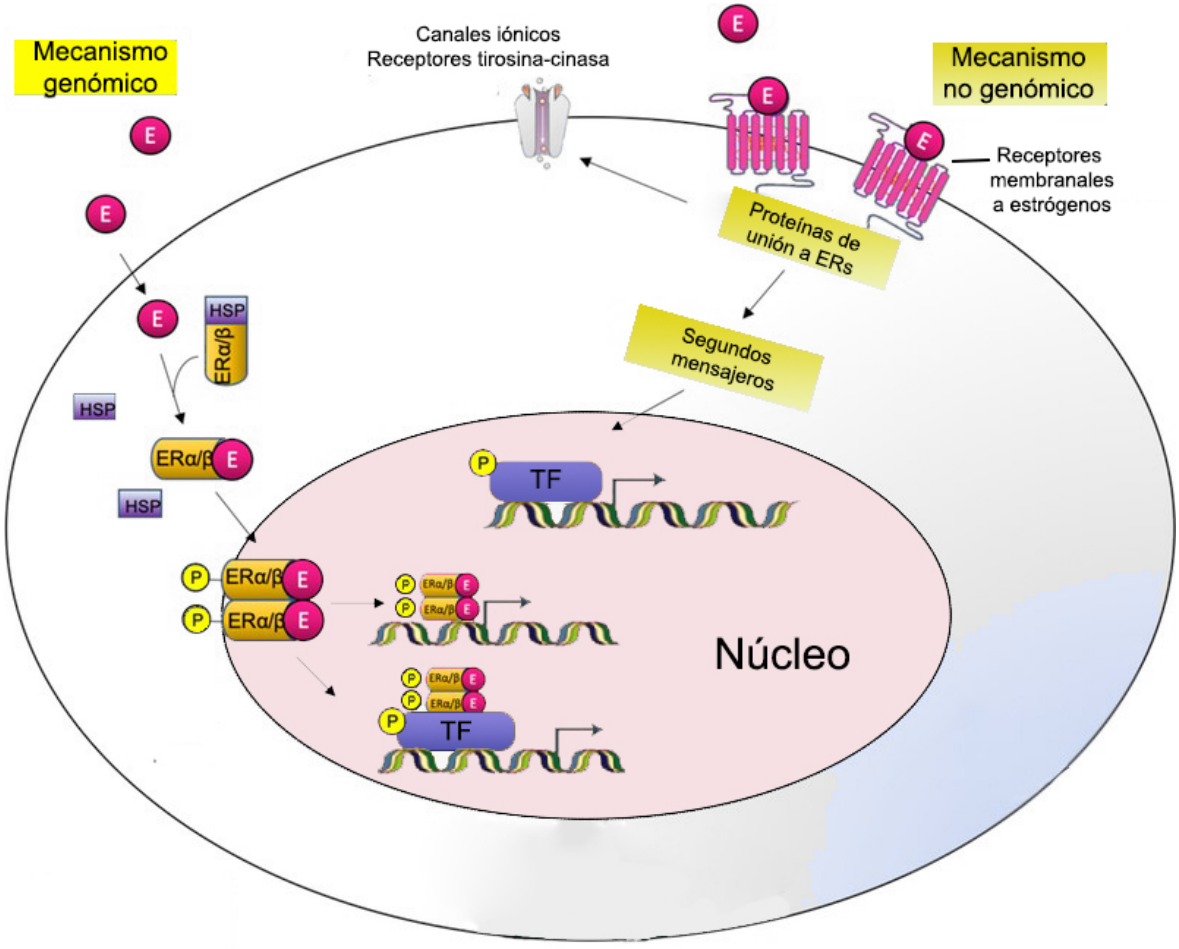

Figura 6: Mecanismos de acción de los receptores a estrógenos. El mecanismo clásico (o genómico) incluye la activación del receptor a estrógenos (ER) por la unión a E2, el ER se dimeriza y transloca a núcleo donde se une directamente a elementos de respuesta a estrógenos (ERE) estimulando la transcripción de genes. El mecanismo no clásico (o no genómico) implica cascadas de señalización que son activadas por la unión del E2 al receptor de estrógenos acoplado a proteína G (GPER o GPR) o al ER translocado a membrana que se dimeriza en respuesta al E2, lo que da como resultado una rápida activación de proteínas G que a su vez activan cinasas como la proteína cinasa activada por mitógeno (MEK); inositol 1,4,5-trisfosfo cinasa (PI3K); cinasas reguladas extracelularmente (ERK). TF: Factor de transcripción. Imagen modificada de Silveyra y Fuentes, 2019.

La respuesta transcripcional mediada por los ERs depende de diversos factores correguladores y de las características de los promotores de los genes [Heldring et al., 2007]. La actividad transcripcional de los ERs está ligada a su interacción con coactivadores que son reclutados por los receptores activados. Los principales reguladores

son la familia de coactivadores de receptores a esteroides (SRC) que consiste de tres miembros: SRC-1, SRC-2 y SRC-3 [Gebhart et al., 2019].

El papel de ERα en diversas neoplasias ha sido ampliamente estudiado, y se ha observado que participa en una gran variedad de procesos carcinogénicos, sin embargo, poco se sabe acerca del ERβ [Tavares et al., 2016]. ERα ha sido propuesto como un promotor de tumores y ha sido descrito que el E2 a través de ERα en líneas celulares cancerosas puede inducir remodelación de la cromatina y cambios en la regulación epigenética de sus genes blanco [Kundakovic, 2017]. ERα y ERβ tienen acciones opuestas en genes involucrados en proliferación, por lo que se ha sugerido que cuando ambos ERs están expresados en la misma célula, ERβ podría antagonizar la activación transcripcional dependiente de ERα mediante mecanismos que actualmente se encuentran en investigación, pero se sugiere que es mediante la alteración del reclutamiento de coactivadores. Se ha observado que cuando ERα y ERβ se expresan en la misma célula, este último puede antagonizar las acciones de ERα mediante la formación de heterodímeros [Heldring et al., 2007].

Existen varios genes que claramente son regulados por estrógenos pero no contienen ERE, hay evidencia de que tanto ERα como ERβ pueden ser reclutados a los genes blanco mediante la interacción directa con otros factores de transcripción como la proteína de especificidad 1 (SP-1), la proteína activadora 1 (AP-1) y p300 que contienen dominios de unión a DNA [Heldring et al., 2011, Mani and O'Malley, 2002]. También ha sido descrito que existe una vía de activación de los ERs que no es dependiente de ligando. La señalización de factores de crecimiento conlleva a la activación de cinasas como PKC, MAPK o PKA que podrían activar ERs por medio de la fosforilación de residuos específicos de serina y tirosina, lo que podría contribuir al crecimiento independiente de hormonas en algunos tumores [Kastrati et al., 2019].

3.3.3. Mecanismo no genómico del estradiol

La vía denominada no genómica de E2 está implicada en la generación de respuestas rápidas a estrógenos y está mediada por subpoblaciones de ERs que después de una serie de modificaciones postraduccionales (como la palmitoilación) se anclan a la membrana celular. Por proximidad, los ERs interactúan con proteínas G, varios receptores membranales como el receptor a insulina, EGFR y cinasas como Src, PI3K o Shc [Romano and Gorelick, 2018]. Las interacciones con estas moléculas promueven la activación de las vías de señalización de MAP cinasas y AKT lo que afecta la regulación transcripcional **(Figura 6)** [Levin, 2008].

Adicionalmente, existe un receptor de E2 acoplado a proteína G (GPER) que regula la expresión génica indirectamente, al activar proteínas que cambian la actividad de factores

de transcripción, en conjunto con la activación de cascadas de señalización intracelular que involucran cinasas como Src, MAPK y PI3K [Barnes et al., 2004]. Ejemplos de los factores de transcripción regulados por este receptor incluyen Elk-1, CREB, C/EBPα, NF-κB y la familia de STAT de activadores de la transcripción [Fuentes and Silveyra, 2019]. Se ha descrito que la activación de GPER mediada por E2 induce diversos procesos como el crecimiento celular, migración e invasión de células tumorales [Lappano et al., 2014]. También se ha localizado a GPER en el cerebro y su activación por E2 promueve neuroprotección en el hipocampo, así como liberación del factor liberador de gonadotropinas (GnRH). La actividad de GPER es independiente de ERα y ERβ, aunque se ha descrito que la convergencia de ambas vías resulta en un aumento de la actividad transcripcional inducida por E2 [Bjornstrom and Sjoberg, 2005].

3.3.4. Estradiol y Glioblastomas

Los estrógenos son hormonas oncogénicas en diferentes tipos de cáncer, tales como mama, próstata, endometrio y pulmón. Sin embargo, aún no se ha dilucidado el papel de estas hormonas en la biología de los GBMs. Recientemente, se reportó que la línea celular U87 derivada de un GBM humano y la línea C6 derivada de GBM de rata pueden metabolizar testosterona y androstenediona a E2, además que se demostró que dichas células sintetizan testosterona a partir de colesterol [Pinacho-Garcia et al., 2020]. Lo anterior sugiere que el E2 podría estar presente en este tipo de tumores y desempeñar un papel crucial en su progresión maligna.

Dueñas y colaboradores han reportado que la concentración de E2 es mayor en GBM que en astrocitomas de grado II, además de que la aromatasa, enzima que metaboliza la testosterona a estradiol, se encuentra sobre-expresada en biopsias de GBM [Dueñas Jiménez et al., 2014]. En la línea U373 derivada de GBM el tratamiento con E2 aumentó la proliferación celular, mientras que el tratamiento con PPT (agonista selectivo de ERα) pero no DPN (agonista selectivo de ERβ) incrementó el número de células U373 [González-Arenas et al., 2012]. Otro estudio reporta un aumento en la migración e invasión de las líneas celulares U87 y T98G al ser tratadas con E2 [Wan et al., 2018]. Aunado a esto, la tibolona (fármaco agonista de los receptores intracelulares a progesterona, y estradiol) induce la proliferación, de las células U87 y U251 [González-Arenas et al., 2019]. De forma contraria, el tratamiento con tamoxifen, un fármaco antagonista de ER, induce muerte por autofagia e incrementa la acción citotóxica de la temozolomida [Baritchii et al., 2016, Graham et al., 2016].

En cuanto a la expresión de los ERs, los reportes indican que en GBM, ERα se expresa en mayor cantidad que ERβ [Dueñas Jiménez et al., 2014]. La activación de ERα en la línea

U87 aumenta el número de células, así como la expresión de ciclina D1, EGFR y VEGF [González-Arenas et al., 2012]. Dueñas y colaboradores observaron que la expresión de ERα está negativamente correlacionada con el grado del tumor y positivamente correlacionada con la esperanza de vida [Dueñas Jiménez et al., 2014]. Se ha identificado que alta expresión de la variante 66 de ERβ (ER-β66) está asociada a resistencia a temozolomida posiblemente a través de la regulación de procesos de autofagia [Qu et al., 2019].

Por otra parte, se ha reportado que ERβ se expresa en tumores astrocíticos y su expresión se relaciona negativamente con el grado del tumor, además de que la baja expresión de este receptor es asociada a pobre expectativa de vida [Batistatou et al., 2004]. Varios fármacos selectivos para ERβ han sido sintetizados y probados para el tratamiento de gliomas ya que el tratamiento de células derivadas de GBMs con agonistas de este receptor redujo el crecimiento tumoral y la proliferación, además de inhibir los mecanismos de reparación de DNA, por lo que se piensa que este receptor actúa como supresor de tumores [Sareddy et al., 2012, Zhou et al., 2019]. Interesantemente, Liu y colaboradores demostraron que a pesar de que la expresión de ERβ disminuye proporcionalmente al grado del tumor, la isoforma ERβ5 incrementa y está involucrada en la activación de la vía de AKT/mTOR [Liu et al., 2018].

Un estudio en xenotrasplantes de la línea celular U87 en cerebros de ratas ovariectomizadas observó que estas tienen una supervivencia media menor a los controles, lo que sugiere que el E2 es un agente protector. No obstante, en el mismo estudio el E2 aumentó significativamente la proliferación celular in vitro, por lo que los autores sugieren que esta hormona regula el microambiente del tumor al modular la respuesta inflamatoria inducida por la implantación ([Barone et al., 2009].

También se ha observado que en líneas celulares derivadas de GBM, el E2 regula la expresión tanto del receptor a progesterona (PR) como de los receptores membranales a progesterona, en ambos casos se observó que al tratar las células con E2 se incrementa la expresión de estos receptores [Valadez-Cosmes et al., 2015, Hansberg-Pastor et al., 2017], por lo que el E2 podría potenciar los efectos de la progesterona (P4) en la progresión de los gliomas. Estudios de nuestro grupo han demostrado que la P4 y sus metabolitos promueven la invasión, migración y proliferación de líneas derivadas de GBM [Valadez-Cosmes et al., 2015, Piña-Medina et al., 2016, Zamora-Sánchez et al., 2018].

3.3.5. Estradiol y EZH2

En cáncer de mama se ha reportado que el E2 participa en la regulación de la actividad de EZH2. La activación de cinasas a través de los receptores membranales a E2 (vía no genómica) provoca la fosforilación de EZH2 lo que regula la actividad catalítica de esta

enzima [Qin et al., 2019]. Majumdar y colaboradores reportan que, en células troncales de cáncer de próstata, ambos ERs (ERα y ERβ activan cascadas de señalización que regulan la actividad de metiltransferasa de EZH2. Sin embargo, la vía activada depende del subtipo de receptor. ERα activa la vía de PI3K/Akt que favorece la actividad de metiltransferasas de H3K4, mientras que ERβ activa la vía de MAPK que conduce a la fosforilación de EZH2 en el residuo de Ser21, inhibiendo la actividad de metiltransferasa de histonas de este último [Majumdar et al., 2019].

Además de la regulación postranscripcional, el gen *EZH2* posee tres EREs en su promotor, lo que sugiere que su expresión puede ser regulada por estrogénos. En líneas celulares derivadas de cáncer de mama se ha demostrado que la expresión de EZH2 es inducida por E2, así como por diversos xenoestrógenos [Bhan et al., 2014]. Aunado a esto, un estudio realizado en las líneas celulares derivadas de cáncer de mama MCF-7 y T47D, encontró que ERα puede ser co-inmunoprecipitado con EZH2, por lo que se sugiere que ERα puede formar parte de PRC2 [Shi et al., 2007].

También hay una relación entre las hormonas y los RNAs no codificantes, por ejemplo, en carcinoma de células renales, la expresión de lncRNA HOTAIR está regulada directamente por ERβ [Ding et al., 2018] y como se mencionó anteriormente (sección 3.2.3), HOTAIR es un lncRNA que se une directamente a EZH2 y recluta al complejo PRC2 al promotor de diversos genes [Margueron and Reinberg, 2011]. En el artículo de Ding y colaboradores se sugiere también que ERβ promueve la progresión del carcinoma de células renales al incrementar la expresión de HOTAIR, el cual podría incrementar la actividad represora de PRC2 o actuar como esponja de miRNAs supresores de tumores [Ding et al., 2018]. Además, el E2 a través de GPER induce la expresión de HOTAIR, un lncRNA que se une directamente a EZH2 y recluta el complejo Polycomb hacia diversos genes blanco [Tao et al., 2015].

4. Justificación

Los glioblastomas son los tumores primarios más frecuentes y agresivos del sistema nervioso central. Desafortunadamente, debido a la falta de estrategias terapéuticas adecuadas, la mayoría de los pacientes no sobrepasan el año de supervivencia posterior al diagnóstico. Debido a que tienen una mayor incidencia en hombres que en mujeres (3:2), el estudio del papel de las hormonas sexuales en estos tumores es de vital importancia. Trabajos anteriores han demostrado que el estradiol (E2) incrementa la proliferación, invasión y migración de células derivadas de GBM humanos; sin embargo, los mecanismos mediante los cuales el E2 ejerce su efecto sobre los GBM no han sido totalmente dilucidados.

Previamente ha sido demostrado que el E2 regula la expresión de la enzima Homóloga del Enhancer de Zeste 2 (EZH2) en cáncer de mama. Varios estudios funcionales han sugerido que la expresión de EZH2 está correlacionada con un aumento en la proliferación, migración e invasión de células derivadas de GBM, mismos procesos que son regulados por el E2. Sin embargo, no se ha investigado si existe una relación directa entre EZH2 y E2 en GBMs. Así pues, los datos sugieren que E2 podría regular la actividad de EZH2 en GBM ya que son tumores que han demostrado ser sensibles a tratamientos hormonales, además de que se caracterizan por una alta expresión de EZH2 y de ERα.

5. Planteamiento del problema

Se sabe que la subunidad catalítica del complejo represor PRC2, EZH2, se encuentra sobre-expresada en biopsias de GBM y que sus niveles están directamente correlacionados con el grado del tumor. También se ha reportado que el E2 induce la expresión de EZH2 en cáncer de mama y promueve la progresión tumoral de GBMs humanos. Sin embargo, se desconoce si el E2 regula la expresión de EZH2 en GBM, así como la participación conjunta de E2 y EZH2 en procesos fundamentales para la progresión tumoral como la proliferación, migración e invasión de GBM.

6. Hipótesis

Tanto el estradiol (E2) como EZH2 regulan procesos similares en glioblastomas (GBM) tales como proliferación, migración e invasión. Por lo tanto, la administración de E2 incrementará la expresión de EZH2 en células derivadas de GBM lo que resultará en un aumento de la represión mediada por Polycomb sobre sus genes blanco aumentando la proliferación, migración e invasión de células derivadas de GBMs humanos.

7. Objetivos

7.1. Objetivo general

Evaluar los efectos del Estradiol (E2) sobre la expresión de la subunidad catalítica de PRC2, EZH2, así como su influencia sobre la proliferación, migración e invasión en células derivadas de glioblastomas humanos.

7.2. Objetivos particulares

- Determinar la expresión basal de EZH2 en las líneas derivadas de GBM humanos: U251, D54 y U87.
- Evaluar el efecto del Estradiol (E2) sobre la expresión de EZH2 en las líneas celulares U87, U251 y D54.
- Evaluar los efectos del silenciamiento de EZH2 sobre la proliferación, invasión y migración de células derivadas de GBM tratadas con E2.

8. Metodología

8.1. Cultivo Celular y tratamientos hormonales

Las células U87, U251 y D54 derivadas de GBM humanos se cultivaron en medio DMEM con rojo de fenol suplementado con suero fetal bovino al 10 % (SFB), piruvato 1 mM, glutamina 2 mM y aminoácidos no esenciales 0.1 mM, a 37ºC en una atmósfera de CO_2 al 5 % humidificada. Una vez alcanzada una confluencia de aproximadamente 80 %, se sembraron $1x10^5$ células por pozo, 24 horas antes de los tratamientos, el medio fue cambiado por DMEM sin rojo de fenol y suplementado con suero fetal bovino filtrado con carbón activado. Las células se trataron con E2 soluble en agua (10 nM, Sigma Aldrich, MO, USA) y Vehículo (V) 0.02 % de ciclodextrina (CDX) durante 3, 6, 12 y 24 horas. Para la curva de concentraciones las células se trataron con E2 (1 nM, 10 nM, 100 nM y 1 µM) o V (0.02 % de CDX) por 12 y 24 horas.

8.2. Extracción de RNA y RT-qPCR

El RNA fue extraído utilizando TRI Reagent, se separó la fase acuosa con cloroformo, el RNA se precipitó con isopropanol y se lavó con etanol. Se cuantificó con el equipo NanoDrop 2000 Spectrophotometer y su integridad fue determinada mediante electroforesis en un gel de agarosa al 1.5 %. Para la síntesis de cDNA se utilizó la enzima M-MLV Reverse Transcriptase (ThermoFisherScientific, MA, USA). En tubos Eppendorf se colocaron los siguientes componentes (cantidades para una reacción): 1 µL de oligo $(dT)_{12-18}$ (500 µg/mL), 1 µg de RNA total y 1 µL de dNTPMix (dATP, dGTP, dCTP y dTTP a una concentración de 10 mM cada uno). La mezcla anterior fue calentada a 65°C durante 5 min y rápidamente transferida a un baño de hielo. Posteriormente, se agregaron 4 µL de buffer de reacción (5X First-Strand Buffer), 2 µL de ditiotreitol (DTT, 0.1 M) y 1 µL de agua. Se homogenizó e incubó a 37°C durante 2 min. Finalmente, se agregó 1 µL de la enzima M-MLV RT a cada tubo de reacción y se incubó a 37°C durante 50 min. Para

inactivar la reacción se calentó a 70°C durante 15 min. Como control de expresión se utilizó RNA total de cultivo primario de astrocitos humanos (ScienCell, cat #1805).

El mRNA se cuantificó mediante qPCR usando el sistema LightCycler y el reactivo FastStart DNA Master SYBR Green I de acuerdo a las especificaciones del fabricante. 2 µL del cDNA obtenido anteriormente fueron utilizados como templado. El programa utilizado fue el siguiente:

- Un ciclo de desnaturalización a 95°C por 10 minutos
- 45 ciclos de amplificación (95°C 10s, 60°C 10s, 72°C 10s)
- Melting Curve (95°C 0s, 65°C 15s, rampa de temperatura 0.1°C/s hasta 95°C)

El análisis de los resultados se realizó por el método de ΔCT [Schmittgen and Livak, 2008]. Los resultados obtenidos se normalizaron con respecto a la subunidad ribosomal 18S, de ahí que los resultados sean expresiones relativas. Se realizaron 4 experimentos independientes.

8.2.1. Oligonucleótidos

Para amplificar al gen EZH2, se utilizó la secuencia de oligonucleótidos previamente reportada por Fuji, et al en 2008. Se comprobó la selectividad de éstos mediante la herramienta PrimerBlast de NCBI disponible en la página electrónica: https://www.ncbi.nlm.nih.gov/tools/ primerblast/.

Los oligonucleótidos para la amplificación del gen 18S se diseñaron con PrimerBlast. Para ambos oligos (EZH2 y 18S) se verificaron los parámetros fisicoquímicos con NetPrimer disponible en: http://www.premierbiosoft.com/netprimer/. Se tomó en cuenta que la longitud de los oligonucleótidos no excediera 24 bases, que su contenido de CG estuviera entre el 50 y 60 %, que la Tm calculada estuviera entre 57 y 60°C y que no hubiera complementariedad entre cada par. Además, se consideró que cada par hibridara en una unión exón-exón. Los oligonucleótidos usados fueron los siguientes:

18S

- Tamaño del amplificado: 167 pb
- Oligonucleótido sentido (5′ → 3′): AGTGAAACTGCAATGGCTC

- Oligonucleótido antisentido (5′ → 3′): CTGACCGGGTTGGTTTTGAT

EZH2 [Fujii et al., 2008]

- Tamaño del amplificado: 120 pb
- Oligonucleótido sentido (5′ → 3′): CCCTGACCTCTGTCTTACTTGTGGA
- Oligonucleótido antisentido (5′ → 3′): ACGTCAGATGGTGCCAGCAATA

8.3. Extracción de proteínas y Western Blot

Después de los tratamientos las células fueron lisadas con buffer RIPA (50 mM Tris-HCl (pH=7.5), 150 mM NaCl, 1 % TRITON y 0.01 % SDS). Los lisados se cuantificaron con el reactivo Pierce® 660 nm ProteinAssay (ThermoScientific, IL, USA) en el equipo NanoDrop 2000®. 20 mg de proteína total fueron separados mediante SDS-PAGE en un gel de acrilamida al 10 % con voltaje constante (100 V). Las proteínas se transfirieron a una membrana de nitrocelulosa utilizando una cámara semi-seca a 60 mA por membrana durante 2 horas y media.

La membrana se bloqueó con una solución de albúmina sérica bovina (BSA) al 5 % en TBS tween 0.1 % durante dos horas y media a 37°C. Se cortó la membrana verticalmente con ayuda del marcador de peso molecular para obtener dos secciones, una con proteínas con peso molecular menor a 60 kDa (mitad inferior) y la otra con pesos mayores a 60 kDa (mitad superior). La mitad superior se incubó con el anticuerpo primario anti-EZH2 (CellSignaling, Rabbit mAb #5246) en dilución 1:1000. La mitad inferior se incubó con el anticuerpo secundario contra γ-tubulina (SIGMA, Rabbit #T3195) en dilución 1:1000, ambos anticuerpos se incubaron durante toda la noche a 4°C y se lavaron con TBS-Tween 0.1 % (5 lavados de 5 min). Como anticuerpo secundario en ambos casos se utilizó uno dirigido contra IgG de conejo, acoplado a peroxidasa de rábano (Santa Cruz, Goat sc-2004) en dilución 1:4500, y se incubó durante 45 minutos a temperatura ambiente. Las membranas se lavaron nuevamente con TBS-Tween y se revelaron por quimioluminiscencia mediante el kit SuperSignal® West Femto Maximum Sensitivity Substrate (ThermoScientific, IL, USA), las imágenes se obtuvieron con el equipo C-DiGit® Blot Scanner (LI-COR, USA).

El análisis densitométrico se realizó con el software ImageJ® [Schneider et al., 2012]. Como control de carga se utilizó γ-tubulina, los resultados se muestran como el cociente entre la densidad de la banda correspondiente a EZH2 y la densidad de la γ-tubulina.

8.4. Inmunofluorescencia

Las células U87, U251 y D54 derivadas de GBM humanos se cultivaron en cajas de 4 en condiciones basales (medio DMEM con rojo de fenol, 37°C y 5 % de CO_2). Las células se fijaron con paraformaldehído (PFA) al 2 % durante 20 minutos a temperatura ambiente, posteriormente se realizaron 3 lavados de 5 minutos con PBS. Posteriormente se bloquearon y permeabilizaron las células con 200 µL una disolución de PBS con 1 % de glicina, 0.2 % de Tritón y 1 % de BSA. Se incubó por 20 minutos a temperatura ambiente, después de este tiempo se retiró la solución y se colocó el anticuerpo primario anti EZH2 en dilución 1:200, se dejó incubar una noche a 4°C posterior a lo cual se lavó 3 veces con PBS. Como anticuerpo secundario se utilizó uno contra IgG de conejo acoplado a Alexa Fluor (ThermoFisher, Goat #A-11011) en dilución 1:1000. Se incubó 1 hora a temperatura ambiente, posteriormente se lavó 3 veces con PBS. Los núcleos se tiñeron con Hoesch (ThermoScientific, IL, USA) a concentración 1.7 µM, se incubó por 7 minutos y se lavó 3 veces con PBS. Las preparaciones se montaron con la solución Aqua-Poly/Mount (Polysciences, PA, USA) y se observaron en el microscopio de fluorescencia confocal Nikon A1R.

8.5. Predicción de elementos de respuesta a estrógenos

La secuencia del gen EZH2 fue obtenida de la base de datos de National Center for Biotechnology Information (NCBI), Estados Unidos. Se obtuvieron las matrices de probabilidad para ERE de las plataformas JASPAR [Khan et al., 2018], HOMER [Heinz et al., 2010] y HOCOMOCO [Kulakovskiy et al., 2018]. Los datos se analizaron con el paquete TFBSTools [Tan and Lenhard, 2016] para R v.3.5. Únicamente los sitios con score mayor a 0.9 y predichos usando al menos dos matrices se consideraron como posibles EREs. Los archivos .bed generados fueron visualizados con el software Integrative Genomics Viewer (IGV) v.2.6.3 [Thorvaldsdóttir et al., 2013].

8.6. Silenciamiento de EZH2

El silenciamiento de EZH2 en las células U251 se llevó a cabo sembrando 200,000 células en cajas de 6 pozos en medio DMEM suplementado con 10 % de SFB. Tras 24 horas, el medio fue reemplazado por medio DMEM sin suplementar. Las células fueron transfectadas con siRNA control (10 nM, Santa Cruz, CA, #37007) o EZH2 siRNA (10 nM, Santa Cruz, CA, #35312) usando el reactivo Lipofectamine RNAiMAX (Thermo Scientific, USA) de acuerdo con las indicaciones del proveedor, el medio de transfección fue removido

después de 12 horas y reemplazado por medio DMEM suplementado con SFB libre de hormonas. Se incubaron las células por 24 horas antes de realizar los ensayos correspondientes. La eficiencia de la transfección fue determinada mediante Western Blot de la forma descrita en la sección 8.3.

8.7. Ensayos de proliferación celular

Posterior a la transfección, las células fueron tratadas con E2 10 nM o Vehículo (DMSO 0.01 %) por 48 horas, posteriores a las cuales se evaluó la proliferación usando el kit BrdU Labeling and Detection I (Roche, USA) de acuerdo con las instrucciones del proveedor. El colorante fluorescente Hoechst 33342 (Thermo Scientific, USA) se utilizó para teñir los núcleos. La señal fue observada con el microscopio de fluorescencia Olympus Bx43F. El número de células con incorporación de BrdU fue medido usando el software ImageJ (National Institute of Healt, USA), el porcentaje de células BrdU-positivas fue calculado considerando el número de núcleos teñidos con Hoechst como el 100 %.

8.8. Ensayos de migración

Después del silenciamiento, las células fueron cultivadas por 24 horas en medio DMEM libre de rojo de fenol suplementado con 10 % SFB libre de hormonas posteriores a las cuales se realizó una herida en la monocapa de células usando una punta de pipeta. El medio fue removido para eliminar las células flotantes y se reemplazó por medio DMEM suplementado con SFB libre de hormonas y adicionado con α-D-arabinofuranosida (Ara-C, 10 µM; Sigma-Aldrich, USA). El Ara-C es una molécula que inhibe la transición de la fase G1 a S del ciclo celular, por lo que es añadido al medio a fin de evitar que los efectos observados sean debido a un aumento en el número de células y no a la migración o invasión per se (Müller and Zahn, 1979). Las células fueron tratadas con E2 10 nM o Vehículo (DMSO 0.01 %) por 24 horas. Fotografías de la herida a las 0 y 24 horas post-tratamiento fueron tomadas con el microscopio invertido Olympus CKX41 y la cámara Infinity 1-2C (Lumenera, CAN). El área de la herida se determinó con el software ImageJ [Schneider et al., 2012].

8.9. Ensayos de invasión

Las células se cultivaron en las condiciones mencionadas anteriormente y 24 horas antes de comenzar el ensayo se cambió el medio por medio DMEM sin rojo no suplementado. El día del ensayo, se diluyó el gel de matriz celular (ECM, Sigma-Aldrich, USA) a una concentración final de 2 mg/mL con medio DMEM sin rojo fenol y sin SFB. Se colocaron los insertos (Corning, USA) en cajas de cultivo de 24 pozos y se añadieron 50 µL de la dilución de ECM en cada uno. Los insertos se incubaron por dos horas a 37°C y 5 % de CO_2 para permitir la gelificación de la matriz. Se sembraron en la parte superior de cada inserto 25,000 células en 150 µL de medio DMEM sin rojo de fenol y sin SFB con Ara-C 10 µM, al cual se le fue añadido el tratamiento correspondiente. En la parte inferior, se adicionaron 500 µL de medio DMEM sin rojo de fenol y 10 % de SFB libre de hormonas. La placa se incubó por 24 horas a 37°C. Transcurrido ese tiempo se eliminó el medio y el gel de ECM. Se fijaron las células con paraformaldehído (PFA, 4 %) por 20 minutos. El exceso de PFA se removió con un lavado de PBS seguido por un lavado con metanol al 100 %. Las células se lavaron nuevamente con PBS y se tiñeron con cristal violeta al 1 % durante 20 minutos, posteriores a los cuales se lavó 3 veces con PBS. Finalmente, el inserto se observó con la cámara Infinity 1-2C acoplada al microscopio invertido Olympus CKX41 a un aumento de 200X. Tres fotografías al azar se tomaron de cada inserto. El número de células se contó con el software ImageJ [Schneider et al., 2012].

8.10. Análisis de datos de secuenciación masiva de RNA (TCGA y GTEx)

Datos de RNA-seq pertenecientes a tumores primarios de los proyectos gliomas de bajo grado y GBMs (TCGA-LGG y TCGA-GBM) fueron descargados del portal Genomic Data Commons del Instituto Nacional del Cáncer (USA, https://gdc.cancer.gov/) usando el paquete “TCGAbiolinks” para R v.3.5 [Colaprico et al., 2016]. Se obtuvieron datos de 196 gliomas de bajo grado (LGG) y 139 GBM. Como tejido normal se utilizó el transcriptoma de 249 muestras de tejido sano de corteza cerebral obtenidas de la base de datos GTEx (https://gtexportal.org/home/). La normalización de datos y el análisis de expresión diferencial se llevaron a cabo con el paquete DESeq2 v.1.22.2 [Love et al., 2014]. Los gráficos fueron construidos con el paquete ggplot2 v3.2.1 [Wickham, 2016].

El análisis de enriquecimiento de sets de genes (GSEA) se llevó a cabo en el software del mismo nombre: GSEA v.4.01 [Subramanian et al., 2005]. Se utilizaron 4 sets de genes validados y reportados en la página web de GSEA

https://www.gsea-msigdb.org/gsea/index.jsp, los cuales se listan en la **Tabla 2**

Tabla 2: Sets de GSEA usados

Nombre	Descripción	Referencia
BENPORATH PRC2 TARGETS	Set de blancos del complejo PRC2 identificados por ChIP en células troncales embrionarias	[Ben-Porath et al., 2008]
HALLMARK ESTROGEN RESPONSE EARLY	Genes relacionados con una respuesta temprana a estrógenos	[Musgrove et al., 2008]
HALLMARK IL6 JAK/STAT3 SIGNALING	Genes regulados al alta por IL-6 a través de STAT3	[Ramadoss et al., 2010]
HALLMARK PI3K AKT MTOR SIGNALING	Genes regulados al alta por la activación de la vía de señalización PI3K/AKT/MTOR	[Grazia et al., 2014]

La base de datos Enrichr (http://amp.pharm.mssm.edu/Enrichr/) fue utilizada para realizar la búsqueda de términos de Ontología Génica (GO) para los genes regulados al alta o a la baja con un valor de $P<0.05$ en cada una de las comparaciones realizadas. Se utilizó la anotación de la base de datos KEGG 2019 HUMAN. Los gráficos presentan el top 10 de procesos biológicos de GO en cada condición.

La base de datos Enrichr (http://amp.pharm.mssm.edu/Enrichr/) fue utilizada para realizar la búsqueda de términos de Ontología Génica (GO) para los genes regulados al alta o a la baja con un valor de $P<0.05$ en cada una de las comparaciones realizadas. Se utilizó la anotación de la base de datos KEGG 2019 HUMAN. Los gráficos presentan el top 10 de procesos biológicos de GO en cada condición.

8.11. Análisis estadístico

Los datos de expresión basal de EZH2 tanto de mRNA como proteína fueron analizados con el software GraphPad Prism 5 para Windows mediante estadística paramétrica, se usó ANOVA de una vía seguida de la prueba post hoc de Tukey. Se consideraron significativos los valores de $p<0.05$. Para los experimentos con E2, así como las mediciones basales con y sin rojo de fenol, los datos se analizaron con una ANOVA de dos vías seguida de la prueba post hoc de Bonferroni. Se consideraron significativos los valores de $P<0.05$.

9. Resultados

9.1 EZH2 se expresa de forma basal en líneas celulares derivadas de GBMs humanos

Para evaluar el nivel de expresión de la subunidad catalítica de PRC2, EZH2, en tres diferentes líneas celulares derivadas de GBM humanos, éstas se cultivaron en medio DMEM con rojo de fenol y suplementado con 10 % de SFB. Como control se utilizó una muestra de RNA proveniente de un cultivo de astrocitos humanos sanos. La expresión relativa a 18S se muestra en la **Figura 7**. Las tres líneas celulares derivadas de GBM humanos (U87, U251 y D54) expresan EZH2 bajo condiciones basales y la expresión en U251 y D54 es mayor a la del cultivo primario de astrocitos. También se encontraron diferencias significativas entre ellas, siendo U251 la línea que mostró la mayor expresión y U87 la menor.

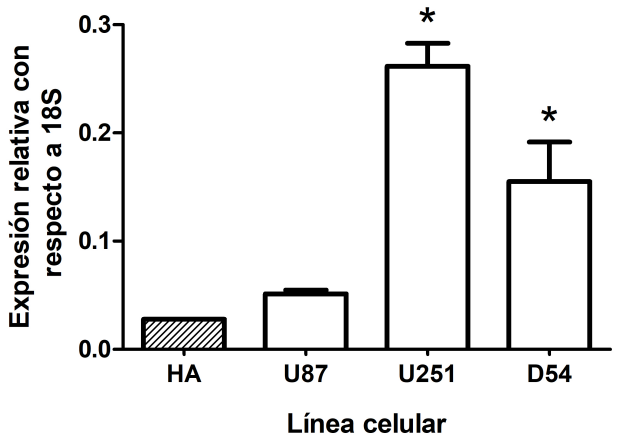

Figura 7: Expresión basal del mRNA de EZH2 en células derivadas de GBM humanos. La cantidad de RNA mensajero correspondiente a EZH2 fue determinada mediante RT-qPCR en tres diferentes líneas celulares derivadas de GBM humanos (U87, U251 y D54) cultivadas bajo condiciones basales y una muestra de astrocitos humanos (HA). *P<0.05 vs U87 y HA. La expresión relativa de EZH2 se calculó por el método de ΔCT usando como referencia al RNA ribosomal 18S. Cada barra representa la media ± E.E. de tres experimentos independientes.

Debido a que se sabe que el rojo de fenol es un ligando del ER [Berthois et al., 1986] y que

el SFB contiene hormonas esteroides [Milo et al., 1976] decidimos evaluar la expresión basal de EZH2 en células cultivadas por 24 horas en medio DMEM sin rojo de fenol y suplementado con SFB filtrado con carbón activado (libre de hormonas) a fin de comparar con los resultados obtenidos anteriormente. En este caso se confirmó que la expresión de EZH2 es diferencial entre las líneas celulares, siendo U87 la que tiene la menor expresión y U251 la mayor, sin embargo, al comparar entre las dos condiciones se observaron diferencias significativas en la expresión de EZH2 en la línea U251 **(Figura 8)**.

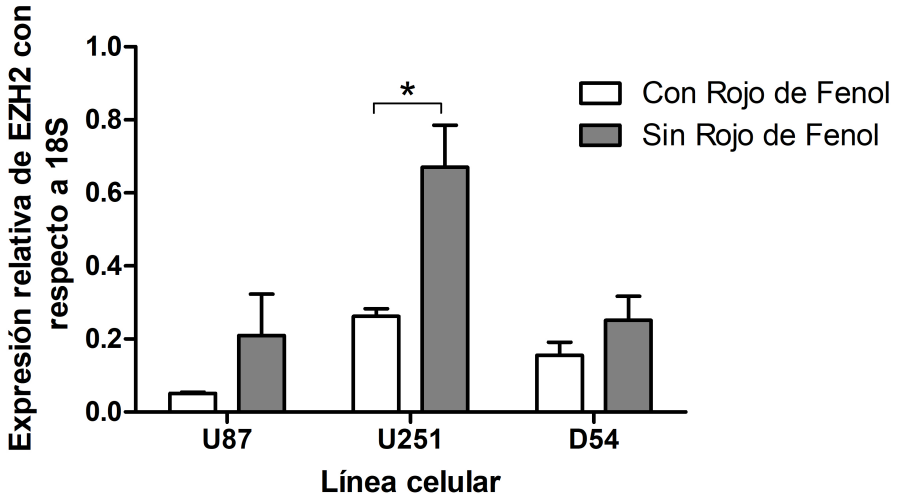

Figura 8: Expresión basal del mRNA de EZH2 en células derivadas de GBM humanos cultivadas en medio sin rojo de fenol. La cantidad de RNA mensajero correspondiente a EZH2 fue determinada mediante RT-qPCR en tres diferentes líneas celulares derivadas de GBM humanos (U87, U251 y D54) cultivadas en medio sin rojo de fenol y suplementado con SFB filtrado con carbón activado y comparada contra células cultivadas en medio DMEM con rojo de fenol suplementado con SFB completo. La expresión relativa de EZH2 se calculó por el método de ΔCT usando como referencia al RNA ribosomal 18S.

*P<0.05. Cada barra representa la media ± E.E. n=3.

Para corroborar que los cambios en los niveles de mRNA de Ezh2 correlacionan con el nivel de proteína, se evaluó por medio de Western blot la expresión basal de EZH2 en las líneas celulares derivadas de GBM humanos U87, U251 y D54 cultivadas en medio DMEM con rojo de fenol. Se observó que todas las líneas expresan la proteína EZH2 en condiciones basales y que la U251 es la que presentó el mayor contenido de esta, mientras que la línea U87 tuvo el menor contenido de dicha proteína **(Figura 9a)**. La misma determinación se realizó en células cultivadas en medio sin rojo de fenol y suplementado con SFB filtrado con carbón activado **(Figura 9b)**, en este caso no se encontraron diferencias significativas entre las líneas celulares.

Con el fin de observar la localización intracelular de EZH2, inmunofluorescencia se evaluó la localización celular de EZH2 en células derivadas de GBM humanos, se observó que en las tres líneas celulares U87, U251 y D54 la proteína se expresa en la totalidad de las

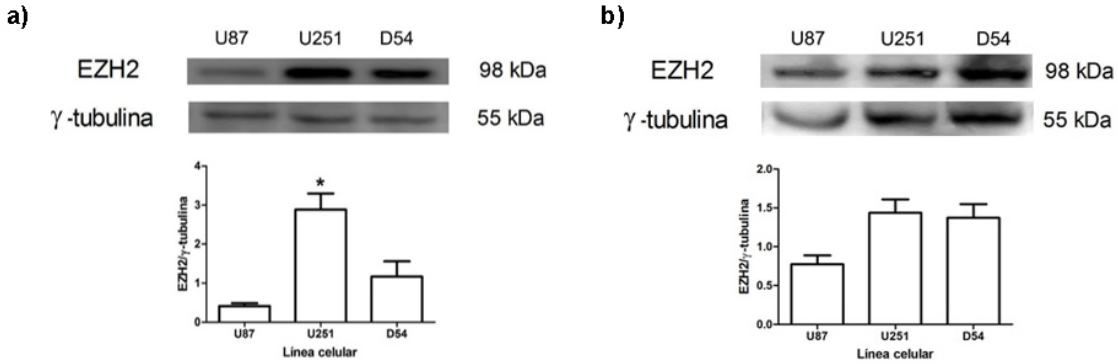

Figura 9: Niveles basales de la proteína EZH2 en células derivadas de GBM humanos. La cantidad de EZH2 fue determinada a nivel proteína mediante Western blot en tres diferentes líneas celulares derivadas de GBM humanos (U87, U251 y D54) cultivadas bajo condiciones basales. a) Determinación con medio DMEM con rojo de fenol y 10 % SFB completo *P<0.05 vs. U87 y D54 . Cada barra representa la media ± E.E. n=3. b) Determinación con medio DMEM sin rojo de fenol y 10 % SFB sin hormonas. La densidad de cada banda se calculó con el software ImageJ, γ-tubulina se usó como control de carga. Cada barra representa la media ± E.E. n=3.

células y se encuentra en el núcleo, ya que co-localiza la señal del anticuerpo con la del colorante Hoechst utilizado para teñir el núcleo, como se muestra en la **Figura 10**. Como control negativo se cultivaron células en condiciones basales y se realizó la inmunofluorescencia sin el anticuerpo monoclonal contra EZH2 (Ver **Figura suplementaria I** en página 81). No se detectó señal para EZH2 en el control negativo.

En resumen, se encontró que las tres líneas evaluadas expresan a EZH2 de forma basal y en niveles mayores que los astrocitos humanos (HA). Las líneas D54 y U251 son las que presentan mayor expresión tanto a nivel de mRNA como de proteína. Además, por medio de inmunofluorescencia se estableció que en las tres líneas celulares EZH2 se encuentra localizado mayormente en el núcleo.

9.2 E2 no incrementa la expresión de EZH2 en GBM humanos

Con el fin de determinar si la expresión de EZH2 puede ser regulada por E2, se realizó un análisis *in silico* para buscar sitios de unión a ERE (**Figura 11**), donde se encontró que la región promotora del gen tiene dos posibles ERE, además de tres probables elementos de respuesta a progesterona (PRE) y dos a andrógenos (ARE). Las secuencias de los sitios de unión se muestran en la **Tabla 3**. También se buscaron en la bibliografía EREs previamente validados en el promotor de EZH2. En particular, Bhan y colaboradores reportaron tres posibles EREs y los validaron mediante ensayos de luciferasa [Bhan et al., 2014].

Para evaluar el efecto *in vitro* del estradiol en la expresión de EZH2 se trataron las células

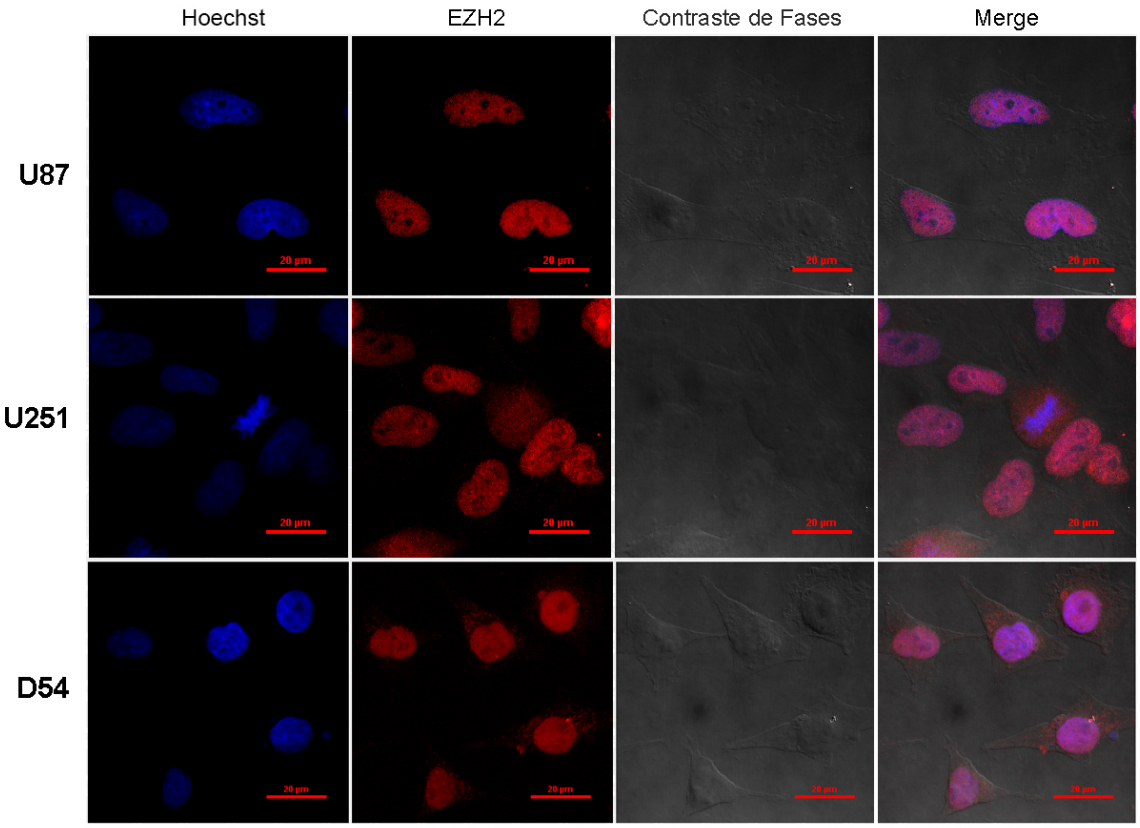

Figura 10: Localización subcelular de EZH2 en las células U87, U251 y D54. Se cultivaron células en condiciones basales y se realizó la inmunofluorescencia utilizando un anticuerpo monoclonal contra EZH2 y un anticuerpo secundario acoplado a Alexa Fluor. Se observa que EZH2 se encuentra en el núcleo ya que co-localiza con la marca obtenida con el colorante Hoechst.

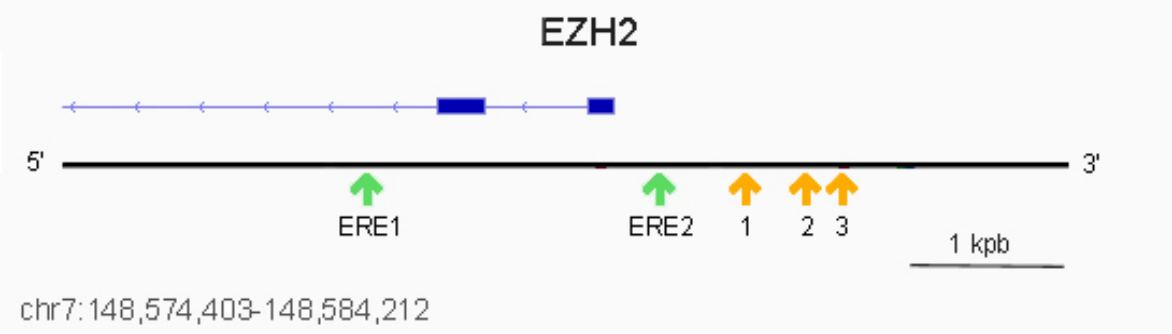

Figura 11: Análisis *in silico* de la presencia de EREs en el promotor del gen EZH2. Representación visual del gen EZH2 (azul). Los ERE predichos por el análisis *in silico* están marcados con flechas verdes. El análisis se realizó en tres plataformas diferentes (JASPAR, HOCOMOCO y HOMER), se consideró un posible sitio de unión aquellos predichos por dos o más bases de datos con un valor de score de 9 o más y $P<0.05$. Las flechas amarillas señalan los sitios de unión predichos y validados por [Bhan et al., 2014].

Tabla 3: Elementos de respuesta a estrógenos en la secuencia promotora del gen EZH2

Elemento	Posición	Hebra	Secuencia
ERE1	-354 a -368	-	ATGTCTCCCGGTCCC
ERE2	+1599 a + 1586	-	TAATAACTTGCTTG
Sitios reportados por Bhan y colaboradores			
1	-846 a -859	-	GACCAGCCTGACC
2	-1238 a -1251	-	CGATCTCCTGACC
3	-1488 a -1501	-	AGGTAGCTTGACC

U251, U87 y U251 con E2 (10 nM) por 3, 6, 12 y 24 horas posteriores a las cuales se evaluó la expresión de EZH2 a nivel de mRNA mediante RT-qPCR. Los datos muestran que el E2 induce la expresión de EZH2 en la línea U87 después de 12 horas de tratamiento, sin embargo, no se observaron cambios significativos en las células U251 ni D54 (**Figura 12)**.

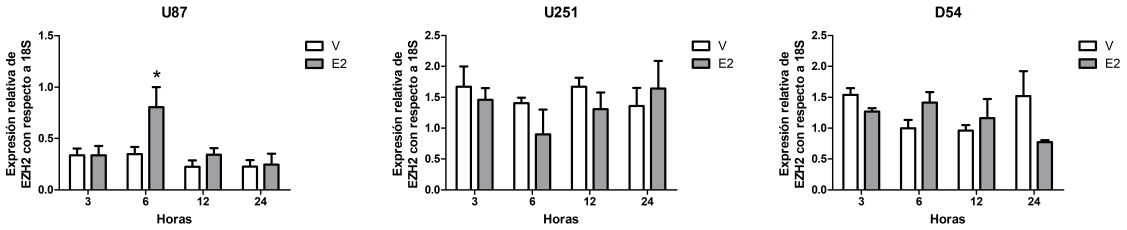

Figura 12: Efecto del E2 en la expresión de EZH2 en líneas celulares derivadas de GBM humanos. Los cambios en la expresión de EZH2 fueron cuantificados mediante RT-qPCR después de que las células fueron tratadas con E2 10 nM o V (CDX 40 nM) por 3, 6, 12 y 24 horas. La expresión relativa de EZH2 se calculó por el método de ΔCT usando como referencia al RNA ribosomal 18S. *P<0.001 vs V. Cada barra representa la media ± E.E. n=3.

Dado que no se observó efecto del E2 en la línea celular U251, se realizó una curva de concentraciones de E2 y se evaluó la expresión de EZH2 por medio de RT-qPCR a las 12 y 24 horas posteriores al tratamiento. Sin embargo, no se detectaron cambios significativos en la expresión del gen EZH2 (**Figura 13**).

Para corroborar los datos obtenidos mediante RT-qPCR, los niveles de proteína se determinaron mediante Western blot, sin embargo, no se observaron cambios significativos inducidos por el E2 en ninguna de las líneas celulares a ninguno de los tiempos evaluados (**Figura 14**). Por lo que se concluye que el E2 no regula la expresión de EZH2 en las líneas celulares U87, U251 y D54.

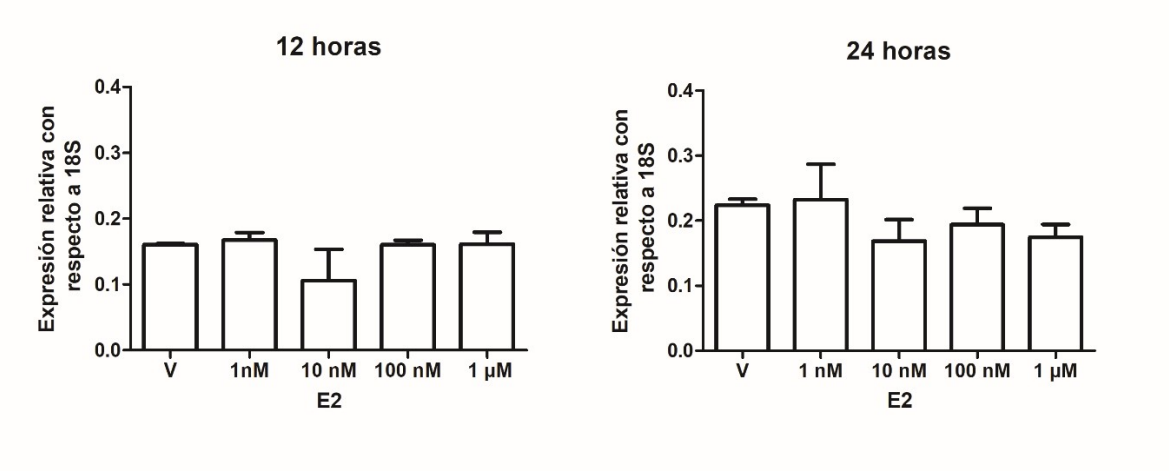

Figura 13: Efecto del E2 en la expresión de EZH2 en la línea celular U251. Los cambios en la expresión de EZH2 fueron cuantificados mediante RT-qPCR después de que las células fueron tratadas con con E2 (1 nM, 10 nM, 100 nM y 1 µM) o V (CDX 40 nM) por 12 y 24 horas. La expresión relativa de EZH2 se calculó por el método de ΔCT usando como referencia al RNA ribosomal 18S. Cada barra representa la media ± E.E. n=3.

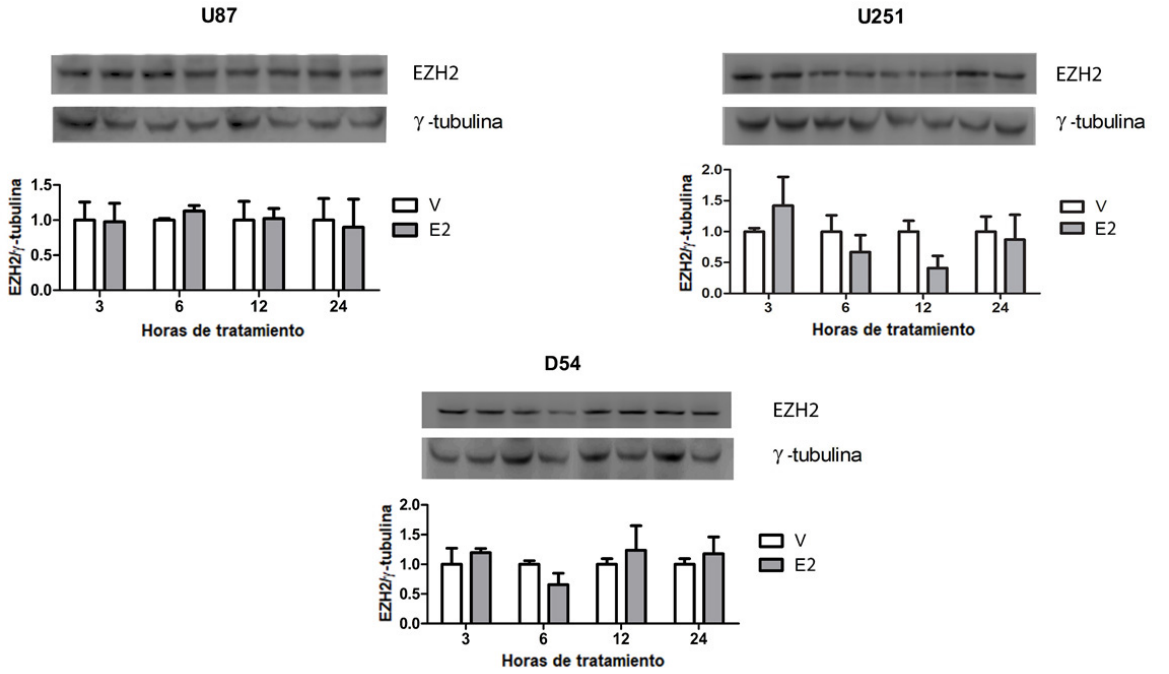

Figura 14: Efecto del E2 sobre la cantidad de proteína EZH2. Los cambios en la cantidad de EZH2 fueron evaluados mediante Western blot después de que las células fueron tratadas con E2 10 nM o V (CDX 40 nM) por 3, 6, 12 y 24 horas. Cada barra representa la media ± E.E. n=4.

9.3 El silenciamiento de EZH2 inhibe la proliferación, invasión y migración inducida por E2

Debido a que se sabe que el E2 puede modular la actividad de EZH2 sin modificar su expresión y que ambas proteínas tienen efectos similares en la proliferación, migración e invasión de las células derivadas de GBM, decidimos evaluar el impacto del silenciamiento vía RNAi de EZH2 sobre los efectos inducidos por E2 en la línea celular U251. Por medio de Western blot se comprobó la eficacia de los siRNAs utilizados en el silenciamiento, se obtuvo un 54 % de disminución en la expresión a EZH2 (**Figura 15a**).

Para evaluar el efecto del silenciamiento de EZH2 en las células U251 tratadas con E2, se realizó un ensayo de BrdU. Brevemente, el ensayo consiste en incubar las células con un análogo de timina (5-bromo-2'-desoxiuridina o BrdU) el cual será incorporado al DNA durante la replicación, las células que han pasado por mitosis pueden ser detectada por inmunofluorescencia usando anticuerpos α-BrdU. Mediante este ensayo, se encontró que en el grupo transfectado con el siRNA control, el E2 indujo la proliferación de las células U251 transfectadas en comparación con V, sin embargo, en el grupo donde fue silenciado EZH2 no se observaron diferencias significativas entre los tratamientos con V o E2 (**Figura 15b,c**). Estos resultados sugieren que EZH2 podría tener un papel importante en la

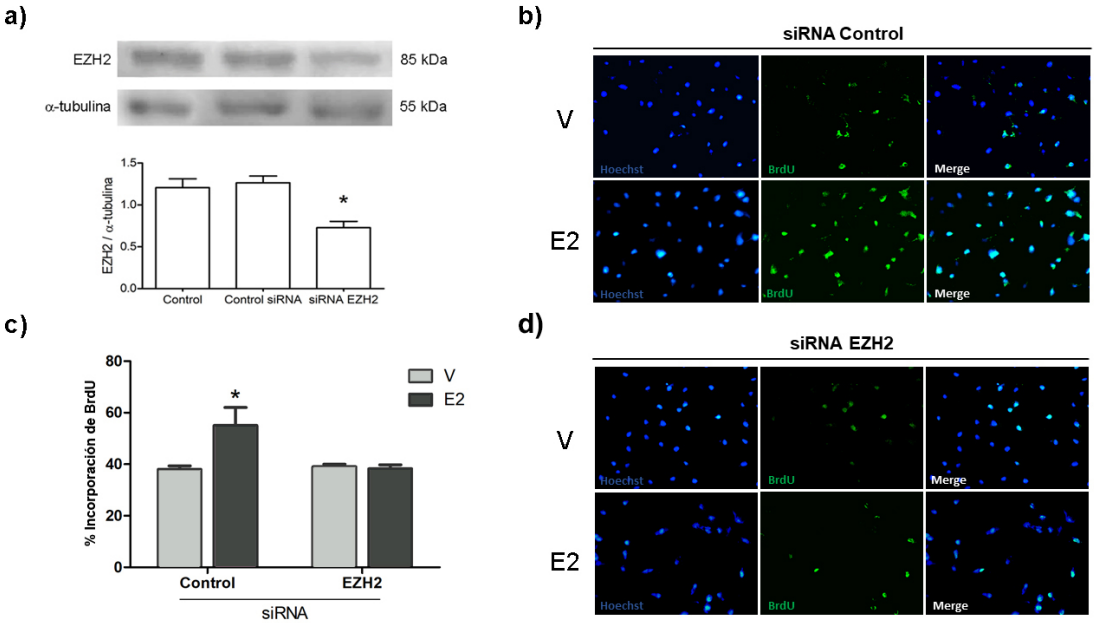

Figura 15: Efecto del silenciamiento de EZH2 en la proliferación inducida por E2. a) La validación del silenciamiento se realizó mediante Western BlotB lot. * P <0.05. vs los demás grupos. b) Fotografías representativas de las células U251 en proliferación con siRNA control o siRNA contra EZH2, tratadas con E2 (10 nM) o V (CDX 40 nM) por 48 horas. c) Porcentaje de células positivas a BrdU en cada tratamiento, *P<0.05. vs los demás grupos.

inducción de la proliferación mediada por E2 en la línea celular U251.

Además de la proliferación, se ha reportado que el E2 induce la migración e invasión de líneas celulares derivadas de GBM. Para evaluar si estos procesos son mediados por E2, se realizaron ensayos de migración en la línea celular U251, en los cuales se observó que en el grupo transfectado con el siRNA control, el tratamiento con E2 presenta una mayor cantidad de células que migraron hacia el interior de la herida en comparación a las células tratadas con V. Por otra parte, en el grupo donde fue silenciado EZH2 no se observaron diferencias significativas entre los tratamientos con V o E2 (**Figura 16a,b**). El mismo efecto se observó en los ensayos de invasión realizados en cámara de Transwell; mientras que en el grupo transfectado con el siRNA control se observa un mayor número de células invasoras al tratar con E2, al silenciar a EZH2 no se observan diferencias significativas entre los tratamientos con V o E2. (**Figura 16c,d**). Las observaciones anteriores indican que la migración e invasión inducidas por E2 en la línea celular U251 podrían estar mediadas en parte por EZH2.

9.4 EZH2 y ERs en biopsias de GBM

Debido a que las observaciones previas sugieren que puede haber una interacción entre las acciones de EZH2 y la de los ERs en GBMs, se analizaron los datos transcriptómicos disponibles en la plataforma de TCGA y GTEx. En total se obtuvieron y analizaron 196 muestras de gliomas de bajo grado (LGG) y 139 de GBM. Como tejido normal se utilizaron 249 muestras de tejido sano proveniente de corteza cerebral.

En las muestras evaluadas, la expresión de ERα es menor en LGG y GBMs con respecto al tejido normal (**Figura 17a**). De manera interesante, la expresión de este receptor en GBM es mayor que en LGG. En cuanto a ERβ, los GBM tienen mayores niveles de este receptor que el tejido sano y los gliomas de bajo grado (**Figura 17b**). Ya que es la primera vez que la expresión de ERα y ERβ es reportada en un set de muestras tan amplio y los análisis bioinformáticos son susceptibles a errores debidos al procesamiento de datos, se incluyó la expresión de EZH2 como control de la anotación de genes y preprocesamiento de cuentas. Es observable que la expresión de EZH2 aumenta conforme progresa el grado del tumor (**Figura 17c**), tal como reportaron Zhang y colaboradores en 2015.

Al comparar los niveles de estos receptores, se encontró que tanto en los tejidos tumorales como en tejido sano la expresión de ERα es mayor que la de ERβ (**Figura 17d**). Para comprobar lo anterior, se dividió la expresión de ERα entre la de ERβ en cada tumor y se graficó esta relación. En la mayoría de los casos el valor es mayor a 1, lo que indica que hay una mayor cantidad de ERα. No se encontraron diferencias significativas, pero se observa una ligera tendencia negativa con respecto al grado del tumor (**Figura 17e**).

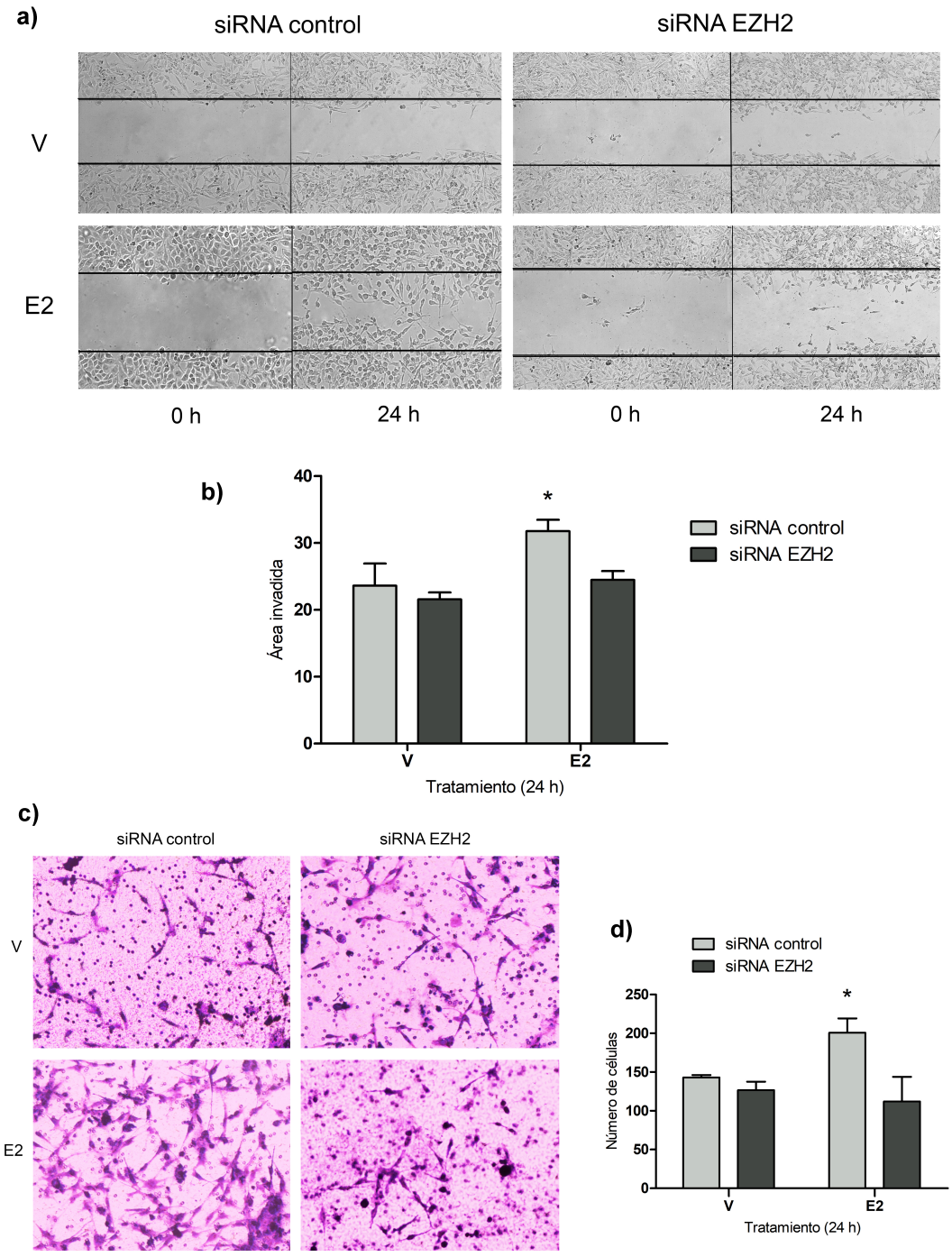

Figura 16: Efecto del silenciamiento de EZH2 en la migración e invasión inducidas por E2. a) Imágenes representativas de los ensayos de migración realizados en la línea celular U251 transfectadas con siRNA control o siRNA contra EZH2, tratadas con E2 (10 nM) o V (CDX 40 nM). b) Comparación del área invadida por las células en los diferentes tratamientos. *P<0.05. vs los demás grupos. c) Fotografías representativas de las células invasoras en los tratamientos previamente descritos. d) Conteo de células invasoras. *P<0.05. vs los demás grupos.

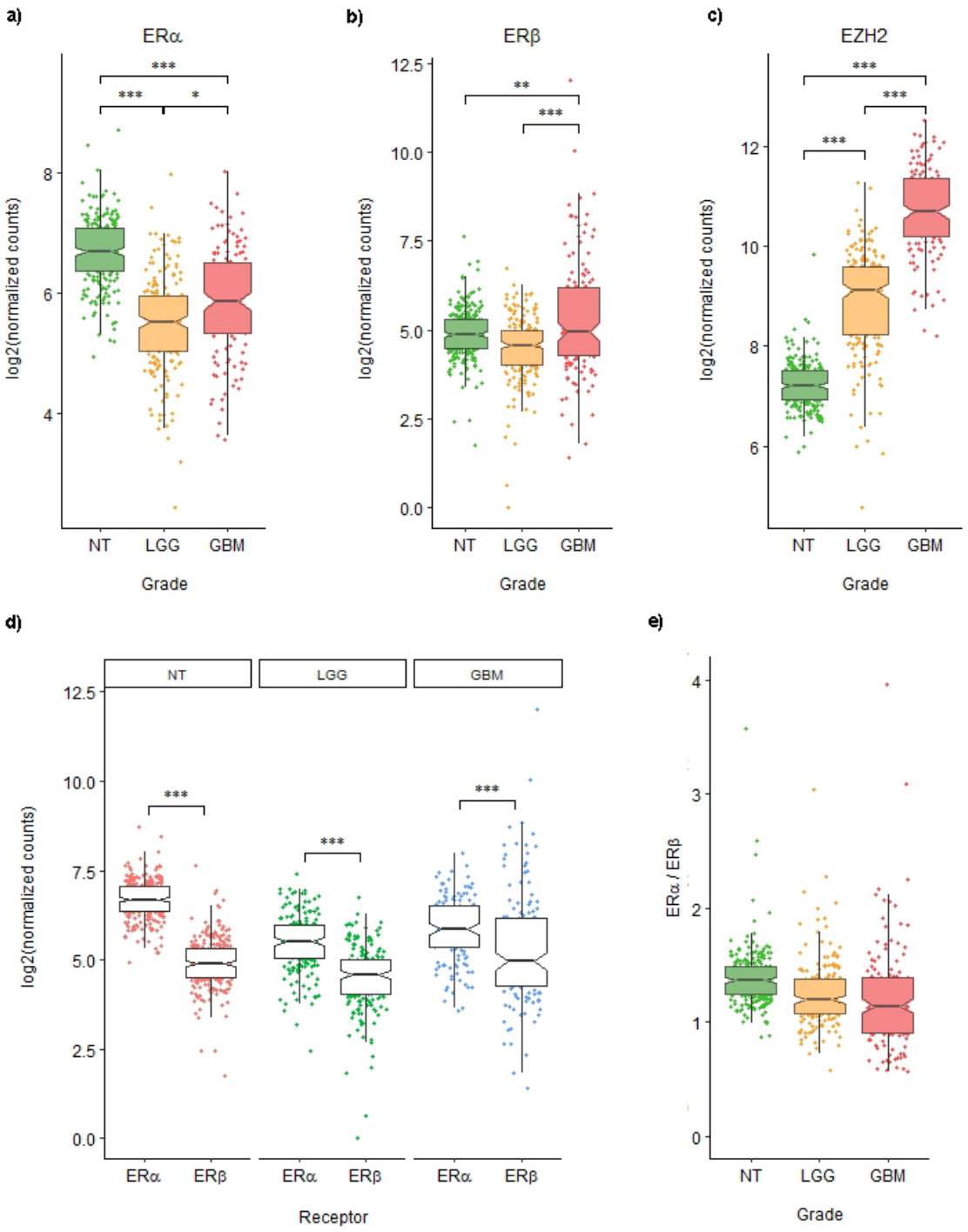

Figura 17: Expresión de EZH2, ERα y ERβ en biopsias de gliomas humanos. Datos de RNA-seq obtenidos de TCGA. Se analizaron 335 gliomas primarios (196 gliomas de bajo grado (LGG) y 139 GBM). 249 muestras procedentes de corteza cerebral sana fueron utilizadas como control (tejido normal, NT). a,b,c) Niveles de EZH2 ERα y ERβ respectivamente en diferentes grados de glioma. *P<0.05, **P<0.01, ***P<0.001. d) Comparación entre los niveles de ERα y ERβ n tejido sano y gliomas humanos. ***P<0.001 vs ERα. e) Relación ERα/ERβ en tejido normal, LGG y GBM.

Debido a que se observa que los GBM presentan heterogeneidad en la expresión de ERα y ERβ se calculó el valor de Z score con el fin de observar la distribución de los datos en las muestras de GBM y tejido normal. Las muestras fueron estratificadas usando el método de agrupamiento jerárquico. Nuestro análisis demostró que son distinguibles tres grupos o clústeres de muestras, como se observa en la **Figura 18a**: el grupo 1 se caracteriza por baja expresión de ERα y ERβ con respecto a tejido normal; el grupo 2 por expresión normal de ERβ y baja de ERα mientras que el grupo 3 por alta expresión de ERβ solamente (**Figura 18b, c**). Los tres grupos tienen alta expresión de EZH2 en comparación con tejido normal, sin embargo, no hay diferencias significativas entre ellos (**Figura 18d**).

A fin de identificar los genes diferencialmente expresados en los tres grupos de muestras, se condujo un análisis de expresión diferencial para obtener una lista de genes

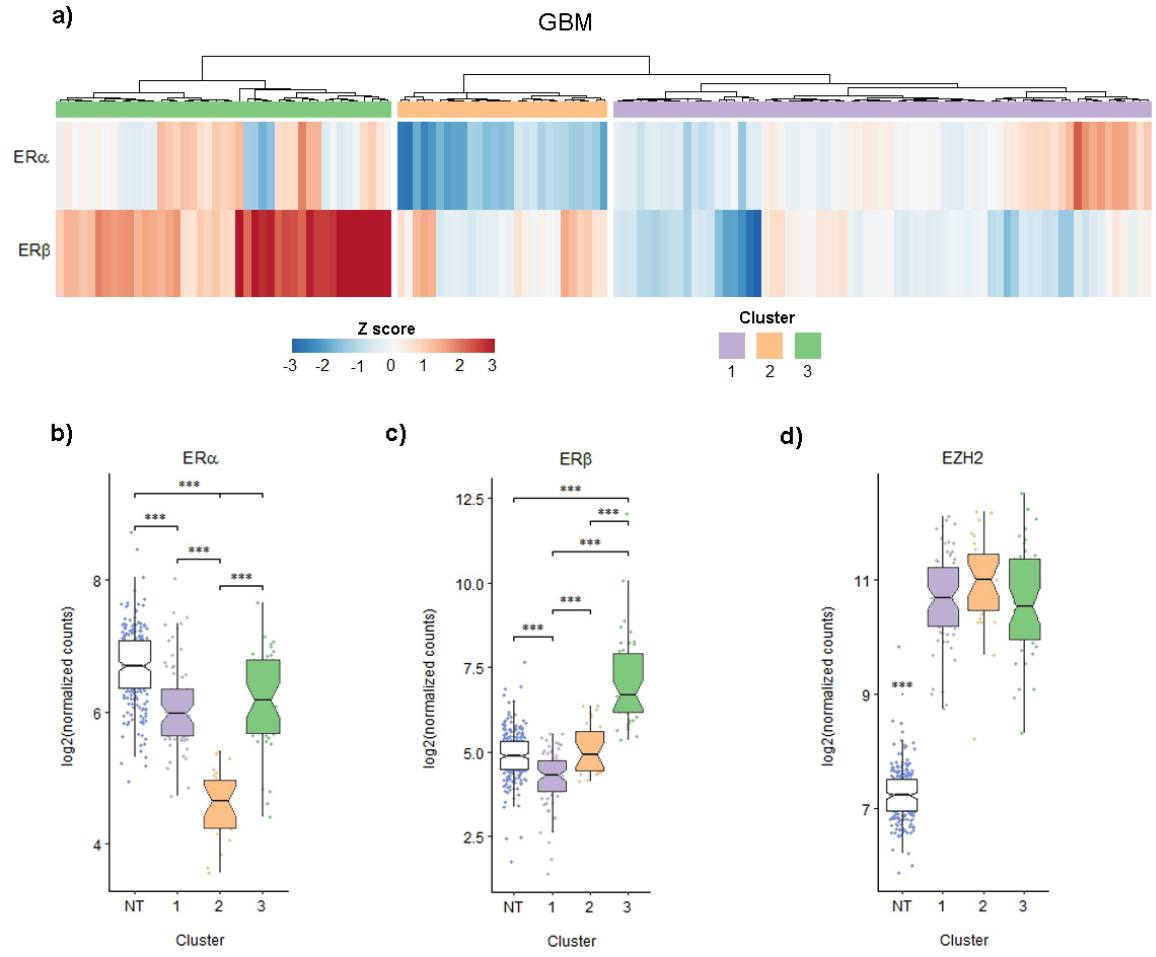

Figura 18: Clústeres de expresión de EZH2, ERα y ERβ en biopsias de GBM humanos. Datos de RNA-seq obtenidos de TCGA. Se analizaron 139 GBM primarios. a) Mapa de calor que muestra la expresión de ERα y ERβ en cada uno de los GBM primarios estudiados. b, c) Niveles de ERα y ERβ respectivamente en los diferentes grupos formados en el inciso a. *** P<0.001. d) Expresión de EZH2 en los diferentes grupos. *** P <0.001 vs el resto de los grupos.

ordenada (de mayor a menor) de acuerdo con la tasa de cambio en su expresión entre los grupos identificados mediante el agrupamiento. Dicha lista fue utilizada para un análisis de Enriquecimiento de Sets de Genes (GSEA) a fin de observar el comportamiento de cuatro sets de expresión previamente reportados.

En primer lugar, para saber si los ERs se encuentran activos en los grupos formados, se utilizó un set de genes validados, característicos de la respuesta a estrógenos. Se observó que el grupo 3 tiene un mayor enriquecimiento de este set en comparación con los grupos 1 y 2. El grupo 1 también presenta mayor expresión en los genes correspondientes a respuesta a estrógenos en comparación con el grupo 2 (**Figura 19**). Para evaluar la expresión de los genes susceptibles a regulación por PRC2, se usó un set de genes que contiene blancos del complejo PRC2 en células troncales derivadas de GBM, validados mediante ChIP de la marca H3K27me3 y que poseen en sus promotores a SUZ12 y EED [Ben-Porath et al., 2008]. Sin embargo, en ninguna de las comparaciones existen diferencias significativas, tampoco se observó una clara tendencia en cuanto a la regulación a la baja o alta de los genes blanco de PRC2 (**Figura 19**).

Se ha reportado en diversos trabajos que la activación de la vía PI3K/AKT promueve la fosforilación de EZH2, inhibiendo su actividad de KMT e induciendo la metilación de

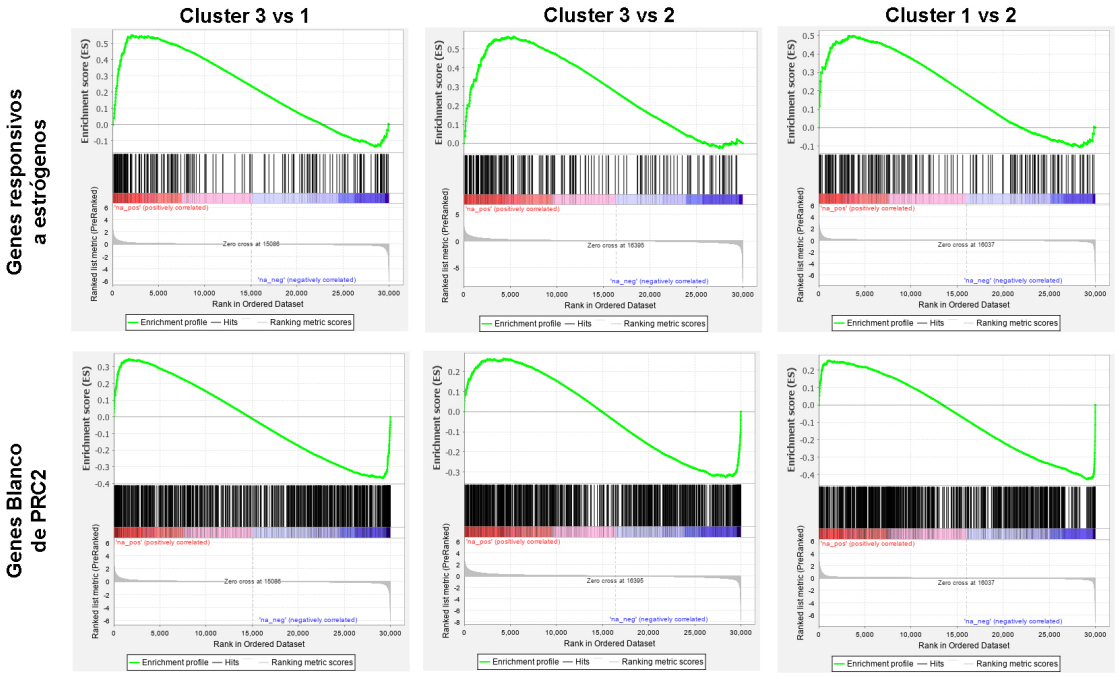

Figura 19: Análisis de Enriquecimiento. Se realizó un análisis de expresión diferencial a fin de identificar los genes que se encuentran principalmente regulados a la alta o baja en los tres grupos de GBMs establecidos. Se evaluaron genes relacionados con la respuesta a estrógenos y blancos comprobados del complejo PRC2.

STAT3 [Kim et al., 2013, Chang et al., 2017, Qin et al., 2019, Loreti et al., 2020]. También es sabido que los receptores a estrógenos a través de su mecanismo de acción no clásico activan esta vía [Fuentes and Silveyra, 2019]. Ya que el grupo 3 presenta un mayor enriquecimiento en la expresión de genes responsivos a estrógenos, se evaluó la expresión de un set de genes característicos de la activación de la vía de señalización JAK/STAT3, así como genes regulados al alta por PI3K/AKT (**Figura 20a**). Es observable que, con respecto a tejido normal, el grupo 3 presenta mayor enriquecimiento en los sets previamente mencionados.

Debido a que previamente se demostró que el E2 promueve la proliferación y migración de células derivadas de GBM y a que el grupo 3 de muestras es el que presenta mayor enriquecimiento de genes característicos de la respuesta a estrógenos, se utilizaron dos sets de genes provenientes de la plataforma Gene Ontology y que están relacionados con los procesos de proliferación (GO:0008283) y migración (GO:0016477) celulares. El grupo 3 presenta mayor enriquecimiento en estos sets en comparación con los grupos 1 y 2 (**Figura 20b**), lo que sugiere que las muestras pertenecientes al clúster 3 tienen una mayor actividad de ER.

Finalmente, para obtener una idea competa de los procesos regulados diferencialmente en el cluster 3 con respecto a los otros dos, se realizó un análisis de expresión diferencial y la correspondiente anotación de los genes con expresión diferencial.

En las **Figuras 21 y 22** se presentan los 10 procesos con menor valor de P tanto a la baja como al alta. En el grupo 3 respecto a los grupos 1 y 2, se encuentran regulados al alta genes involucrados en la adhesión focal, en la interacción con la matriz extracelular, diversos procesos relacionados con linajes hematopoyéticos, e interesantemente, la vía de señalización PI3K/AKT. Por otra parte, a la baja se encuentran procesos relacionados con estrés oxidativo, ya que los principales genes están involucrados en la cadena respiratoria o pertenecen al metabolismo mitocondrial.

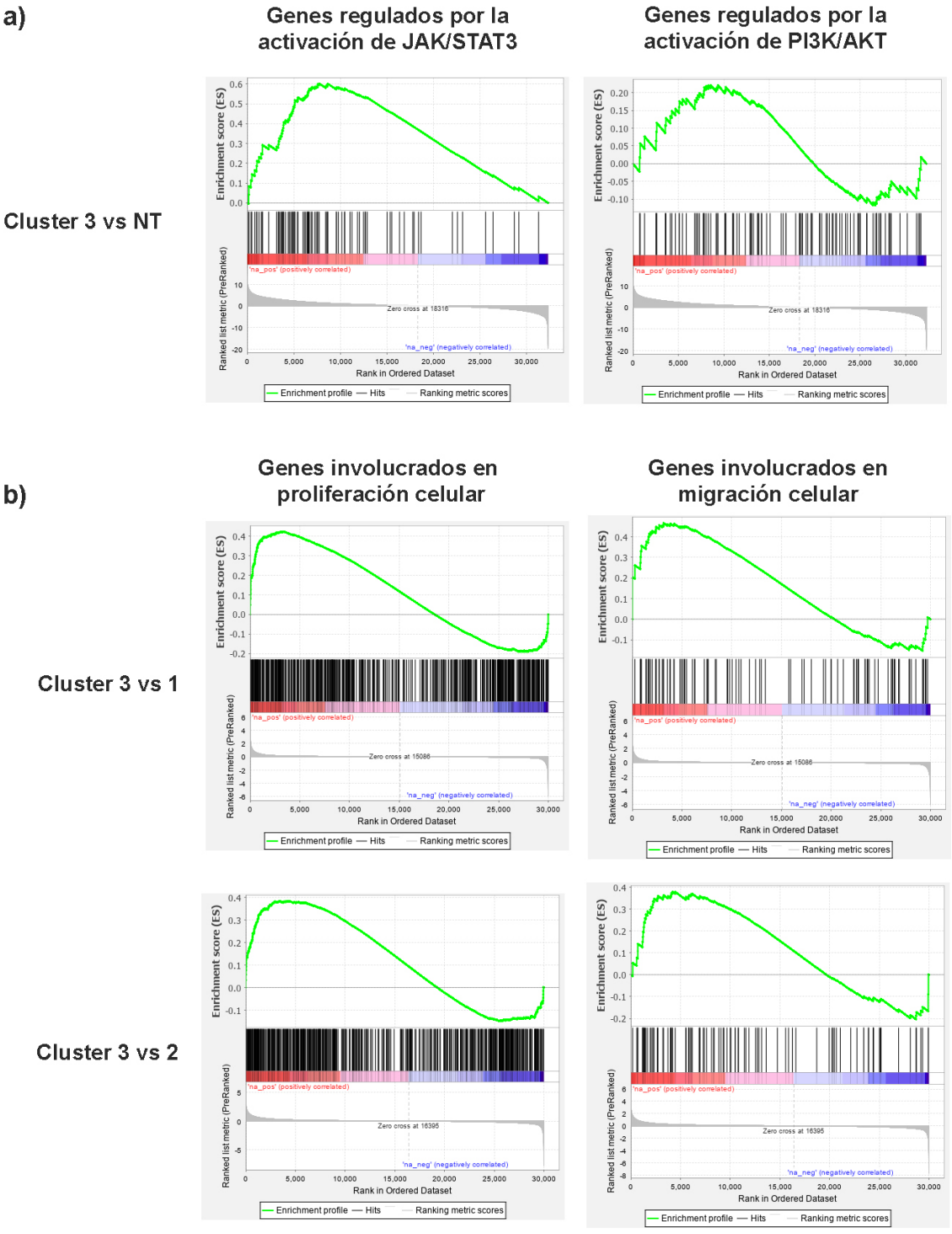

Figura 20: Análisis de Enriquecimiento en grupo 3 de muestras de GBM. a) Se realizó el análisis de expresión diferencial entre el grupo 3 de biopsias de GBM y las muestras de tejido normal. Se muestra el análisis de enriquecimiento de genes involucrados en la respuesta a la activación de la vía JAK/STAT3 y la vía de PI3K/AKT. b) Comparación en el enriquecimiento de genes involucrados en los procesos de proliferación y migración en el grupo 3 con respecto a los grupos 1 y 2.

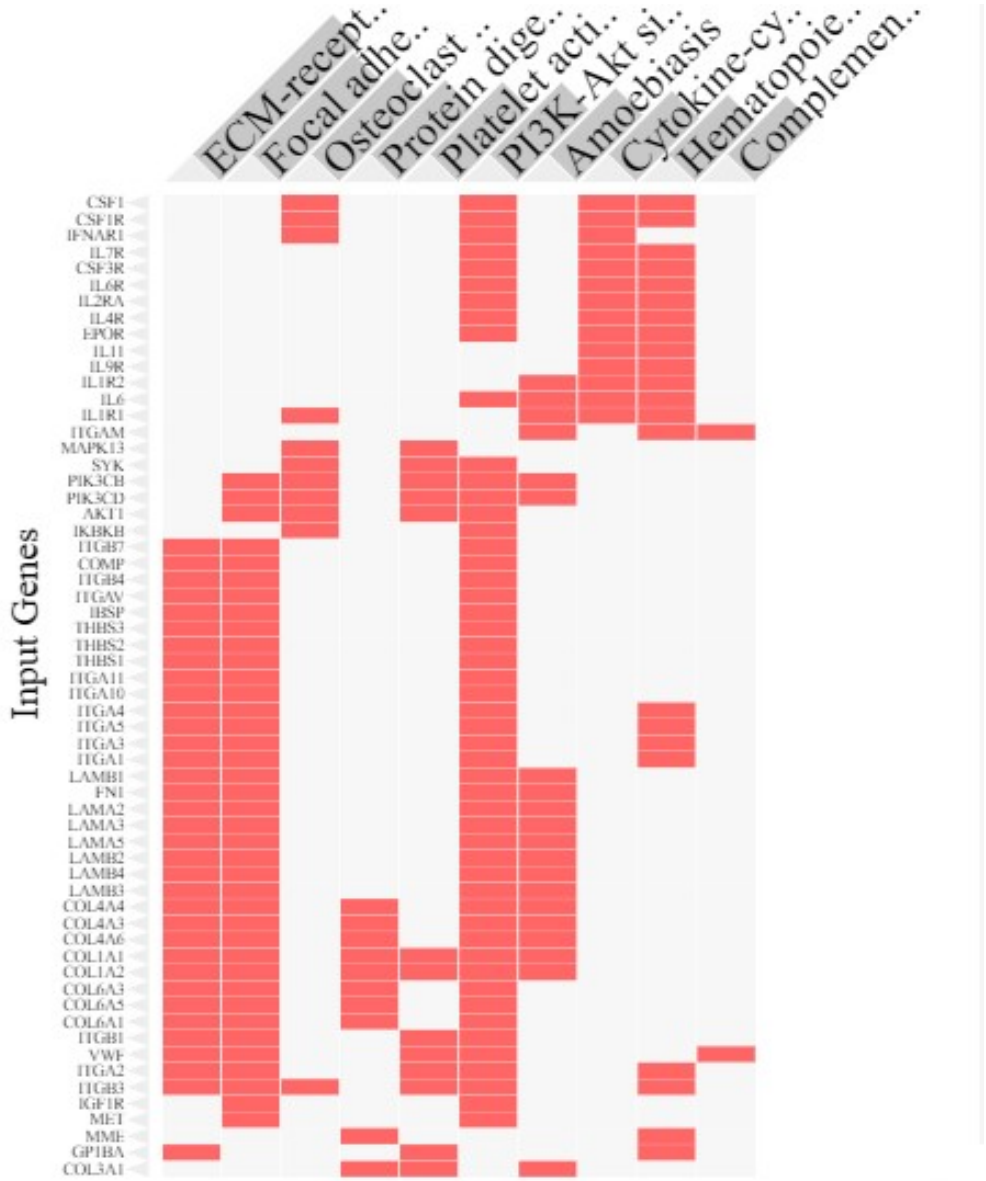

Name	P-value	Adjusted p-value	Odds Ratio	Combined score
ECM-receptor interaction	2.614e-13	8.052e-11	3.51	101.75
Focal adhesion	8.137e-10	1.253e-7	2.25	47.03
Osteoclast differentiation	2.117e-8	0.000002173	2.45	43.23
Protein digestion and absorption	2.127e-7	0.00001637	2.61	40.11
Platelet activation	3.127e-7	0.00001926	2.32	34.79
PI3K-Akt signaling pathway	3.561e-7	0.00001828	1.73	25.75
Amoebiasis	0.000001068	0.00004699	2.45	33.65
Cytokine-cytokine receptor interaction	0.000002017	0.00007765	1.75	22.99
Hematopoietic cell lineage	0.000004299	0.0001471	2.34	28.96
Complement and coagulation cascades	0.000005202	0.0001602	2.49	30.35

Figura 21: Procesos biológicos diferencialmente regulados al alta en el grupo 3 vs los grupos 1 y 2. Se tomaron como genes regulados al alta a aquellos con P <0.05 y log2 Fold Change mayor a 0.

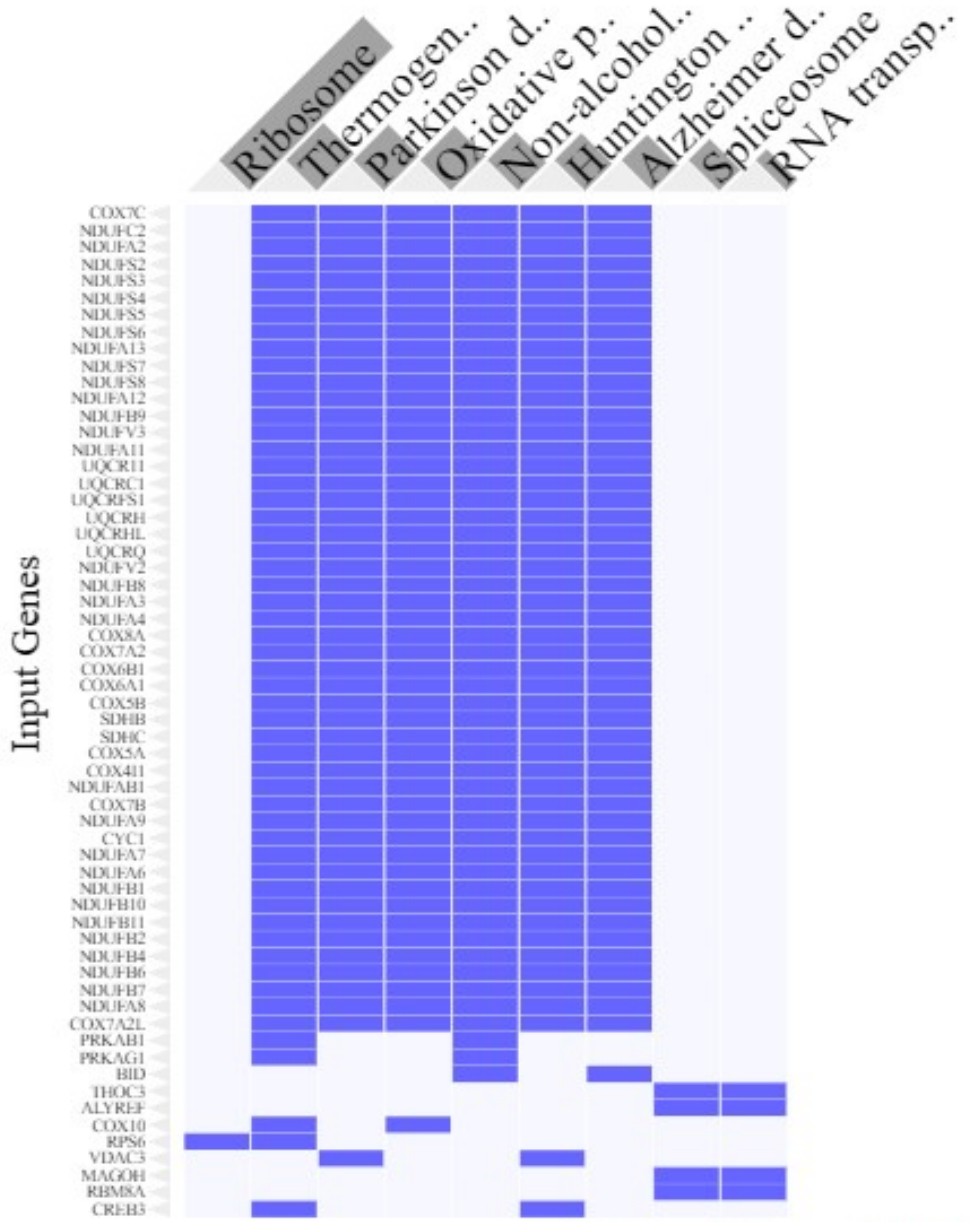

Name	P-value	Adjusted p-value	Odds Ratio	Combined score
Ribosome	3.929e-60	1.210e-57	5.17	707.00
Thermogenesis	3.297e-16	5.078e-14	2.52	89.86
Parkinson disease	2.335e-15	2.397e-13	2.94	98.93
Oxidative phosphorylation	6.507e-15	5.010e-13	2.97	97.11
Non-alcoholic fatty liver disease (NAFLD)	1.733e-12	1.068e-10	2.65	71.86
Huntington disease	7.206e-12	3.699e-10	2.38	61.16
Alzheimer disease	2.450e-11	1.078e-9	2.44	59.58
Spliceosome	1.762e-9	6.784e-8	2.47	49.74
Proteasome	2.115e-8	7.238e-7	3.51	62.11
RNA transport	0.00002510	0.0007731	1.87	19.85

Figura 22: Procesos biológicos diferencialmente regulados a la baja en el grupo 3 vs los grupos 1 y 2. Se tomaron como genes regulados al alta a aquellos con P <0.05 y log2 Fold Change mayor a 0.

10. Discusión

Las líneas celulares U87, U251 y D54 expresan EZH2 de forma basal

En este trabajo se evaluó el efecto del E2 en la regulación de la expresión y actividad de la enzima metiltransferasa EZH2 en células de GBM humanos. Anteriormente ha sido reportado que EZH2 se encuentra sobreexpresado en biopsias de pacientes con GBM y que dicha expresión está directamente relacionada con el grado del tumor [Zhang et al., 2015a]. EZH2 se ha visto involucrado en procesos como proliferación, invasión y migración [Yin et al., 2016], mismos que se ven afectados por tratamientos hormonales en células derivadas de GBM humanos [González-Arenas et al., 2012, Piña-Medina et al., 2016].

Para demostrar que EZH2 se expresa en líneas celulares derivadas de GBMs humanos, se evaluó su expresión basal en las líneas U87, U251 y D54 utilizando RNA procedente de astrocitos humanos como control de tejido sano. Se encontró que las tres líneas evaluadas expresan a EZH2 de forma basal y en mayor cantidad que el control. La observación anterior concuerda con las funciones que ya se han reportado para EZH2 y PRC2, en especial, se ha demostrado que PRC2 está implicado en la proliferación celular y la tumorigénesis [Scelfo et al., 2015], además de que se sobreexpresa en diversos tipos de tumores, incluyendo GBM por lo que las líneas celulares U87, U251 y D54 concuerdan con lo reportado para biopsias de GBM [Zhang et al., 2015a]. Las líneas D54 y U251 presentan mayor expresión de EZH2 que la línea U87, lo que podría estar relacionado con el tiempo de duplicación de las células, ya que para U87 se ha calculado en 30.6 horas [Oraiopoulou et al., 2017] mientras que para U251 y D54 es de 24 horas [Cowley et al., 2014]. Debido a que EZH2 regula varias proteínas involucradas en checkpoints del ciclo celular, particularmente la transición G1/S [Sauvageau and Sauvageau, 2010], es factible pensar que una alta expresión de EZH2 involucraría una alta tasa de proliferación. Por medio de inmunofluorescencia se estableció que en las tres líneas celulares EZH2 se expresa en la totalidad de las células y se encuentra localizado mayormente en el núcleo, lo que sugiere que la proteína es funcional y por lo tanto, se esperaría un aumento en la marca H3K27me3 en los promotores de los genes blanco de PRC2 en comparación con tejido no neoplásico.

Por otra parte, se sabe que el rojo de fenol es un ligando del ER [Berthois et al., 1986] y que el SFB contiene hormonas esteroides [Milo et al., 1976], se comparó la expresión de EZH2 en células cultivadas por 24 horas en medio DMEM con rojo de fenol y suplementado con SFB contra células cultivadas en medio DMEM sin rojo de fenol y suplementado con SFB filtrado con carbón activado (libre de hormonas). Se observaron diferencias significativas en las células cultivadas en medio libre de hormonas contra las cultivadas en medio con rojo de fenol y SFB completo. Este fenómeno no puede ser adjudicado en su totalidad a la presencia o ausencia de rojo de fenol, sino que debe tomarse en cuenta que la composición del SFB filtrado con carbón activado varía en gran medida con la del SFB completo respecto a la cantidad de factores de crecimiento, hormonas y citocinas presentes que son removidas por el proceso de filtrado [Sikora et al., 2016]. Debido a las diferencias encontradas, el resto de los experimentos se condujeron estrictamente en medio DMEM libre de rojo de fenol y suplementado con SFB filtrado con carbón activado.

Efecto del E2 sobre la expresión de EZH2 en líneas celulares derivadas de GBM

Mediante un análisis *in silico*, se encontraron dos potenciales EREs en la región promotora de EZH2 adicionales a los previamente reportados por Bhan y colaboradores. En el mismo trabajo, se demostró que el tanto el E2 como una colección de xenoestrógenos inducen la expresión de EZH2 en células derivadas de cáncer de mama [Bhan et al., 2014]. Esto sugiere que la transcripción de EZH2 puede ser regulada por E2. Para evaluar lo anterior experimentalmente, se realizaron tratamientos con E2 (10 nM) ya que en estudios previos se ha reportado que a esta concentración se induce la proliferación, migración e invasión de células derivadas de GBM humanos [González-Arenas et al., 2012, Wan et al., 2018], además de que es cercana a los niveles encontrados de forma natural en el torrente sanguíneo de humanos. No se observaron cambios significativos inducidos por el E2 en las líneas celulares a ninguno de los tiempos evaluados tanto a nivel del RNA como de la proteína. Diferentes concentraciones de E2 (1nM a 1μM) se probaron a 12 y 24 horas en la línea celular U251 a fin de comprobar que el E2 no induce la expresión de EZH2, incluso a diferentes dosis de la hormona. La observación anterior es contraria a lo descrito por Bhan y colaboradores previamente, sin embargo, es importante remarcar que sus observaciones fueron realizadas en líneas celulares de cáncer de mama. Si bien tanto los GBMs como el cáncer de mama son tumores responsivos a estrógenos, se encuentran embebidos en contextos biológicos distintos, por lo que es altamente probable que los mecanismos que regulan la expresión de EZH2 sean diferentes entre ambos tipos de tumor. Anteriormente se ha manejado la idea de que la expresión de EZH2 depende tanto del contexto biológico en el que se encuentran las células neoplásicas como de la célula de origen [Margueron and Reinberg, 2011]. Dicha hipótesis surgió a partir de observación de que EZH2 actúa como oncogén en diversas neoplasias como cáncer de mama, de próstata, GBMs entre otros [Sørensen and Ørntoft, 2010], pero es un supresor de tumores en varios linfomas, cáncer de ovario y gliomas pediátricos [Scelfo et al., 2015, Mohammad et al., 2017]. Por las razones

anteriores, es factible pensar que la expresión de EZH2 está regulada por finos mecanismos que son dependientes del contexto celular.

Por otra parte, se ha descrito que el E2, a través de sus receptores membranales, puede activar cascadas de cinasas que conducen a la fosforilación de EZH2, lo que regula su actividad [Lu et al., 2016]. Teniendo en cuenta lo anterior, es probable que no sea necesario que aumente la cantidad de EZH2 total para que se vea un efecto en el cambio de actividad de KMT, en específico, existen reportes de que la fosforilación de EZH2 disminuye la afinidad de esta proteína por H3K27, por lo que podría disminuir la cantidad global de H3K27me3 [Qin et al., 2019].

EZH2 es indispensable para la inducción de migración, invasión y proliferación dependiente de E2

A pesar de no observar un efecto del E2 sobre la expresión de EZH2, trabajos previos han demostrado, que esta hormona induce la proliferación, migración e invasión de líneas celulares derivadas de GBM humanos, mismos procesos que son regulados por EZH2 también en GBM. Por tal motivo, se decidió evaluar el impacto del silenciamiento de EZH2 en procesos inducidos por E2. Como a se ha descrito previamente, el tratamiento con E2 indujo la migración, invasión y proliferación de la línea U251. Al tratar con E2 10 nM las células U251 transfectadas con siRNA control, se observó un aumento significativo en la proliferación, migración e invasión con respecto al grupo tratado con Vehículo. Interesantemente, al silenciar a EZH2 se abate el efecto inducido por E2 10 nM en la migración, proliferación e invasión celulares. Esto es un indicio de que los efectos de E2 sobre los procesos mencionados anteriormente podrían estar en parte mediados por EZH2.

Como ya se mencionó anteriormente, la actividad de EZH2 puede ser regulada por la modificación postraduccional de varios residuos. Entre las modificaciones de EZH2 más estudiadas, se encuentra la fosforilación de la Ser21. La activación de la vía de AKT ha sido comprobada como necesaria para la fosforilación de EZH2 en este residuo [Cha et al., 2005], misma vía que es activada por la unión de E2 a los ERs anclados a membrana. Esta modificación disminuye la afinidad de EZH2 por H3K27 pero favorece que esta enzima metile sustratos no histónicos, entre ellos al factor de transcripción STAT3 [Fouse and Costello, 2013].

STAT3 es uno de los factores de trascripción oncogénicos más estudiados en los últimos años, ya que está involucrado en varios procesos clásicos del cáncer como metástasis, resistencia a la quimioterapia y evasión del sistema inmune [Qin et al., 2019]. La activación persistente de STAT3 podría ser crucial para la progresión tumoral y la transición epitelio-mesénquima [Chang et al., 2017]. Por consecuencia, el estudio de los mecanismos que regulan la actividad de este factor es necesario para el entendimiento de los GBM y el

desarrollo de nuevas terapias.

EZH2 podría promover la proliferación, migración e invasión de células derivadas de GBM a través de STAT3

Para tratar de aclarar un poco la relación entre EZH2 y los ERs en GBMs, se analizó el transcriptoma de un set de muestras de glioma procedentes de TCGA y se comparó la expresión de ERα, ERβ y EZH2 entre LGG, GBM y tejido normal. En un primer acercamiento se aprecia que la expresión de ERα es menor en LGG y GBM con respecto al tejido normal, mientras que la expresión de ERβ es mayor en GBM respecto a LGG y tejido normal. Estudios anteriores han indicado que, en gliomas, la expresión de ERα está negativamente relacionada con el grado del tumor [Dueñas Jiménez et al., 2014], tal y como se observó en este set de muestras. De forma contraria, en la literatura se ha establecido que la expresión de ERβ es menor en muestras de GBM que en gliomas de bajo grado [Batistatou et al., 2004, Liu et al., 2018]. Cabe recalcar que en los estudios mencionados anteriormente se han utilizado grupos de muestras reducidos, la cuantificación de los receptores se ha hecho principalmente a través de WB y no se han utilizado controles de tejido sano. Hasta ahora no se había reportado el análisis de la expresión de los receptores en el set de muestras disponibles en la base de datos de TCGA y GTEx. Se observó también que en GBM, LGG y en tejido sano la expresión de ERα es mayor a la de ERβ lo cual concuerda con reportes previos [González-Arenas et al., 2012, Dueñas Jiménez et al., 2014]. A modo de control positivo del análisis realizado, se presenta la expresión de EZH2 debido a que ya ha sido reportado en otro trabajo que utilizó el mismo grupo de muestras que este gen está sobre-expresado en GBM con respecto a tejido normal y que la expresión es dependiente del grado del tumor [Zhang et al., 2015a].

Contrariamente al caso de EZH2 en el que la sobre-expresión de este es evidente en GBM, la expresión de ERα y ERβ parece ser un tanto heterogénea, con varias muestras con expresión similar al tejido sano. Por tal motivo se realizó un agrupamiento jerárquico de las muestras de GBM tomando en cuenta la expresión de ambos ERs, encontrándose que estas pueden ser organizadas en tres grupos. El grupo 1 se caracteriza por expresión de ERα y ERβ más baja que el tejido normal. El grupo 2 por baja expresión de ERα (menor que en los grupos 1 y 3) y niveles de ERβ similares a los del tejido sano. Finalmente, el clúster 3 se caracteriza por alta expresión de ERβ y baja de ERα respecto a tejido sano. En concordancia con los datos experimentales, no hay diferencias en la expresión de EZH2 entre los grupos, lo que sugiere que, en biopsias, la expresión de EZH2 no está relacionada con los ERs.

Al realizar el análisis de enriquecimiento de vías, el grupo 3 presenta enriquecimiento de los genes regulados por estrógenos comparado con los grupos 1 y 2, sin embargo, al comparar la expresión de genes blanco de PRC2, no hay diferencia entre los grupos, por lo que podría

ser posible que la actividad de metiltransferasa de EZH2 no se vea afectada por la actividad de los ERs.

Debido al mecanismo antes ya mencionado sobre la regulación de STAT3 mediante la trimetilación del residuo K180 mediada por EZH2 [Fouse and Costello, 2013] (ver **Figura 5** en página 20), se realizó un análisis de enriquecimiento con un set validado de genes regulados al alta por la activación de la vía de JAK/STAT en el grupo 3, el cual presenta el mayor enriquecimiento en genes responsivos a estrógenos. También se incluyó un set de genes sobre-expresados cuando se encuentra activa la vía de PI3K/AKT. Interesantemente, el grupo 3 presenta enriquecimiento de ambos sets. La vía de PI3K/ AKT puede ser activada por acción de los receptores de estrógenos anclados a membrana [Saczko et al., 2017]. En específico, se ha descrito que él ERα anclado a la membrana al unirse a E2, activa a PI3K, que a su vez fosforila a AKT [Majumdar et al., 2019]. AKT activo fosforila a EZH2 de acuerdo con Kim y colaboradores, mientras que pEZH2 metila a STAT3 aumentando su actividad de factor de transcripción [Fouse and Costello, 2013]. Sin embargo, en un trabajo más reciente, se reportó que la sobreexpresión de la isoforma 5 de ERβ (ERβ5) provoca la fosforilación de AKT y la activación de STAT3, además de promover la migración de células derivadas de GBM humanos [Liu et al., 2018]. Esto es importante tomando en cuenta que el grupo 3 es el que presenta mayor expresión de ERβ en el set de muestras de GBM evaluado, por lo que podría ser probable que las acciones de E2 en GBM sean en parte mediadas por el mecanismo extranuclear de EZH2.

Al analizar la expresión de un set de genes relacionados con la proliferación y migración celular, se observa que el grupo 3 tiene un mayor enriquecimiento comparado con los grupos 1 y 2. Al ser el grupo con mayor respuesta a estrógenos, concuerda con las observaciones experimentales que sugieren que el E2 promueve dichos procesos.

Finalmente, al evaluar los procesos biológicos en los cuales están involucrados los genes sobre-expresados o sub-expresados en el grupo 3 de GBMs en comparación con el 1 y 2, es notable que los procesos al alta incluyen en su mayor parte regulación de la adhesión a matriz extracelular, lo cual concuerda con los procesos de migración e invasión. Muy notablemente, se encuentra la vía de PI3K/AKT en los primeros lugares, lo cual refuerza la hipótesis de que esta vía se encuentra activa por acción de los ERs. Cabe señalar que además de las vías mostradas (correspondientes al top 10), también se encontraron enriquecidos diferentes grupos de genes relacionados con la regulación de la respuesta inmune y el control de la proliferación celular. Estos procesos están regulados por la acción de STAT3, debido a que este factor de transcripción tiene como blancos genes que promueven el escape de la respuesta inmunológica por parte de los tumores, al mantenimiento del fenotipo de célula troncal y la progresión del ciclo celular [Qin et al., 2019].

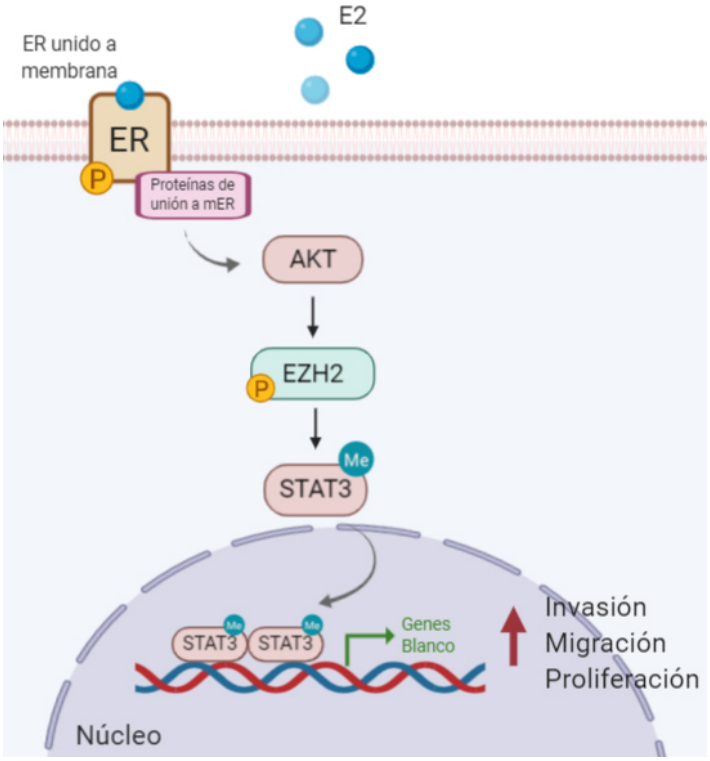

Figura 23: Modelo propuesto para la acción de E2 vía EZH2 en GBMs humanos.

En resumen, los datos obtenidos sugieren que el E2 promueve la proliferación, migración e invasión de GBMs humanos y dichos efectos están mediados por EZH2 a través de la activación del factor de transcripción STAT3 (**Figura 23**).

Sin duda el estudio de la regulación hormonal del gen EZH2 presenta una gran oportunidad de dilucidar los mecanismos epigenéticos involucrados en la malignidad de los glioblastomas y por consiguiente es una oportunidad para encontrar nuevos blancos terapéuticos. Dado que los tratamientos disponibles para los glioblastomas no resultan efectivos, el estudio del papel que desempeñan las hormonas sexuales y los mecanismos mediante los cuales actúan en GBMs humanos podrían aportar información valiosa para el desarrollo de nuevas terapias e incluso dar un nuevo enfoque al estudio de los glioblastomas. Actualmente se ha evaluado al tamoxifen (inhibidor de los ERs) como posible terapia para los pacientes con GBM [Graham et al., 2016, Balça-Silva et al., 2015] y se han obtenido resultados prometedores. De la misma forma, numerosos fármacos inhibidores de EZH2 se encuentran en desarrollo (fases clínicas II y III) con resultados positivos en leucemia [Yin et al., 2016], por lo que en el futuro podría ser de utilidad evaluar la posibilidad de que exista un efecto sinérgico en combinación de inhibidores de ER y EZH2, el cual podría contribuir a mejorar la expectativa de vida de los pacientes.

11. Conclusiones

- EZH2 se expresa en líneas celulares de GBM humanos y se encuentra localizado en núcleo.
- La expresión de EZH2 no es regulada por E2 en líneas celulares ni en biopsias de GBM.
- El E2 induce la proliferación, migración e invasión de las células de la línea U251 derivada de GBM humanos y dicha inducción es mediada por EZH2.
- El E2 en GBM humanos podría ejercer sus efectos en migración, proliferación e invasión a través de la fosforilación de EZH2 y la subsecuente metilación del factor de transcripción STAT3.

12. Perspectivas

Ya que los efectos del E2 sobre la migración, invasión y proliferación de lineas celulares derivadas de GBMs humanos depende de la represión de EZH2 resulta interesante evaluar los cambios en la expresión y en la localización de la marca H3K27me3 al tratar la célula con E2 a fin de obtener un mejor panorama de los genes cuya expresión se ve afectada directamente por el cambio en la actividad de EZH2 inducido por E2.

De la misma forma, para comprobar que STAT3 es parte fundamental del mecanismo de acción de EZH2 en el contexto de este estudio, resultaría útil repetir los experimentos de proliferación, migración e invasión utilizando esta vez un siRNA contra STAT3, además de verificar la fosforilación de esta proteína al añadir E2.

13. Bibliografía

[Atif et al., 2015] Atif, F., Yousuf, S., and Stein, D. G. (2015). Anti-tumor effects of progesterone in human glioblastoma multiforme: role of PI3K/Akt/mTOR signaling. *The Journal of steroid biochemistry and molecular biology*, 146:62–73.

[Azcoitia et al., 2011] Azcoitia, I., Yague, J., and Garcia-Segura, L. M. (2011). Estradiol synthesis within the human brain. *Neuroscience*, 191:139–147.

[Balça-Silva et al., 2015] Balça-Silva, J., Matias, D., do Carmo, A., Girão, H., Moura-Neto, V., Sarmento-Ribeiro, A. B., and Lopes, M. C. (2015). Tamoxifen in combination with temozolomide induce a synergistic inhibition of pkc-pan in gbm cell lines. *Biochimica et Biophysica Acta (BBA)-General Subjects*, 1850(4):722–732.

[Baritchii et al., 2016] Baritchii, A., Jurj, A., Soritau, O., Tomuleasa, C., Raduly, L., Zanoaga, O., Cernea, D., Braicu, C., Neagoe, I., and Stefan Florian, I. (2016). Sensitizer drugs for the treatment of temozolomide-resistant glioblastoma. *J buon*, 21:199–207.

[Barnes et al., 2004] Barnes, C., Vadlamudi, R. K., and Kumar, R. (2004). Novel estrogen receptor coregulators and signaling molecules in human diseases. *Cellular and Molecular Life Sciences CMLS*, 61(3):281–291.

[Barone et al., 2009] Barone, T. A., Gorski, J. W., Greenberg, S. J., and Plunkett, R. J. (2009). Estrogen increases survival in an orthotopic model of glioblastoma. *Journal of neuro-oncology*, 95(1):37–48.

[Batistatou et al., 2004] Batistatou, A., Stefanou, D., Goussia, A., Arkoumani, E., Papavassiliou, A. G., and Agnantis, N. J. (2004). Estrogen receptor beta (ERβ) is expressed in brain astrocytic tumors and declines with dedifferentiation of the neoplasm. *Journal of cancer research and clinical oncology*, 130(7):405–410.

[Ben-Porath et al., 2008] Ben-Porath, I., Thomson, M. W., Carey, V. J., Ge, R., Bell, G. W., Regev, A., and Weinberg, R. A. (2008). An embryonic stem cell–like gene expression signature in poorly differentiated aggressive human tumors. *Nature genetics*, 40(5):499.

[Berdasco and Esteller, 2019] Berdasco, M. and Esteller, M. (2019). Clinical epigenetics: seizing opportunities for translation. *Nature Reviews Genetics*, 20(2):109–127.

[Berger et al., 2009] Berger, S. L., Kouzarides, T., Shiekhattar, R., and Shilatifard, A. (2009). An operational definition of epigenetics. *Genes & development*, 23(7):781–783.

[Berthois et al., 1986] Berthois, Y., Katzenellenbogen, J. A., and Katzenellenbogen, B. S. (1986). Phenol red in tissue culture media is a weak estrogen: implications concerning the study of estrogen-responsive cells in culture. *Proceedings of the National Academy of Sciences*, 83(8):2496–2500.

[Bhan et al., 2014] Bhan, A., Hussain, I., Ansari, K. I., Bobzean, S. A., Perrotti, L. I., and Mandal, S. S. (2014). Histone methyltransferase EZH2 is transcriptionally induced by estradiol as well as estrogenic endocrine disruptors bisphenol-A and diethylstilbestrol. *Journal of molecular biology*, 426(20):3426–3441.

[Bjornstrom and Sjoberg, 2005] Bjornstrom, L. and Sjoberg, M. (2005). Mechanisms of estrogen receptor signaling: convergence of genomic and nongenomic actions on target genes. *Molecular endocrinology*, 19(4):833–842.

[Brown, 2006] Brown, J. L. (2006). Reproductive endocrinology. *Biology, Medicine, and Surgery of Elephants*, pages 377–388.

[Cha et al., 2005] Cha, T.-L., Zhou, B. P., Xia, W., Wu, Y., Yang, C.-C., Chen, C.-T., Ping, B., Otte, A. P., and Hung, M.-C. (2005). Akt-mediated phosphorylation of EZH2 suppresses methylation of lysine 27 in histone H3. *Science*, 310(5746):306–310.

[Chang et al., 2017] Chang, N., Ahn, S. H., Kong, D.-S., Lee, H. W., and Nam, D.-H. (2017). The role of STAT3 in glioblastoma progression through dual influences on tumor cells and the immune microenvironment. *Molecular and cellular endocrinology*, 451:53–65.

[Chow, 2010] Chow, A. (2010). Cell cycle control by oncogenes and tumor suppressors: driving the transformation of normal cells into cancerous cells. *Nature Education*, 3(9):7.

[Colaprico et al., 2016] Colaprico, A., Silva, T. C., Olsen, C., Garofano, L., Cava, C., Garolini, D., Sabedot, T. S., Malta, T. M., Pagnotta, S. M., Castiglioni, I., et al. (2016). TCGAbiolinks: an R/Bioconductor package for integrative analysis of TCGA data. *Nucleic acids research*, 44(8):e71–e71.

[Comet et al., 2016] Comet, I., Riising, E. M., Leblanc, B., and Helin, K. (2016). Maintaining cell identity: PRC2-mediated regulation of transcription and cancer. *Nature Reviews Cancer*, 16(12):803.

[Cowley et al., 2014] Cowley, G. S., Weir, B. A., Vazquez, F., Tamayo, P., Scott, J. A., Rusin, S., East-Seletsky, A., Ali, L. D., Gerath, W. F., Pantel, S. E., et al. (2014). Parallel genome-scale loss of function screens in 216 cancer cell lines for the identification of context-specific genetic dependencies. *Scientific data*, 1:140035.

[Davidovich et al., 2013] Davidovich, C., Zheng, L., Goodrich, K. J., and Cech, T. R. (2013). Promiscuous RNA binding by Polycomb repressive complex 2. *Nature structural & molecular biology*, 20(11):1250.

[Dawson and Kouzarides, 2012] Dawson, M. A. and Kouzarides, T. (2012). Cancer epigenetics: from mechanism to therapy. *Cell*, 150(1):12–27.

[de Vries et al., 2015] de Vries, N. A., Hulsman, D., Akhtar, W., de Jong, J., Miles, D. C., Blom, M., van Tellingen, O., Jonkers, J., and van Lohuizen, M. (2015). Prolonged Ezh2 depletion in glioblastoma causes a robust switch in cell fate resulting in tumor progression. *Cell reports*, 10(3):383–397.

[Dillon et al., 2005] Dillon, S. C., Zhang, X., Trievel, R. C., and Cheng, X. (2005). The SET-domain protein superfamily: protein lysine methyltransferases. *Genome biology*, 6(8):227.

[Ding et al., 2018] Ding, J., Yeh, C.-R., Sun, Y., Lin, C., Chou, J., Ou, Z., Chang, C., Qi, J., and Yeh, S. (2018). Estrogen receptor β promotes renal cell carcinoma progression via regulating LncRNA HOTAIR-miR-138/200c/204/217 associated CeRNA network. *Oncogene*, 37(37):5037–5053.

[Dueñas Jiménez et al., 2014] Dueñas Jiménez, J., Arellano Candanedo, A., Santerre, A., Suárez Orozco, S., Sánchez Sandoval, H., Romero Feria, I., López-Elizalde, R., Venegas Alonso, M., Netel, B., de la Torre Valdovinos, B., et al. (2014). Aromatase and estrogen receptor alpha mRNA expression as prognostic biomarkers in patients with astrocytomas. *Journal of neuro-oncology*, 119(2):275–284.

[Esteller, 2011] Esteller, M. (2011). Epigenetic changes in cancer. *F1000 biology reports*, 3(9).

[Fan et al., 2014] Fan, T.-Y., Wang, H., Xiang, P., Liu, Y.-W., Li, H.-Z., Lei, B.-X., Yu, M., and Qi, S.-T. (2014). Inhibition of EZH2 reverses chemotherapeutic drug TMZ chemosensitivity in glioblastoma. *International journal of clinical and experimental pathology*, 7(10):6662.

[Felsenfeld and Groudine, 2003] Felsenfeld, G. and Groudine, M. (2003). Controlling the double helix. *Nature*, 421(6921):448–453.

[Ferlay et al., 2019] Ferlay, J., Colombet, M., Soerjomataram, I., Mathers, C., Parkin, D., Piñeros, M., Znaor, A., and Bray, F. (2019). Estimating the global cancer incidence and

mortality in 2018: GLOBOCAN sources and methods. *International journal of cancer*, 144(8):1941–1953.

[Finlay-Schultz et al., 2015] Finlay-Schultz, J., Cittelly, D. M., Hendricks, P., Patel, P., Kabos, P., Jacobsen, B. M., Richer, J. K., and Sartorius, C. A. (2015). Progesterone downregulation of mir-141 contributes to expansion of stem-like breast cancer cells through maintenance of progesterone receptor and Stat5a. *Oncogene*, 34(28):3676–3687.

[Fouse and Costello, 2013] Fouse, S. D. and Costello, J. F. (2013). Cancer stem cells activate STAT3 the EZ way. *Cancer cell*, 23(6):711–713.

[Fuentes and Silveyra, 2019] Fuentes, N. and Silveyra, P. (2019). Estrogen receptor signaling mechanisms. *Advances in protein chemistry and structural biology*, 116:135.

[Fujii et al., 2008] Fujii, S., Ito, K., Ito, Y., and Ochiai, A. (2008). Enhancer of zeste homologue 2 (EZH2) down-regulates RUNX3 by increasing histone H3 methylation. *Journal of Biological Chemistry*, 283(25):17324–17332.

[Furnari et al., 2007] Furnari, F. B., Fenton, T., Bachoo, R. M., Mukasa, A., Stommel, J. M., Stegh, A., Hahn, W. C., Ligon, K. L., Louis, D. N., Brennan, C., et al. (2007). Malignant astrocytic glioma: genetics, biology, and paths to treatment. *Genes & development*, 21(21):2683–2710.

[Gebhart et al., 2019] Gebhart, V. M., Caldwell, J. D., Rodewald, A., Kalyvianaki, K., Kampa, M., and Jirikowski, G. F. (2019). Estrogen receptors and sex hormone binding globulin in neuronal cells and tissue. *Steroids*, 142:94–99.

[Germán-Castelán et al., 2014] Germán-Castelán, L., Manjarrez-Marmolejo, J., González-Arenas, A., González-Morán, M. G., and Camacho-Arroyo, I. (2014). Progesterone induces the growth and infiltration of human astrocytoma cells implanted in the cerebral cortex of the rat. *BioMed research international*, 2014.

[Giretti and Simoncini, 2008] Giretti, M. S. and Simoncini, T. (2008). Rapid regulatory actions of sex steroids on cell movement through the actin cytoskeleton. *Steroids*, 73(9-10):895–900.

[Godard et al., 2003] Godard, S., Getz, G., Delorenzi, M., Farmer, P., Kobayashi, H., Desbaillets, I., Nozaki, M., Diserens, A.-C., Hamou, M.-F., Dietrich, P.-Y., et al. (2003). Classification of human astrocytic gliomas on the basis of gene expression: a correlated group of genes with angiogenic activity emerges as a strong predictor of subtypes. *Cancer research*, 63(20):6613–6625.

[González-Arenas et al., 2019] González-Arenas, A., De la Fuente-Granada, M., Camacho-Arroyo, I., Zamora-Sánchez, C. J., Piña-Medina, A. G., Segura-Uribe, J., and Guerra-Araiza, C. (2019). Tibolone Effects on Human Glioblastoma Cell Lines. *Archives of medical research*, 50(4):187–196.

[González-Arenas et al., 2012] González-Arenas, A., Hansberg-Pastor, V., Hernández-Hernández, O. T., González-García, T. K., Henderson-Villalpando, J., Lemus-Hernández, D., Cruz-Barrios, A., Rivas-Suárez, M., and Camacho-Arroyo, I. (2012). Estradiol increases cell growth in human astrocytoma cell lines through ERα activation and its interaction with SRC-1 and SRC-3 coactivators. *Biochimica et Biophysica Acta (BBA)-Molecular Cell Research*, 1823(2):379–386.

[Graham et al., 2016] Graham, C. D., Kaza, N., Klocke, B. J., Gillespie, G. Y., Shevde, L. A., Carroll, S. L., and Roth, K. A. (2016). Tamoxifen induces cytotoxic autophagy in glioblastoma. *Journal of Neuropathology & Experimental Neurology*, 75(10):946–954.

[Grazia et al., 2014] Grazia, G., Vegetti, C., Benigni, F., Penna, I., Perotti, V., Tassi, E., Bersani, I., Nicolini, G., Canevari, S., Carlo-Stella, C., et al. (2014). Synergistic anti-tumor activity and inhibition of angiogenesis by cotargeting of oncogenic and death receptor pathways in human melanoma. *Cell death & disease*, 5(10):e1434–e1434.

[Gruber et al., 2004] Gruber, C. J., Gruber, D. M., Gruber, I. M., Wieser, F., and Huber, J. C. (2004). Anatomy of the estrogen response element. *Trends in endocrinology & metabolism*, 15(2):73–78.

[Gusyatiner and Hegi, 2018] Gusyatiner, O. and Hegi, M. E. (2018). Glioma epigenetics: from subclassification to novel treatment options. In *Seminars in cancer biology*, volume 51, pages 50–58. Elsevier.

[Hadjipanayis and Van Meir, 2009] Hadjipanayis, C. G. and Van Meir, E. G. (2009). Brain cancer propagating cells: biology, genetics and targeted therapies. *Trends in molecular medicine*, 15(11):519–530.

[Hamza and Gilbert, 2014] Hamza, M. A. and Gilbert, M. (2014). Targeted therapy in gliomas. *Current oncology reports*, 16(4):379.

[Han et al., 2012] Han, L., Zhang, K., Shi, Z., Zhang, J., Zhu, J., Zhu, S., Zhang, A., Jia, Z., Wang, G., Yu, S., et al. (2012). LncRNA profile of glioblastoma reveals the potential role of lncRNAs in contributing to glioblastoma pathogenesis. *International journal of oncology*, 40(6):2004–2012.

[Hanahan and Weinberg, 2011] Hanahan, D. and Weinberg, R. A. (2011). Hallmarks of cancer: the next generation. *Cell*, 144(5):646–674.

[Hansberg-Pastor et al., 2017] Hansberg-Pastor, V., González-Arenas, A., and Camacho-Arroyo, I. (2017). CCAAT/enhancer binding protein β negatively regulates progesterone receptor expression in human glioblastoma cells. *Molecular and cellular endocrinology*, 439:317–327.

[Heinz et al., 2010] Heinz, S., Benner, C., Spann, N., Bertolino, E., Lin, Y. C., Laslo, P., Cheng, J. X., Murre, C., Singh, H., and Glass, C. K. (2010). Simple combinations of lineage-determining transcription factors prime cis-regulatory elements required for macrophage and B cell identities. *Molecular cell*, 38(4):576–589.

[Heldring et al., 2011] Heldring, N., Isaacs, G. D., Diehl, A. G., Sun, M., Cheung, E., Ranish, J. A., and Kraus, W. L. (2011). Multiple sequence-specific DNA-binding proteins mediate estrogen receptor signaling through a tethering pathway. *Molecular endocrinology*, 25(4):564–574.

[Heldring et al., 2007] Heldring, N., Pike, A., Andersson, S., Matthews, J., Cheng, G., Hartman, J., Tujague, M., Strom, A., Treuter, E., Warner, M., et al. (2007). Estrogen receptors: how do they signal and what are their targets. *Physiological reviews*, 87(3):905–931.

[Holoch and Margueron, 2017] Holoch, D. and Margueron, R. (2017). Mechanisms regulating PRC2 recruitment and enzymatic activity. *Trends in biochemical sciences*, 42(7):531–542.

[Ivanchuk et al., 2001] Ivanchuk, S. M., Mondal, S., Dirks, P. B., and Rutka, J. T. (2001). The INK4A/ARF locus: role in cell cycle control and apoptosis and implications for glioma growth. *Journal of neuro-oncology*, 51(3):219–229.

[Jermann et al., 2014] Jermann, P., Hoerner, L., Burger, L., and Schübeler, D. (2014). Short sequences can efficiently recruit histone H3 lysine 27 trimethylation in the absence of enhancer activity and dna methylation. *Proceedings of the National Academy of Sciences*, 111(33):E3415–E3421.

[Johannessen and Bjerkvig, 2012] Johannessen, T.-C. A. and Bjerkvig, R. (2012). Molecular mechanisms of temozolomide resistance in glioblastoma multiforme. *Expert review of anticancer therapy*, 12(5):635–642.

[Kabat et al., 2010] Kabat, G. C., Etgen, A. M., and Rohan, T. E. (2010). Do steroid hormones play a role in the etiology of glioma? *Cancer Epidemiology and Prevention Biomarkers*, 19(10):2421–2427.

[Kaneko et al., 2013] Kaneko, S., Son, J., Shen, S. S., Reinberg, D., and Bonasio, R. (2013). PRC2 binds active promoters and contacts nascent RNAs in embryonic stem cells. *Nature structural & molecular biology*, 20(11):1258.

[Kassis and Brown, 2013] Kassis, J. A. and Brown, J. L. (2013). Polycomb group response elements in Drosophila and vertebrates. In *Advances in genetics*, volume 81, pages 83–118. Elsevier.

[Kastrati et al., 2019] Kastrati, I., Semina, S., Gordon, B., and Smart, E. (2019). Insights into how phosphorylation of estrogen receptor at serine 305 modulates tamoxifen activity in breast cancer. *Molecular and cellular endocrinology*, 483:97–101.

[Katoh, 2016] Katoh, M. (2016). Mutation spectra of histone methyltransferases with canonical SET domains and EZH2-targeted therapy. *Epigenomics*, 8(2):285–305.

[Khalil et al., 2009] Khalil, A. M., Guttman, M., Huarte, M., Garber, M., Raj, A., Morales, D. R., Thomas, K., Presser, A., Bernstein, B. E., van Oudenaarden, A., et al. (2009). Many human large intergenic noncoding RNAs associate with chromatin-modifying complexes and affect gene expression. *Proceedings of the National Academy of Sciences*, 106(28):11667–11672.

[Khan et al., 2018] Khan, A., Fornes, O., Stigliani, A., Gheorghe, M., Castro-Mondragon, J. A., van der Lee, R., Bessy, A., Cheneby, J., Kulkarni, S. R., Tan, G., et al. (2018). JASPAR 2018: update of the open-access database of transcription factor binding profiles and its web framework. *Nucleic acids research*, 46(D1):D260–D266.

[Kim et al., 2013] Kim, E., Kim, M., Woo, D.-H., Shin, Y., Shin, J., Chang, N., Oh, Y. T., Kim, H., Rheey, J., Nakano, I., et al. (2013). Phosphorylation of EZH2 activates STAT3 signaling via STAT3 methylation and promotes tumorigenicity of glioblastoma stem-like cells. *Cancer cell*, 23(6):839–852.

[Kim et al., 1991] Kim, T. S., Halliday, A. L., Hedley-Whyte, E. T., and Convery, K. (1991). Correlates of survival and the daumas-duport grading system for astrocytomas. *Journal of neurosurgery*, 74(1):27–37.

[Kleihues et al., 2002] Kleihues, P., Louis, D. N., Scheithauer, B. W., Rorke, L. B., Reifenberger, G., Burger, P. C., and Cavenee, W. K. (2002). The WHO classification of tumors of the nervous system. *Journal of Neuropathology & Experimental Neurology*, 61(3):215–225.

[Kondo et al., 2014] Kondo, Y., Katsushima, K., Ohka, F., Natsume, A., and Shinjo, K. (2014). Epigenetic dysregulation in glioma. *Cancer science*, 105(4):363–369.

[Kulakovskiy et al., 2018] Kulakovskiy, I. V., Vorontsov, I. E., Yevshin, I. S., Sharipov, R. N., Fedorova, A. D., Rumynskiy, E. I., Medvedeva, Y. A., Magana-Mora, A., Bajic, V. B., Papatsenko, D. A., et al. (2018). HOCOMOCO: towards a complete collection of transcription factor binding models for human and mouse via large-scale ChIP-Seq analysis. *Nucleic acids research*, 46(D1):D252–D259.

[Kundakovic, 2017] Kundakovic, M. (2017). Sex-specific epigenetics: implications for environmental studies of brain and behavior. *Current environmental health reports*, 4(4):385–391.

[Lappano et al., 2014] Lappano, R., Pisano, A., and Maggiolini, M. (2014). GPER function in breast cancer: an overview. *Frontiers in endocrinology*, 5:66.

[Lappin et al., 2006] Lappin, T. R., Grier, D. G., Thompson, A., and Halliday, H. L. (2006). HOX genes: seductive science, mysterious mechanisms. *The Ulster medical journal*, 75(1):23.

[Lee et al., 2018] Lee, C.-H., Yu, J.-R., Kumar, S., Jin, Y., LeRoy, G., Bhanu, N., Kaneko, S., Garcia, B. A., Hamilton, A. D., and Reinberg, D. (2018). Allosteric activation dictates PRC2 activity independent of its recruitment to chromatin. *Molecular cell*, 70(3):422–434.

[Levin, 2008] Levin, E. R. (2008). Rapid signaling by steroid receptors. *American Journal of Physiology-Regulatory, Integrative and Comparative Physiology*, 295(5):R1425–R1430.

[Lindroth et al., 2008] Lindroth, A. M., Park, Y. J., McLean, C. M., Dokshin, G. A., Persson, J. M., Herman, H., Pasini, D., Miro, X., Donohoe, M. E., Lee, J. T., et al. (2008). Antagonism between DNA and H3K27 methylation at the imprinted Rasgrf1 locus. *PLoS genetics*, 4(8).

[Liu et al., 2020] Liu, J., Ali, M., and Zhou, Q. (2020). Establishment and evolution of heterochromatin. *Annals of the New York Academy of Sciences*.

[Liu et al., 2018] Liu, J., Sareddy, G. R., Zhou, M., Viswanadhapalli, S., Li, X., Lai, Z., Tekmal, R. R., Brenner, A., and Vadlamudi, R. K. (2018). Differential effects of estrogen receptor β isoforms on glioblastoma progression. *Cancer research*, 78(12):3176–3189.

[Loreti et al., 2020] Loreti, M., Shi, D.-L., and Carron, C. (2020). The regulatory proteins DSCR6 and Ezh2 oppositely regulate Stat3 transcriptional activity in mesoderm patterning during Xenopus development. *Journal of Biological Chemistry*, 295(9):2724–2735.

[Louis et al., 2016] Louis, D. N., Perry, A., Reifenberger, G., Von Deimling, A., Figarella-Branger, D., Cavenee, W. K., Ohgaki, H., Wiestler, O. D., Kleihues, P., and Ellison, D. W. (2016). The 2016 World Health Organization classification of tumors of the central nervous system: a summary. *Acta neuropathologica*, 131(6):803–820.

[Love et al., 2014] Love, M. I., Huber, W., and Anders, S. (2014). Moderated estimation of fold change and dispersion for RNA-seq data with DESeq2. *Genome biology*, 15(12):550.

[Lu et al., 2016] Lu, H., Li, G., Zhou, C., Jin, W., Qian, X., Wang, Z., Pan, H., Jin, H., and Wang, X. (2016). Regulation and role of post-translational modifications of enhancer of zeste homologue 2 in cancer development. *American journal of cancer research*, 6(12):2737.

[Majumdar et al., 2019] Majumdar, S., Rinaldi, J. C., Malhotra, N. R., Xie, L., Hu, D.-P., Gauntner, T. D., Grewal, H. S., Hu, W.-Y., Kim, S. H., Katzenellenbogen, J. A., et al.

(2019). Differential Actions of Estrogen Receptor α and β via Nongenomic Signaling in Human Prostate Stem and Progenitor Cells. *Endocrinology*, 160(11):2692–2708.

[Mani and O'Malley, 2002] Mani, S. K. and O'Malley, B. W. (2002). Mechanism of progesterone receptor action in the brain. In *Hormones, brain and behavior*, pages 643–682. Elsevier.

[Margueron et al., 2008] Margueron, R., Li, G., Sarma, K., Blais, A., Zavadil, J., Woodcock, C. L., Dynlacht, B. D., and Reinberg, D. (2008). Ezh1 and Ezh2 maintain repressive chromatin through different mechanisms. *Molecular cell*, 32(4):503–518.

[Margueron and Reinberg, 2011] Margueron, R. and Reinberg, D. (2011). The Polycomb complex PRC2 and its mark in life. *Nature*, 469(7330):343–349.

[Marsh et al., 2014] Marsh, D. J., Shah, J. S., and Cole, A. J. (2014). Histones and their modifications in ovarian cancer–drivers of disease and therapeutic targets. *Frontiers in oncology*, 4:144.

[Martin et al., 2006] Martin, C., Cao, R., and Zhang, Y. (2006). Substrate preferences of the EZH2 histone methyltransferase complex. *Journal of Biological Chemistry*, 281(13):8365–8370.

[Melmed and Conn, 2007] Melmed, S. and Conn, P. M. (2007). *Endocrinology: basic and clinical principles*. Springer Science & Business Media.

[Miller, 2013] Miller, W. L. (2013). Steroid hormone synthesis in mitochondria. *Molecular and cellular endocrinology*, 379(1-2):62–73.

[Milo et al., 1976] Milo, G. E., Malarkey, W. B., Powell, J. E., Blakeslee, J. R., and Yohn, D. S. (1976). Effects of steroid hormones in fetal bovine serum on plating and cloning of human cells in vitro. *In vitro*, 12(1):23–30.

[Mohammad et al., 2017] Mohammad, F., Weissmann, S., Leblanc, B., Pandey, D. P., Højfeldt, J. W., Comet, I., Zheng, C., Johansen, J. V., Rapin, N., Porse, B. T., et al. (2017). EZH2 is a potential therapeutic target for H3K27M-mutant pediatric gliomas. *Nature medicine*, 23(4):483.

[Musgrove et al., 2008] Musgrove, E. A., Sergio, C. M., Loi, S., Inman, C. K., Anderson, L. R., Alles, M. C., Pinese, M., Caldon, C. E., Schütte, J., Gardiner-Garden, M., et al. (2008). Identification of functional networks of estrogen-and c-Myc-responsive genes and their relationship to response to tamoxifen therapy in breast cancer. *PloS one*, 3(8).

[Noble, 2015] Noble, D. (2015). Conrad Waddington and the origin of epigenetics. *Journal of Experimental Biology*, 218(6):816–818.

[Oraiopoulou et al., 2017] Oraiopoulou, M.-E., Tzamali, E., Tzedakis, G., Vakis, A., Papamatheakis, J., and Sakkalis, V. (2017). In vitro/in silico study on the role of doubling time heterogeneity among primary glioblastoma cell lines. *BioMed research international*, 2017.

[Ostrom et al., 2018] Ostrom, Q. T., Gittleman, H., Truitt, G., Boscia, A., Kruchko, C., and Barnholtz-Sloan, J. S. (2018). CBTRUS statistical report: primary brain and other central nervous system tumors diagnosed in the united states in 2011–2015. *Neuro-oncology*, 20(suppl_4):iv1–iv86.

[Ott et al., 2012] Ott, M., Litzenburger, U. M., Sahm, F., Rauschenbach, K. J., Tudoran, R., Hartmann, C., Marquez, V. E., von Deimling, A., Wick, W., and Platten, M. (2012). Promotion of glioblastoma cell motility by enhancer of zeste homolog 2 (EZH2) is mediated by AXL receptor kinase. *PloS one*, 7(10).

[Piña-Medina et al., 2016] Piña-Medina, A. G., Hansberg-Pastor, V., González-Arenas, A., Cerbón, M., and Camacho-Arroyo, I. (2016). Progesterone promotes cell migration, invasion and cofilin activation in human astrocytoma cells. *Steroids*, 105:19–25.

[Pinacho-Garcia et al., 2020] Pinacho-Garcia, L. M., Valdez, R. A., Navarrete, A., Cabeza, M., Segovia, J., and Romano, M. C. (2020). The effect of finasteride and dutasteride on the synthesis of neurosteroids by glioblastoma cells. *Steroids*, 155:108556.

[Qin et al., 2019] Qin, J.-J., Yan, L., Zhang, J., and Zhang, W.-D. (2019). STAT3 as a potential therapeutic target in triple negative breast cancer: a systematic review. *Journal of Experimental & Clinical Cancer Research*, 38(1):195.

[Qu et al., 2019] Qu, C., Ma, J., Zhang, Y., Han, C., Huang, L., Shen, L., Li, H., Wang, X., Liu, J., and Zou, W. (2019). Estrogen receptor variant ER-α36 promotes tamoxifen agonist activity in glioblastoma cells. *Cancer science*, 110(1):221–234.

[Ramadoss et al., 2010] Ramadoss, P., Chiappini, F., Bilban, M., and Hollenberg, A. N. (2010). Regulation of hepatic six transmembrane epithelial antigen of prostate 4 (STEAP4) expression by STAT3 and CCAAT/enhancer-binding protein α. *Journal of Biological Chemistry*, 285(22):16453–16466.

[Reifenberger et al., 2017] Reifenberger, G., Wirsching, H.-G., Knobbe-Thomsen, C. B., and Weller, M. (2017). Advances in the molecular genetics of gliomas—implications for classification and therapy. *Nature reviews Clinical oncology*, 14(7):434.

[Rinn et al., 2007] Rinn, J. L., Kertesz, M., Wang, J. K., Squazzo, S. L., Xu, X., Brugmann, S. A., Goodnough, L. H., Helms, J. A., Farnham, P. J., Segal, E., et al. (2007). Functional demarcation of active and silent chromatin domains in human HOX loci by noncoding RNAs. *Cell*, 129(7):1311–1323.

[Rodríguez-Lozano et al., 2019] Rodríguez-Lozano, D. C., Piña-Medina, A. G., Hansberg-Pastor, V., Bello-Alvarez, C., and Camacho-Arroyo, I. (2019). Testosterone promotes glioblastoma cell proliferation, migration, and invasion through androgen receptor activation. *Frontiers in endocrinology*, 10:16.

[Romano and Gorelick, 2018] Romano, S. N. and Gorelick, D. A. (2018). Crosstalk between nuclear and G protein-coupled estrogen receptors. *General and comparative endocrinology*, 261:190–197.

[Rossetti et al., 2016] Rossetti, M. F., Cambiasso, M. J., Holschbach, M., and Cabrera, R. (2016). Oestrogens and progestagens: synthesis and action in the brain. *Journal of neuroendocrinology*, 28(7).

[Saczko et al., 2017] Saczko, J., Michel, O., Chwiłkowska, A., Sawicka, E., Mączyńska, J., and Kulbacka, J. (2017). Estrogen receptors in cell membranes: Regulation and signaling. In *Transport Across Natural and Modified Biological Membranes and its Implications in Physiology and Therapy*, pages 93–105. Springer.

[Sareddy et al., 2012] Sareddy, G. R., Nair, B. C., Gonugunta, V. K., Zhang, Q.-g., Brenner, A., Brann, D. W., Tekmal, R. R., and Vadlamudi, R. K. (2012). Therapeutic significance of estrogen receptor β agonists in gliomas. *Molecular cancer therapeutics*, 11(5):1174–1182.

[Sarkar et al., 2009] Sarkar, C., Jain, A., Suri, V., et al. (2009). Current concepts in the pathology and genetics of gliomas. *Indian journal of cancer*, 46(2):108.

[Sauvageau and Sauvageau, 2010] Sauvageau, M. and Sauvageau, G. (2010). Polycomb group proteins: multi-faceted regulators of somatic stem cells and cancer. *Cell stem cell*, 7(3):299–313.

[Scelfo et al., 2015] Scelfo, A., Piunti, A., and Pasini, D. (2015). The controversial role of the Polycomb group proteins in transcription and cancer: how much do we not understand polycomb proteins? *The FEBS journal*, 282(9):1703–1722.

[Schmitges et al., 2011] Schmitges, F. W., Prusty, A. B., Faty, M., Stützer, A., Lingaraju, G. M., Aiwazian, J., Sack, R., Hess, D., Li, L., Zhou, S., et al. (2011). Histone methylation by PRC2 is inhibited by active chromatin marks. *Molecular cell*, 42(3):330–341.

[Schmittgen and Livak, 2008] Schmittgen, T. D. and Livak, K. J. (2008). Analyzing real-time PCR data by the comparative C T method. *Nature protocols*, 3(6):1101.

[Schneider et al., 2012] Schneider, C. A., Rasband, W. S., and Eliceiri, K. W. (2012). NIH Image to ImageJ: 25 years of image analysis. *Nature methods*, 9(7):671–675.

[Schwartz et al., 2016] Schwartz, N., Verma, A., Bivens, C. B., Schwartz, Z., and Boyan, B. D. (2016). Rapid steroid hormone actions via membrane receptors. *Biochimica et Biophysica Acta (BBA)-Molecular Cell Research*, 1863(9):2289–2298.

[Shi et al., 2007] Shi, B., Liang, J., Yang, X., Wang, Y., Zhao, Y., Wu, H., Sun, L., Zhang, Y., Chen, Y., Li, R., et al. (2007). Integration of estrogen and wnt signaling circuits by the polycomb group protein EZH2 in breast cancer cells. *Molecular and cellular biology*, 27(14):5105–5119.

[Sikora et al., 2016] Sikora, M. J., Johnson, M. D., Lee, A. V., and Oesterreich, S. (2016). Endocrine response phenotypes are altered by charcoal-stripped serum variability. *Endocrinology*, 157(10):3760–3766.

[Singh et al., 2004] Singh, S. K., Hawkins, C., Clarke, I. D., Squire, J. A., Bayani, J., Hide, T., Henkelman, R. M., Cusimano, M. D., and Dirks, P. B. (2004). Identification of human brain tumour initiating cells. *nature*, 432(7015):396–401.

[Smits et al., 2010] Smits, M., Nilsson, J., Mir, S. E., van der Stoop, P. M., Hulleman, E., Niers, J. M., de Witt Hamer, P. C., Marquez, V. E., Cloos, J., Krichevsky, A. M., et al. (2010). mir-101 is down-regulated in glioblastoma resulting in EZH2-induced proliferation, migration, and angiogenesis. *Oncotarget*, 1(8):710.

[Sørensen and Ørntoft, 2010] Sørensen, K. D. and Ørntoft, T. F. (2010). Discovery of prostate cancer biomarkers by microarray gene expression profiling. *Expert review of molecular diagnostics*, 10(1):49–64.

[Subramanian et al., 2005] Subramanian, A., Tamayo, P., Mootha, V. K., Mukherjee, S., Ebert, B. L., Gillette, M. A., Paulovich, A., Pomeroy, S. L., Golub, T. R., Lander, E. S., et al. (2005). Gene set enrichment analysis: a knowledge-based approach for interpreting genome-wide expression profiles. *Proceedings of the National Academy of Sciences*, 102(43):15545–15550.

[Suvà et al., 2009] Suvà, M.-L., Riggi, N., Janiszewska, M., Radovanovic, I., Provero, P., Stehle, J.-C., Baumer, K., Le Bitoux, M.-A., Marino, D., Cironi, L., et al. (2009). EZH2 is essential for glioblastoma cancer stem cell maintenance. *Cancer research*, 69(24):9211–9218.

[Svotelis et al., 2011] Svotelis, A., Bianco, S., Madore, J., Huppé, G., Nordell-Markovits, A., Mes-Masson, A.-M., and Gévry, N. (2011). H3K27 demethylation by JMJD3 at a poised enhancer of anti-apoptotic gene bcl2 determines erα ligand dependency. *The EMBO journal*, 30(19):3947–3961.

[Tamm-Rosenstein et al., 2013] Tamm-Rosenstein, K., Simm, J., Suhorutshenko, M., Salumets, A., and Metsis, M. (2013). Changes in the transcriptome of the human endometrial ishikawa cancer cell line induced by estrogen, progesterone, tamoxifen, and mifepristone (RU486) as detected by RNA-sequencing. *PLoS One*, 8(7).

[Tan and Lenhard, 2016] Tan, G. and Lenhard, B. (2016). Tfbstools: an R/bioconductor package for transcription factor binding site analysis. *Bioinformatics*, 32(10):1555–1556.

[Tao et al., 2015] Tao, S., He, H., and Chen, Q. (2015). Estradiol induces HOTAIR levels via GPER-mediated mir-148a inhibition in breast cancer. *Journal of translational medicine*, 13(1):131.

[Tavares et al., 2016] Tavares, C. B., Gomes-Braga, F. d. C. S., Costa-Silva, D. R., Escórcio-Dourado, C. S., Borges, U. S., Conde-Junior, A. M., Barros-Oliveira, M. d. C., Sousa, E. B., Barros, L. d. R., Martins, L. M., et al. (2016). Expression of estrogen and progesterone receptors in astrocytomas: a literature review. *Clinics*, 71(8):481–486.

[Thorvaldsdóttir et al., 2013] Thorvaldsdóttir, H., Robinson, J. T., and Mesirov, J. P. (2013). Integrative Genomics Viewer (IGV): high-performance genomics data visualization and exploration. *Briefings in bioinformatics*, 14(2):178–192.

[Trošelj et al., 2016] Trošelj, K. G., Kujundzic, R. N., and Ugarkovic, D. (2016). Polycomb repressive complex's evolutionary conserved function: The role of EZH2 status and cellular background. *Clinical epigenetics*, 8(1):55.

[Turner, 2005] Turner, B. M. (2005). Reading signals on the nucleosome with a new nomenclature for modified histones. *Nature structural & molecular biology*, 12(2):110–112.

[Valadez-Cosmes et al., 2015] Valadez-Cosmes, P., Germán-Castelán, L., González-Arenas, A., Velasco-Velázquez, M. A., Hansberg-Pastor, V., and Camacho-Arroyo, I. (2015). Expression and hormonal regulation of membrane progesterone receptors in human astrocytoma cells. *The Journal of steroid biochemistry and molecular biology*, 154:176–185.

[Verhaak et al., 2010] Verhaak, R. G., Hoadley, K. A., Purdom, E., Wang, V., Qi, Y., Wilkerson, M. D., Miller, C. R., Ding, L., Golub, T., Mesirov, J. P., et al. (2010). Integrated genomic analysis identifies clinically relevant subtypes of glioblastoma characterized by abnormalities in PDGFRA, IDH1, EGFR, and NF1. *Cancer cell*, 17(1):98–110.

[Wan et al., 2018] Wan, S., Jiang, J., Zheng, C., Wang, N., Zhai, X., Fei, X., Wu, R., and Jiang, X. (2018). Estrogen nuclear receptors affect cell migration by altering sublocalization of AQP2 in glioma cell lines. *Cell death discovery*, 4(1):1–12.

[Wang et al., 2017] Wang, Q., Hu, B., Hu, X., Kim, H., Squatrito, M., Scarpace, L., deCarvalho, A. C., Lyu, S., Li, P., Li, Y., et al. (2017). Tumor evolution of glioma-intrinsic gene expression subtypes associates with immunological changes in the microenvironment. *Cancer cell*, 32(1):42–56.

[Weller et al., 2015] Weller, M., Wick, W., Aldape, K., Brada, M., Berger, M., Pfister, S. M., Nishikawa, R., Rosenthal, M., Wen, P. Y., Stupp, R., et al. (2015). Glioma. *Nature reviews Disease primers*, 1(1):1–18.

[Wickham, 2016] Wickham, H. (2016). *ggplot2: elegant graphics for data analysis*. Springer.

[Wiles and Selker, 2017] Wiles, E. T. and Selker, E. U. (2017). H3K27 methylation: a promiscuous repressive chromatin mark. *Current opinion in genetics & development*, 43:31–37.

[Wu et al., 2013] Wu, H., Zeng, H., Dong, A., Li, F., He, H., Senisterra, G., Seitova, A., Duan, S., Brown, P. J., Vedadi, M., et al. (2013). Structure of the catalytic domain of EZH2 reveals conformational plasticity in cofactor and substrate binding sites and explains oncogenic mutations. *PloS one*, 8(12).

[Yan et al., 2017] Yan, K.-S., Lin, C.-Y., Liao, T.-W., Peng, C.-M., Lee, S.-C., Liu, Y.-J., Chan, W. P., and Chou, R.-H. (2017). EZH2 in cancer progression and potential application in cancer therapy: a friend or foe? *International journal of molecular sciences*, 18(6):1172.

[Yen et al., 2017] Yen, S.-Y., Chuang, H.-M., Huang, M.-H., Lin, S.-Z., Chiou, T.-W., and Harn, H.-J. (2017). n-Butylidenephthalide regulated tumor stem cell genes EZH2/AXL and reduced its migration and invasion in glioblastoma. *International journal of molecular sciences*, 18(2):372.

[Yin et al., 2016] Yin, Y., Qiu, S., and Peng, Y. (2016). Functional roles of enhancer of zeste homolog 2 in gliomas. *Gene*, 576(1):189–194.

[Zamora-Sánchez et al., 2018] Zamora-Sánchez, C. J., Moral-Morales, D., Hernández-Vega, A. M., Hansberg-Pastor, V., Salido-Guadarrama, I., Rodríguez-Dorantes, M., Camacho-Arroyo, I., et al. (2018). Allopregnanolone alters the gene expression profile of human glioblastoma cells. *International journal of molecular sciences*, 19(3):864.

[Zhang et al., 2015a] Zhang, J., Chen, L., Han, L., Shi, Z., Zhang, J., Pu, P., and Kang, C. (2015a). Ezh2 is a negative prognostic factor and exhibits pro-oncogenic activity in glioblastoma. *Cancer letters*, 356(2):929–936.

[Zhang et al., 2015b] Zhang, K., Sun, X., Zhou, X., Han, L., Chen, L., Shi, Z., Zhang, A., Ye, M., Wang, Q., Liu, C., et al. (2015b). Long non-coding RNA HOTAIR promotes glioblastoma cell cycle progression in an ezh2 dependent manner. *Oncotarget*, 6(1):537.

[Zhao et al., 2007] Zhao, X. D., Han, X., Chew, J. L., Liu, J., Chiu, K. P., Choo, A., Orlov, Y. L., Sung, W.-K., Shahab, A., Kuznetsov, V. A., et al. (2007). Whole-genome mapping of histone H3 Lys4 and 27 trimethylations reveals distinct genomic compartments in human embryonic stem cells. *Cell stem cell*, 1(3):286–298.

[Zhou et al., 2019] Zhou, M., Sareddy, G. R., Li, M., Liu, J., Luo, Y., Venkata, P. P., Viswanadhapalli, S., Tekmal, R. R., Brenner, A., and Vadlamudi, R. K. (2019). Estrogen

receptor beta enhances chemotherapy response of GBM cells by down regulating DNA damage response pathways. *Scientific reports*, 9(1):1–10.

[Zong et al., 2015] Zong, H., Parada, L. F., and Baker, S. J. (2015). Cell of origin for malignant gliomas and its implication in therapeutic development. *Cold Spring Harbor perspectives in biology*, 7(5):a020610.

14. ANEXOS

14.1. Figuras suplementarias

Figura suplementaria 1

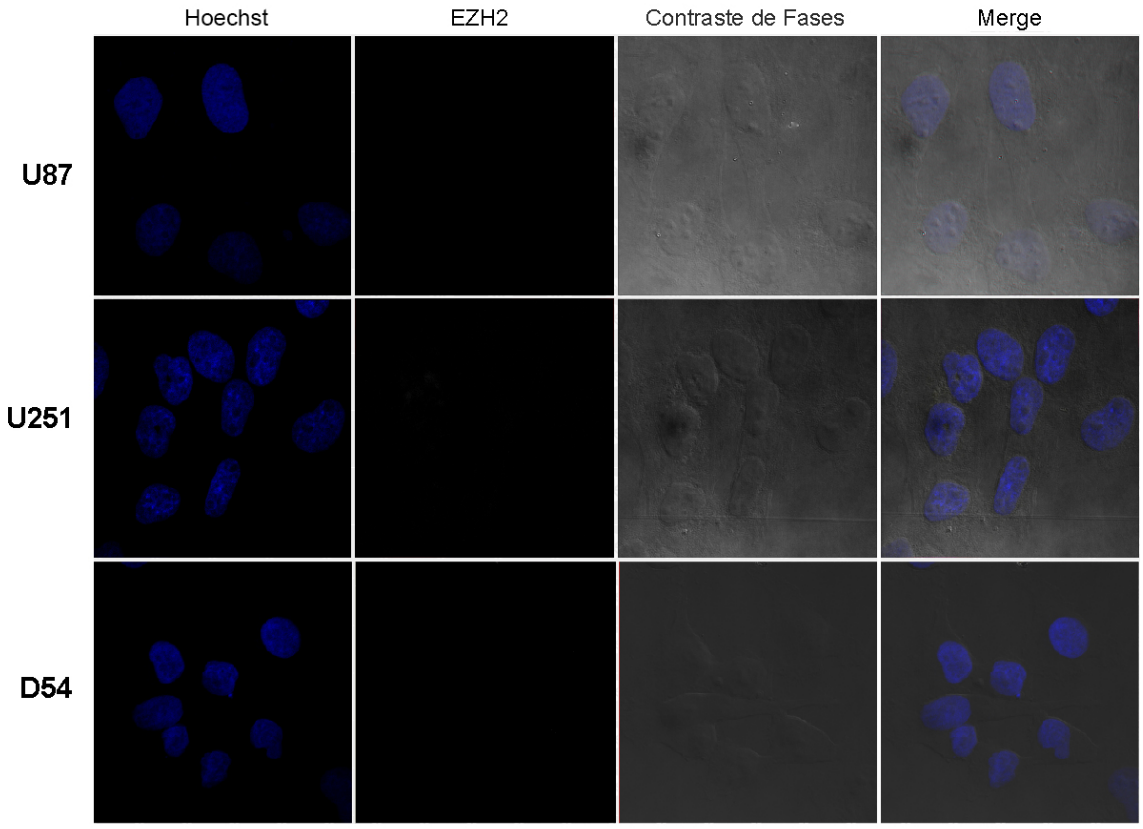

Control negativo del anticuerpo primario contra EZH2 Se cultivaron células en condiciones basales y se realizó la inmunofluorescencia sin el anticuerpo monoclonal contra EZH2, se utilizó un anticuerpo secundario acoplado a Alexa Fluor. Se observa que no se detectó señal en el canal correspondiente a EZH2 pero si se distinguen los núcleos marcados con el colorante Hoechst.

14.2. Artículos relacionados con el proyecto publicados en revistas indizadas.

International Journal of
Molecular Sciences

MDPI

Article

Allopregnanolone Alters the Gene Expression Profile of Human Glioblastoma Cells

Carmen J. Zamora-Sánchez [1], Aylin del Moral-Morales [1], Ana M. Hernández-Vega [1], Valeria Hansberg-Pastor [2], Ivan Salido-Guadarrama [3], Mauricio Rodríguez-Dorantes [3] and Ignacio Camacho-Arroyo [1,*]

1 Unidad de Investigación en Reproducción Humana, Instituto Nacional de Perinatología-Facultad de Química, Universidad Nacional Autónoma de México (UNAM), 04510 Mexico City, Mexico; carmenjzamora@gmail.com (C.J.Z.-S.); aylindmm@hotmail.com (A.d.M.-M.); anahdzvg@gmail.com (A.M.H.-V.)
2 Departamento de Biología, Facultad de Química, Universidad Nacional Autónoma de México (UNAM), 04510 Mexico City, Mexico; valeriahp@gmail.com
3 Instituto Nacional de Medicina Genómica, 14610 Mexico City, Mexico; silvervann@gmail.com (I.S.-G.); mrodriguez@inmegen.gob.mx (M.R.-D.)
* Correspondence: camachoarroyo@gmail.com; Tel.: +52-55-5622-3732; or +52-55-5520-9900

Received: 10 January 2018; Accepted: 23 February 2018; Published: 15 March 2018

Abstract: Glioblastomas (GBM) are the most frequent and aggressive brain tumors. In these malignancies, progesterone (P4) promotes proliferation, migration, and invasion. The P4 metabolite allopregnanolone (3α-THP) similarly promotes cell proliferation in the U87 human GBM cell line. Here, we evaluated global changes in gene expression of U87 cells treated with 3α-THP, P4, and the 5α-reductase inhibitor, finasteride (F). 3α-THP modified the expression of 137 genes, while F changed 90. Besides, both steroids regulated the expression of 69 genes. After performing an over-representation analysis of gene ontology terms, we selected 10 genes whose products are cytoskeleton components, transcription factors, and proteins involved in the maintenance of DNA stability and replication to validate their expression changes by RT-qPCR. 3α-THP up-regulated six genes, two of them were also up-regulated by F. Two genes were up-regulated by P4 alone, however, such an effect was blocked by F when cells were treated with both steroids. The remaining genes were regulated by the combined treatments of 3α-THP + F or P4 + F. An in-silico analysis revealed that promoters of the six up-regulated genes by 3α-THP possess cyclic adenosine monophosphate (cAMP) responsive elements along with CCAAT/Enhancer binding protein alpha (CEBPα) binding sites. These findings suggest that P4 and 3α-THP regulate different sets of genes that participate in the growth of GBMs.

Keywords: allopregnanolone; progesterone metabolites; finasteride; astrocytomas; glioblastomas

1. Introduction

Astrocytomas represent 40–50% of all primary Central Nervous System (CNS) neoplasms and at least 70% of all gliomas. The World Health Organization (WHO) classifies astrocytomas into four grades of malignancy (I–IV) [1]. Grade IV astrocytomas, also known as glioblastoma (GBM), constitute the most common and aggressive brain tumors due to their highly proliferative and infiltrative potential [2]. Steroid hormones such as progesterone (P4), participate in stimulating astrocytomas' growth [3,4].

Neurons and glial cells metabolize P4, and its metabolites exert numerous actions in the CNS. The main metabolic pathway of P4 comprises two reduction reactions: First, the enzyme 5α-reductase (5αR1/2), which irreversibly reduces the double bond on C4–C5 of P4, metabolizes the hormone to 5α-dihydroprogesterone (5α-DHP). Subsequently, 5α-DHP is reduced by the enzyme 3α-hydroxysteroid dehydrogenase (3αHSD) into allopregnanolone (3α-THP) [5,6].

3α-THP is one of the most extensively studied neurosteroids, given its neuroprotective and myelination effects [7,8], and its role in regulating neural stem cells proliferation [9–11]. Regarding its mechanisms of actions, three main pathways have been described: (1) γ-aminobutyric acid receptor A ($GABA_AR$) positive modulation [12]; (2) membrane P4 receptors (mPRs) direct activation [13,14]; and (3) pregnane xenobiotic receptor (PXR) interaction. Different reports show that $GABA_AR$ and mPRs signaling pathways increase cyclic adenosine monophosphate (cAMP) levels thus activating the transcription factor cAMP response binding element protein (CREB) [15], even a crosstalk between both has been suggested [13]. As a ligand-activated transcription factor, PXR induces target gene expression by binding to specific response elements [16].

Recently, we reported that the human GBM cell line U87 expresses 5αR1 and 2. Besides, 3α-THP induces GBM cell proliferation and regulates oncogene expression [17]. Despite these effects, neither the mechanisms of action involved in promoting GBM cell proliferation nor its role in modulating gene expression have been elucidated. Here we report the effects of 3α-THP, P4, and the 5αR inhibitor finasteride (F) on the gene expression profile of U87 cells. Interestingly, both 3α-THP and F induced the expression of genes involved in the maintenance of DNA integrity, DNA replication, and cytoskeleton reorganization.

2. Results

2.1. 3α-THP and F Promote Gene Expression Changes in U87 Cells

Recently, we reported that both 3α-THP and P4 promote U87 cell proliferation after 72 h of treatment [17]. In line with such results, we evaluated the gene expression profile in U87 cells at 72 h of treatment with 3α-THP (10 nM), P4 (10 nM), and F (100 nM). We performed a differential expression analysis by comparing all treatments against the vehicle. The data discussed in this publication have been deposited in NCBI's Gene Expression Omnibus [18] and are accessible through GEO Series accession number GSE108998 at [19]. Our results show that 3α-THP and F changed the expression of 137 and 90 genes respectively, while P4 modified only six (Figure 1a). Most of the differentially expressed genes were up-regulated by 3α-THP and F (132 and 86, respectively), whereas only five and four genes were down-regulated by each steroid, respectively. P4 up-regulated three genes and down-regulated another three (Figure 1a). Additionally, we performed the comparisons between P4 vs. F, 3α-THP vs. P4, and 3α-THP vs. F. In the first comparison, P4 up- and down-regulated five genes. In the second analysis, 3α-THP up-regulated 33 genes, while in the third comparison it up-regulated two and down-regulated three genes (Figure 1a). Then, we investigated if there were transcripts whose levels were regulated by more than one steroid. Interestingly, 3α-THP and F changed the level of 69 transcripts, while 3α-THP and P4 changed the level of one gene. Furthermore, 66 genes were regulated by 3α-THP alone, 20 by F, and four by P4. One gene was regulated by the three steroids (Figure 1b). The lists of the differentially expressed genes are included in the Tables S1–S6. Principal Component Analysis (PCA) graph of normalized files and heatmaps are in the Supplementary Material (Figure S1). PCA reveals that samples were tightly grouped by steroid treatments except P4, which showed a similar distribution as compared with vehicle (Figure S1a). Heatmaps were performed to determine hierarchical clusters of genes up- or down-regulated by 3α-THP, P4, or F in comparison with vehicle (Figure S1b–d) or by the comparison between steroids (Figure S1e–g). These results are summarized in Figure 1a.

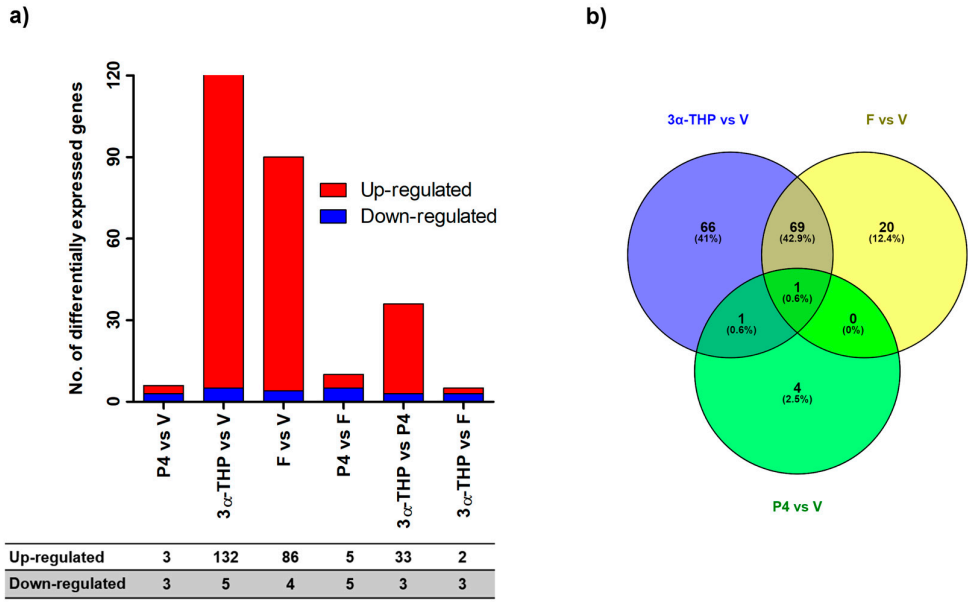

Figure 1. Progesterone (P4), allopregnanolone (3α-THP), and finasteride (F) promote changes in the gene expression profile of U87 cell line. (**a**) The number of differentially expressed genes with a Fc > ±1.5 and $p < 0.05$ between different treatment comparisons. The table shows the number of up- and down-regulated genes. (**b**) The genes that changed their expression under the treatment of P4, 3α-THP, and F vs. vehicle (V), respectively were used to build a Venn's diagram with the program Venny. 3α-THP and F differentially regulated 69 genes while 3α-THP and P4 regulated one, and the three steroids regulated the expression of one transcript.

2.2. 3α-THP and F Increase the mRNA Levels of Proteins Involved in Several Cellular and Metabolic Processes

We performed an enrichment analysis of gene ontology categories using the database PANTHER to identify possible biological processes altered by 3α-THP or F at 72 h of treatment in U87 cells. Cross-examination using the DAVID enrichment algorithm [20,21] confirmed the results. 125 out of the 132 genes up-regulated by 3α-THP treatment were classified under one or more Gene Ontology (GO) categories. The most enriched categories were "cellular process" and "metabolic process", which included 51 and 32 genes, respectively. Other enriched categories were "biological regulation" (23 genes), "cellular component organization or biogenesis" and "localization" each with 16 genes, and "response to stimulus" (15 genes) (Figure 2a,b). Among the 51 enriched genes in the "cellular process" category, a sub-classification analysis showed that twelve genes code for proteins relevant for cell communication, and eleven for cell cycle processes. The rest of the genes were enriched in the sub-categories "chromosome segregation" (3), "cellular component movement" (7), and "cytokinesis" (2). The analysis for the "metabolic process" category showed that among the 32 enriched genes, 27 were sub-classified into "primary metabolic process". The remaining genes were classified into the next categories: biosynthetic process (14), nitrogen compound metabolic process (17), phosphate-containing compound metabolic process (9), and catabolic process (10) (Figure 2a).

According to the GO over-representation analysis for F up-regulated genes (Figure 2a,c), the enriched categories were "cellular process", "biological regulation", and "metabolic process", represented by 51, 23, and 32 genes respectively. The analysis of the "cellular process" category showed the enrichment of nine genes in "cell cycle" and in "cell communication" categories, respectively. The remaining genes were sub-classified in "cellular component movement" (7), "cytokinesis" (3), and "chromosome segregation" (2). Moreover, genes grouped in the category of "metabolic process" were sub-classified into the categories: biosynthetic process (10), nitrogen compound metabolic process

(10), catabolic process (6), and primary metabolic process (17). These data show that both 3α-THP and F could regulate the same type of genes.

a) Gene ontology terms

	Comparisons:	3α-THP vs V		F vs V	
	Category name (accession)	#	%H	#	%H
I	biological regulation (GO:0065007)	23	18.4	14	16.9
II	cellular component organization or biogenesis (GO:0071840)	16	12.8	13	15.7
III	cellular process (GO:0009987)	51	40.8	34	41.0
IV	developmental process (GO:0032502	5	4.0	6	7.2
V	immune system process (GO:0002376)	1	0.8	1	1.2
VI	localization (GO:0051179)	16	12.8	10	12.0
VII	locomotion (GO:0040011)	2	1.6	2	2.4
VIII	metabolic process (GO:0008152)	32	25.6	21	25.3
IX	multicellular organismal process (GO:0032501)	7	5.6	4	4.8
X	reproduction (GO:0000003)	1	0.8	2	2.4
XI	response to stimulus (GO:0050896)	15	12.0	10	12.0

Comparisons:	3α-THP vs V		F vs V	
Cellular process	#	%H	#	%H
cell cycle (GO:0007049)	11	21.6	9	26.5
chromosome segregation (GO:0007059)	3	5.9	2	5.9
cell communication (GO:0007154)	12	23.5	9	26.5
cellular component movement (GO:0006928)	7	13.7	5	14.7
cytokinesis (GO:0000910)	2	3.9	3	8.8

Comparisons:	3α-THP vs V		F vs V	
Metabolic process	#	%H	#	%H
biosynthetic process (GO:0009058)	14	43.8	10	47.6
nitrogen compound metabolic process (GO:0006807)	17	53.1	10	47.6
phosphate-containing compound metabolic process (GO:0006796)	9	28.1	5	23.8
catabolic process (GO:0009056)	10	31.3	6	28.6
primary metabolic process (GO:0044238)	27	84.4	17	81.0

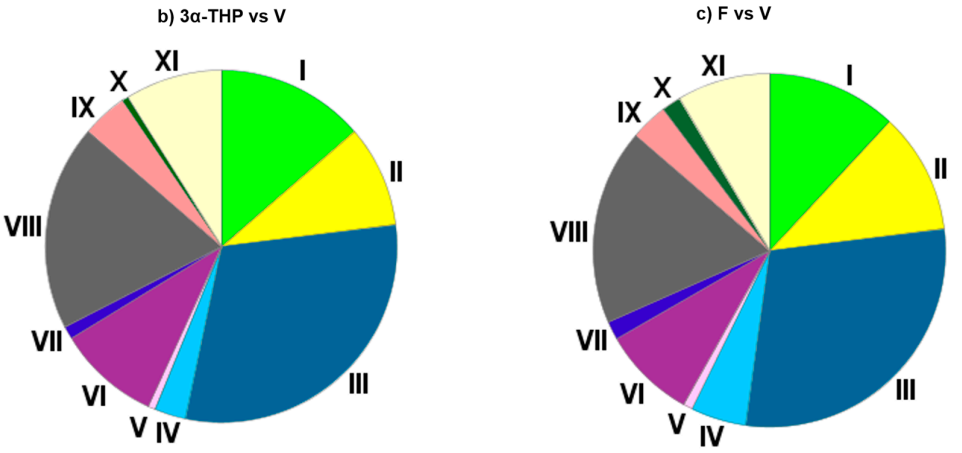

Figure 2. Enrichment analysis of the group of genes regulated by 3α-THP and F. The proteins coded by the differentially expressed genes after 3α-THP and F treatments were analyzed with PANTHER. (**a**) The diverse biological processes (categories) in which the gene products participate are shown in the left table. As the categories of cellular process and metabolic process were ones of the most enriched by 3α-THP and F, we performed a second analysis to determine sub-categories. In the three different tables, the number of genes in each category (column **#**), and the percentage of gene hits against the total number of genes (column %H) for each treatment are indicated. (**b**,**c**) The pie charts show the enriched categories (marked with roman numbers) for the two treatment comparisons.

2.3. 3α-THP and F Increase the Expression Level of Genes Selected for Validation

Considering the results of both the microarrays and the GO over-representation analyses, we chose ten interesting genes that participate in diverse cell processes for validation (their function is described in Table S7). We selected the genes according to their Fc and *p* values, as well as for their occurrence in the most enriched categories (Table 1). However, among the selected genes, *ESF1* and *RIF1* caught our interest due to their high Fc (*ESF1*: Fc = 3.7, $p = 0.010$, *RIF1*: Fc = 2.69, $p = 0.015$) despite not being included in any PANTHER protein class. Besides, *CCDC91* (Fc = 1.68, $p = 0.037$) was enriched in a Golgi-proteins cluster when the gene enrichment analysis was performed in DAVID, but not in PANTHER.

For the gene expression validation, we included the treatments used for the microarray analysis (V, 3α-THP, P4, and F) as well as the combined treatments of P4 + F and 3α-THP + F. The latter two were used to determine if 5αR inhibition interfered with the effects of P4 and to discard the fact that F could affect the actions of 3α-THP. The RT-qPCR experiments shown in Figure 3 denote with grey bars the gene expression changes obtained by the microarray analysis. Accordingly, 3α-THP increased the expression of six out of the ten genes chosen for validation, and F changed the expression levels of only one gene (Figure 3).

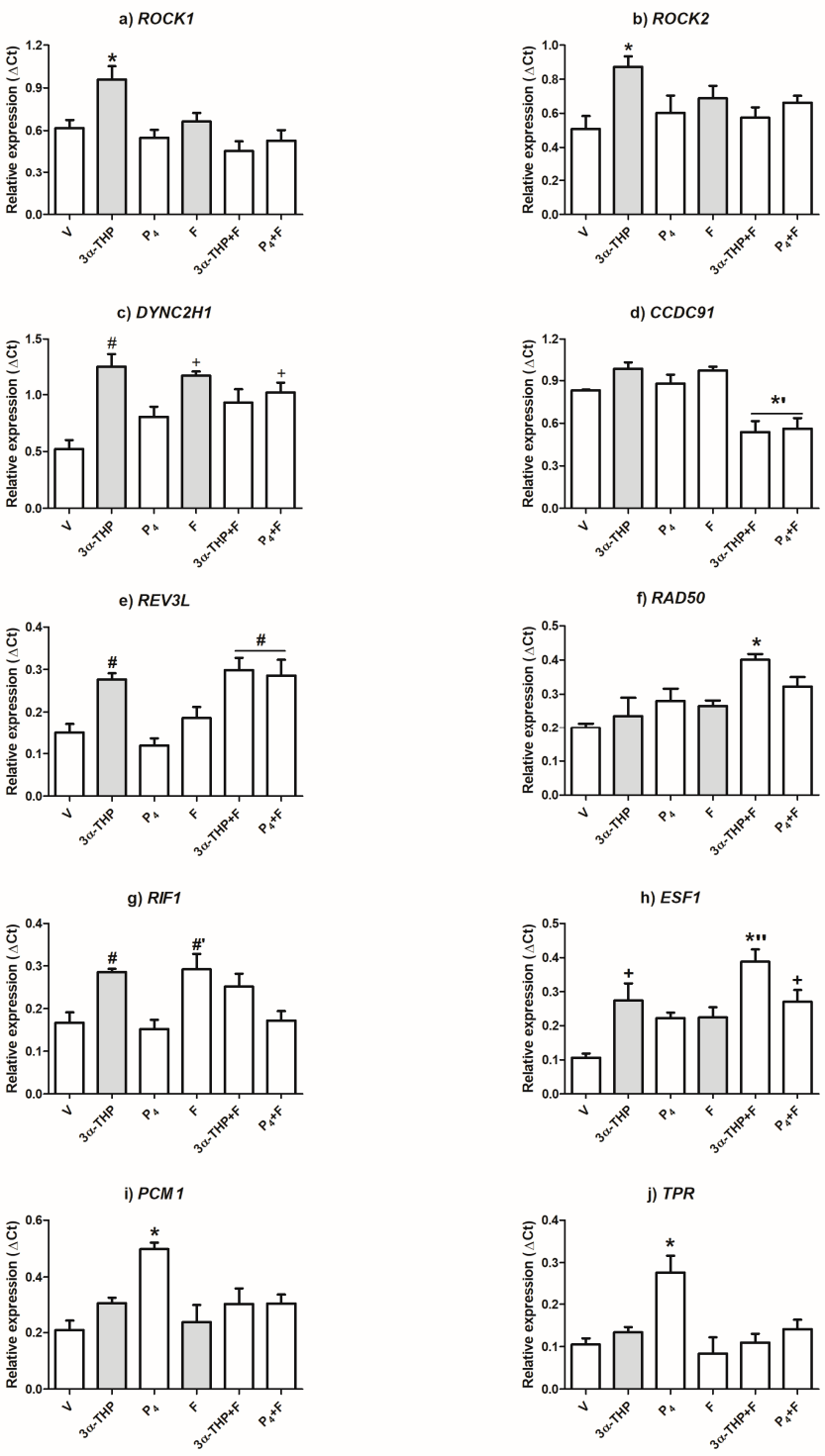

Figure 3. 3α-THP, P4, and F regulate the expression of genes selected for validation. RT-qPCR was used to validate ten genes with a Fc > 1.5 in the microarray analysis. U87 cells were treated for 72 h with 3α-THP (10 nM), P4 (10 nM), F (100 nM), 3α-THP + F, and P4 + F. The internal control gene 18S ribosomal RNA was used to calculate the relative expression of each gene according to the ΔCt mathematic method. The grey bars represent the microarray results of the up-regulated genes by 3a-THP and/or F. Each column represents the mean ± standard error of mean (SEM), $n = 3$. + $p < 0.05$ vs. V; # $p < 0.05$ vs. V, and P4; #′ $p < 0.05$ vs. V, P4, and P4 + F; * $p < 0.05$ vs. all other treatments; *′ $p < 0.05$ vs. V and single treatments; *″ $p < 0.05$ vs. V, P4, and F.

Table 1. The microarray data (Fc and *p*-value) and the ontogeny analysis of the selected genes for validation.

Gene Full Name	Treatment vs. V (Fc)		Treatment vs. V (*p*-Value)		Ontogeny Categories
	3α-THP	F	3α-THP	F	
ESF1 nucleolar pre-rRNA processing protein homolog (*ESF1*)	3.07	2.01	0.0103	0.044	ND
Translocated promoter region, nuclear basket protein (*TPR*)	2.75	-	0.010	-	• Biological regulation • Cellular component organization or biogenesis • Cellular process • Localization
Replication timing regulatory factor 1 (*RIF1*)	2.69	-	0.015	-	ND
RAD50 double-strand break repair protein (*RAD50*)	2.31	2.16	0.010	0.022	• Biological regulation • Cellular component organization or biogenesis • Cellular process • Metabolic process • Reproduction • Response to stimulus
Rho-associated coiled-coil containing protein kinase 1 (*ROCK1*)	1.94	2.04	0.009	0.018	• Cellular process • Developmental process • Localization
Rho-associated coiled-coil containing protein kinase 2 (*ROCK2*)	1.94	1.8	0.041	0.034	• Cellular process • Developmental process • localization
REV3-like, DNA directed polymerase zeta catalytic subunit (*REV3L*)	1.86	-	0.014	-	• Cellular process • Metabolic process
Pericentriolar material 1 protein (*PCM1*)	1.68	1.54	0.037	0.044	• Biological regulation • Cellular component organization or biogenesis • Cellular process • Localization
Dynein cytoplasmic 2 heavy chain 1 (*DYNC2H1*)	1.64	1.55	0.001	0.023	• Cellular process • Localization
Coiled-coil domain containing 91, P56 protein (*CCDC91*)	1.63	-	0.04	-	ND

Note: ND = not determined; - = no changes in gene expression under this comparison.

The microarray experiments showed that ROCK1 and ROCK2 expression increases with 3α-THP and F treatments. Remarkably, the RT-qPCR data indicate that only 3α-THP regulates the expression of these two genes and that F blocked such an effect as shown in the 3α-THP + F treatment (Figure 3a,b). DYNC2H1 expression regulation coincides with the microarray data, and the P4 + F treatment also up-regulated this gene (Figure 3c). Interestingly, the expression level of CCDC91 did not change with any of the single treatments, but it significantly decreased with 3α-THP + F and P4 + F (Figure 3d). The levels of REV3L mRNA augmented with 3α-THP as in the microarray data, and an increase was also observed for both combined treatments (Figure 3e). Concerning RAD50, its expression levels were modified only by 3α-THP + F, but not by the single treatments of 3α-THP and F as expected (Figure 3f). The expression of RIF1 was elevated by 3α-THP according to the microarray results, although F also augmented its expression (Figure 3g). ESF1 was expected to be up-regulated by 3α-THP and F according to the microarray analysis, but the validation showed an increase with the combined treatments (Figure 3h).

Lastly, neither 3α-THP nor F modified the expression of PCM1 or TPR (Figure 3i,j, respectively) as in the microarray data. In the case of both genes, P4 promotes an increase in their expression and F significantly abolished this effect as seen in the combined treatment of P4 + F. As 3α-THP up-regulates the expression of six genes chosen for validation, we explored through a bioinformatic analysis the possible mechanism by which 3α-THP could regulate the expression of such genes.

2.4. CREB1 and CEBPa Could Mediate 3α-THP-Dependent Transcriptional Effects

As 3α-THP regulates the expression of six out of the ten genes chosen for validation, we performed an in-silico analysis for putative transcription factor binding sites (TFBS) in their promoter regions. The bioinformatic analysis focused on the transcription factors CCAAT/Enhancer binding protein alpha (CEBPα), CREB1, and PXR, which are known to participate in 3α-THP mechanisms of action. Four bioinformatic tools were used for the prediction of the TFBS: JASPAR, Unipro UGENE v.1.26.3, UCSC Genome Browser, and TRANSFAC. UGENE software was used to compile the data. Only the binding sites predicted by two or more programs (similarity score > 0.8, $p < 0.05$) were considered as positive hits. The selected genes for this analysis were DYNC2H1 (Figure 4a), ESF1 (Figure 4b), REV3L (Figure 4c), RIF (Figure 4d), ROCK1 (Figure 4e), and ROCK2 (Figure 4f). In every analyzed gene regulatory region, the most abundant TFBS were for CREB1 and CEBPα and few for PXR. Except for REV3L, most of the binding sites are located in the promoter regions. These data suggest that these factors should regulate the 3α-THP-dependent transcription of the selected genes.

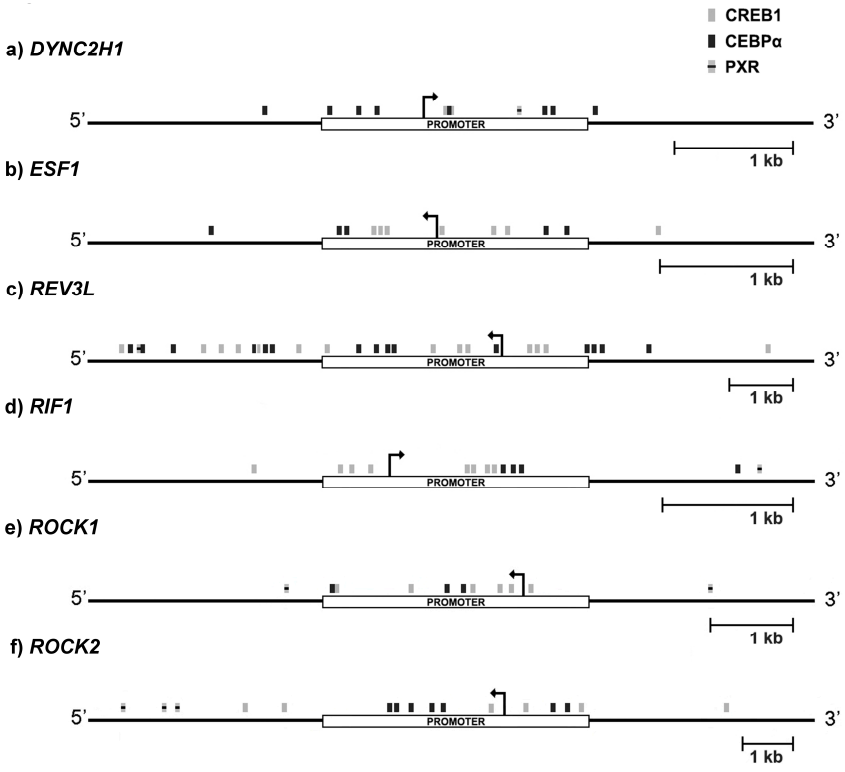

Figure 4. In silico analysis of the regulatory region of the genes up-regulated by 3α-THP. Six of the validated genes were analyzed for their promoter regions and scanned for putative transcription factor binding sites with several bioinformatic tools: JASPAR, UCSC Genome Browser, UGENE, and TRANSFAC. For each gene, a white rectangle indicates the promoter region, and the continuous black lines represent the adjacent regulatory region. Black arrows indicate the transcription start site and the gene transcription direction. The putative binding sites for CREB1 (grey box), CEBPα (black box), and PXR (black lined grey box) are denoted. According to each gene, the scale bar of 1 kb is defined.

3. Discussion

This study aimed to evaluate the gene expression profile changes produced by 3α-THP, P4, and F in U87 cells, and correlate them with our previous proliferation data [17]. First, we performed a PCA of the microarray data after their normalization. Displaying the principal components of the microarray data allows possible batch effects to be identified, such as technical variables affecting the interesting biological variability between conditions [22], in this case, 3α-THP, P4, and F treatments. This analysis let us identify some additional changes in gene expression more precisely related to 3α-THP and F treatments, than with the simple normalization without determining principal components. We found a tight grouping between treatments, except for P4 and V. This correlates with the fact that P4 and vehicle treatments display a very similar expression profile, since P4 altered the expression of only six genes as compared with vehicle. Moreover, the microarray analysis showed that 3α-THP promotes more changes in the gene expression profile of U87 cells than P4. This difference could be due to their specific mechanisms of action. There are two main mechanisms of action of P4: the classical and the non-classical. The first one depends on the binding of P4 to its intracellular receptor (PR) that functions as a transcription factor, and the second one is mediated by mPRs, which are G protein-coupled receptors that activate different signaling pathways involving the production of second messengers (for review see [23]). We and others have reported that P4 induces the expression of cyclins, growth factors such as vascular endothelial growth factor (VEGF) or epidermal growth factor (EGF), and receptors like EGF(R) through PR activation [24]. However, these effects had been detected at 12 h or less of treatment [24,25]. The few changes in gene expression with P4 at 72 h of treatment could be associated with its mechanism of action: once PR is active, the ligand-dependent phosphorylation of the receptor that increases its transcriptional activity [26,27] also promotes its degradation by de 26S proteasome. PR degradation has been reported to occur between 4 and 12 h in breast cancer cells [28], whereas in the human astrocytoma cell line U373 takes 3–5 h [26]. Nevertheless, we have previously reported that 3α-THP promotes U87 cell proliferation in a very similar manner as P4 at 72 h of treatment [17], despite not presenting affinity to PR [29].

Another interesting observation of our microarrays results is that groups of 3α-THP and F are more related in the PCA analysis. According to this, we found many regulated-genes by both F and 3α-THP, than those discovered with a simple normalization and gene expression analysis. F regulates 69 genes also modified by 3α-THP. When the gene ontology analysis of up-regulated genes by 3α-THP or F was performed, we found a higher enrichment in the category of "cellular process", specifically in the subcategories of "cell cycle", "cell communication" and "cell component movement". The category of "metabolic process" was highly enriched in all the subcategories reported. Despite F being a well-known 5αR inhibitor, it also modifies the expression of a wide range of genes in different biological systems [30–32]. However, the mechanisms by which F exerts its agonistic effects are not fully elucidated. Wu (2013) and coworkers proposed that, due to their steroid-based structure, F could interact with the androgen receptor (AR) and modulate the expression of target genes such as the prostate-specific antigen in prostate cancer cell lines. Nevertheless, these effects might depend on the inherent cellular characteristics. Another hypothesis suggests that F and/or other 5αR inhibitors with steroid structure could interfere with the formation of the active complex of the AR and its natural ligand, dihydrotestosterone [33,34]. Besides, F could modify the levels of other steroids susceptible to 5α-reduction including testosterone, androstenedione, aldosterone, cortisol, and deoxycorticosterone. These steroids modulate gene expression, and their effects could be affected by the F treatment [35]. Additionally, there are other P4 metabolites whose synthesis does not directly depend on 5αR. For example, there is 3α-hydroxy-4-pregnen-20-one (3αHP), which is the product of the direct reduction of P4 by the enzyme 3αHSD. This metabolite has a similar mechanism of action as 3α-THP [36], and it is also a positive modulator of $GABA_AR$ [37]. Therefore, F treatment could enhance alternative P4 metabolic pathways as described. Despite the fact that F did not increase proliferation in U87 GBM cell line in our previous work [17], here we suggest that F and 3α-THP should enhance

the malignancy of the cells since the genes regulated by these steroids are related with cell migration, DNA repair and cell cycle.

Particularly interesting is the 3α-THP-dependent regulation of *ROCK1* and *ROCK2* expression, which are key regulators of cell morphology, cell invasion, migration, and proliferation [38–40]. In fact, Rho/ROCK is one of the most important pathways that favors GBM cell migration, as ROCK phosphorylation targets include essential proteins involved in actomyosin contraction [41,42]. Recently, reports show that 3α-THP promotes rat Schwann cell migration in culture [43], suggesting that the induction of ROCK expression should increase GBM cell migration.

Remarkably, both 3α-THP and F regulated RIF1, indicating that other metabolites besides 3α-THP, whose levels might be modified by the treatment of F, could be responsible for this increase. Besides, the promoter of this gene presented many CREB1 binding sites. CREB acts downstream of the signaling pathway of $GABA_AR$, a receptor targeted by 3α-THP and other P4 metabolites. RIF1 is of particular interest, given its relevance for the maintenance of the DNA stability and induction of DNA replication [44,45].

In contrast, 3α-THP, F, and the combined treatment of P4 + F regulate DYNC2H1 expression, suggesting different mechanisms of action promoted by other P4 metabolites such as the ones synthesized by 3αHSD. The cytoplasmic localization of DYNC2H1 protein has been associated with resistance to the primary GBM chemotherapeutic agent temozolomide [46].

Furthermore, *REV3L* and *ESF1* were regulated by 3α-THP and by the two combined treatments, suggesting that the effect of 3α-THP is maintained even with F treatment. Besides, 5αR-independent P4 metabolism could contribute to the up-regulation of such genes when treated with P4 + F. Interestingly, at least one of the combined treatments induced the expression of genes such as *CCDC91* and *RAD50*, and thus, they might be regulated differently. In the case of *TPR* and *PCM1*, both involved in cell division, P4 alone increased the expression of both genes, and its effect was blocked by F as observed in the combined treatment. This result also indicates that the P4-dependent expression of *PCM1* and *TPR* could be mediated by other 5α-reduced metabolites such as 5α-DHP, which can directly activate PR [29].

As mentioned before, reports indicate that 3α-THP could bind to specific mPRs. These receptors comprise the class II of the progesterone and adipoQ receptor family (PAQR) which includes five members: PAQR7 (mPRα), PAQR8 (mPRβ), PAQR5 (mPRγ), PAQR6 (mPRδ), and PAQR9 (mPRε). It has been suggested that the first three members are coupled to inhibitory G-proteins (G_i), whereas the lasts two activate stimulatory G-proteins (G_s) (for review see [47]). The high affinity of 3α-THP for mPRδ [14] could lead to the activation of the adenylyl cyclase, followed by an increase of intracellular cAMP levels, activation of the protein kinase A (PKA), and phosphorylation of CREB transcription factor. In fact, Shimizu and coworkers (2015) reported that H-89, a PKA inhibitor, blocked the effect of 3α-THP on the drebrin clusters density, an important protein in the formation of dendritic spines [15]. The prediction of a high number of CREB binding sites in the promoter region of the validated genes suggests that 3α-THP promote gene expression in a CREB-dependent manner in GBM. Besides, CREB expression and activation is directly related with the astrocytoma grade [48] and participates in the up-regulation of genes involved in DNA repair such as RAD50 as well as genes promoting cell proliferation and cytokinesis in PC12 cells [49]. Interestingly, 3α-THP (10 nM) induces CREB phosphorylation in rat Schwann cells [50]. Also, CREB binding sites are commonly found near CEBPα and CEBPβ sites, and both transcription factors are required to obtain a robust expression of different genes [51,52]. In U87 cells, there is evidence of a high CEBPα expression [53], which led us to determine the presence of CEBPα sites along with CREB sites in the promoter of the validated genes.

Regarding PXR, we cannot discard the possibility that this receptor regulates the expression of the evaluated genes, given that 3α-THP can directly activate it in vivo [16]. PXR modulates the expression of genes whose products are mainly involved in xenobiotic metabolism [54].

This work shows the importance of determining 3α-THP mechanisms of action in GBMs, and to take into consideration steroid hormone metabolism when studying its effects. Besides, it opens new questions regarding the activation of CREB and its participation along with CEBP in regulating the

expression of the validated genes. Nevertheless, it is crucial to determine the role of the studied genes in the molecular and cellular biology of GBMs while considering physiological P4 levels and their metabolites, since they could participate in cancer progression.

4. Materials and Methods

4.1. Cell Culture and Treatments

U87 human glioblastoma cell line (purchased from ATCC, Georgetown, WA, USA) was cultured in phenol red and high glucose Dulbecco's Modified Eagle's medium (DMEM, In vitro, Mexico City, Mexico) supplemented with 10% fetal bovine serum (FBS), 1 mM pyruvate, 2 mM glutamine, and 0.1 mM non-essential amino acids, at 37 °C in a humidified 5% CO_2 atmosphere. 2×10^5 cells were plated in 12-well plates for the microarray experiments. 8×10^4 cells were plated in 6-well plates to validate the microarray data. 24 h before steroids treatments, the medium was changed for phenol red-free and high glucose DMEM (In vitro, Mexico City, Mexico), supplemented with charcoal-stripped FBS. Treatments for microarray analysis were: vehicle (V, 0.1% DMSO), P4 (10 nM), 3α-THP (10 nM), F (100 nM). Treatments for gene expression validation by RT-qPCR were: (V, 0.1% DMSO), P4 (10 nM), 3α-THP (10 nM), F (100 nM), P4 + F and 3α-THP + F (same concentrations) for 72 h; all hormones were purchased from Sigma Aldrich (St. Louis, MO, USA).

4.2. RNA Extraction and Microarrays

After 72 h of treatment, total RNA was extracted by the phenol-guanidine isothiocyanate-chloroform method using TRI Reagent (Molecular Research Center Inc., Cincinnati, OH, USA) according to the manufacturer's recommendations. RNA concentration and purity were determined with the NanoDrop 2000 Spectrophotometer (Thermo Fisher Scientific, Waltham, MA, USA). RNA integrity was assessed on the Agilent 2100 Bioanalyzer (Agilent Technologies, Santa Clara, CA, USA) and the software 2100 Expert. Samples with an RNA integrity number (RIN) value above 8.0 were used for further processing. Microarray experiments were performed in the Microarray Core Facility at the National Institute of Genomic Medicine (INMEGEN, Mexico City, Mexico). The WT cDNA Synthesis and Amplification kit (Thermo Fisher Scientific, Waltham, MA, USA) was used to obtain the double strand cDNA, while the cRNA was obtained by in vitro transcription. The hybridization was performed with the GeneChipTM Human Gene 1.0 ST arrays (Thermo Scientific, Waltham, MA, USA) according to the standard protocol, and exogenous controls were included.

Raw microarray intensity data were pre-processed and quantile normalized using the Transcriptomic Analysis Console (TAC) Software 4.0.1. (Thermo Fisher Scientific). The principal component analysis of the normalized data is shown in Figure S1. We performed an unpaired one-way ANOVA and a false discovery rate (FDR) analysis. For further confirmation, we used different Bioconductor packages in the statistical platform R. We first employed a robust multiarray analysis (RMA) to transform and normalize the data into log2 data. Then, differential expression analysis with the Linear Models of Microarray Data (LIMMA) package was performed using the moderated *t*-test and the Benjamini-Hochberg FDR as statistical analyses. Here, we report the results obtained with the TAC Software 4.0.1. Differential gene expression with a fold change (Fc) <-1.5 or >1.5 and $p < 0.05$ was considered as statistically significant and non-random. After the normalization and statistical analysis of the raw microarray data, all steroid treatments were compared against the vehicle (V, 0.1% DMSO).

The lists of differentially expressed genes among conditions were then exported to Venny 2.1.0 [55], and then to the Protein Analysis Through Evolutionary Relationships (PANTHER) database [56–58] (available at [59]) to determine the biological processes enrichment. With the Database for Annotation, Visualization and Integrated Discovery (DAVID) v6.8 [20,21], available at [60], the ontology results were also confirmed.

4.3. Validation of Selected Differentially Expressed Genes by RT-qPCR

The genes with the highest Fc among treatment comparisons and with relevance in the enriched biological processes were selected. To validate the expression of the chosen genes, we designed oligonucleotides in the primer-BLAST tool from the National Center for Biotechnology Information (NCBI) database available at [61]. The oligonucleotide sequences and the amplicon lengths are shown in Table 2.

Total RNA was extracted after 72 h of treatment with vehicle, P4, 3α-THP, F, P4 + F, and 3α-THP + F as described. The concentration and purity of RNA were determined using the NanoDrop, as well as its integrity in a 1.5% agarose gel electrophoresis. cDNA was synthesized from 1 µg of total RNA using the M-MVL reverse transcriptase according to the manufacturer's instructions (Invitrogen, Carlsbad, CA, USA) with oligo-$dT_{12–18}$ as primers. qPCR was performed in a LightCycler 1.5 using the FastStart DNA Master SYBR Green I reagent (Roche Diagnostics, Mannheim, Germany) according to the manufacturer's protocol. Briefly, 1 µg of cDNA of the previous reaction was used to perform qPCR, and each gene was amplified (Table 2) along with the endogenous reference gene *18S* ribosomal RNA to quantify the relative expression by the Δ*C*t method [62,63]. Duplicate samples for each of the three independent experiments were included.

Table 2. Designed primers used for different gene amplifications.

Gene	Primer Sequence 5′→3′	Amplified Fragment (bp)
ESF1	FW: GCTCCTCGTGCTGATGAGATTA RV: TGCTCTTCCTTCATCCTCTCCT	176
PCM1	FW: TCAAGACAAGAAAAGCGTCTGC RV: GGGCTGAATGTCTGTTCCTACT	180
TPR	FW: TTTGGCACAGTTTCGGCTAC RV: TCTTCCTCAGTTCCTACAGGTG	164
RIF1	FW: TAATAAGGTTCGCCGTGTCTCC RV: CCTTTGGCTGAAGTGGTATTATGC	177
REV3L	FW: TGAGAAATGAGGTGGCTCTAAC RV: CACGGACACGGCTAACATAA	168
RAD50	FW: GCCTCACTCATCATTCGCCT RV: AAGCTGGAAGTTACGCTGCT	168
ROCK1	FW: ATGGAACCAGTACAACAAGCTGA RV: GCATCTTCGACACTCTAGGGC	159
ROCK2	FW: GAAGAGCAGCAGAAGTGGGT RV: GGCAGTTAGCTAGGTTTGTTTGG	170
CCDC91	FW: AAGTCAGGAAACTGTTAAGGCAG RV: ACAGGCTTCTTTGGCGGAT	152
DYNC2H1	FW: GCTTGGCGGAGCAGATTAAA RV: CCAGGATGCCCGATTCAGTAT	159
18S	FW: AGTGAAACTGCAATGGCTC RV: CTGACCGGGTTGGTTTTGAT	167

Note: FW = forward primer; RV = reverse primer. Official full names of the genes are shown in Table 1.

The data were analyzed and plotted in the GraphPad Prism 5 software for Windows XP (GraphPad Software, Version 5.01, La Jolla, CA, USA). The statistical analysis of the relative gene expression levels was one-way ANOVA followed by a Tukey post-hoc test. Values of $p < 0.05$ were considered statistically significant.

4.4. Bioinformatic Analysis of Transcription Factor Binding Sites

The putative transcription factor binding sites (TFBS) analysis for the selected genes was performed using several bioinformatic tools. First, promoters and gene sequences were obtained from the NCBI database [64]. Then, the promoter regions and transcription start site (TSS) were determined with the Ensembl database [65] and confirmed by the Eukaryotic Promoter Database (EPD) [66]. We searched for putative binding sites for CREB1, CEBPα and PXR using JASPAR [67], UCSC Genome Browser [68], Unipro UGENE v.1.26.3 software [69], and TRANSFAC software [70]. For all analyzed genes, we established as potential TFBS the ones predicted by two or more databases with a matrix similarity score greater than 0.8 and a value of $p < 0.05$.

5. Conclusions

In this work, we show that 3α-THP promotes the expression of genes involved in DNA stability maintenance and replication, in the reorganization of the cytoskeleton, and the transport of different cargo compounds in U87 GBM cell line. Besides, F blocked the effects of P4 on the expression of genes involved in cell division (TPR and PCM1), suggesting that the inhibition of 5αR should affect GBM progression. Further investigation is necessary to determine whether F could enhance the malignancy of GMB cells since many genes related to this process were regulated by both 3α-THP and F.

Supplementary Materials: Supplementary materials can be found at www.mdpi.com/1422-0067/19/3/864/s1.

Acknowledgments: This work was financially supported by Consejo Nacional de Ciencia y Tecnología (CONACYT, grant CB250866), Mexico City.

Author Contributions: Carmen J. Zamora-Sánchez and Ignacio Camacho-Arroyo conceived the study and wrote the paper. Carmen J. Zamora-Sánchez, Aylin del Moral-Morales, Ana M. Hernández-Vega and Ivan Salido-Guadarrama performed and analyzed the experiments. Valeria Hansberg-Pastor, Ivan Salido-Guadarrama and Mauricio Rodríguez-Dorantes participated in the experimental design, provided technical assistance and contributed to the preparation of the figures. All authors reviewed the results and approved the final version of the manuscript.

Conflicts of Interest: The authors declare no conflict of interest.

References

1. Ostrom, Q.T.; Gittleman, H.; Liao, P.; Rouse, C.; Chen, Y.; Dowling, J.; Wolinsky, Y.; Kruchko, C.; Barnholtz-Sloan, J. CBTRUS Statistical Report: Primary Brain and Central Nervous System Tumors Diagnosed in the United States in 2008–2012. *Neuro-Oncol.* **2015**, *17*, iv1–iv62. [CrossRef] [PubMed]
2. Schwartzbaum, J.A.; Fisher, J.L.; Aldape, K.D.; Wrensch, M. Epidemiology and molecular pathology of glioma. *Nat. Clin. Pract. Neurol.* **2006**, *2*, 494–503; [CrossRef] [PubMed]
3. Piña-Medina, A.G.; Hansberg-Pastor, V.; González-Arenas, A.; Cerbón, M.; Camacho-Arroyo, I. Progesterone promotes cell migration, invasion and cofilin activation in human astrocytoma cells. *Steroids* **2016**, *105*, 19–25. [CrossRef] [PubMed]
4. Gutiérrez-Rodríguez, A.; Hansberg-Pastor, V.; Camacho-Arroyo, I. Proliferative and Invasive Effects of Progesterone-Induced Blocking Factor in Human Glioblastoma Cells. *Biomed. Res. Int.* **2017**, *2017*, 1295087. [CrossRef] [PubMed]
5. Faroni, A.; Magnaghi, V. The neurosteroid allopregnanolone modulates specific functions in central and peripheral glial cells. *Front. Endocrinol.* **2011**, *2*, 103. [CrossRef] [PubMed]
6. Schumacher, M.; Mattern, C.; Ghoumari, A.; Oudinet, J.P.; Liere, P.; Labombarda, F.; Sitruk-Ware, R.; de Nicola, A.F.; Guennoun, R. Revisiting the roles of progesterone and allopregnanolone in the nervous system: Resurgence of the progesterone receptors. *Prog. Neurobiol.* **2014**, *113*, 6–39. [CrossRef] [PubMed]
7. Djebaili, M.; Guo, Q.; Pettus, E.H.; Hoffman, S.W.; Stein, D.G. The neurosteroids progesterone and allopregnanolone reduce cell death, gliosis, and functional deficits after traumatic brain injury in rats. *J. Neurotrauma* **2005**, *22*, 106–118. [CrossRef] [PubMed]

8. VanLandingham, J.W.; Cutler, S.M.; Virmani, S.; Hoffman, S.W.; Covey, D.F.; Krishnan, K.; Hammes, S.R.; Jamnongjit, M.; Stein, D.G. The enantiomer of progesterone acts as a molecular neuroprotectant after traumatic brain injury. *Neuropharmacology* **2006**, *51*, 1078–1085. [CrossRef] [PubMed]
9. Wang, J.M.; Johnston, P.B.; Ball, B.G.; Brinton, R.D. The neurosteroid allopregnanolone promotes proliferation of rodent and human neural progenitor cells and regulates cell-cycle gene and protein expression. *J. Neurosci.* **2005**, *25*, 4706–4718. [CrossRef] [PubMed]
10. Yu, S.-C.; Ping, Y.-F.; Yi, L.; Zhou, Z.-H.; Chen, J.-H.; Yao, X.-H.; Gao, L.; Wang, J.M.; Bian, X.-W. Isolation and characterization of cancer stem cells from a human glioblastoma cell line U87. *Cancer Lett.* **2008**, *265*, 124–134. [CrossRef] [PubMed]
11. Karout, M.; Miesch, M.; Geoffroy, P.; Kraft, S.; Hofmann, H.D.; Mensah-Nyagan, A.G.; Kirsch, M. Novel analogs of allopregnanolone show improved efficiency and specificity in neuroprotection and stimulation of proliferation. *J. Neurochem.* **2016**, *139*, 782–794. [CrossRef] [PubMed]
12. Pinna, G.; Uzunova, V.; Matsumoto, K.; Puia, G.; Mienville, J.M.; Costa, E.; Guidotti, A. Brain allopregnanolone regulates the potency of the GABA(A) receptor agonist muscimol. *Neuropharmacology* **2000**, *39*, 440–448. [CrossRef]
13. Thomas, P.; Pang, Y. Membrane progesterone receptors: Evidence for neuroprotective, neurosteroid signaling and neuroendocrine functions in neuronal cells. *Neuroendocrinology* **2012**, *96*, 162–171. [CrossRef] [PubMed]
14. Pang, Y.; Dong, J.; Thomas, P. Characterization, neurosteroid binding and brain distribution of human membrane progesterone receptors δ and ε (mPRδ and mPRε) and mPRδ involvement in neurosteroid inhibition of apoptosis. *Endocrinology* **2013**, *154*, 283–295. [CrossRef] [PubMed]
15. Shimizu, H.; Ishizuka, Y.; Yamazaki, H.; Shirao, T. Allopregnanolone increases mature excitatory synapses along dendrites via protein kinase A signaling. *Neuroscience* **2015**, *305*, 139–145. [CrossRef] [PubMed]
16. Langmade, S.J.; Gale, S.E.; Frolov, A.; Mohri, I.; Suzuki, K.; Mellon, S.H.; Walkley, S.U.; Covey, D.F.; Schaffer, J.E.; Ory, D.S. Pregnane X receptor (PXR) activation: A mechanism for neuroprotection in a mouse model of Niemann-Pick C disease. *Proc. Natl. Acad. Sci. USA* **2006**, *103*, 13807–13812. [CrossRef] [PubMed]
17. Zamora-Sánchez, C.J.; Hansberg-Pastor, V.; Salido-Guadarrama, I.; Rodríguez-Dorantes, M.; Camacho-Arroyo, I. Allopregnanolone promotes proliferation and differential gene expression in human glioblastoma cells. *Steroids* 2017. [CrossRef] [PubMed]
18. Edgar, R.; Domrachev, M.; Lash, A.E. Gene Expression Omnibus: NCBI gene expression and hybridization array data repository. *Nucleic Acids Res.* **2002**, *30*, 207–210. [CrossRef] [PubMed]
19. GEO Accession Viewer. Available online: https://www.ncbi.nlm.nih.gov/geo/query/acc.cgi (accessed on 24 February 2018).
20. Huang, D.W.; Sherman, B.T.; Lempicki, R.A. Systematic and integrative analysis of large gene lists using DAVID bioinformatics resources. *Nat. Protoc.* **2009**, *4*, 44–57. [CrossRef] [PubMed]
21. Huang, D.W.; Sherman, B.T.; Lempicki, R.A. Bioinformatics enrichment tools: Paths toward the comprehensive functional analysis of large gene lists. *Nucleic Acids Res.* **2009**, *37*, 1–13. [CrossRef] [PubMed]
22. Leek, J.T.; Scharpf, R.B.; Bravo, H.C.; Simcha, D.; Langmead, B.; Johnson, W.E.; Geman, D.; Baggerly, K.; Irizarry, R.A. Tackling the widespread and critical impact of batch effects in high-throughput data. *Nat. Rev. Genet.* **2010**, *11*, 733–739. [CrossRef] [PubMed]
23. Thomas, P. Characteristics of membrane progestin receptor alpha (mPRα) and progesterone membrane receptor component 1 (PGMRC1) and their roles in mediating rapid progestin actions. *Front. Neuroendocrinol.* **2008**, *29*, 292–312. [CrossRef] [PubMed]
24. Hernández-Hernández, O.T.; González-García, T.K.; Camacho-Arroyo, I. Progesterone receptor and SRC-1 participate in the regulation of VEGF, EGFR and Cyclin D1 expression in human astrocytoma cell lines. *J. Steroid Biochem. Mol. Biol.* **2012**, *132*, 127–134. [CrossRef] [PubMed]
25. González-Arenas, A.; Cabrera-Wrooman, A.; Díaz, N.; González-García, T.; Salido-Guadarrama, I.; Rodríguez-Dorantes, M.; Camacho-Arroyo, I. Progesterone receptor subcellular localization and gene expression profile in human astrocytoma cells are modified by progesterone. *Nucl. Recept. Res.* **2014**, *1*, 1–10. [CrossRef]
26. González-Arenas, A.; Peña-Ortiz, M.Á.; Hansberg-Pastor, V.; Marquina-Sánchez, B.; Baranda-Ávila, N.; Nava-Castro, K.; Cabrera-Wrooman, A.; González-Jorge, J.; Camacho-Arroyo, I. PKCα and PKCδ Activation Regulates Transcriptional Activity and Degradation of Progesterone Receptor in Human Astrocytoma Cells. *Endocrinology* **2015**, *156*, 1010–1022. [CrossRef] [PubMed]

27. Faivre, E.J.; Daniel, A.R.; Hillard, C.J.; Lange, C.A. Progesterone receptor rapid signaling mediates serine 345 phosphorylation and tethering to specificity protein 1 transcription factors. *Mol. Endocrinol.* **2008**, *22*, 823–837. [CrossRef] [PubMed]
28. Lange, C.A.; Shen, T.; Horwitz, K.B. Phosphorylation of human progesterone receptors at serine-294 by mitogen-activated protein kinase signals their degradation by the 26S proteasome. *Proc. Natl. Acad. Sci. USA* **2000**, *97*, 1032–1037. [CrossRef] [PubMed]
29. Rupprecht, R.; Reul, J.M.H.M.; Trapp, T.; Steensel, B.v.; Wetzel, C.; Damm, K.; Zieglgänsberger, W.; Holsboer, F. Progesterone receptor-mediated effects of neuroactive steroids. *Neuron* **1993**, *11*, 523–530. [CrossRef]
30. Tian, H.; Zhao, C.; Wu, H.; Xu, Z.; Wei, L.; Zhao, R.; Jin, D. Finasteride reduces microvessel density and expression of vascular endothelial growth factor in renal tissue of diabetic rats. *Am. J. Med. Sci.* **2015**, *349*, 516–520. [CrossRef] [PubMed]
31. Duarte-Guterman, P.; Langlois, V.S.; Hodgkinson, K.; Pauli, B.D.; Cooke, G.M.; Wade, M.G.; Trudeau, V.L. The aromatase inhibitor fadrozole and the 5-reductase inhibitor finasteride affect gonadal differentiation and gene expression in the frog Silurana tropicalis. *Sex Dev.* **2009**, *3*, 333–341. [CrossRef] [PubMed]
32. Huynh, H.; Seyam, R.M.; Brock, G.B. Reduction of Ventral Prostate Weight by Finasteride Is Associated with Suppression of Insulin-like Growth Factor I (IGF-I) and IGF-I Receptor Genes and with an Increase in IGF Binding Protein 3 Reduction of Ventral Prostate Weight by Finasteride Is Asso. *Cancer Res.* **1998**, *58*, 215–218. [PubMed]
33. Chhipa, R.R.; Halim, D.; Cheng, J.; Zhang, H.Y.; Mohler, J.L.; Ip, C.; Wu, Y. The direct inhibitory effect of dutasteride or finasteride on androgen receptor activity is cell line specific. *Prostate* **2013**, *73*, 1483–1494. [CrossRef] [PubMed]
34. Wu, Y.; Godoy, A.; Azzouni, F.; Wilton, J.H.; Ip, C.; Mohler, J.L. Prostate cancer cells differ in testosterone accumulation, dihydrotestosterone conversion, and androgen receptor signaling response to steroid 5α-reductase inhibitors. *Prostate* **2013**, *73*, 1470–1482. [CrossRef] [PubMed]
35. Azzouni, F.; Godoy, A.; Li, Y.; Mohler, J. The 5 alpha-reductase isozyme family: A review of basic biology and their role in human diseases. *Adv. Urol.* **2012**, *2012*, 530121. [CrossRef] [PubMed]
36. Wiebe, J.P.; Muzia, D.; Hu, J.; Szwajcer, D.; Hill, S.A.; Seachrist, J.L. The 4-pregnene and 5α-pregnane progesterone metabolites formed in nontumorous and tumorous breast tissue have opposite effects on breast cell proliferation and adhesion. *Cancer Res.* **2000**, *60*, 936–943. [PubMed]
37. Beck, C.A.; Wolfe, M.; Murphy, L.D.; Wiebe, J.P. Acute, nongenomic actions of the neuroactive gonadal steroid, 3α-hydroxy-4-pregnen-20-one (3αHP), on FSH release in perifused rat anterior pituitary cells. *Endocrine* **1997**, *6*, 221–229. [CrossRef] [PubMed]
38. Hsu, C.-Y.; Chang, Z.-F.; Lee, H.-H. Immunohistochemical evaluation of ROCK activation in invasive breast cancer. *BMC Cancer* **2015**, *15*, 943. [CrossRef] [PubMed]
39. Katoh, K.; Kano, Y.; Noda, Y. Rho-associated kinase-dependent contraction of stress fibres and the organization of focal adhesions. *J. R. Soc. Interface* **2011**, *8*, 305–311. [CrossRef] [PubMed]
40. Li, B.; Zhao, W.-D.; Tan, Z.-M.; Fang, W.-G.; Zhu, L.; Chen, Y.-H. Involvement of Rho/ROCK signalling in small cell lung cancer migration through human brain microvascular endothelial cells. *FEBS Lett.* **2006**, *580*, 4252–4260. [CrossRef] [PubMed]
41. Qin, E.Y.; Cooper, D.D.; Abbott, K.L.; Lennon, J.; Nagaraja, S.; Mackay, A.; Jones, C.; Vogel, H.; Jackson, P.K.; Monje, M. Neural Precursor-Derived Pleiotrophin Mediates Subventricular Zone Invasion by Glioma. *Cell* **2017**, *170*, 845–859e19. [CrossRef] [PubMed]
42. Xu, S.; Guo, X.; Gao, X.; Xue, H.; Zhang, J.; Guo, X.; Qiu, W.; Zhang, P.; Li, G. Macrophage migration inhibitory factor enhances autophagy by regulating *ROCK1* activity and contributes to the escape of dendritic cell surveillance in glioblastoma. *Int. J. Oncol.* **2016**, *49*, 2105–2115. [CrossRef] [PubMed]
43. Melfi, S.; Montt Guevara, M.M.; Bonalume, V.; Ruscica, M.; Colciago, A.; Simoncini, T.; Magnaghi, V. Src and phospho-FAK kinases are activated by allopregnanolone promoting Schwann cell motility. *J. Neurochem.* **2017**, *141*, 165–178. [CrossRef] [PubMed]
44. Yamazaki, S.; Ishii, A.; Kanoh, Y.; Oda, M.; Nishito, Y.; Masai, H. *RIF1* regulates the replication timing domains on the human genome. *EMBO J.* **2012**, *31*, 3667–3677. [CrossRef] [PubMed]
45. Wang, H.; Zhao, A.; Chen, L.; Zhong, X.; Liao, J.; Gao, M.; Cai, M.; Lee, D.H.; Li, J.; Chowdhury, D.; et al. Human RIF1 encodes an anti-apoptotic factor required for DNA repair. *Carcinogenesis* **2009**, *30*, 1314–1319. [CrossRef] [PubMed]

46. Wang, H.; Feng, W.; Lu, Y.; Li, H.; Xiang, W.; Chen, Z.; He, M.; Zhao, L.; Sun, X.; Lei, B.; et al. Expression of dynein, cytoplasmic 2, heavy chain 1 (DHC2) associated with glioblastoma cell resistance to temozolomide. *Sci. Rep.* **2016**, *6*, 28948. [CrossRef] [PubMed]
47. Valadez-Cosmes, P.; Vázquez-Martínez, E.R.; Cerbón, M.; Camacho-Arroyo, I. Membrane progesterone receptors in reproduction and cancer. *Mol. Cell. Endocrinol.* **2016**, *434*, 166–175. [CrossRef] [PubMed]
48. Daniel, P.; Filiz, G.; Brown, D.V.; Hollande, F.; Gonzales, M.; D'Abaco, G.; Papalexis, N.; Phillips, W.A.; Malaterre, J.; Ramsay, R.G.; et al. Selective CREB-dependent cyclin expression mediated by the PI3K and MAPK pathways supports glioma cell proliferation. *Oncogenesis* **2014**, *3*, e108. [CrossRef] [PubMed]
49. Impey, S.; McCorkle, S.R.; Cha-Molstad, H.; Dwyer, J.M.; Yochum, G.S.; Boss, J.M.; McWeeney, S.; Dunn, J.J.; Mandel, G.; Goodman, R.H. Defining the CREB regulon: A genome-wide analysis of transcription factor regulatory regions. *Cell* **2004**, *119*, 1041–1054. [CrossRef] [PubMed]
50. Magnaghi, V.; Parducz, A.; Frasca, A.; Ballabio, M.; Procacci, P.; Racagni, G.; Bonanno, G.; Fumagalli, F. GABA synthesis in Schwann cells is induced by the neuroactive steroid allopregnanolone. *J. Neurochem.* **2010**, *112*, 980–990. [CrossRef] [PubMed]
51. Routes, J.M.; Colton, L.A.; Ryan, S.; Klemm, D.J. CREB (cAMP response element binding protein) and C/EBPalpha (CCAAT/enhancer binding protein) are required for the superstimulation of phosphoenolpyruvate carboxykinase gene transcription by adenoviral E1a and cAMP. *Biochem. J.* **2000**, *352 Pt 2*, 335–342. [CrossRef]
52. Zhang, J.W.; Klemm, D.J.; Vinson, C.; Lane, M.D. Role of CREB in Transcriptional Regulation of CCAAT/Enhancer-binding Protein β Gene during Adipogenesis. *J. Biol. Chem.* **2004**, *279*, 4471–4478. [CrossRef] [PubMed]
53. Katara, R.; Mir, R.A.; Shukla, A.A.; Tiwari, A.; Singh, N.; Chauhan, S.S. Wild type p53-dependent transcriptional upregulation of cathepsin L expression is mediated by C/EBPa in human glioblastoma cells. *Biol. Chem.* **2010**, *391*, 1031–1040. [CrossRef] [PubMed]
54. Hariparsad, N.; Chu, X.; Yabut, J.; Labhart, P.; Hartley, D.P.; Dai, X.; Evers, R. Identification of pregnane-X receptor target genes and coactivator and corepressor binding to promoter elements in human hepatocytes. *Nucleic Acids Res.* **2009**, *37*, 1160–1173. [CrossRef] [PubMed]
55. Oliveros, J.C. Venny. An Interactive Tool for Comparing Lists with Venn's Diagrams. Available online: http://bioinfogp.cnb.csic.es/tools/venny/index.html (accessed on 31 August 2017).
56. Thomas, P.D. PANTHER: A Library of Protein Families and Subfamilies Indexed by Function. *Genome Res.* **2003**, *13*, 2129–2141. [CrossRef] [PubMed]
57. Mi, H.; Dong, Q.; Muruganujan, A.; Gaudet, P.; Lewis, S.; Thomas, P.D. PANTHER version 7: Improved phylogenetic trees, orthologs and collaboration with the Gene Ontology Consortium. *Nucleic Acids Res.* **2009**, *38*, 204–210. [CrossRef] [PubMed]
58. Thomas, P.D.; Kejariwal, A.; Guo, N.; Mi, H.; Campbell, M.J.; Muruganujan, A.; Lazareva-Ulitsky, B. Applications for protein sequence-function evolution data: MRNA/protein expression analysis and coding SNP scoring tools. *Nucleic Acids Res.* **2006**, *34*, 645–650. [CrossRef]
59. PANTHER—Gene List Analysis. Available online: http://pantherdb.org/ (accessed on 24 February 2018).
60. DAVID Functional Annotation Bioinformatics Microarray Analysis. Available online: https://david.ncifcrf.gov/ (accessed on 24 February 2018).
61. BLAST: Basic Local Alignment Search Tool. Available online: https://blast.ncbi.nlm.nih.gov/Blast.cgi (accessed on 24 February 2018).
62. Pfaffl, M.W. A new mathematical model for relative quantification in real-time RT-PCR. *Nucleic Acids Res.* **2001**, *29*, 2003–2007. [CrossRef]
63. Schmittgen, T.D.; Livak, K.J. Analyzing real-time PCR data by the comparative CT method. *Nat. Protoc.* **2008**, *3*, 1101–1108. [CrossRef] [PubMed]
64. Human Genome Resources at NCBI. Available online: https://www.ncbi.nlm.nih.gov/genome/guide/human/ (accessed on 24 February 2018).
65. Yates, A.; Akanni, W.; Amode, M.R.; Barrell, D.; Billis, K.; Carvalho-Silva, D.; Cummins, C.; Clapham, P.; Fitzgerald, S.; Gil, L.; et al. Ensembl 2016. *Nucleic Acids Res.* **2016**, *44*, D710–D716. [CrossRef] [PubMed]
66. Dreos, R.; Ambrosini, G.; Périer, R.C.; Bucher, P. The Eukaryotic Promoter Database: Expansion of EPDNew and new promoter analysis tools. *Nucleic Acids Res.* **2015**, *43*, D92–D96. [CrossRef] [PubMed]

67. Khan, A.; Fornes, O.; Stigliani, A.; Gheorghe, M.; Castro-Mondragon, J.A.; van der Lee, R.; Bessy, A.; Chèneby, J.; Kulkarni, S.R.; Tan, G.; et al. JASPAR 2018: Update of the open-access database of transcription factor binding profiles and its web framework. *Nucleic Acids Res.* **2018**, *46*, D260–D266. [CrossRef] [PubMed]
68. Kent, W.J.; Sugnet, C.W.; Furey, T.S.; Roskin, K.M. The Human Genome Browser at UCSC W. *J. Med. Chem.* **1976**, *19*, 1228–1231. [CrossRef]
69. Okonechnikov, K.; Golosova, O.; Fursov, M.; Varlamov, A.; Vaskin, Y.; Efremov, I.; German Grehov, O.G.; Kandrov, D.; Rasputin, K.; Syabro, M.; et al. Unipro UGENE: A unified bioinformatics toolkit. *Bioinformatics* **2012**, *28*, 1166–1167. [CrossRef] [PubMed]
70. Matys, V. TRANSFAC(R) and its module TRANSCompel(R): Transcriptional gene regulation in eukaryotes. *Nucleic Acids Res.* **2006**, *34*, D108–D110. [CrossRef] [PubMed]

© 2018 by the authors. Licensee MDPI, Basel, Switzerland. This article is an open access article distributed under the terms and conditions of the Creative Commons Attribution (CC BY) license (http://creativecommons.org/licenses/by/4.0/).

Life Sciences 230 (2019) 111–120

Contents lists available at ScienceDirect

Life Sciences

journal homepage: www.elsevier.com/locate/lifescie

Hypothyroidism induces uterine hyperplasia and inflammation related to sex hormone receptors expression in virgin rabbits

Julia Rodríguez-Castelán[a,b], Aylin Del Moral-Morales[c], Ana Gabriela Piña-Medina[d], Dafne Zepeda-Pérez[e], Marlenne Castillo-Romano[e], Maribel Méndez-Tepepa[a], Marlen Espindola-Lozano[a], Ignacio Camacho-Arroyo[c], Estela Cuevas-Romero[f,*]

[a] Doctorado en Ciencias Biológicas, Universidad Autónoma de Tlaxcala, Tlaxcala, Mexico
[b] Departamento de Neurobiología Celular y Molecular, Instituto de Neurobiología, Universidad Nacional Autónoma de, Mexico
[c] Unidad de Investigación en Reproducción Humana, Instituto Nacional de Perinatología-Facultad de Química, Universidad Nacional Autónoma de México, Ciudad de México, Mexico
[d] Facultad de Química, Departamento de Biología, Universidad Nacional Autónoma de México, Ciudad de México, Mexico
[e] Maestría en Ciencias Biológicas, Universidad Autónoma de Tlaxcala, Tlaxcala, Mexico
[f] Centro Tlaxcala de Biología de la Conducta, Universidad Autónoma de Tlaxcala, Tlaxcala, Mexico

ARTICLE INFO

Keywords:
Estrogen receptor
Progesterone receptor
Thyroid hormone receptor
Perilipin
Malondialdehyde
Vascular endothelial growth factor

ABSTRACT

Aims: In women, uterine alterations have been associated with sex steroid hormones. Sex hormones regulate the expression of thyroid hormone receptors (TRs) in the uterus, but an inverse link is unknown. We analyzed the impact of hypothyroidism on histological characteristics, vascular endothelial growth factor (VEGF-A), progesterone receptors (PR), estrogen receptors (ER), thyroid hormone receptors (TRs), perilipin (PLIN-A), and lipid content in the uterus of virgin rabbits.

Main methods: Twelve Chinchilla-breed adult female rabbits were grouped into control (n = 6) and hypothyroid (n = 6; 0.02% of methimazole for 30 days). The thickness of endometrium and myometrium, number of uterine glands, and infiltration of immune cells were analyzed. The expression of VEGF-A, PR, ERα, and PLIN-A was determined by RT-PCR and western blot. The uterine content of triglycerides (TAG), total cholesterol (TC), and malondialdehyde (MDA) was quantified.

Key findings: Hypothyroidism promoted uterine hyperplasia and a high infiltration of immune cells into the endometrium, including macrophages CD163+. It also increased the expression of VEGF-A, TRA, and ERα-66 but reduced that of PR and ERα-46. The uterine content of PLIN-A, TAG, and TC was reduced, but that of MDA was augmented in hypothyroid rabbits.

Significance: Our results suggest that uterine hyperplasia and inflammation promoted by hypothyroidism should be related to changes in the VEGF-A, PR, ER, and TRs expression, as well as to modifications in the PLIN-A expression, lipid content, and oxidative status. These results suggest that hypothyroidism should affect the fertility of females.

1. Introduction

In women, endometriosis, uterine hyperplasia, dysfunctional uterine bleeding and myomas have been associated with alterations in serum levels of estradiol (E2), testosterone, and progesterone (P4) [1,2], as well as with changes in the uterine expression of progesterone (PRs) and estrogen (ERs) receptors [3,4]. Uterine alterations have also been related to a high expression of vascular endothelial growth factor (VEGF) [5], immune cells infiltration [5,6], and significant uterine lipid peroxidation [7]. Furthermore, uterine abnormalities are correlated with dyslipidemias and body weight gain [8], and recently with hypothyroidism [9–12].

Particularly, the impact of hypothyroidism on the uterus has been mostly studied in pregnant laboratory animals. In rats, this thyroid dysfunction increases gestational length, modifies myometrial contractions, and decreases litter size [13]. It also modifies the expression of thyroid hormones receptors (TRs) [14], promotes inflammation and alters the immune profile in the uterus affecting the trophoblast migration [15]. In rabbits, hypothyroidism reduces the thoracic size of embryos and increases the thickness of the endometrium, as well as

* Corresponding author at: Centro Tlaxcala de Biología de la Conducta, Universidad Autónoma de Tlaxcala, Carretera Tlaxcala-Puebla Km 1.5, C.P. 90062, Mexico.
E-mail address: ecuevas@uatx.mx (E. Cuevas-Romero).

https://doi.org/10.1016/j.lfs.2019.05.063
Received 12 March 2019; Received in revised form 22 May 2019; Accepted 23 May 2019
Available online 24 May 2019
0024-3205/ © 2019 Elsevier Inc. All rights reserved.

reduces the content of total cholesterol (TC) and triacylglycerol (TAG), and the expression of 3β-hydroxysteroid dehydrogenase (3β-HSD) in the uterine horn [16]. However, there are limited studies about the effect of hypothyroidism on the uterus from non-pregnant animal models. In young rats, hypothyroidism induces a low uterine anti-oxidative status [17]. A reduction in the uterus volume and luminal epithelium thickness have been found in hypothyroid non-pregnant rats [18]. It is necessary to perform more studies to analyze the impact of hypothyroidism on the uterus of non-pregnant animals.

The TRs and thyrotropin receptors (TSHR) are present in the endometrium and myometrium [19,20]. The expression or activity of these receptors can be modified by circulating E2 and P4 [16,21,22]. In contrast, the influence of thyroid hormones on the uterine expression of ERs and PRs is little known.

The present study aimed to analyze the impact of hypothyroidism on the histology, immune cells infiltration, vascularization, and expression of VEGF-A, PRs, ERα, TRs, and perilipin (PLIN-A), as well as the lipid content and lipid peroxidation in the uterus of adult virgin female rabbits.

2. Material and methods

Twelve chinchilla-breed nulliparous female rabbits (*Oryctolagus cuniculus*, 8–9 months of age) were housed under controlled temperature (20 ± 2 °C) and light: dark cycle of 16:8 h. This condition maintained most females in early proestrus [23]. They were daily provided with pellet food (120 g/day) and tap water *ad libitum*. Hypothyroidism was induced with a one-month administration of 0.02% methimazole (Sigma, MO, USA; approximate diary dosage of 10 mg/kg) in drinking water for 30 days. This treatment is useful to induce hypothyroidism in female rabbits [24]. At the end of this treatment, control (n = 6) and hypothyroid (n = 6) rabbits were anesthetized with sodium pentobarbital (90 mg/kg, i.p.), and subsequently euthanized with an overdose of the same anesthetic. Cardiac blood was obtained and serum concentrations of total triiodothyronine (T3), thyroxine (T4) and free T4 were quantified using chemiluminescence by the Diagnóstico Molecular y Servicio de Referencia S.A. de C.V. (Diagmo laboratory; México). Immediately after death, right and left uterine horns were excised. The Ethics Committee from the Universidad Autónoma de Tlaxcala approved this experimental design, according to the Guidelines of the Mexican Law for Production, Care and Use of Laboratory Animals.

A piece from the middle portion of the left uterine horn was collected and histologically processed to be cut in the cryostat at 5 μm. Another piece from the middle portion of the left uterine horn was embedded in paraplast X-tra (Sigma, MO, USA) and transversally cut at a thickness of 5 μm using a microtome (Thermo Scientific, Model Finesse 325, MA, USA). The middle portion of the right uterine horn was frozen at −80 °C for biochemical measures.

2.1. Morphometry of the uterine horns

One slide with six slices of the left uterine horn cut with microtome per animal was deparaffinized, rehydrated and stained with Masson's trichrome. Slides were observed and photographed. In the best-stained slice, pictures at 4× (Zeiss Axio Imager A1, Oberkochen, Germany) were taken. The area covered by endometrium and thickness of endometrium and myometrium (in 20 microscopic fields from one slice per animal) were measured using the software AxioVision 4.8 (Carl Zeiss Micro Imaging, Inc.). Histograms of the measurements for the thickness of endometrium and myometrium were obtained, and the percentage of the measurements > 1400 μm for endometrium and > 1000 μm for myometrium were calculated. In pictures at 400 magnifications, randomly pictures from 16 microscopic fields of the endometrium were taken per rabbit. The number, thickness and external cross-sectional area (CSA) of closed uterine glands were measured. The number of uterine fused glands was also counted. Moreover, the number of blood vessels and areas covered by them were quantified in 8 random fields per uterus. Additionally, other slides were stained with hematoxylin-eosin to detect the presence of immune cells inside epithelium in pictures at 1000 magnifications in 30 microscopic fields randomly selected.

Other slides were deparaffinized and processed for immunohistochemistry. Endogenous peroxidases were quenched, and endogenous binding was blocked with 10% of donkey serum (Jackson Immuno Research Inc. PA, USA). Independent sections were incubated with primary antibody to detect macrophages CD163 positives (1:20, goat polyclonal antibody Santa Cruz Biotechnology, TX, USA; sc-18794) for overnight at 4 °C. Subsequently, they were incubated with secondary antibodies (1:250; donkey anti-goat antibody Santa Cruz Biotechnology, TX, USA) and diluted in PBST for 2 h at 37 °C. Immunostaining was developed using the ABC method and sections were washed and counterstained with Mayer's hematoxylin. Macrophages CD163 positives secrete both pro- and anti-inflammatory cytokines and pro-angiogenic factors [25].

2.2. Expression of VEGF, ERα, PR, TRA, TRB, and PLIN in the uterine horns

A portion of the right uterine horn (~50 mg) was homogenized in trizol reagent (Invitrogen, CA, USA) according to manufacturer's protocol. The quantity and purity of RNA were measured using a NanoDrop 2000 spectrophotometer (Thermo Scientific, MA, USA). The RNA integrity was determined by electrophoresis. For this, 1 μg of each RNA sample in a 1.5% agarose gel with 0.5× tris-borate buffer (TB), and only total RNA samples with 260/280 and 230/260 relations close to 2.0, and integrity represented by two defined 28S and 18S bands without smear visualized on an agarose gel were used for RT-PCR. Then, 1 μg of RNA was used to synthesize the first-strand cDNA with the Moloney murine leukemia virus (M-MLV) reverse transcriptase (Thermo Scientific, MA, USA) following the manufacturer's instructions. Posteriorly, 2 μl of this reaction were subjected for PCR to amplify VEGF-A, PR, ERα and thyroid hormone receptors (alpha, TRA; and beta, TRB). Sense and antisense primers were purchased from Sigma-Aldrich (MO, USA). Table 1 contains all the information of the primers for PCR. Negative controls without cDNA were included in all experiments. The PCR reaction was performed as follows: an initial PCR activation step at 94 °C (5 min), 30 cycles of denaturation at 94 °C (20 s), annealing at 60 °C (30 s), and elongation at 72 °C (30 s). A final extension cycle was performed at 72 °C (3 min). The number of cycles performed was within the exponential phase of the amplification process. PCR products were separated by electrophoresis in a 1.5% agarose gel at 70 V for 120 min and stained with EpiQuik (Epigentek, NY, USA). The gel image was captured under a UV trans-illuminator and analyzed for band densitometry using the Image J software (National Institute of Health, USA). The expression of VEGF-A, PR, ERα, TRA, and TRB was

Table 1
Primers used for gene amplifications.

Gene	Primer sequence	Amplified fragment
VEGF-A	FW: 5′-CCACACCGCCACCACCGACA-3′	149
VEGF-A	RV: 5′-CCAATTCCAAGAGGGCCCGT-3′	
PR	FW: 5′-GTCCTTGGAGGGCGAAAGTT-3′	163
PR	RV: 5′-ACAGGTTGATTAGAGGGGGA-3′	
ERα	FW: 5′-AGGGTTCCAGGCTTTGTGGA-3′	181
ERα	RV: 5′ CCACCATGCCCTCTACACATT-3′	
THRA	FW: 5′-ACAGTGCCAGGTCACCAGAT-3′	195
THRA	RV: 5′-GGATTGTGCGGCGAAAGAAG-3′	
THRB	FW: 5′-ACCTTGAACGGGGAAATGGC-3′	170
THRB	RV: 5′-CCTGGGCGATCTGAGGACAT-3′	
18S	FW: 5′-AGTGAAACTGCAATGGCTC-3′	167
18S	RV: 5′-CTGACCGGGTTGGTTTTGAT-3′	

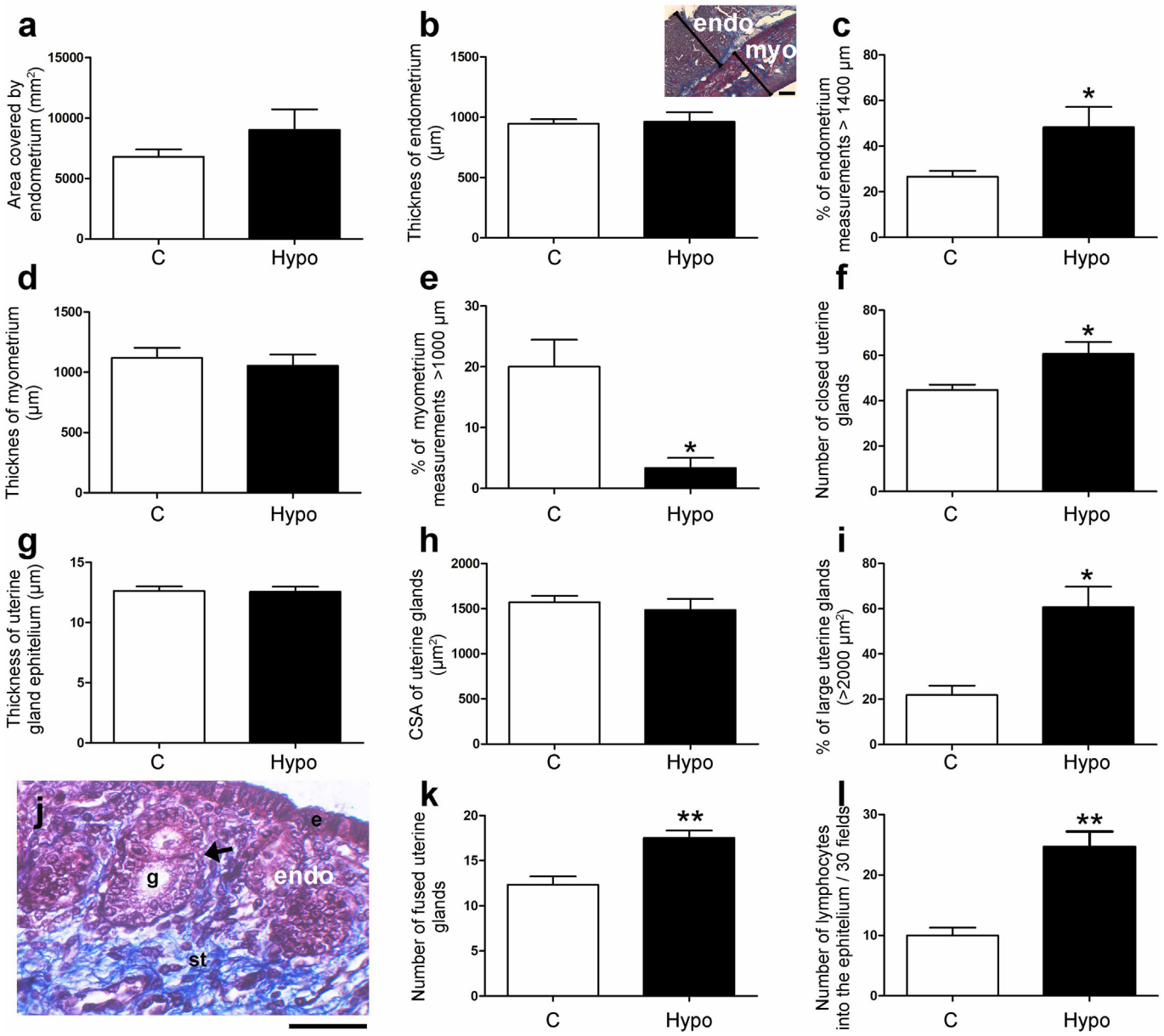

Fig. 1. Histological characteristics of the uterine horn from control (C, white bars) and hypothyroid (hypo, black bars) rabbits. Endometrium (endo; **a,** area covered; **b,** thickness; and **c,** percentage of measurements > 1400 µm). Myometrium (myo; **d,** thickness; **e**; percentage of measurements > 1000 µm). Uterine glands (**f,** number of closed glands; **g**, thickness of epithelium; **h**, CSA of glands; **i**, percentage of large glands; **j**, examples of fused glands; **k**, number of fused glands; and **l**, infiltration of lymphocytes). Results are expressed as mean ± S.E.M. $*p \leq 0.05$; $**p \leq 0.01$. Other abbreviations: g, uterine gland; st, stroma, e, epithelium. Scale: b = 400 µm and j = 50 µm. Arrow indicates a fused uterine gland.

normalized to that of the internal control 18S rRNA.

A portion of the right uterine horn (~50 mg) was disrupted in lysis buffer as reported elsewhere [26]. Total proteins were obtained by centrifugation at 15000 rpm, at 4 °C for 30 min and quantified using a NanoDrop 2000 spectrophotometer (Thermo Scientific, MA, USA). Protein extracts (VEGF-A, 20 µg; ERα, 30 µg; PR, 60 µg; and PLIN-A, 30 µg) were resolved onto SDS-PAGE and transferred to nitrocellulose membranes (Bio-Rad Laboratories Headquarters, CA, USA). The PLIN-A regulates the lipid storage into droplets on tissues [27], and its expression is regulated by hypothyroidism in the ovary [26]. Membranes were stained with Ponceau's Red to confirm that protein content was equal in all lines. Membranes were soaked as indicated: 3.0% nonfat dry milk plus 2.0% bovine serum albumin (BSA) (PLIN-A, PR, and ERα) or 15% non-dry milk (VEGF-A), all diluted in PBS containing 0.2% Tween-20 (PBST). Then, they were incubated overnight at 4 °C with the following antibodies: rabbit polyclonal anti VEGF-A (0.5 µg/ml; Santa Cruz Biotechnology, sc-152); goat polyclonal anti PLIN-A (1 µg/ml, Abcam, MA, USA; ab60269), mouse monoclonal anti-PR (1 µg/ml, Abcam, ab58565) and mouse monoclonal anti-ERα (0.5 µg/ml; Santa Cruz Biotechnology, TX, USA; sc-8002). Following an incubation with a secondary antibody (VEGF-A: 1:20000 mouse anti-rabbit; Santa Cruz Biotechnology, sc-2357; PLIN-A: 1:2000 mouse anti-goat, Santa Cruz Biotechnology, sc-2354; PR and ERα: 1:5000 goat anti-mouse; Pierce, 1,858,413) conjugated with horseradish peroxidase at room temperature under constant agitation for 45 min. Chemiluminescent signals were detected exposing membranes to Kodak Biomax Light films (Sigma-Aldrich, MO, USA) using a chemiluminescence kit (West Pico Signal, Thermo Scientific, MA, USA). The band density for the antigen-antibody complex was calculated in a semi-quantitative way using a 14.1 megapixels digital Canon camera (SD1400IS, Canon, Mexico) and

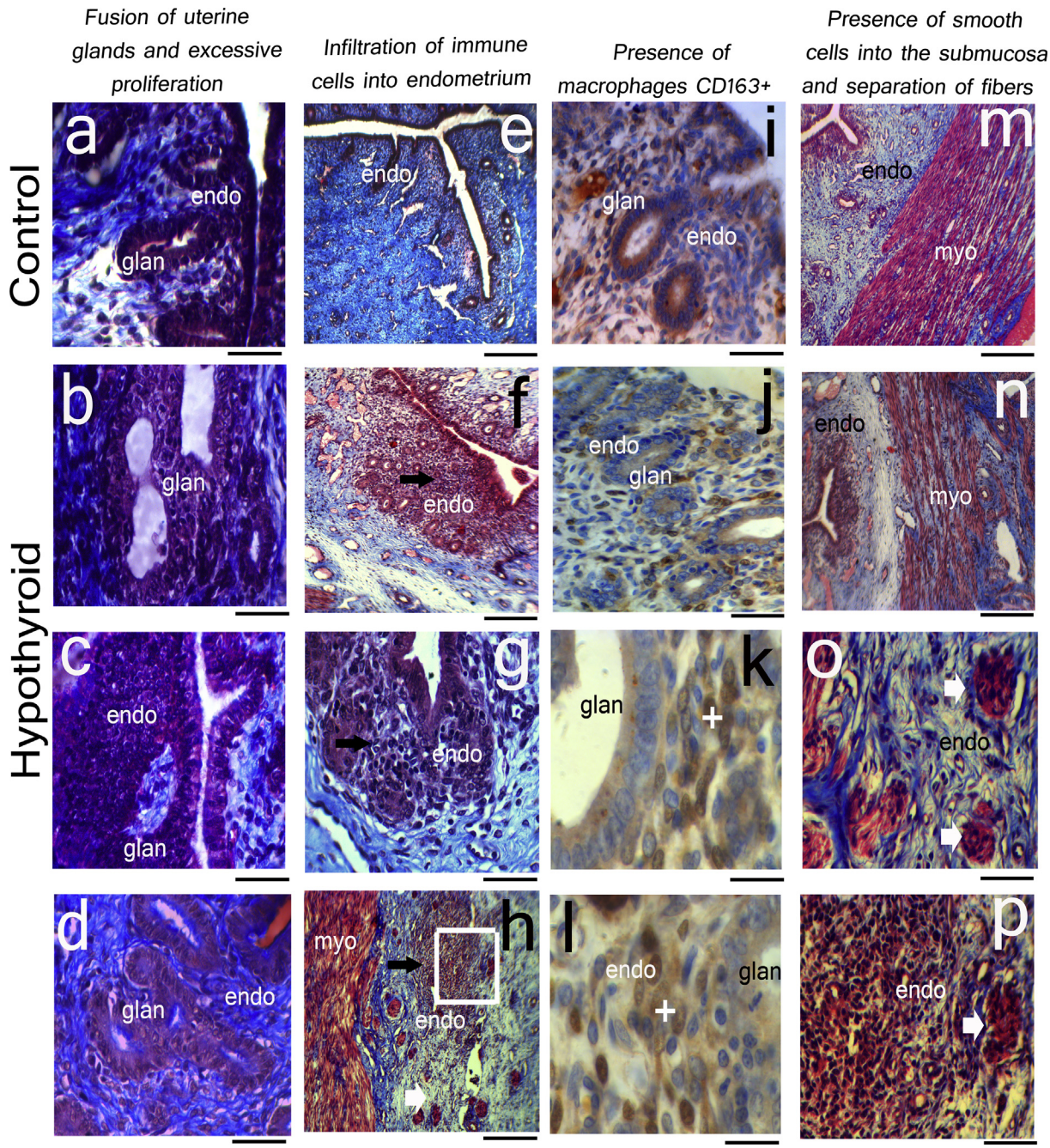

Fig. 2. Characteristics of the endometrium (endo) and myometrium (myo) of control and hypothyroid rabbits. Compared to control (**a**), hypothyroidism promoted the thickening of the glandular epithelium and the fusion of uterine glands (glan; **b–d**). A great infiltration of immune cells (black arrows) into the endometrium was observed in hypothyroid rabbits (**f–g**), even showing some points of inflammation (**h**) that were not observed in the uterus from control rabbits (**e**). Many of these immune cells were macrophages CD163+ (+) (control, **i**; hypothyroid, **j–l**). The organization of smooth muscle fibers of the myometrium was compacted in the control group (**m**) but separated in the hypothyroid group (**n**). Also, groups of smooth muscle cells were observed into the endometrium (white arrows; **o–p**) near inflammatory points. The picture **p** is the enlargement from the white square of the picture **h**. Scale a–d, g, i–j, and o–p = 50 μm; e–f, h, and m–n = 500 μm; k–i = 20 μm.

the Image J 14.45S software (National Institute of Health, USA). To correct differences in the total protein loaded in each lane VEGF-A, PR, ERα, and PLIN-A, protein content was normalized to that of α-tubulin. Therefore, blots were stripped with a 0.1 M glycine solution (pH 2.5, 0.5% SDS) for 2 h at 37 °C and incubated with mouse monoclonal anti-α-tubulin (0.7 μg/ml, Santa Cruz Biotechnology, sc-5286) at 4 °C overnight. Blots were then incubated with a goat-anti-mouse secondary antibody (1:5000; Pierce, 1,858,413) at room temperature for 45 min under constant agitation. Immunoblot chemiluminescent signals were detected as described.

2.3. Lipids in the uterine horns

The quantification of TC and TAG were done in samples of the right uterine horn (~100 mg) by using the method of Folch as reported elsewhere [16]. Enzymatic method-based kits of ELITech Clinical Systems (Sees, France) were used to measure TC (CHSL-0507) and TAG (TGML-0425). Uterine TC and TAG concentrations were expressed as mg of TC or TAG per gram of the uterus.

A portion of the right uterine horn (25 mg) was homogenated in ice-cold tris-buffer (20 mM, pH 7.4) and centrifuged at 3000 rpm for 10 min

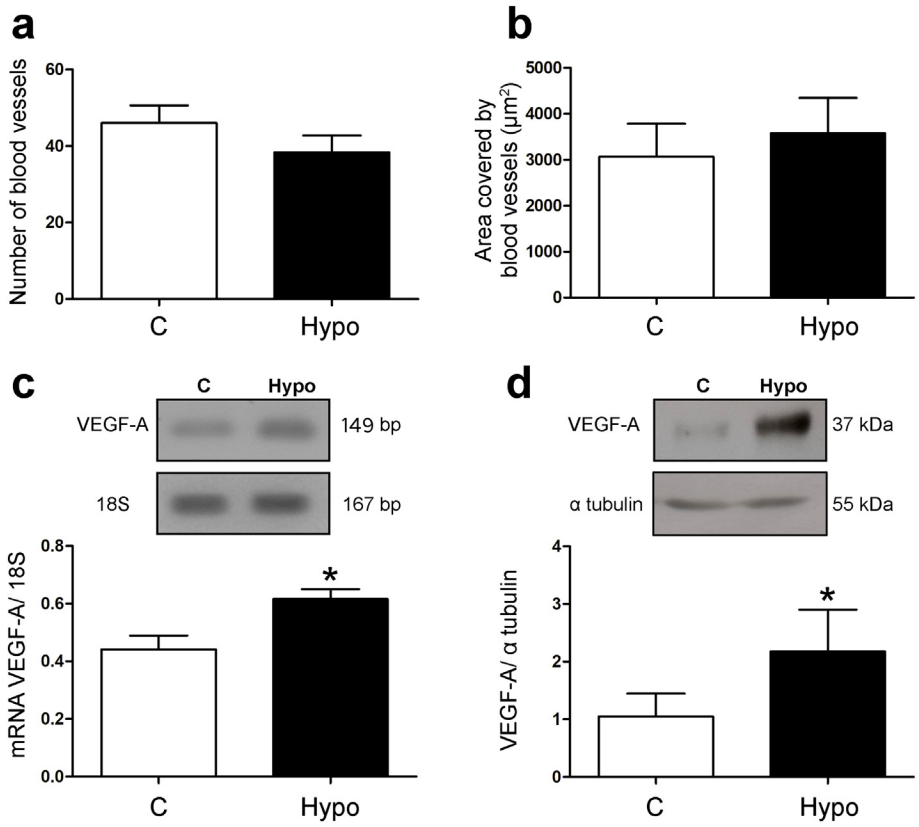

Fig. 3. (**a, b**) Blood vessel characteristics in the uterine horn from control (C, white bars) and hypothyroid (hypo, black bars) rabbits. Representative PCR or western blot (upper panel) and densitometry analysis showing the VEGF-A mRNA (**c**) and protein (**d**) expression in the uterine horn. Results are expressed as mean ± S.E.M. *$p \leq 0.05$.

at 4 °C, and then the supernatant was collected and immediately tested for lipid peroxidation with ALDetect lipid peroxidation assay kit (BML-AK170-0001, Enzo Life Sciences, Ann Arbor, MI, USA). The kit uses a chromatographic reagent which reacts with malondialdehyde (MDA) at 70 °C, yielding a stable chromophore with maximum absorbance at 586 nm. Uterine MDA concentrations were expressed as µM de MDA/ mg of the uterus.

Additionally, a slide with left uterine horn slices cut in cryostat was stained with Sudan black to detect oxidative lipids, counterstained with Harris hematoxylin, and mounted in glycerol. Sections were observed in a light microscope (Zeiss Axio Imager A1, Oberkochen, Germany) and pictures were made with a digital camera (ProgRES, Jenoptik, Jena Germany) at 400 and 1000 magnifications. The presence of granules of oxidative lipids in the endometrium (luminal epithelium, uterine glands, and stroma) was evaluated semi-qualitatively as previously described [26]. Categories were established: (+++) for a high proportion of stained granules; (++) for a moderate proportion of stained granules; and (+) for a low proportion of stained granules.

2.4. Statistical analysis

Statistical analyses were performed with the GraphPad Prism v 5.01 software (GraphPad Sofware, Inc., CA, USA). Results were expressed as mean ± S.E.M. Student *t*-tests were performed to determine significant differences between control and hypothyroid rabbits. The values of $p \leq 0.05$ were considered statistically significant.

3. Results

The area covered by the endometrium and their media thickness was similar between control and hypothyroid groups (Fig. 1a–b; see in the picture the measurements for the thickness of endometrium and myometrium). However, the percentage of the measurements of the thickness of the endometrium (> 1400 µm) was significantly high in the hypothyroid group (Fig. 1c). No differences were found in the thickness of myometrium between groups (Fig. 1d), but a low percentage of measurements > 1000 µm were found in the hypothyroid group (Fig. 1e). The number of closed uterine glands was higher in hypothyroid dams (Fig. 1f), but the thickness and the CSA of closed uterine glands were not modified (Fig. 1g–h). The percentage of large uterine glands (> 2000 µm^2) was higher in the hypothyroid group (Fig. 1i). Hypothyroidism also increased the number of fused uterine glands, which were commonly found near the luminal epithelium (Fig. 1j–k). The number of lymphocytes into the luminal epithelium of the uterine horn from hypothyroid rabbits was higher than in control ones (Fig. 1l).

Tissue characteristics for endometrium and myometrium from control and hypothyroid rabbits are shown in Fig. 2. Compared to controls (Fig. 2a), hypothyroidism promoted the thickening of the glandular epithelium and the fusion of uterine glands (Fig. 2b–d). Although the infiltration of immune cells in the endometrium from control rabbits is common (Fig. 2e), a great infiltration was observed in hypothyroid rabbits (Fig. 2f–g). Even it was possible to observe some points of inflammation (Fig. 2h). Many of these immune cells infiltrated into the endometrium were macrophages CD163+ (Fig. 2i; for controls; and Fig. 2j–l for hypothyroid). For the control group, myometrium was observed uniform and the smooth muscle fibers were together (Fig. 2m). However, the hypothyroid group showed myometrium with separated muscle fibers (Fig. 2n). Even some groups of smooth muscle cells were observed into the endometrium near of inflammatory points forming circle or oval forms (Fig. 2o–p). The number and area covered by capillaries were similar between females from the control and hypothyroid groups (Fig. 3a–b). However, the expression of VEGF-A mRNA and protein levels was higher in the hypothyroid group (Fig. 3c–d).

Hypothyroidism decreased PR mRNA expression in the uterine horn (Fig. 4a) as well as the content of its two isoforms (PR-A and PR-B) (Fig. 4b). The expression of ERα mRNA was unmodified by

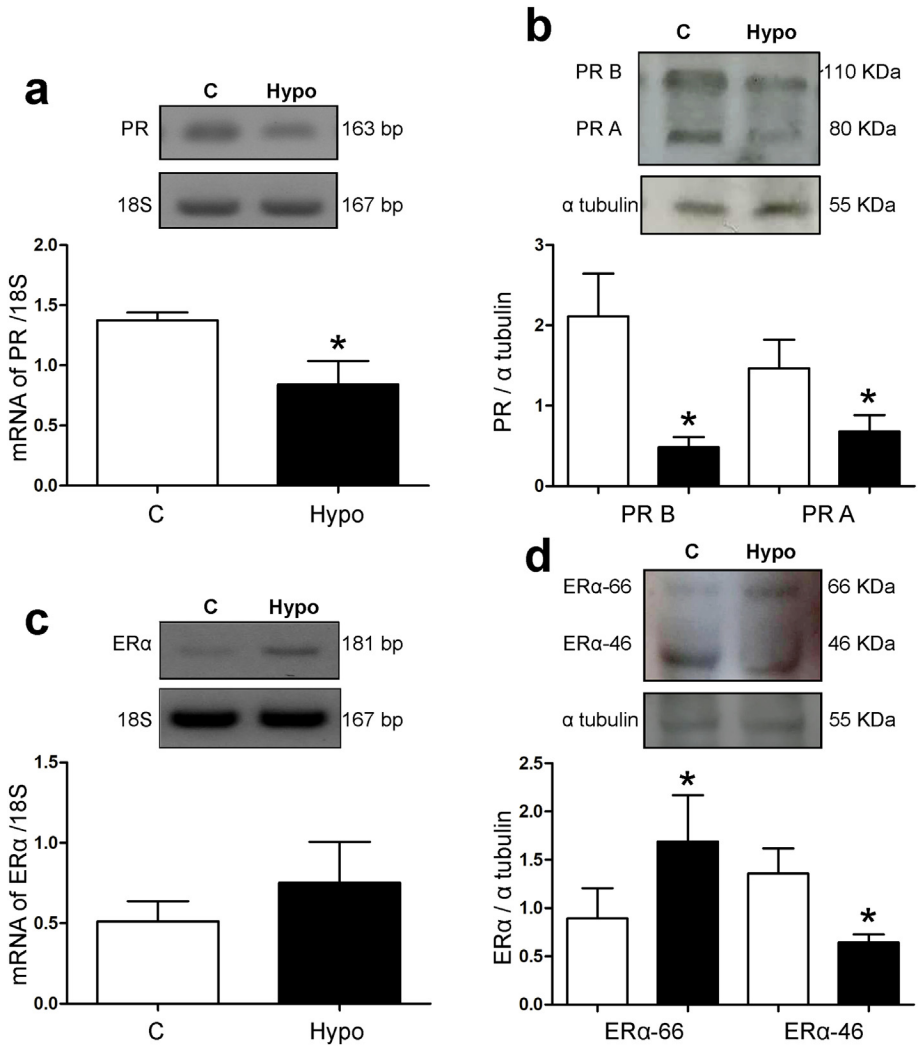

Fig. 4. Hypothyroidism affects the PR and ERα expression in the uterine horn of rabbits. Representative PCR (upper panel) and densitometry analysis showing PR (**a**) or ERα (**c**) mRNA expression of control (C, white bars, n = 6) and hypothyroid (Hypo, black bars, n = 6). Representative western blot detection of PR (**b**) and ERα (**d**) in control (C, white bars, n = 6) and hypothyroid (Hypo, black bars, n = 6). Results are expressed as mean ± S.E.M. *$p \leq 0.05$.

hypothyroidism (Fig. 4c). However, uterine expression of the large isoform (66 kDa) of ERα in hypothyroid female rabbits was higher than that in controls, the opposite was found for the truncated isoform (46 kDa, Fig. 4d).

In addition, hypothyroid rabbits showed a tendency to have a lower concentration of T4 and free T4 index ($p = 0.06$) and presented a significant reduction in the concentration of T3 as compared to control animals (Fig. 5a–c). Hypothyroid rabbits showed an increased expression of TRA (Fig. 5d) and a tendency to present a high expression of TRB (Fig. 5e; $p = 0.06$).

The expression of PLIN-A in the uterine horn in the hypothyroid group was lower compared to controls (Fig. 6a). The content of TAG and TC was also lower in hypothyroid rabbits (Fig. 6b–c). In contrast, a high concentration of MDA was found in the hypothyroid group (Fig. 6d). The presence of oxidative lipids identified by Sudan black stain in the epithelium, uterine glands, and stroma in the hypothyroid group was lower than in controls (Fig. 6e–g). However, the gland secretion showed higher staining to Sudan black in the hypothyroid group.

4. Discussion

Our results show that in the uterine horn of virgin rabbits, hypothyroidism promoted several histological alterations such as endometrial hyperplasia, with high infiltration of immune cells that in some cases can be observed as points of inflammation. This inflammation is associated with high epithelial proliferation and fusion of glands. Even a detachment of epithelial tissue can be found. Our results are essential considering the involving of thyroid hormones in the development of possible myomas and uterine adherent tissues affecting the fertility of hypothyroid females [9,10,12]. In general, endometrial fibrosis has been associated with intrauterine adhesions, in which there is a differentiation between epithelium, fibroblasts, and myoblasts promoted by transforming growth factor (TGF)-β, and remodeling of the extracellular matrix [28]. In this regard, hypothyroidism stimulates the proliferation of epithelium from the intestine, oviduct, lung, and thyroid [24,29], now we extended this finding in the uterus of virgin females. In concordance to our results, endometrial hyperplasia caused by prenatal hypothyroidism was confirmed by the vast number of fused uterine glands [16]. This could be considered as mild cystic hyperplasia of superficial glands [30]. Additionally, a low thickness in the myometrium layer was observed. This could be related to the abnormal uterine contraction patterns reported in non-pregnant hypothyroid rats [31]. In this regard, T3 regulates the expression of alpha-smooth muscle actin in cardiomyocytes [32] and aorta [33]. In addition, thyroid hormones can modulate chemotaxis, lipoperoxidation, and cytokines production in several immune cells [34]. A great infiltration of CD163+ macrophages was observed in hypothyroid uterine horn, suggesting

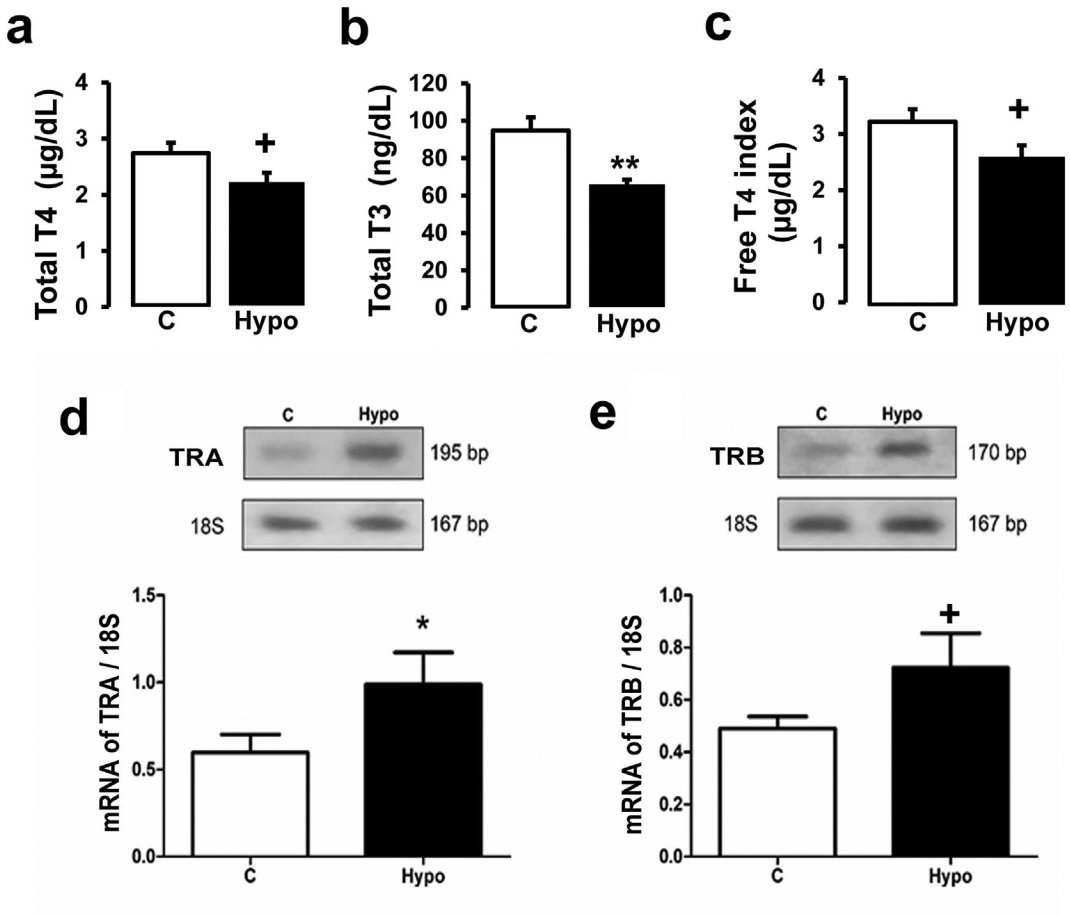

Fig. 5. Concentrations of total T4 (**a**) and T3 (**b**) in the serum of control (C; white bars, n = 6) and hypothyroid (Hypo; black bars, n = 6) female rabbits and free T4 index (**c**). Representative RT-PCR and densitometry analysis showing the TRA (**d**) and TRB (**e**) mRNA expression. Results are expressed as mean ± S.E.M. $^{*}p \leq 0.05$; $^{*}p \leq 0.01$; $+p = 0.06$.

endometritis [6]. Macrophages CD163+ secrete TNF-α, IL-6, MCP-1, and VEGF-A [25], supporting the presence of uterine inflammation.

Although hypothyroidism did not affect the number nor the area covered by blood vessels, a high expression of VEGF-A in the uterine horn was found. Uterine hyperplasia and pyometra are associated with a major expression of VEGF-A, improving the blood flow and reducing the vascular resistance [35]. Moreover, VEGF is regulated by P4 [36] and E2 [37]. Uterine hyperplasia and inflammation are related to an increase in ER and a decrease in PR expression [2–4,9,38]. In contrast, P4 has opposite effects on the hyperplasia induced by E2 [39]. In addition, we reported that hypothyroidism causes endometrial hyperplasia in pregnant rabbits, associated with an increase in the 3β-hydroxysteroid dehydrogenase (3β-HSD) [16], this is hypothyroidism may affect the local synthesis of sex hormones in the uterus.

As we confirmed in the present study, the methimazole dose (10 mg/kg) used is effective to reduce thyroid hormones concentrations in serum [24]. Besides, the expression of TRs was higher in hypothyroid animals. In contrast, hypothyroidism down-regulates the expression of TRs and TSHR in the uterine horn at the implantation period in rats [41]. In this regard, it is known that the expression of TRs in the rat uterus varies with the phase of the estrous cycle, being lower at the proestrus and diestrus [40]. This suggests differential regulation of TRs depending on the sex hormones status. According to other studies [23], our rabbits were at proestrus, and we have previously shown that hypothyroidism does not modify the concentration of estradiol and progesterone in non-pregnant rabbits [24]. This suggests that the increment in the expression of uterine TRs should depend on the reduced concentrations of thyroid hormones in serum and on the modifications in the expression of sex hormones receptors in the uterus.

Thus, the direct effects of thyroid hormones on TRs to regulate the expression of mRNA and protein of PR and ER in the uterus [19–21] may be proposed. In this regard, a decrease in the PR-A is necessary for implantation [42], an excessive reduction in the expression and activity of PR promotes a shortened luteal phase affecting the endometrial development [42]. A decrease in the synthesis of P4 and expression of PR has been associated with a higher activity of pro-inflammatory cytokines, metalloproteases and chemokines [42] Also, a deficiency in P4 and PR-aberrant is related to miscarriage and myomas [43]. Two isoforms of ERα (one large of 66 kDa, and other short of 46 kDa) were found in the uterus of rabbits, as previously reported in women [44]. Hypothyroidism increased the long form of ERα and diminished the short one. In concordance, it has been reported that ERα-46 modulates the expression of ERα-66 in the mammary gland and endometrium [44,45]. In the mammary gland, hypothyroidism affects the expression of PR (A and B) and ERα involving the regulation of nuclear receptor co-activator (NCOA) [46].

Hypothyroidism in female rabbits induces hypercholesterolemia [47]. However, it reduces the content of TAG and TC, the expression of PLIN-A, and the presence of oxidized lipid granules in virgin rabbits. The importance of these results lies in the role of cholesterol as a cell membrane component and precursor of sex hormones. The uterus has a *novo* synthesis of cholesterol since express lanosterol 14alpha-demethylase, which can be regulated by estrogens [48]. The triglycerides reduction in hypothyroid rabbits could affect prostaglandin synthesis [49]. The content of oxidized lipids may have an important role in the implantation [50]. In contrast, a great lipoperoxidation was observed in

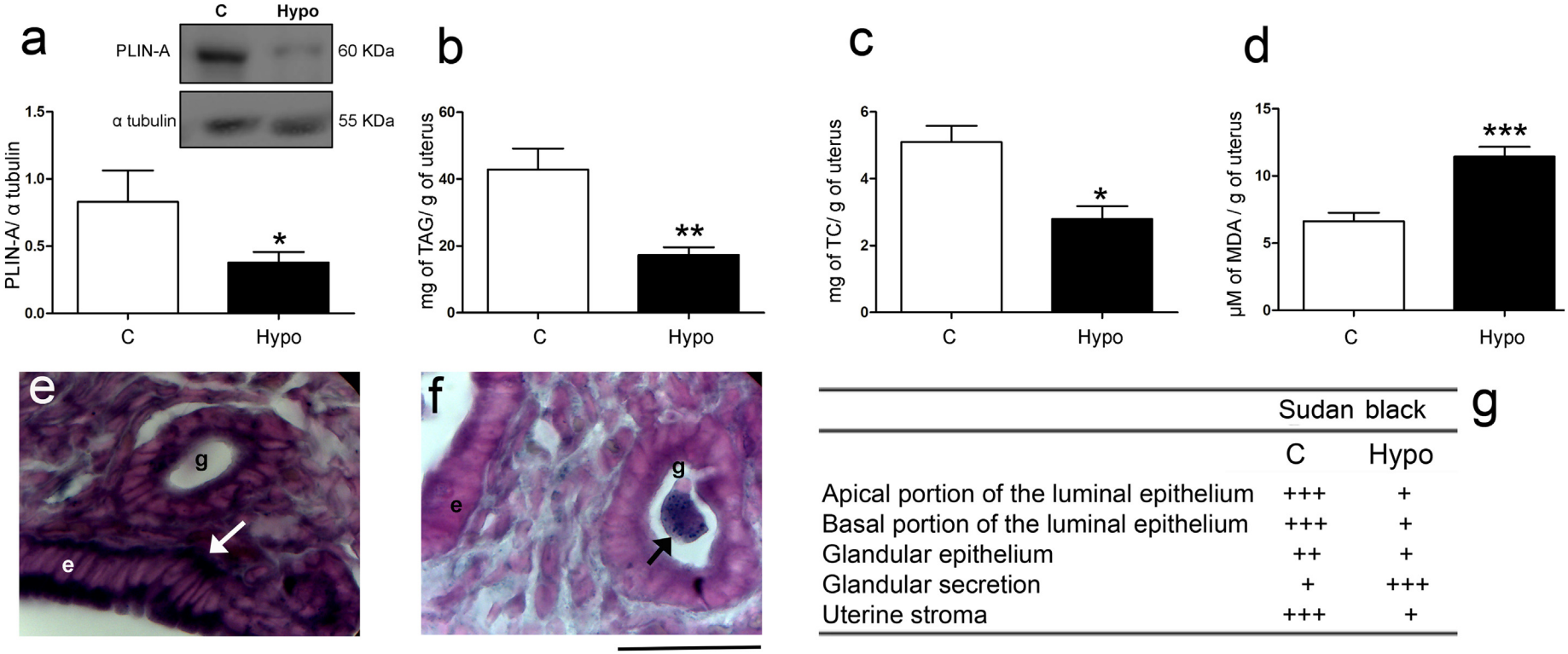

Fig. 6. Lipids in the uterine horn of control (C, white bars) and hypothyroid (hypo, black bars) rabbits. Expression of PLIN-A (**a**), as well as the content of triglycerides (TAG; **b**), total cholesterol (TC; **c**), and malondialdehyde (MDA; **f**). Results are expressed as mean ± S.E.M. *$p \leq 0.05$; **$p \leq 0.01$; ***$p \leq 0.001$. The uterus of control (**d**) and hypothyroid (**e**) was stained with Sudan black. Categories were established: (+ + +) for a high proportion of stained granules; (+ +) for a moderate proportion of stained granules; and (+) for a low proportion of stained granules. Scale = 50 µm. Arrows indicate oxidized lipids droplets in the uterine gland, g, and epithelium, e.

the hypothyroid uterus. In agreement, the high content of MDA with low activity of antioxidant enzymes has been reported in women with hyperplasia [7]. Changes in the uterine lipoperoxidation have been observed in young hypothyroid rats [17]. The content of uterine lipids and oxidative status of the endometrium could be affected by local synthesis of E2 and P4 or their respective receptors [51].

These variations in the lipid content of the uterus from the hypothyroid group could be related to modifications in the steroidogenesis, considering that hypothyroidism modifies the expression of P450scc [52], 3β-HSD [16] and 17β-HSD [53], and aromatase [47] in the ovaries and uterine horn of virgin or pregnant females. Both steroidogenesis and sexual hormones signaling may have an important role in the uterine hyperplasia and inflammation observed in hypothyroid rabbits, possibly mediating the expression of steroidogenic factor 1 (SF1), which has been related to abnormal uterine gland morphogenesis, an inhibition of steroid hormone signaling, and activation of an immune response [54].

In contrast to rats, rabbits reflex ovulatory and can stay in continuous early proestrus by light/dark cycle regulation [23]. This permits to manipulate the levels of thyroid hormones, with a stable concentration of sex hormones [24]. Moreover, rabbits have been chosen as an animal model for uterine adenocarcinoma, knowing the normal and pathology histology of their uterus [55]. Our study suggests that hypothyroidism is another cause of uterine hyperplasia.

5. Conclusion

Findings of the present study confirm that the hypothyroidism induces uterine hyperplasia and inflammation in virgin females, which is associated with an increase in the VEGF-A, a decrease in the expression of PR (A and B), and modifications in that of ERα. Also, hyperplasia involves changes in the uterine content of lipids and lipoperoxidation. Therefore, our findings indicate a direct effect of thyroid hormones on the uterine horn, regulating actions of sex hormones. Present results might be helpful to clarify the relationship between hypothyroidism and abnormal bleeding and miscarriage in females. Even female secondary infertility may be linked to hypothyroidism.

Acknowledgments

Authors thank the Consejo Nacional de Ciencia y Tecnología (CONACyT) of Mexico for supporting this research (Grant no. 257549 to ECR, Proyecto apoyado por el Fondo Sectorial de Investigación para la Educación) and for providing research fellowships to students.

Declaration of Competing Interest

The authors disclose any financial or personal relationships with other people or organizations that could inappropriately bias or influence in the work.

References

[1] J.Y. Wong, E.B. Gold, W.O. Johnson, J.S. Lee, Circulating sex hormones and risk of uterine fibroids: Study of Women's Health across the Nation (SWAN), J. Clin. Endocrinol. Metab. 101 (2015) 123–130, https://doi.org/10.1210/jc.2015-2935.

[2] K. Upson, K.H. Allison, S.D. Reed, C.D. Jordan, K.M. Newton, E.M. Swisher, J.A. Doherty, R.L. Garcia, Biomarkers of progestin therapy resistance and endometrial hyperplasia progression, Am. J. Obstet. Gynecol. 207 (2012) e1–e8, https://doi.org/10.1016/j.ajog.2012.05.012.

[3] B. Pieczyńska, S. Wojtylak, A. Zawrocki, W. Biernat, Analysis of PTEN, estrogen receptor α and progesterone receptor expression in endometrial hyperplasia using tissue microarray, Pol. J. Pathol. 62 (2011) 133–138.

[4] E. Laas, M. Ballester, A. Cortez, J. Gonin, G. Canlorbe, E. Daraï, O. Graesslin, Supervised clustering of immunohistochemical markers to distinguish atypical and non-atypical endometrial hyperplasia, Gynecol. Endocrinol. 31 (2015) 282–285, https://doi.org/10.3109/09513590.2014.989981.

[5] A.K. Elfayomy, S.M. Almasry, G.M. Attia, F.A. Habib, Enhanced expression of vascular endothelial growth factor and increased microvascular density in women with endometrial hyperplasia: a possible relationship with uterine natural killer cells, Romanian J. Morphol. Embryol. 56 (2015) 725–734.

[6] A. Cominelli, H.P. Gaide Chevronnay, P. Lemoine, P.J. Courtoy, E. Marbaix, P. Henriet, Matrix metalloproteinase-27 is expressed in CD163 + /CD206 + M2 macrophages in the cycling human endometrium and in superficial endometriotic lesions, Mol. Hum. Reprod. 20 (2014) 767–775, https://doi.org/10.1093/molehr/gau034.

[7] S. Pejić, A. Todorović, V. Stojiljković, J. Kasapović, S.B. Pajović, Antioxidant enzymes and lipid peroxidation in endometrium of patients with polyps, myoma, hyperplasia and adenocarcinoma, Reprod. Biol. Endocrinol. 7 (2009) 149, , https://doi.org/10.1186/1477-7827-7-149.

[8] S. Özdemir, G. Batmaz, S. Ates, C. Celik, F. Incesu, C. Peru, Relation of metabolic syndrome with endometrial pathologies in patients with abnormal uterine bleeding, Gynecol. Endocrinol. 31 (2015) 725–729, https://doi.org/10.3109/09513590.2015.1058355.

[9] E. Soleymani, K. Ziari, O. Rahmani, M. Dadpay, M. Taheri-Dolatabadi, K. Alizadeh, N. Ghanbarzadeh, Histopathological findings of endometrial specimens in abnormal uterine bleeding, Arch. Gynecol. Obstet. 289 (2014) 845–849, https://doi.org/10.1007/s00404-013-3043-1.

[10] Y. Hu, Q. Wang, G. Li, X. Sun, C. Liu, Ultrasonic morphology of uterus and ovaries in girls with pituitary hyperplasia secondary to primary hypothyroidism, Horm. Metab. Res. 45 (2013) 669–674, https://doi.org/10.1055/s-0033-1345141.

[11] N.S. Ajmani, V. Sarbhai, N. Yadav, M. Paul, A. Ahmad, A.K. Ajmani, Role of thyroid dysfunction in patients with menstrual disorders in tertiary care center of Walled city of Delhi, J. Obstet. Gynaecol. India. 66 (2016) 115–119, https://doi.org/10.1007/s13224-014-0650-0.

[12] J. Ott, C. Kurz, R. Braun, R. Promberger, R. Seemann, E. Vytiska-Binstorfer, K. Walch, Overt hypothyroidism is associated with the presence of uterine leiomyoma: a retrospective analysis, Eur. J. Obstet. Gynecol. Reprod. Biol. 177 (2014) 19–22, https://doi.org/10.1016/j.ejogrb.2014.03.003.

[13] F. Bagheripuor, M. Ghanbari, A. Piryaei, A. Ghasemi, Effects of fetal hypothyroidism on uterine smooth muscle contraction and structure of offspring rats, Exp. Physiol. 103 (2018) 683–692, https://doi.org/10.1113/EP086564.

[14] A.S.M. Sayem, N. Giribabu, S. Muniandy, N. Salleh, Effects of thyroxine on expression of proteins related to thyroid hormone functions (TR-α, TR-β, RXR and ERK1/2) in uterus during peri-implantation period, Biomed. Pharmacother. 96 (2017) 1016–1021, https://doi.org/10.1016/j.biopha.2017.11.128.

[15] J.F. Silva, N.M. Ocarino, R. Serakides, Maternal thyroid dysfunction affects placental profile of inflammatory mediators and the intrauterine trophoblast migration kinetics, Reproduction 147 (2014) 803–816, https://doi.org/10.1530/REP-13-0374.

[16] J. Rodríguez-Castelán, D. Zepeda-Pérez, M. Méndez-Tepepa, M. Castillo-Romano, M. Espindola-Lozano, A. Anaya-Hernández, P. Berbel, E. Cuevas-Romero, Hypothyroidism modifies the uterine lipid levels in pregnant rabbits and affects the fetal size, Endocr Metab Immune Disord Drug Targets (2018), https://doi.org/10.2174/1871530318666181102093621 Epub ahead of Print.

[17] L. Kong, Q. Wei, J.S. Fedail, F. Shi, K. Nagaoka, G. Watanabe, Effects of thyroid hormones on the antioxidative status in the uterus of young adult rats, J. Reprod. Dev. 61 (2015) 219–227, https://doi.org/10.1262/jrd.2014-129.

[18] I.M. Inuwa, M.A. Williams, A morphometric study on the endometrium of rat uterus in hypothyroid and thyroxine treated hypothyroid rats, Ups. J. Med. Sci. 111 (2006) 215–225.

[19] M. Hulchiy, H. Zhang, J.M. Cline, A.L. Hirschberg, L. Sahlin, Receptors for thyrotropin-releasing hormone, thyroid-stimulating hormone, and thyroid hormones in the macaque uterus: effects of long-term sex hormone treatment, Menopause 19 (2012) 1253–1259, https://doi.org/10.1097/gme.0b013e318252e450.

[20] J. Rodríguez-Castelán, A. Anaya-Hernández, M. Méndez-Tepepa, M. Martínez-Gómez, F. Castelán, E. Cuevas-Romero, Distribution of thyroid hormone and thyrotropin receptors in reproductive tissues of adult female rabbits, Endocr. Res. 42 (2017) 59–70, https://doi.org/10.1080/07435800.2016.1182185.

[21] A.S.M. Sayem, N. Giribabu, K. Karim, L.K. Si, S. Muniandy, N. Salleh, Differential expression of the receptors for thyroid hormone, thyroid stimulating hormone, vitamin D and retinoic acid and extracellular signal-regulated kinase in uterus of rats under influence of sex-steroids, Biomed. Pharmacother. 100 (2018) 132–141, https://doi.org/10.1016/j.biopha.2018.02.008.

[22] H.S. Keeping, A.M. Newcombe, P.H. Jellinck, Modulation of estrogen-induced peroxidase activity in the rat uterus by thyroid hormones, J. Steroid. Biochem. 16 (1982) 45–49.

[23] T.M. Mousa-Balabel, R.A. Mohamed, Effect of different photoperiods and melatonin treatment on rabbit reproductive performance, Vet. Q. 31 (2011) 165–171, https://doi.org/10.1080/01652176.2011.642533.

[24] A. Anaya-Hernández, J. Rodríguez-Castelán, L. Nicolás, M. Martínez-Gómez, I. Jiménez-Estrada, F. Castelán, E. Cuevas, Hypothyroidism affects differentially the cell size of epithelial cells among oviductal regions of rabbits, Reprod. Domest. Anim. 50 (2015) 104–111, https://doi.org/10.1111/rda.12455.

[25] A.L. Jensen, J. Collins, E.P. Shipman, C.R. Wira, P.M. Guyre, P.A. Pioli, A subset of human uterine endometrial macrophages is alternatively activated, Am. J. Reprod. Immunol. 68 (2012) 374–386, https://doi.org/10.1111/j.1600-0897.2012.01181.x.

[26] J. Rodríguez-Castelán, M. Méndez-Tepepa, J. Rodríguez-Antolín, F. Castelán, E. Cuevas-Romero, Hypothyroidism affects lipid and glycogen content and peroxisome proliferator-activated receptor δ expression in the ovary of the rabbit, Reprod. Fertil. Dev. 30 (2018) 1380–1387, https://doi.org/10.1071/RD17502.

[27] H. Itabe, T. Yamaguchi, S. Nimura, N. Sasabe, Perilipins: a diversity of intracellular lipid droplet proteins, Lipids Health Dis. 16 (2017) 83, , https://doi.org/10.1186/s12944-017-0473-y.

[28] H.Y. Zhu, T.X. Ge, Y.B. Pan, S.Y. Zhang, Advanced role of Hippo signaling in endometrial fibrosis: implications for intrauterine adhesion, Chin. Med. J. 130 (2017) 2732–2737, https://doi.org/10.4103/0366-6999.218013.
[29] C. Frau, M. Godart, M. Plateroti, Thyroid hormone regulation of intestinal epithelial stem cell biology, Mol. Cell. Endocrinol. 459 (2017) 90–97, https://doi.org/10.1016/j.mce.2017.03.002.
[30] N. Reusche, A. Beineke, C. Urhausen, M. Beyerbach, M. Schmicke, S. Kramer, A.R. Günzel-Apel, Proliferative and apoptotic changes in the healthy canine endometrium and in cystic endometrial hyperplasia, Theriogenology. 114 (2018) 14–24, https://doi.org/10.1016/j.theriogenology.2018.03.018.
[31] S. Corriveau, S. Blouin, É. Raiche, M.A. Nolin, É. Rousseau, J.C. Pasquier, Levothyroxine treatment generates an abnormal uterine contractility patterns in an *in vitro* animal model, J. Clin. Transl. Endocrinol. 2 (2015) 144–149, https://doi.org/10.1016/j.jcte.2014.09.005.
[32] M.A. Gosteli-Peter, B.A. Harder, H.M. Eppenberger, J. Zapf, M.C. Schaub, Triiodothyronine induces over-expression of alpha-smooth muscle actin, restricts myofibrillar expansion and is permissive for the action of basic fibroblast growth factor and insulin-like growth factor I in adult rat cardiomyocytes, J. Clin. Invest. 98 (1996) 1737–1744.
[33] X. Wang, Z. Sun, Thyroid hormone induces artery smooth muscle cell proliferation: discovery of a new TRalpha1-Nox1 pathway, J. Cell. Mol. Med. 14 (2010) 368–380.
[34] E.L. Jara, N. Muñoz-Durango, C. Llanos, C. Fardella, P.A. González, S.M. Bueno, A.M. Kalergis, C.A. Riedel, Modulating the function of the immune system by thyroid hormones and thyrotropin, Immunol. Lett. 184 (2017) 76–83, https://doi.org/10.1016/j.imlet.2017.02.010.
[35] G.A. Veiga, R.H. Miziara, D.S. Angrimani, P.C. Papa, B. Cogliati, C.I. Vannucchi, Cystic endometrial hyperplasia-pyometra syndrome in bitches: identification of hemodynamic, inflammatory, and cell proliferation changes, Biol. Reprod. 96 (2017) 58–69, https://doi.org/10.1095/biolreprod.116.140780.
[36] M. Kim, H.J. Park, J.W. Seol, J.Y. Jang, Y. Cho, J.P. Lydon, F.J. Demayo, M. Shibuya, N. Ferrara, H.K. Sung, A. Nagy, K. Alitalo, G.Y. Koh, VEGF-A regulated by progesterone governs uterine angiogenesis and vascular remodeling during pregnancy, EMBO Mol. Med. 5 (2013) 1415–1430, https://doi.org/10.1002/emmm.201302618.
[37] J. Zhang, H. Song, Y. Lu, H. Chen, S. Jiang, L. Li, Effects of estradiol on VEGF and bFGF by Akt in endometrial cancer cells are mediated through the NF-κB pathway, Oncol. Rep. 36 (2016) 705–714, https://doi.org/10.3892/or.2016.4888.
[38] A.V. Kubyshkin, L.L. Aliev, I.I. Fomochkina, Y.P. Kovalenko, S.V. Litvinova, T.G. Filonenko, N.V. Lomakin, V.A. Kubyshkin, O.V. Karapetian, Endometrial hyperplasia-related inflammation: its role in the development and progression of endometrial hyperplasia, Inflamm. Res. 65 (2016) 785–794, https://doi.org/10.1007/s00011-016-0960-z.
[39] A. Gompel, Progesterone, progestins and the endometrium in perimenopause and in menopausal hormone therapy, Climacteric 21 (2018) 321–325, https://doi.org/10.1080/13697137.2018.1446932.
[40] A.S.M. Sayem, N. Giribabu, K. Karim, L.K. Si, S. Muniandy, N. Salleh, Differential expression of the receptors for thyroid hormone, thyroid stimulating hormone, vitamin D and retinoic acid and extracellular signal-regulated kinase in uterus of rats under influence of sex-steroids, Biomed. Pharmacother. 100 (2018) 132–141, https://doi.org/10.1016/j.biopha.2018.02.008.
[41] N. Salleh, A.S.M. Sayem, N. Giribabu, S.L. Khaing, Expression of proteins related to thyroid hormone function in the uterus is down-regulated at the day of implantation in hypothyroid pregnant rats, Cell Biol. Int. 43 (2019) 486–494, https://doi.org/10.1002/cbin.11114.
[42] M. Wetendorf, S.P. Wu, X. Wang, C.J. Creighton, T. Wang, R.B. Lanz, L. Blok, S.Y. Tsai, M.J. Tsai, J.P. Lydon, F.J. DeMayo, Decreased epithelial progesterone receptor A at the window of receptivity is required for preparation of the endometrium for embryo attachment, Biol. Reprod. 96 (2017) 313–326, https://doi.org/10.1095/biolreprod.116.144410.
[43] B. Patel, S. Elguero, S. Thakore, W. Dahoud, M. Bedaiwy, S. Mesiano, Role of nuclear progesterone receptor isoforms in uterine pathophysiology, Hum. Reprod. Update 21 (2015) 155–173, https://doi.org/10.1093/humupd/dmu056.
[44] G. Flouriot, H. Brand, S. Denger, R. Metivier, M. Kos, G. Reid, V. Sonntag-Buck, F. Gannon, Identification of a new isoform of the human estrogen receptor-alpha (hER-alpha) that is encoded by distinct transcripts and that is able to repress hER-alpha activation function 1, EMBO J. 19 (2000) 4688–4700, https://doi.org/10.1093/emboj/19.17.4688.
[45] C.M. Klinge, K.A. Riggs, N.S. Wickramasinghe, C.G. Emberts, D.B. McConda, P.N. Barry, J.E. Magnusen, Estrogen receptor alpha 46 is reduced in tamoxifen resistant breast cancer cells and re-expression inhibits cell proliferation and estrogen receptor alpha 66-regulated target gene transcription, Mol. Cell. Endocrinol. 323 (2010) 268–276, https://doi.org/10.1016/j.mce.2010.03.013.
[46] F. Campo-VerdeArboccó, C.V. Sasso, D.L. Nasif, M.B. Hapon, G.A. Jahn, Effect of hypothyroidism on the expression of nuclear receptors and their co-regulators in mammary gland during lactation in the rat, Mol. Cell. Endocrinol. 412 (2015) 26–35, https://doi.org/10.1016/j.mce.2015.05.026.
[47] J. Rodríguez-Castelán, M. Méndez-Tepepa, Y. Carrillo-Portillo, A. Anaya-Hernández, J. Rodríguez-Antolín, E. Zambrano, F. Castelán, E. Cuevas-Romero, Hypothyroidism reduces the size of ovarian follicles and promotes hypertrophy of periovarian fat with infiltration of macrophages in adult rabbits, Biomed. Res. Int. 2017 (2017) 3795950, , https://doi.org/10.1155/2017/3795950.
[48] X. Song, P. Tai, J. Yan, B. Xu, X. Chen, H. Ouyang, M. Zhang, G. Xia, Expression and regulation of lanosterol 14alpha-demethylase in mouse embryo and uterus during the peri-implantation period, Reprod. Fertil. Dev. 20 (2008) 964–972.
[49] M.A. Chaud, A.M. Franchi, M. Viggiano, A.L. Gimeno, M.A. Gimeno, Effect of exogenous phospholipase A2 and triacylglycerol lipase on the synthesis and release of monoenoic and bisenoic prostaglandins from isolated rat uterus, Prostaglandins Leukot. Essent. Fatty Acids. 44 (1991) 211–215.
[50] C. Alberto-Rincon Mdo, C.S. de Paiva, P.A. Abrahamsohn, T.M. Zorn, Histochemical demonstration of phospholipid containing choline in the cytoplasm of murine decidual cells, Acta Anat. 150 (1994) 119–126.
[51] M.M. Singh, R.N. Trivedi, S.C. Chauhan, V.M. Srivastava, A. Makker, S.R. Chowdhury, V.P. Kamboj, Uterine estradiol and progesterone receptor concentration, activities of certain antioxidant enzymes and dehydrogenases and histoarchitecture in relation to time of secretion of nidatory estrogen and high endometrial sensitivity in rat, J. Steroid Biochem. Mol. Biol. 59 (1996) 215–224.
[52] J.J. Chen, S.W. Wang, E.J. Chien, P.S. Wang, Direct effect of propylthiouracil on progesterone release in rat granulosa cells, Br. J. Pharmacol. 139 (2003) 1564–1570, https://doi.org/10.1038/sj.bjp.0705392.
[53] D. Sarkar, A. Chakraborty, D. Mahapatra, A.K. Changra, Morphological and functional alterations of female reproduction after exposure of bamboo shoots of North East India, Asian Pac, J. Reprod. 6 (2017) 151, https://doi.org/10.12980/apjr.6.20170402.
[54] Y.M. Vasquez, S.P. Wu, M.L. Anderson, S.M. Hawkins, C.J. Creighton, M. Ray, S.Y. Tsai, M.J. Tsai, J.P. Lydon, F.J. DeMayo, Endometrial expression of steroidogenic factor 1 promotes cystic glandular morphogenesis, Mol. Endocrinol. 30 (2016) 518–532, https://doi.org/10.1210/me.2015-1215.
[55] C.A. Bertram, K. Müller, R. Klopfleisch, Genital tract pathology in female pet rabbits (Oryctolagus cuniculus): a retrospective study of 854 necropsy examinations and 152 biopsy samples, J. Comp. Pathol. 164 (2018) 17–26, https://doi.org/10.1016/j.jcpa.2018.08.003.

Hormones and Cancer
https://doi.org/10.1007/s12672-020-00381-7

The Role of mPRδ and mPRε in Human Glioblastoma Cells: Expression, Hormonal Regulation, and Possible Clinical Outcome

Aylin Del Moral-Morales[1] · Juan Carlos González-Orozco[1] · José Moisés Capetillo-Velázquez[1] · Ana Gabriela Piña-Medina[2] · Ignacio Camacho-Arroyo[1]

© Springer Science+Business Media, LLC, part of Springer Nature 2020

Abstract

Glioblastomas (GBM) are the most frequent and aggressive primary tumor of the central nervous system. In recent years, it has been proposed that sex hormones such as progesterone play an essential role in GBM biology. Membrane progesterone receptors (mPRs) are a group of G protein–coupled receptors with a wide distribution and multiple functions in the organism. There are five mPRs subtypes described in humans: mPRα, mPRβ, mPRγ, mPRδ, and mPRε. It has been reported that human-derived GBM cells express the mPRα, mPRβ, and mPRγ subtypes, and that progesterone promotes GBM progression in part by mPRα specific activation; however, it is still unknown if mPRδ and mPRε are also expressed in this type of tumor cells. In this study, we characterized the expression and hormonal regulation of mPRδ and mPRε in human GBM cells. We also analyzed a set of biopsies from TCGA. We found that the expression of these receptors is dependent on the tumor's grade and that mPRδ expression is directly correlated to patients' survival while the opposite is observed for mPRε. By RT-qPCR, Western blot, and immunofluorescence, the expression of mPRδ and mPRε was detected for the first time in human GBM cells. An in silico analysis showed possible progesterone response elements in the promoter regions of mPRδ and mPRε, and progesterone treatments downregulated the expression of these receptors. Our results suggest that mPRδ and mPRε are expressed in human GBM cells and that they are relevant to GBM biology.

Keywords Membrane progesterone receptors · Glioblastoma · Brain tumors · Progesterone · Astrocytoma

Introduction

Glioblastoma multiforme (GBM) is the most frequent and aggressive central nervous system (CNS) tumor that arises from the malignization of glial cells, glial progenitor cells, or transformed neural stem cells [1]. These tumors are characterized as fast-growing due to their high proliferative and invasive capabilities and for the low survival time of the patients after diagnosis, which goes from 12 to 16 months [1–3]. Therefore, it is crucial to elucidate the molecular mechanisms involved in the progression of GBM. Moreover, it is known that these tumors are more frequent in men than in women, in a proportion of 3:2; however, the factors involved in this gender bias have not been elucidated [1]. Regarding this issue, in recent years, it has been proposed that sex hormones, such as progesterone (P4), play an essential role in GBM biology [4].

P4 is a steroid hormone produced in ovaries, adrenal glands, and placenta, and is involved in the regulation of critical reproductive functions, including menstrual cycle and maintenance of pregnancy [5]. Also, it is synthesized and metabolized in various regions of the CNS [6], where it regulates sexual behavior, mood, neuroprotection, myelination, learning, and memory, as well as tumor growth in pathological conditions [6, 7]. P4 exerts its effects on target cells by two mechanisms: the genomic and the non-genomic ones. Through the genomic pathway, P4 permeates the plasmatic membrane to attach to its intracellular progesterone receptor (PR), which functions as a transcription factor that binds to specific DNA sequences named progesterone response

Electronic supplementary material The online version of this article (https://doi.org/10.1007/s12672-020-00381-7) contains supplementary material, which is available to authorized users.

✉ Ignacio Camacho-Arroyo
camachoarroyo@gmail.com

[1] Unidad de Investigación en Reproducción Humana, Instituto Nacional de Perinatología-Facultad de Química, Universidad Nacional Autónoma de México (UNAM), 04510 Mexico City, Mexico

[2] Departamento de Biología, Facultad de Química, UNAM, 04510 Mexico City, Mexico

Published online: 20 February 2020

elements (PRE), which are commonly localized in various promoter regions, thus regulating the expression of several genes [8–10]. Meanwhile, the non-genomic pathway of P4 is associated with rapid cell signaling changes induced via PR ligand-independent activation by membrane-associated kinases, or via the activation of different G protein–coupled membrane receptors to progesterone (mPRs) [11–13].

mPRs are G protein–coupled surface receptors that belong to the progestin and AdipoQ receptor family (PAQR). There are five mPRs subtypes described in humans: mPRα (PAQR7), mPRβ (PAQR8), mPRγ (PAQR5), mPRδ (PAQR6), and mPRε (PAQR9); the mPRα, mPRβ, and mPRγ subtypes are paired to inhibitory G proteins while the mPRδ and mPRε are associated to stimulatory G proteins [14–17]. Activation of these mPRs by P4 or by some of its metabolites such as dihydroprogesterone and allopregnanolone initiates intracellular signaling cascades linked to the modulation of cAMP levels, mobilization of intracellular Ca^{2+}, or the activation of kinases such as MAPKs, PI3K, Akt, and c-Src [11, 13, 14]. These mPRs regulate physiological processes involved in reproduction, development, immunological, and neuroendocrine responses [16, 18–22], and its participation in breast and ovarian cancer progression has also been demonstrated [23–25].

Previous works have suggested that P4 contributes to the tumor progression of GBM since human-derived GBM cells express several PR; plus, this hormone increases proliferation, migration, and invasion of GBM cells in both in vitro and in vivo models [26, 27, 28]. Additionally, it has been demonstrated that P4 enhances the infiltration of GBM cells from the tumor area into healthy tissue in the cerebral cortex [2930]. However, the use of the pharmacological antagonist of the PR mifepristone (RU486) partially blocks P4 effects on GBM cells [27282930], suggesting the participation of other mechanisms triggered by P4 in these cells, such as those activated by mPRs.

Our group has demonstrated that human-derived GBM cell lines U87 and U251 express the mPRα, mPRβ, and mPRγ subtypes [31]. Furthermore, it was demonstrated that mPRα activation by the specific mPR agonist 10-ethenyl-19-norprogesterone (Org OD 02-0) promotes the proliferation, migration, and invasion in these cells, and that these effects are mediated by the phosphorylation of Akt and Src kinases [32]. Despite this, it is still unknown if the mPRδ and mPRε subtypes are expressed in GBM and if these receptors could have any role in this type of cancer.

For this reason, in the present study, we characterized the mPRδ and mPRε subtypes expression in human GBM by using a set of biopsies data obtained from The Cancer Genome Atlas (TCGA), and in experiments carried out in the cell lines U87 and U251 derived from human GBM. The hormonal regulation of these receptors by P4 was also studied in the mentioned cell lines. Our results showed that the expression of mPRδ is positively correlated to the patients' survival, while mPRε levels are negatively correlated to clinical outcome. We also found out that both receptors are expressed in GBM cell lines and that their expression is downregulated by P4.

Material and Methods

TCGA Data Analysis

RNA-Seq counts from normal tissue (5), and human astrocytoma primary tumors (55 grade II, 112 grade III, 155 grade IV) were obtained from the Glioblastoma and Low-Grade Glioma projects of The Cancer Genome Atlas (TCGA) repository (https://portal.gdc.cancer.gov/). The data were downloaded and processed using TCGAbiolinks package version 2.12.6 [33] for R. DESeq2 version 1.34.1 [34] was used for the differential expression analysis and data normalization. Samples were stratified according to gene expression into three groups: "low" corresponding to the first quartile, "medium" for the second and third quartile, and "high" for the upper. Survival plots were generated with TCGA_analyze_survival tool from TCGAbiolinks.

Cell Culture and Treatments

U87 and U251 human GBM cell lines (purchased from ATCC, Georgetown, WA, USA) were cultured in phenol red and high glucose Dulbecco's modified Eagle's medium (DMEM, In vitro, Mexico City, Mexico) supplemented with 10% fetal bovine serum (FBS), 1 mM pyruvate, 2 mM glutamine, and 0.1 mM non-essential amino acids, at 37 °C in a humidified 5% CO_2 atmosphere. Both cell lines were tested for mycoplasma contamination using the Universal Mycoplasma Detection Kit (ATCC, Georgetown, WA, USA); all samples were negative (Supplementary Material 1). 2×10^5 cells were plated into 6-well plates. Twenty-four hours before treatments, the medium was changed for phenol red-free and high glucose DMEM (In vitro, Mexico City, Mexico), supplemented with charcoal-stripped FBS (HyClone, PA, USA). Treatments for RT-qPCR and Western blot were P4 (coupled to cyclodextrin, 1 nM, 10 nM, 100 nM, and 1 μM) and vehicle (V, 0.02% cyclodextrin) for 12 and 24 h; P4 was purchased from Sigma-Aldrich (St. Louis, MO, USA).

RNA Isolation and RT-qPCR

After treatments, total RNA was extracted using TRIzol LS Reagent (Thermo Fisher Scientific, MA, USA) according to the manufacturer's protocol. RNA concentration and purity were assessed through the NanoDrop 2000 Spectrophotometer (Thermo Fisher Scientific, MA, USA).

The integrity of the samples was determined with a 1.5% agarose gel electrophoresis. Healthy human astrocyte (HA) total RNA was obtained from ScienCell (cat: 1805, ScienCell, CA, USA). One microgram of total RNA was reverse transcribed to cDNA using the M-MLV reverse transcriptase (Invitrogen, Carlsbad, CA, USA) and oligo-$dT_{12–18}$ as primers. Two microliters from the previous reaction was subjected to qPCR using the FastStart DNA Master SYBR Green I reagent kit for LightCycler 1.5 (Roche Diagnostics, Mannheim, Germany) according to the manufacturer's protocol. The relative abundance of PAQR6 (mPRδ) and PAQR9 (mPRε) mRNA was calculated using 18S mRNA as an endogenous reference. Relative expression levels were calculated by the ΔCt method. Three biological replicates for each experiment were done. Primers used and the sequences of the fragments amplified are addressed in Supplemental Material 2.

Western Blot

After treatments, cells were detached from culture plates with PBS-EDTA and centrifuged. Cell pellets were lysed with RIPA buffer plus protease inhibitors (1 mM EDTA, 2 μg/ml leupeptin, 2 μg/ml aprotinin, 1 mM PMSF). Total protein was obtained by centrifugation at 14,000 rpm (4 °C for 5 min). The concentration of each sample was determined using Pierce 660 nm Protein Assay reagent (Thermo Fisher Scientific, MA, USA) and NanoDrop 2000 Spectrophotometer (Thermo Scientific, MA, USA) according to the manufacturer's protocol. Thirty micrograms of protein were subjected to SDS-PAGE in a 12% acrylamide gel. Proteins were transferred to a PVDF membrane for 2 h (60 mA at semi-dry conditions). Membranes were blocked with 5% bovine serum albumin (BSA; In Vitro, Mexico City, Mexico) and then incubated at 37 °C for 3 h with one of the following antibodies: mPRδ (cat: NBP1-59428; Novus Biologicals, CO, USA) in dilution 1:1000 or mPRε (cat: ab185466; Abcam, USA) in dilution 1:400. Blots were then incubated with a 1:7500 dilution of goat anti-rabbit secondary antibody conjugated to horseradish peroxidase (cat: sc-2004 Santa Cruz Biotechnology, TX, USA) at room temperature for 45 min. mPR content was normalized to γ-tubulin. Blots were stripped with glycine (0.1 M, pH 2.5, 0.5% SDS) at room temperature for 30 min, and incubated with anti-γ-tubulin antibody (cat: T3195-.2ML, Sigma-Aldrich, MO, USA) at 4 °C overnight. Membranes were incubated with a 1:7500 dilution of goat anti-rabbit secondary antibody as previously described. Bands were detected exposing blots to Kodak Biomax Light Film (Sigma-Aldrich, MO, USA) after incubation with Super Signal West Femto Maximum Sensitivity Substrate (Thermo Scientific, MA, USA). Densitometry of the bands was performed with ImageJ 1.45S software (National Institutes of Health, WA, USA). Three independent cultures for each experiment were done.

Immunofluorescence

U87 and U251 cells were fixed using 4% paraformaldehyde solution at room temperature for 20 min, followed by three washes in PBS. Then, for intracellular detection of the mPRs, fixed cells were permeabilized and blocked with 1% BSA and 0.2% Triton X-100 (Sigma-Aldrich, MO, USA) in PBS at room temperature for 30 min, while for cell membrane detection, fixed cells were just blocked with 1% BSA in PBS at room temperature for 30 min. Next, permeabilized and non-permeabilized cells were incubated with primary antibody rabbit anti-mPRδ (cat: NBP1-59428; Novus Biologicals, CO, USA) or anti-mPRε (cat: ab185466; Abcam, USA) in dilution 1:100 at 4 °C for 24 h. Cells were washed three times in PBS and then incubated with secondary antibody goat anti-rabbit Alexa Fluor 568 (Thermo Fisher Scientific, MA, USA) in dilution 1:500 at room temperature for 60 min. Cells were rinsed three times in PBS, and nuclei were stained with 1 mg/ml Hoechst 33342 solution (Thermo Fisher Scientific, MA, USA). Finally, cells were coverslipped using fluorescence mounting medium (Polysciences Inc., PA, USA), and visualized in an Olympus Bx43 microscope. Immunofluorescence negative controls consisted of cells incubated without the primary antibody.

Bioinformatic Analysis of Progesterone Response Elements

Gene sequences were obtained from the Human Genome Resources at NCBI (https://www.ncbi.nlm.nih.gov/genome/gdv/browser/?context=genome&acc=GCF_000001405.38). The promoter regions and transcription start site (TSS) were determined through the Ensembl database [35]. Putative binding sites for PR were searched with JASPAR [36], Unipro UGENE software v.1.26.3 [37], and TRANSFAC [38] algorithms. For all analyzed genes, the binding sites predicted by two or more databases with a matrix similarity score higher than 0.8 or P value < 0.05 were established as potential progesterone response element (PRE).

Statistical Analysis

Data from TCGA were plotted and analyzed using R version 3.5.2. To examine the relation between tumor grade and the level of expression of each mPR, a chi-square test of independence was performed. Experimental data were analyzed and plotted using the GraphPad Prism 5.0 software (GraphPad Software, CA, USA). Statistical analysis between groups was performed using a one-way ANOVA with a Tukey post-test. A P value < 0.05 was considered statistically significant.

Results

mPRδ and mPRε Expression in GBM Is Dependent of Tumor Grade and Correlates to Clinical Outcome

Expression data from TCGA were analyzed in order to find out the mPRs that are differentially expressed in GBM with respect to healthy tissue. In total, expression profiles from 5 normal tissues and 155 GBM were compared. Differential expression analysis shows that mPRβ, mPRδ, and mPRε are downregulated in GBM (Fig. 1a). As mPRβ expression and hormonal regulation in GBM have been previously described [31], we decided to focus on mPRδ and mPRε. In order to find out if their expression is dependent on the astrocytoma grade, data from 55 grade II, 112 grade III, 155 grade IV tumors (GBMs), and 5 normal tissue samples were stratified by quartiles according to the expression level of mPRδ and mPRε, where quartile 1 has the samples with the lowest levels of expression and quartile 4 the highest (Fig. 1b). A chi-square test of independence was performed to examine the relation between the quartile the samples belong to and the tumor's grade. We found that mPRδ expression is negatively correlated to the tumor grade X^2 (9, $N = 327$) = 86.454, P value < 0.0001, while mPRε expression is independent of the tumor grade, X^2 (9, $N = 327$) = 17.388, P value = 0.043.

To further analyze the possible clinical outcome of mPRs expression, samples were classified into *low* (first quartile), *medium* (second and third), and *high* (fourth quartile). Low expression of mPRδ was correlated to poor prognosis, while the opposite is observed regarding mPRε, where patients with low expression live longer than those with higher levels (Fig. 1c). Since gender bias in GBM incidence is well known and expression levels of mPRδ and mPRε are relevant to patient clinical outcomes, samples were stratified by gender in order to test for differences in survival time. No differences were detected for mPRδ since both females and males have a better prognosis if they have a high expression of this gene (Fig. 2a, Supplementary Material 3); on the contrary, males with high levels of mPRε have a significantly lower survival time after diagnosis, while women's prognosis is independent of mPRε expression. (Fig. 2b, Supplementary Material 3).

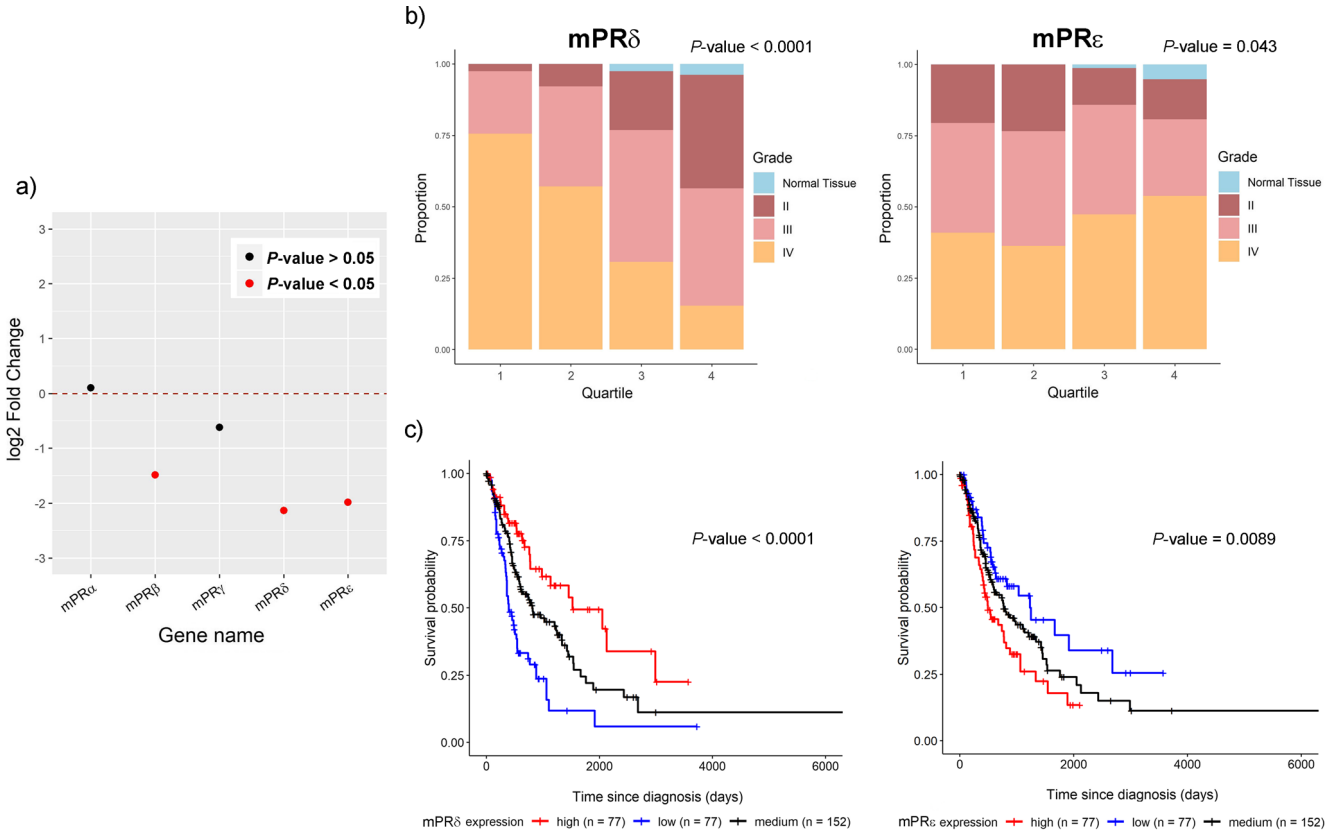

Fig. 1 mPRs expression in human astrocytoma primary tumor biopsies. RNA-Seq data from 322 astrocytoma primary tumors (55 grade II, 112 grade III, 155 grade IV, or GBM) and 5 normal tissues were obtained from TCGA repository. **a** Log2 fold change of mPRs in GBM compared with normal tissue, significant changes ($P < 0.05$) are denoted in red. **b** Samples were stratified in quartiles according to expression of mPRδ or mPRε and plotted by tumor grade, and a chi-square test of independence was performed in order to evaluate the correlation between the quartile the samples belong to and the tumor grade. **c** Survival plots of patients with *low* (first quartile, blue), *medium* (second and third, black), and *high* (fourth quartile, red) expression of mPRδ or mPRε

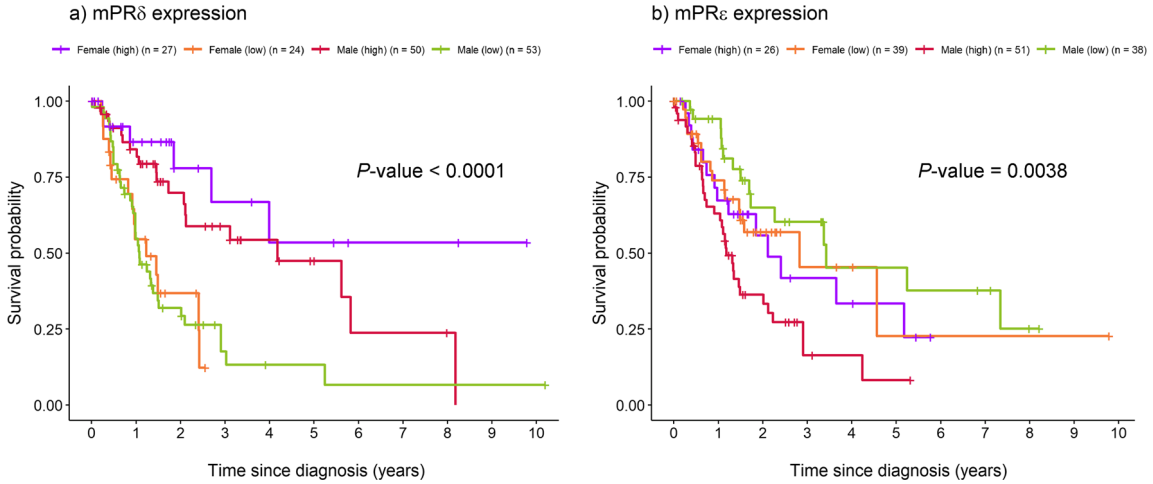

Fig. 2 Differences in survival by patients' gender. Samples from TCGA repository were classified into high and low levels of **a** mPRδ or **b** mPRε expression and stratified by gender in order to test for differences in survival time. *P* values were obtained by a log-rank test performed with the TCGAbiolinks package for R version 3.5.2

mPRδ and mPRε Are Expressed in Human GBM Cells Under Basal Conditions

In order to confirm the observations made, basal expression levels of mPRδ (PAQR6) and mPRε (PAQR9) were analyzed by RT-qPCR and Western blot in human GBM cell lines and compared with those in healthy human astrocytes (HA). Interestingly, mPRδ expression was lower in U251 and U87 cells as compared with that in HA. In contrast, mPRε expression was higher in both GBM cell lines with respect to that in HA. Furthermore, mPRδ levels were 100 times higher than those of mPRε in both cell lines (Fig. 3a). It is important to address that this is the first time that the expression of mPRδ and mPRε is demonstrated in human GBM cells. Western blot experiments showed a band of around 35 kDa for both receptor subtypes (Fig. 3b) in U87 and U251 cells. Both proteins had similar expression patterns in U87 and U251 cells; no significant

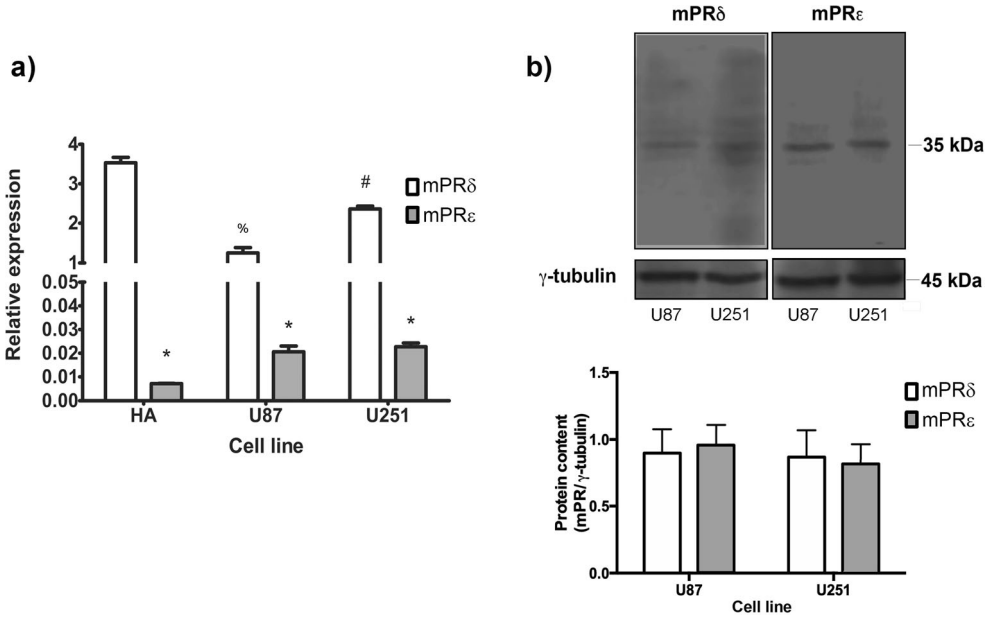

Fig. 3 mPRs mRNA and protein expression in human astrocytoma cell lines. **a** RNA extraction followed by RT-qPCR was carried out in U87 and U251 cells cultured under basal conditions. mPRs relative expression (normalized to 18S ribosomal RNA by ΔCt method) is shown. Healthy human astrocytes total RNA (HA) was used as normal tissue control. **b** U251 and U87 cells were lysed, and mPRs were evaluated by Western blot. Densitometry of each band was plotted. Three independent cultures for each experiment were done. Results are expressed as the mean ± S.E.M. (∗) *P* value < 0.001 vs all groups. (#) *P* value < 0.001 vs U87 and HA, (%) *P* value < 0.001 vs U251 and HA

differences were found between the mPRδ and mPRε protein content (Fig. 3b).

Intracellular and cell membrane localization of mPRδ and mPRε was also analyzed by immunofluorescence in GBM permeabilized and non-permeabilized cells (Fig. 4). For both receptors, U87 and U251 permeabilized cells showed positive staining distributed in the cytoplasm and the nucleus, while in non-permeabilized cells, positive staining resulted in punctuated marks distributed across the plasmatic membrane. Permeabilized and non-permeabilized GBM cells incubated without primary antibody were used as negative controls (Supplementary Material 4).

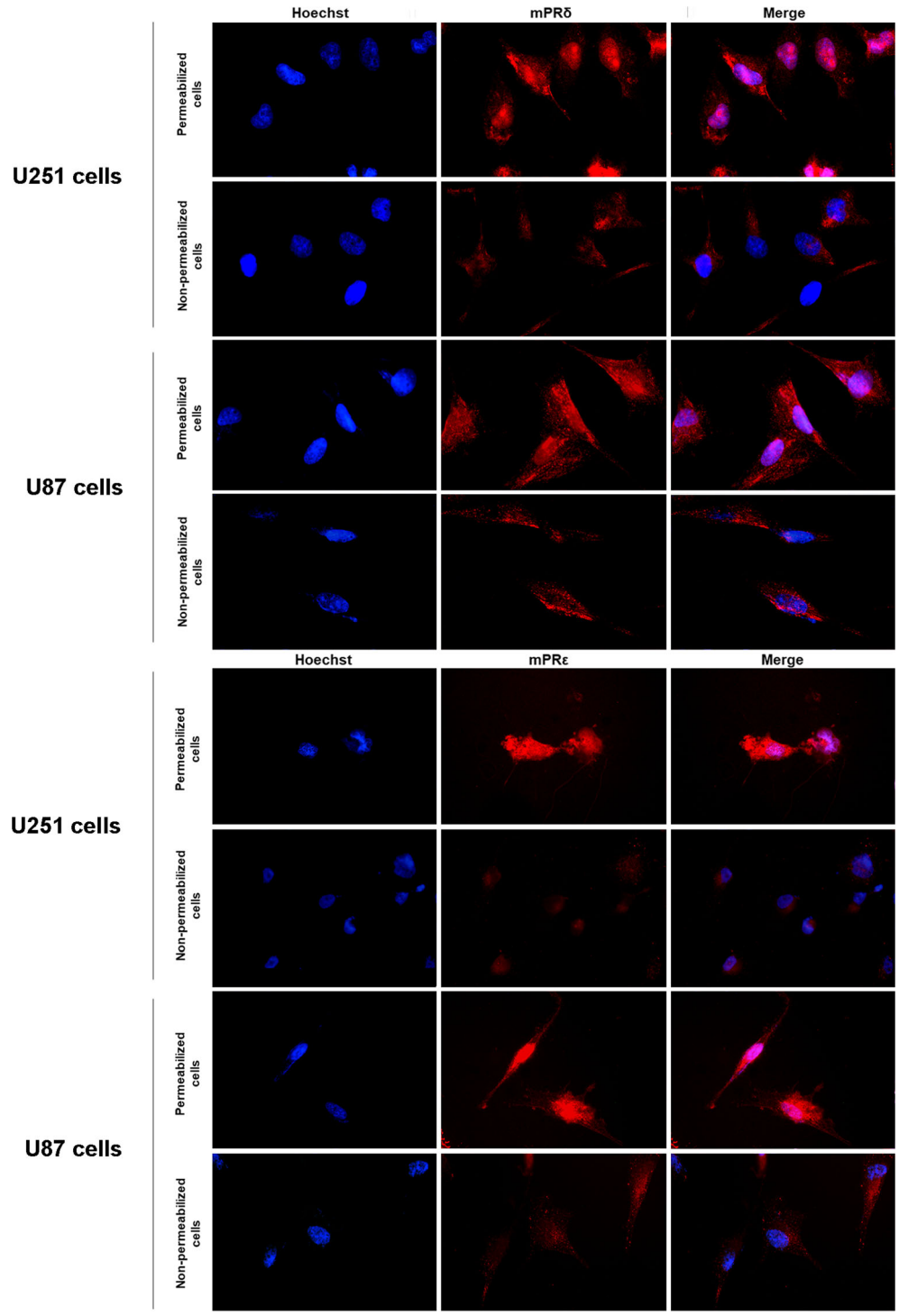

Fig. 4 Cellular localization of mPRδ and mPRε in GBM cells. Intracellular and cell membrane localization of mPRδ and mPRε was detected in U87 and U251 cells by immunofluorescence. Nuclei (blue), mPR positive stain (red), and merge are shown in permeabilized and non-permeabilized cells. All images were captured with a × 600 amplification

P4 Regulation of mPR⊠ and mPRε in U87 Cells

As previously described by Valadez-Cosmes et al. [30], mPRs expression can be regulated by sex hormones such as P4. In order to predict a possible regulation of mPRδ and mPRε by this hormone, an in silico analysis was performed to find putative PRE. Promoter sequences of PAQR6 (mPRδ) and PAQR9 (mPRε) genes were obtained from ENSEMBL (core promoter region, as indicated in the database) and analyzed with several bioinformatic tools (JASPAR, TRANSFAC, UGENE). Only PRE predicted by two or more algorithms (identity score > 0.8 or *P* value < 0.05) were considered as positive hits. In both promoters, potential PRE were found; according to the analysis, PAQR6 has three possible PR binding sites, whereas PAQR9 presents only one (Fig. 5).

RT-qPCR assays were performed in order to evaluate the P4 regulation of mPRδ and mPRε expression in U87 cells. Cells were treated with P4 at different concentrations (1 nM, 10 nM, 100 nM, and 1 μM) or vehicle (V, 0.02% cyclodextrin) for 12 or 24 h. mPRδ mRNA levels were reduced by P4 100 nM and 1 μM after 12 h of treatment as compared with V; this inhibition was maintained after 24 h of treatment only by P4 100 nM (Fig. 6). mPRε expression was inhibited by P4 10 nM, 100 nM, and 1 μM after 12 h of treatment. At 24 h, all the concentrations of P4 inhibited mPRε expression (Fig. 6).

Western blot analysis in U87 cells showed that P4 (1nM and 100 nM) decreased mPRδ content after 12 h of treatment compared with V; however, only P4 (1 μM) significantly decreased mPRδ content after 24 h. No significant changes in mPRε protein content were observed after 12 h with any of the P4 concentrations; however, after 24 h, P4 1 nM, 100 nM, and 1 μM decreased mPRε content as compared with the V (Fig. 7).

Discussion

GBMs are the most aggressive primary tumors of the CNS due to their poor prognosis. Recent studies have suggested that P4 and its receptors are relevant for GBM progression [26–29]. It has been demonstrated that P4 enhances the infiltration of GBM cells from the tumor area into healthy tissue in the cerebral cortex [29, 30] and that increases proliferation, migration, and invasion of human GBM cell lines [26–28]. However, the use of the pharmacological antagonist of the PR mifepristone (RU486), only partially blocks P4 effects on GBM cells [27, 28, 30], suggesting the participation of other mechanisms triggered by P4 in these cells such as those activated by mPRs.

In particular, our group has focused on mPRs, which are a group of G protein–coupled receptors associated with rapid cell signaling changes induced by P4. There are five mPRs subtypes described in humans: mPRα, mPRβ, mPRγ, mPRδ, and mPRε [12, 15, 17]. By analyzing the data from the

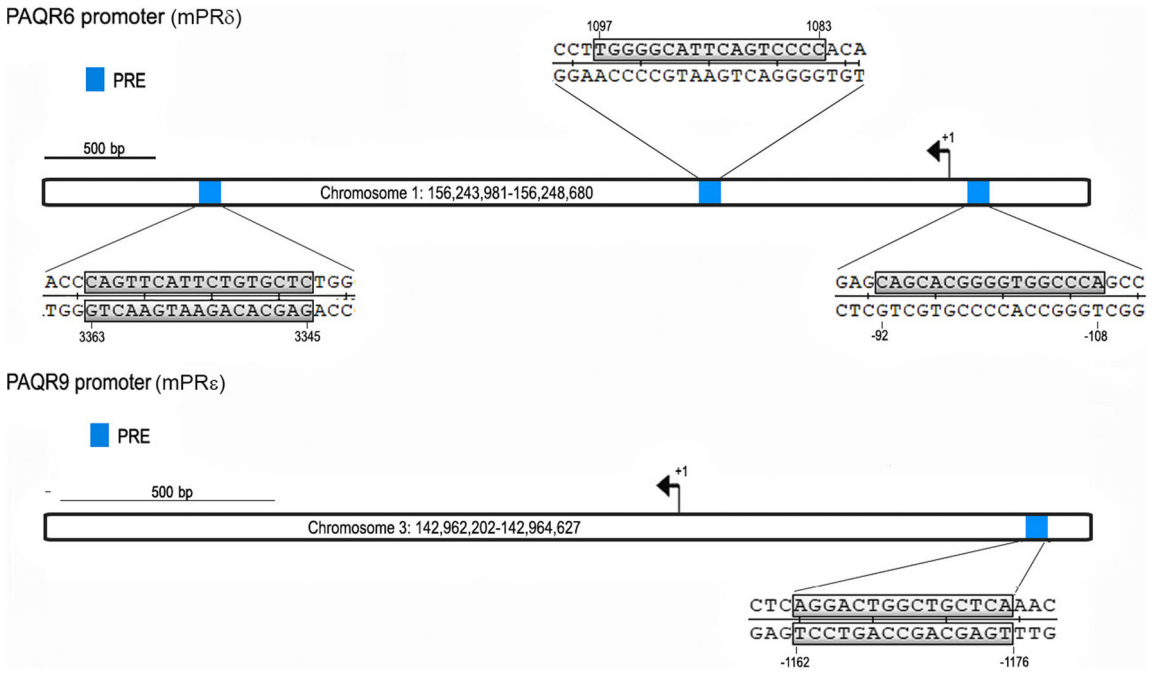

Fig. 5 In silico analysis of promoter sequences of PAQR6 (mPRδ) and PAQR9 (mPRε). Promoter sequences were obtained from the ENSEMBL database (core promoter region) and analyzed for putative PRE with several bioinformatic tools: JASPAR, TRANSFAC, and UGENE. For each gene, a white rectangle indicates the promoter region. Black arrows indicate the transcription start site and the gene transcription direction. The putative PRE are denoted with a blue square. A scale bar of 500 bp is included

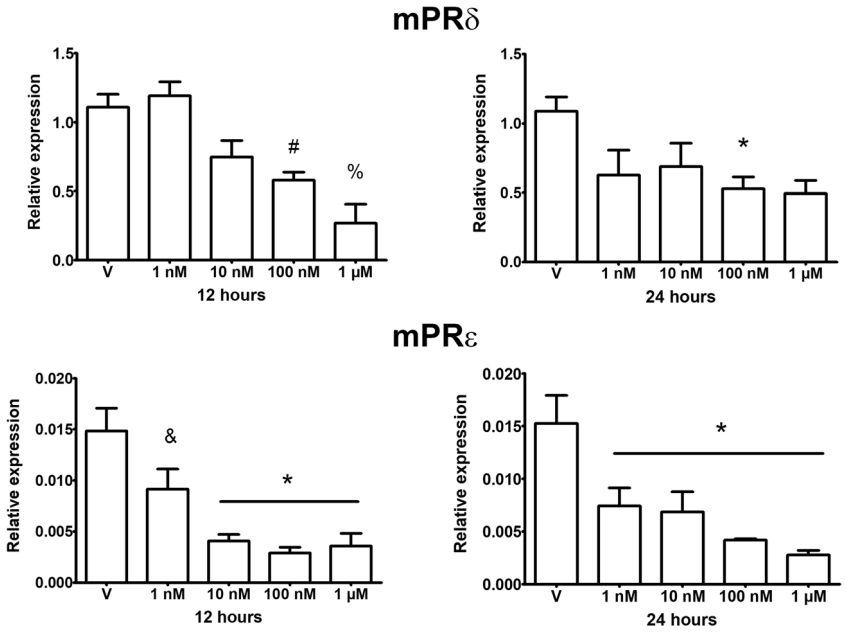

Fig. 6 P4 effects on mPRδ and mPRε expression. U87 GBM cells were treated with P4 at different concentrations (1 nM, 10 nM, 100 nM, and 1 μM) or V (0.02% cyclodextrin) for 12 or 24 h. PAQR6 and PAQR9 mRNA levels were quantified by RT-qPCR. Three independent experiments were performed for each sample. mPRs relative expression (normalized to 18S ribosomal RNA by ΔCt method) is shown. Results are expressed as the mean ± S.E.M. (*) P value < 0.05 vs V, (#) P value < 0.05 vs V and P4 1 nM, (%) P value < 0.05 vs V, P4 1 nM and P4 10 nM, (&) P value < 0.05 vs P4 100 nM

TCGA, it was observed that mPRβ, mPRδ, and mPRε are downregulated in GBM with respect to healthy tissue, which suggests that these receptors are relevant to tumor progression. Previous studies from our group have demonstrated that human-derived GBM cell lines U87 and U251 express mPRα, mPRβ, and mPRγ [31] and that mPRα activation increases cell proliferation and invasion by Akt and Src phosphorylation [32]. However, no research was conducted before on mPRδ and mPRε subtypes in GBM.

It was found that mPRδ and mPRε expression is dependent on the tumor grade. There is evidence that mPRδ mRNA is upregulated in prostate cancer cells and this correlates with lower survival rates, suggesting that mPRδ expression in prostate cancer should be considered as a predictor of malignancy [39]. However, in this study, it was shown that patients with high expression of mPRδ have a better prognosis than those with lower levels regardless of gender. On the contrary, high levels of mPRε are associated with poor prognosis, and this effect depends on the patients' gender, which suggests a possible hormone regulation.

By using RT-qPCR and Western blot approaches, we detected the expression of both receptors at mRNA and protein levels in U87 and U251 cell lines with predominant expression of the PAQR6 mRNA in both cell lines (100 times greater) as seen by RT-qPCR. This differential expression had been previously described by Pang et al. in several regions of the human brain such as the forebrain, corpus callosum, hypothalamus, and spinal cord [14]. It is also important to denote that this is the first time that the expression of these receptors is described in GBM cell lines. Expression levels of both receptors were compared in GBM cell lines and normal tissue. mPRδ expression was lower in U251 and U87 cells compared with HA. However, mPRε expression was higher in both GBM cell lines with respect to HA, which suggests that these receptors have a different role in GBM biology. Analysis of TCGA data of the low-grade glioma and GBM projects confirmed that mPRε expression is lower than that of mPRδ in both astrocytoma and normal tissue, and that the expression of both receptors is correlated to the tumor grade. However, Western blot assays revealed no significant differences in the expression of both receptors. It is essential to mention that mPRδ and mPRε signals detected in Western blot under basal conditions appeared as a single band in the expected molecular weight (~35 kDa); interestingly, the Western blot for the P4 treatments shows a double band which has already been observed for the mPRβ in glioma spheroids by Hiavaty et al. [40].

Meanwhile, by immunofluorescence, we detected in non-permeabilized U87 and U251 cells positive marks of mPRδ and mPRε in the cell membrane of both cell lines. As reported before, mPRδ is mainly detected in membrane preparations, and it is associated with Gs α-subunits [14]. Remarkably, we also detected positive marks of both mPRs expression in cytoplasm and nucleus which is not unexpected since mPRα and mPRβ intracellular localization has been reported in GBM cells due to the synthesis, transport to membrane, or degradation pathways that occur in membrane receptors [31].

P4 downregulates mPRδ and mPRε in U87 GBM cells after 12 h of exposure; furthermore, we observed by an in silico analysis that mPRδ and mPRε gene promoter regions contain PRE sequences, which explains their regulation by P4. One of the molecular functions of P4 in its target cells is to regulate the expression of its own receptors; previously we

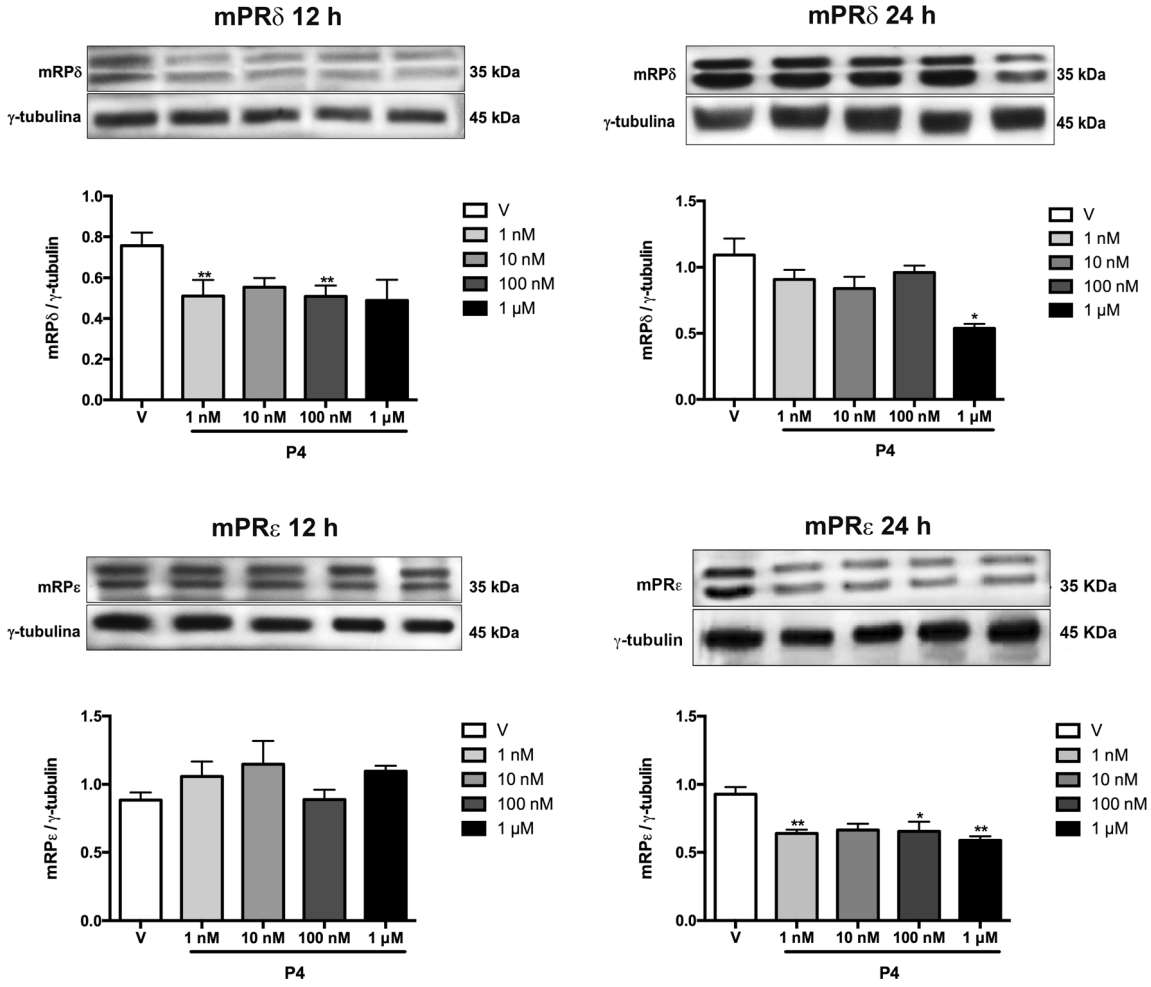

Fig. 7 P4 effects on mPRδ and mPRε protein content in U87 human GBM cells. Cells were treated with P4 (1 nM, 10 nM, 100 nM, and 1 μM) or V (0.02% cyclodextrin) during 12 or 24 h. Cells were lysed, and proteins (30 μg) were separated by electrophoresis on 12% SDS-PAGE gel, transferred to a PVDF membrane, and incubated with an antibody against mPRδ or mPRε. Each experiment was performed three times. Results are expressed as the mean ± S.E.M. *P value < 0.05 vs V; **P value < 0.01 vs V

have reported that P4 downregulates the expression of the PR and the mPRα, whereas it upregulates the expression of the mPRβ in human GBM cells [31, 41]. Gonzalez-Orozco et al. demonstrated that the activation of mPRα in U87 and U251 cells by the specific mPR agonist Org OD 02-0 increases cell proliferation, migration, and invasion [32].

Respecting the mechanisms of action of mPRδ and mPRε, it has been shown that these receptors mediate the neuroprotective effects of P4 and its metabolite allopregnanolone in neurons of the hippocampus in a model of starvation, by increasing the intracellular levels of cAMP, indicating that both membrane receptors are coupled to stimulatory G proteins. Interestingly, in that study, it was also observed that recombinant human mPRδ and mPRε expression in transfected MDA-MB-231 breast cancer cells diminished starvation-induced apoptosis [14].

Both mPRδ and mPRε have high affinity for P4 (Kd ~ 3 nM) [14], and it has been shown that allopregnanolone increases proliferation of GBM cells, which suggests that this metabolite should exert its effects by mPRδ binding, since it has been reported that allopregnanolone has a higher affinity for this receptor subtype compared with PR [42]. These data suggest that P4 and allopregnanolone should induce rapid P4 signaling in GBM cells through the activation of mPRδ or mPRε.

Conclusion

mPRδ and mPRε are relevant to GBM biology. An analysis of TCGA data revealed that mPRδ expression is directly correlated to patients' survival, while the opposite is observed for mPRε. We also demonstrated that human GBM cell lines U87 and U251 express the mPRδ and mPRε subtypes, showing that mPRδ exhibits high content and membrane localization. Moreover, in the U87 cell line, both mPRs are downregulated by P4.

Author Contributions All authors contributed to the study conception and design. Material preparation, data collection, and analysis were performed by Aylin del Moral-Morales, Juan Carlos González-Orozco, and José Moisés Capetillo-Velázquez. The first draft of the manuscript was written by Aylin del Moral-Morales and Juan Carlos González-Orozco, and all authors commented on previous versions of the manuscript. All authors read and approved the final manuscript.

Funding Information This work was supported by Grant No. 250866 from Consejo Nacional de Ciencia y Tecnología, México.

Compliance with Ethical Standards

Conflict of Interest The authors declare that they have no conflict of interest.

References

1. Louis DN, Perry A, Reifenberger G, von Deimling A, Figarella-Branger D, Cavenee WK, Ellison DW (2016) The 2016 World Health Organization classification of tumors of the central nervous system: a summary. Acta Neuropathol 131(6):803–820. https://doi.org/10.1007/s00401-016-1545-1
2. Furnari FB, Fenton T, Bachoo RM, Mukasa A, Stommel JM, Stegh A, Cavenee WK (2007) Malignant astrocytic glioma: genetics, biology, and paths to treatment. Genes Dev 21(21):2683–2710. https://doi.org/10.1101/gad.1596707
3. Nachbichler SB, Schupp G, Ballhausen H, Niyazi M, Belka C (2017) Temozolomide during radiotherapy of glioblastoma multiforme. Strahlenther Onkol 193(11):890–896. https://doi.org/10.1007/s00066-017-1110-4
4. Braga Tavares C, Gomes-Braga F, Costa-Silva D et al (2016) Expression of estrogen and progesterone receptors in astrocytomas: a literature review. Clinics. 71(8):481–486. https://doi.org/10.6061/clinics/2016(08)12
5. Wu SP, Li R, DeMayo FJ (2018) Progesterone receptor regulation of uterine adaptation for pregnancy. Trends Endocrinol Metab 29(7):1–11. https://doi.org/10.1016/j.tem.2018.04.001
6. Schumacher M, Mattern C, Ghoumari A, Oudinet JP, Liere P, Labombarda F et al (2014) Revisiting the roles of progesterone and allopregnanolone in the nervous system: resurgence of the progesterone receptors. Prog Neurobiol 113:6–39. https://doi.org/10.1016/j.pneurobio.2013.09.004
7. Schumacher M, Hussain R, Gago N, Oudinet JP, Mattern C, Ghoumari AM (2012) Progesterone synthesis in the nervous system: implications for myelination and myelin repair. Front Neurosci. 6(FEB):1–22. https://doi.org/10.3389/fnins.2012.00010
8. Liu T, Ogle T (2002) Signal transducer and activator of transcription 3 is expressed in the decidualized mesometrium of pregnancy and associates with the progesterone receptor through protein-protein interactions. Biol Reprod 67:114–118. https://doi.org/10.1095/biolreprod67.1.114
9. Camacho-Arroyo I, Villamar-Cruz O, González-Arenas A, Guerra-Araiza C (2002) Participation of the 26S proteasome in the regulation of progesterone receptor concentrations in the rat brain. Neuroendocrinology. 76(5):267–271. https://doi.org/10.1159/000066623
10. Boonyaratanakornkit V, Bi Y, Rudd M, Edwards DP (2008) The role and mechanism of progesterone receptor activation of extranuclear signaling pathways in regulating gene transcription and cell cycle progression. Steroids. 73:922–928
11. Zhu Y, Rice CD, Pang Y, Pace M, Thomas P (2003) Cloning, expression, and characterization of a membrane progestin receptor and evidence it is an intermediary in meiotic maturation of fish oocytes. Proc Natl Acad Sci 100:2231–2236. https://doi.org/10.1073/pnas.0336132100
12. Valadez-Cosmes P, Vázquez-Martínez ER, Cerbón M, Camacho-Arroyo I (2016) Membrane progesterone receptors in reproduction and cancer. Mol Cell Endocrinol 434:166–175. https://doi.org/10.1016/j.mce.2016.06.027
13. Zhu Y, Bond J, Thomas P (2003) Identification, classification, and partial characterization of genes in humans and other vertebrates homologous to a fish membrane progestin receptor. Proc Natl Acad Sci U S A 100(5):2237–2242. https://doi.org/10.1073/pnas.0436133100
14. Pang Y, Dong J, Thomas P (2013) Characterization, neurosteroid binding and brain distribution of human membrane progesterone receptors δ and ε (mPRδ and mPRε) and mPRδ involvement in neurosteroid inhibition of apoptosis. Endocrinology. 154(1):283–295. https://doi.org/10.1210/en.2012-1772
15. Tang YT, Hu T, Arterburn M, Boyle B, Bright JM, Emtage PC, Funk WD (2005) PAQR proteins: a novel membrane receptor family defined by an ancient 7-transmembrane pass motif. J Mol Evol 61(3):372–380. https://doi.org/10.1007/s00239-004-0375-2
16. Thomas P (2008) Characteristics of membrane progestin receptor alpha (mPRalpha) and progesterone membrane receptor component 1 (PGMRC1) and their roles in mediating rapid progestin actions. Front Neuroendocrinol 29(2):292–312 https://doi.org/10.1016/j.yfrne.2008.01.001
17. Thomas P, Pang Y, Dong J, Groenen P, Kelder J, de Vlieg J, Zhu Y, Tubbs C (2007) Steroid and G protein binding characteristics of the seatrout and human progestin membrane receptor alpha subtypes and their evolutionary origins. Endocrinology. 148(2):705–718 https://doi.org/10.1210/en.2006-0974
18. Fernandes MS, Pierron V, Michalovich D, Astle S, Thornton S, Peltoketo H, Brosens JJ (2005) Regulated expression of putative membrane progestin receptor homologues in human endometrium and gestational tissues. J Endocrinol 187(1):89–101. https://doi.org/10.1677/joe.1.06242
19. Macias H, Hinck L (2012) Mammary gland development. Wiley Interdiscip Rev Dev Biol 1(4):533–557. https://doi.org/10.1002/wdev.35
20. Mesiano S, Wang Y, Norwitz ER (2011) Progesterone receptors in the human pregnancy uterus. Reprod Sci 18(1):6–19. https://doi.org/10.1177/1933719110382922
21. Sleiter N, Pang Y, Park C, Horton TH, Dong J, Thomas P, Levine JE (2009) Progesterone receptor a (PRA) and PRB-independent effects of progesterone on gonadotropin-releasing hormone release. Endocrinology. 150(8):3833–3844. https://doi.org/10.1210/en.2008-0774
22. Dosiou C, Hamilton AE, Pang Y, Overgaard MT, Tulac S, Dong J, Thomas P, Giudice LC (2008) Expression of membrane progesterone receptors on human T lymphocytes and Jurkat cells and activation of G-proteins by progesterone. J Endocrinol 196:67–77. https://doi.org/10.1677/JOE-07-0317
23. Dressing GE, Thomas P (2007) Identification of membrane progestin receptors in human breast cancer cell lines and biopsies and their potential involvement in breast cancer. Steroids. 72(2):111–116. https://doi.org/10.1016/j.steroids.2006.10.006
24. Dressing GE, Alyea R, Pang Y, Thomas P (2012) Membrane progesterone receptors (mPRs) mediate progestin induced antimorbidity in breast cancer cells and are expressed in human breast tumors. Hormones Cancer 3(3):101–112. https://doi.org/10.1007/s12672-012-0106-x
25. Charles N, Thomas P, Lange C (2010) Expression of membrane progesterone receptors (mPR/PAQR) in ovarian cancer cells: implications for progesterone induced signaling events. Hormones Cancer 1(4):167–176. https://doi.org/10.1007/s12672-010-0023-9

26. González-Arenas A, Cabrera-Wrooman A, Díaz N, González-García T, Salido-Guadarrama I, Rodríguez-Dorantes M, Camacho-Arroyo I (2014) Progesterone receptor subcellular localization and gene expression profile in human astrocytoma cells are modified by progesterone. Nucl Recept Res 1:1–10. https://doi.org/10.11131/2014/101098
27. González-Agüero G, Gutiérrez AA, González-Espinosa D, Solano JD, Morales R, González-Arenas A, Camacho-Arroyo I (2007) Progesterone effects on cell growth of U373 and D54 human astrocytoma cell lines. Endocrine. 32(2):129–135. https://doi.org/10.1007/s12020-007-9023-0
28. Piña-Medina AG, Hansberg-Pastor V, González-Arenas A, Cerbón M, Camacho-Arroyo I (2016) Progesterone promotes cell migration, invasion and cofilin activation in human astrocytoma cells. Steroids. 105:19–25. https://doi.org/10.1016/j.steroids.2015.11.008
29. Germán-Castelán L, Manjarrez-Marmolejo J, González-Arenas A, Camacho-Arroyo I (2016) Intracellular progesterone receptor mediates the increase in glioblastoma growth induced by progesterone in the rat brain. Arch Med Res 47:419–426. https://doi.org/10.1016/j.arcmed.2016.10.002
30. Germán-Castelán L, Manjarrez-Marmolejo J, González-Arenas A, González-Morán MG, Camacho-Arroyo I (2014) Progesterone induces the growth and infiltration of human astrocytoma cells implanted in the cerebral cortex of the rat. Biomed Res 2014:1–8. https://doi.org/10.1155/2014/393174
31. Valadez-Cosmes P, Germán-Castelán L, González-Arenas A, Velasco-Velázquez MA, Hansberg-Pastor V, Camacho-Arroyo I (2015) Expression and hormonal regulation of membrane progesterone receptors in human astrocytoma cells. J Steroid Biochem Mol Biol 154:176–185. https://doi.org/10.1016/j.jsbmb.2015.08.006
32. González-Orozco JC, Hansberg-Pastor V, Valadez-Cosmes P, Nicolas-Ortega W, Bastida-Beristain Y, Fuente-Granada MDL et al (2018) Activation of membrane progesterone receptor-alpha increases proliferation, migration, and invasion of human glioblastoma cells. Mol Cell Endocrinol 477:81–89. https://doi.org/10.1016/j.mce.2018.06.004
33. Colaprico A, Silva TC, Olsen C, Garofano L, Cava C, Garolini D, Sabedot T, Malta TM, Pagnotta SM, Castiglioni I, Ceccarelli M, Bontempi G, Noushmehr H (2016) TCGAbiolinks: an R/bioconductor package for integrative analysis of TCGA data. Nucleic Acids Res 44(8):e71. https://doi.org/10.1093/nar/gkv1507
34. Love MI, Huber W, Anders S (2014) Moderated estimation of fold change and dispersion for RNA-seq data with DESeq2. Genome Biol 15:550. https://doi.org/10.1186/s13059-014-0550-8
35. Zerbino DR, Achuthan P, Akanni W, Amode MR, Barrell D, Bhai J, Billis K, Cummins C, Gall A, Girón CG, Gil L, Gordon L, Haggerty L, Haskell E, Hourlier T, Izuogu OG, Janacek SH, Juettemann T, To JK, Laird MR, Lavidas I, Liu Z, Loveland JE, Maurel T, McLaren W, Moore B, Mudge J, Murphy DN, Newman V, Nuhn M, Ogeh D, Ong CK, Parker A, Patricio M, Riat HS, Schuilenburg H, Sheppard D, Sparrow H, Taylor K, Thormann A, Vullo A, Walts B, Zadissa A, Frankish A, Hunt SE, Kostadima M, Langridge N, Martin FJ, Muffato M, Perry E, Ruffier M, Staines DM, Trevanion SJ, Aken BL, Cunningham F, Yates A, Flicek P (2018) Ensembl 2018. Nucleic Acids Res 46(D1):D754–D761. https://doi.org/10.1093/nar/gkx1098
36. Khan A, Fornes O, Stigliani A, Gheorghe M, Castro-Mondragon JA, van der Lee R, Bessy A, Chèneby J, Kulkarni SR, Tan G, Baranasic D, Arenillas DJ, Sandelin A, Vandepoele K, Lenhard B, Ballester B, Wasserman WW, Parcy F, Mathelier A (2018) JASPAR 2018: update of the open-access database of transcription factor binding profiles and its web framework. Nucleic Acids Res 46(D1):D260–D266. https://doi.org/10.1093/nar/gkx1126
37. Okonechnikov K, Golosova O, Fursov M (2012) Unipro UGENE: a unified bioinformatics toolkit. Bioinformatics. 28(8):1166–116710. https://doi.org/10.1093/bioinformatics/bts091
38. Wingender E, Schoeps T, Haubrock M, Krull M, Dönitz J (2018) TFClass: expanding the classification of human transcription factors to their mammalian orthologs. Nucleic Acids Res 46(D1):D343–D347. https://doi.org/10.1093/nar/gkx987
39. Li B, Lin Z, Liang Q, Hu Y, Xu WF (2018) PAQR6 expression enhancement suggest a worse prognosis in prostate cancer patients. Open Life Sci 13:511–517. https://doi.org/10.1515/biol-2018-0061
40. Hiavaty J, Ertl R, Miller I, Cordula G (2016) Expression of progesterone receptor membrane component 1 (PGRMC1), progestin and AdipoQ receptor 7 (PAQPR7), and plasminogen activator inhibitor 1 RNA-binding protein (PAIRBP1) in glioma spheroids in vitro. Biomed Res Int 2016:1–12. https://doi.org/10.1155/2016/8065830
41. Cabrera-Muñoz E, González-Arenas A, Saqui-Salces M, Camacho J, Larrea F, García-Becerra R et al (2009) Regulation of progesterone receptor isoforms content in human astrocytoma cell lines. J Steroid Biochem Mol Biol 113:80–84. https://doi.org/10.1016/j.jsbmb.2008.11.009
42. Zamora-Sánchez CJ, Hansberg-Pastor V, Salido-Guadarrama I, Rodriguez-Dorantes M, Camacho-Arroyo I (2017) Allopregnanolone promotes proliferation and differential gene expression in human glioblastoma cells. Steroids. 119:36–42. https://doi.org/10.1016/j.steroids.2017.01.004

Publisher's Note Springer Nature remains neutral with regard to jurisdictional claims in published maps and institutional affiliations.

cells

MDPI

Article

Progesterone through Progesterone Receptor B Isoform Promotes Rodent Embryonic Oligodendrogenesis

Juan Carlos González-Orozco, Aylin Del Moral-Morales and Ignacio Camacho-Arroyo *

Unidad de Investigación en Reproducción Humana, Instituto Nacional de Perinatología-Facultad de Química, Universidad Nacional Autónoma de México (UNAM), Ciudad de Mexico 04510, Mexico; g.orozco221@gmail.com (J.C.G.-O.); aylindmm@gmail.com (A.D.M.-M.)

* Correspondence: camachoarroyo@gmail.com

Received: 12 March 2020; Accepted: 28 March 2020; Published: 14 April 2020

Abstract: Oligodendrocytes are the myelinating cells of the central nervous system (CNS). These cells arise during the embryonic development by the specification of the neural stem cells to oligodendroglial progenitor cells (OPC); newly formed OPC proliferate, migrate, differentiate, and mature to myelinating oligodendrocytes in the perinatal period. It is known that progesterone promotes the proliferation and differentiation of OPC in early postnatal life through the activation of the intracellular progesterone receptor (PR). Progesterone supports nerve myelination after spinal cord injury in adults. However, the role of progesterone in embryonic OPC differentiation as well as the specific PR isoform involved in progesterone actions in these cells is unknown. By using primary cultures obtained from the embryonic mouse spinal cord, we showed that embryonic OPC expresses both PR-A and PR-B isoforms. We found that progesterone increases the proliferation, differentiation, and myelination potential of embryonic OPC through its PR by upregulating the expression of oligodendroglial genes such as neuron/glia antigen 2 (NG2), sex determining region Y-box9 (SOX9), myelin basic protein (MBP), 2′,3′-cyclic-nucleotide 3′-phosphodiesterase (CNP1), and NK6 homeobox 1 (NKX 6.1). These effects are likely mediated by PR-B, as they are blocked by the silencing of this isoform. The results suggest that progesterone contributes to the process of oligodendrogenesis during prenatal life through specific activation of PR-B.

Keywords: oligodendrocyte progenitor cells; oligodendrogenesis; myelination; progesterone; progesterone receptor

1. Introduction

Central nervous system (CNS) myelination is a process that begins in late stages of mammalian prenatal life and extends to adulthood [1,2]; however, the oligodendrocytes responsible of this process arise earlier in embryonic neurodevelopment by the specification of neural stem cells (NSC) into oligodendroglial progenitor cells (OPC) after the neurogenic phase [3], which occurs approximately on day 12.5 of the mouse embryonic development and between gestational weeks 16–18 in the human [4,5].

The first site of OPC specification during mammalian neurodevelopment has been identified in the ventral region of the neural tube, in the prospective cervical portion of the spinal cord [4,6,7]. In this region, after the first wave of generation of the motoneurons of the spinal cord, the morphogen sonic hedgehog (Shh) promotes the induction of the NSC into OPC by upregulating the expression of a transcriptional program associated to the oligodendroglial lineage [6,8]; among the upregulated genes in this early specification stage are the transcription factors sex determining region Y-box9/10 (Sox9/10), oligodendrocyte transcription factor 1/2 (Olig1/2), NK6 homeobox 1/2 (Nkx 6.1/6.2) and the receptor α for the platelet-derived growth factor (PDGFRa) [8–10]. Then, newly specified OPC actively proliferate and migrate to establish a homogenous distribution [4,7,11].

The proliferation and migratory phenotype of early OPC is maintained by the platelet-derived growth factor (PDGF) and the fibroblast growth factor 2 (FGF2) [7,12], whereas mitotic arrest and subsequent oligodendrocyte differentiation is promoted by several elements such as thyroid hormones [13,14], the ciliary neurotrophic factor (CNTF), the extracellular matrix component laminin α2 (merosin), and the presence of neuronal activity [15–17]; final maturation to myelinating oligodendrocytes is induced by the upregulation of promyelinating genes such as the myelin basic protein (MBP), myelin proteolipid protein (PLP), and 2′,3′-cyclic-nucleotide 3′-phosphodiesterase (CNP1) [17,18].

Along with these elements, some studies have shown that progesterone also has a role in developmental oligodendrogenesis and the myelination process [19]; in fact, because the main role of this hormone lies in the maintenance of pregnancy, progesterone is constitutively present in the maternal and embryo-fetal circulation throughout development [20], and continues to be synthesized in the CNS of both females and males after birth [21]. In the adult, it regulates different functions such as neuroprotection, neurogenesis, neuronal plasticity, sexual behavior, mood, learning, and memory [22,23].

Progesterone exerts its effects mainly through two pathways: a directly genomic pathway and a non-genomic pathway. Through the genomic pathway, it interacts with its intracellular receptor (PR), a transcription factor that, once activated, binds to specific DNA sequences named progesterone response elements (PRE) that are mainly located in gene promoter regions, thus regulating their expression [24,25]. Meanwhile, the non-genomic pathway is related to rapid cellular responses triggered by the activation of different G protein-coupled membrane receptors to progesterone (mPRs) or PR ligand-independent activation [26,27].

There are two PR isoforms, PR-A and PR-B, which are encoded in the same gene but from different transcription start sites [28], which makes the PR-A isoform an N-terminally truncated form of the complete PR-B isoform [29,30]. In the brain and the spinal cord, they present a different expression pattern, regulation, and function [31–35]. Generally, given that the PR-B is a more potent transcription activator than the PR-A, the former is the positive regulator of the genomic effects of progesterone, whereas PR-A is mainly a transcriptional repressor [36–38].

The effects of progesterone on developmental oligodendrogenesis and myelination have been documented in cerebellar organotypic cultures obtained from postnatal rats and mice. It was demonstrated that the addition of progesterone to the culture medium immediately increases OPC proliferation, and after 1 week it increases the number of differentiated oligodendrocytes and its potential of nerve myelination, as seen by an increasing in MBP expression, effects that were found to be mediated by a genomic mechanism of action because the use of the PR antagonist mifepristone blocked them [39,40]. In addition, it was reported that OPC from the brain of newborn rats actively synthetizes and metabolizes progesterone during its proliferative phase prior to its differentiation into oligodendrocytes, suggesting that autocrine and paracrine actions of progesterone contribute to oligodendrocyte development and nerve myelination [41].

Moreover, progesterone also has effects on CNS remyelination in adulthood because it increases the number of differentiated oligodendrocytes and upregulates the expression of genes involved in myelin repair in adult rats with spinal cord injury. Therefore, progesterone has been proposed to treat demyelinating lesions [42,43].

Despite these studies, it is unknown if progesterone also promotes differentiation of OPC during embryonic life, as well as the specific PR isoform involved in progesterone actions in these glial cells, which is relevant to understand the mechanisms underlying the developmental oligodendrogenesis and thus elaborate therapeutic strategies to treat demyelinating lesions in postnatal life. In this work, we studied the effects of progesterone and the role of PR in the proliferation, differentiation, and myelination potential of OPC, as well the effects of progesterone on the regulation of genes associated with developmental oligodendrogenesis by using isolated OPC from the embryonic mouse spinal cord. Finally, we studied the specific role of PR-B in the embryonic OPC.

2. Materials and Methods

2.1. Animals

Female CD-1 mice with 14.5 days of pregnancy were used in this study. For this purpose, female mice purchased from the animal facility of Instituto de Investigaciones Biomédicas (UNAM, México) were mated with expert male mice for 12 h, and then maintained in individual cages with free access to food and water until the day of use. Day 0 of pregnancy was defined as the day on which the vaginal plug was observed. Animals were euthanized by cervical dislocation and embryos were extracted and transferred to a cold sterile phosphate-buffered saline (PBS) solution. All animals used in this study were handled following the bioethical guidelines approved by the internal committee for the care and use of laboratory animals (CICUAL) of Facultad de Química (UNAM, México).

2.2. OPC Culture

The cervical segments of the spinal cord of E14.5 mouse embryos were dissected and disaggregated in 0.1% trypsin (ThermoFisher Scientific, Waltham, MA, USA) during 20 min at 37 °C. Cellular suspension was centrifuged at 1000× *g* for 3 min and then resuspended in DMEM/F-12 (Dulbecco's Modified Eagle Medium/Nutrient Mixture F-12) with HEPES buffer, no phenol red culture medium (ThermoFisher Scientific) supplemented with B-27 (ThermoFisher Scientific). Then, 10 µL per 1 mL of disaggregated cells were mixed with 10 µL of trypan blue (ThermoFisher Scientific) and manually counted on a hemocytometer. Approximately 5×10^5 cells were plated per well in 12-well plates, with the addition of FGF2 (20 ng/mL) and the epidermal growth factor (EGF; 20 ng/mL) (Peprotech, Rocky Hill, NJ, USA), which were added every 2 days. After 1 week, the formation of cell spheroid aggregates (neurospheres) was observed. Then, neurospheres were disaggregated with 0.025% trypsin during 10 min at 37 °C; cells were counted as described before and 1.5×10^5 cells were plated under the same conditions; however, from the second day on culture, the growth factor PDGF (10 ng/mL) (Peprotech) was added in replacement of EGF. OPC selective expansion was obtained by platting 8×10^4 cells (derived from the disintegration of second passage neurospheres) per well in 12-well plates pretreated with 0.01% poly-L-lysine (Merck, Kenilworth, NJ, USA) with the addition of the growth factors FGF2 (10 ng/mL) and PDGF (10 ng/mL). Approximately 1 week later, cell confluence was observed; then, OPC were detached with 0.025% trypsin during 10 min at 37 °C and subcultured under the same conditions for approximately 1 week. Cells from the 3rd to 10th passage were used to perform the experiments. To perform the cell proliferation and differentiation experiments, the following pharmacological agents were used: triiodo-L-thyronine (T3; Sigma-Aldrich, St. Louis, MO, USA), progesterone (P4; Sigma-Aldrich), RU486 (mifepristone; Sigma-Aldrich), R5020 (promegestone; PerkinElmer Inc., Waltham, MA, USA), and Org OD 02-0 (10-ethenyl-19-norprogesterone; Sigma-Aldrich).

2.3. Immunofluorescence

Cells were fixed using 4% paraformaldehyde solution (Sigma-Aldrich) at room temperature for 20 min followed by three washes in PBS. Then, cells were permeabilized and blocked in a PBS solution with 1% bovine serum albumin (BSA; In Vitro, MEX), 1% glycine (Sigma-Aldrich), and 0.2% Triton X-100 (Sigma-Aldrich) at room temperature for 30 min. Cells were incubated at 4 °C for 12 h with primary antibodies at the following dilutions: 1:500 mouse anti- sex determining region Y-box2 (Sox2) (Santa Cruz, Dallas, TX, USA; sc-365964), 1:200 mouse anti-neuron/glia antigen 2 (NG2) (Millipore, Burlington, MA, USA; mab5384), 1:300 mouse anti-oligodendrocyte marker O4 (Millipore; mab345), 1:500 mouse anti-myelin basic protein (MBP) (Millipore; 05-675), 1:100 rabbit anti-microtubule-associated protein 2 (MAP2) (Invitrogen, Waltham, MA, USA; pa5-17646), 1:200 rabbit anti-Ki67 antigen (Millipore; ab9260), and 1:500 rabbit anti-glial fibrillary acidic protein (GFAP) (Abcam, Cambridge, UK; ab7260). Cells were rinsed three times in PBS and then incubated with secondary antibodies goat anti-mouse Alexa Fluor 488 or goat anti-rabbit Alexa Fluor 568, both at dilution 1:500 (ThermoFisher Scientific) at room temperature for 60 min. Nuclei were stained for 5 min

with 1 mg/mL Hoechst 33,342 solution (ThermoFisher Scientific). Finally, cells were coverslipped with fluorescence mounting medium (Polysciences Inc., Warrington, PA, USA) and visualized in an Olympus Bx43 microscope (JPN). All immunofluorescence images were captured with a 400X magnification from three random fields per coverslip in each independent experiment. All images were captured under the same gain, exposure time and light intensity conditions. The percentage of immunopositive cells was calculated considering the nuclei stained with Hoechst as the total (100%) number of cells using the "Cell counter" plugin in the ImageJ software ver. 1.51 (NIH, Bethesda, MD, USA). Fluorescence density was measured as "Integrated density" from the Analyze menu of ImageJ, whereas oligodendrocyte branching was measured as "Area" from the same menu options.

2.4. RNA Isolation and PCR Experiments

Total RNA was extracted using TRIzol LS reagent (ThermoFisher Scientific) following the manufacturer's instructions. One microgram of total RNA was used to synthesize the first strand of complementary DNA using the Moloney Murine Leukemia Virus (M-MLV) reverse transcriptase (TermoFisher Scientific) following the manufacturer's protocol. Two microliters from the previous reaction was used to perform RT-PCR or RT-qPCR experiments using the Platinum Taq DNA Polymerase (ThermoFisher Scientific) and the FastStart DNA Master SYBR Green I reagent kit (Roche, Basel, Switzerland), respectively. RT-PCR results were visualized in a 1.5% agarose (Sigma-Aldrich) gel electrophoresis. RT-qPCR experiments were performed on a LightCycler 1.5 (Roche) and relative expression levels were calculated by the ΔCt method. The used primers were: NG2: FW 5′-GCCCGTGCCCTCAGC-3′ RV 5′-CAAGTCTGACCTGGAGGCAT-3′; PDGFRa: FW 5′-GGAAGAGGATGACTCTGCCAT-3′ RV 5′-CGAAGCCTTTCTCGTGGACA-3′; OLIG1: FW 5′-GCAGCCACCTATCTCCTCAT-3′ RV 5′-GTGGCAATCTTGGAGAGCTT-3′; SOX9: FW 5′-GAGCTGGAAGTCGGAGAGC-3′ RV 5′-CTCTCGTTCAGCAGCCTCCA-3′; SOX10: FW 5′-AGCCCAGGTGAAGACAGAGA-3′ RV 5′-AGTCAAACTGGGGTCGTGAG-3′; MBP: FW 5′-TCACAGAAGAGACCCTCACA-3′ RV 5′-GCCGTAGTGGGTAGTTCTTG-3′; CNP1: FW 5′-TCCACGAGTGCAAGACGCTATTCA-3′ RV 5′-TGTAAGCATCAGCGGACACCATCT-3′; NKX 6.1: FW 5′-CTTCTGGCCCGGAGTGATG-3′ RV 5′-GGGTCTGGTGTGTTTTCTCTTC-3′; NKX 6.2: FW 5′-CTTCTGGCCCGGAGTGATG-3′ RV 5′-CGGTTGTATTCGTCATCGTC-3′; PR-B: FW 5′-ACCTGAGGCCAGATTCAGAAG-3′ RV 5′-GTATCCCCCACATGCACGTAT-3′ and 18S ribosomal RNA: FW 5′-AGTGAAACTGCAATGGCTC-3′ RV 5′-CTGACCGGGTTGGTTTTGAT-3′.

2.5. Analysis of Potential Progesterone Response Elements

The promoter sequences and transcription start sites were obtained from the Eukaryotic Promoter Database (EPD) (https://epd.epfl.ch//index.php); potential binding sites for PR were searched using the algorithms contained in JASPAR [44], TRANSFAC [45], and NUBIscan [46] databases. The binding sites predicted by two or more databases with a matrix similarity score higher than 0.8 were established as potential PRE.

2.6. Western Blot

OPC were detached from culture plates using PBS-EDTA (ethylenediaminetetraacetic acid; Sigma-Aldrich) and cell scraper (Corning, New York, NY, USA). Cells were centrifuged and obtained pellets were lysed with radioimmunoprecipitation assay (RIPA) buffer and protease inhibitors (1 mM EDTA, 2 μg/mL leupeptin, 2 μg/mL aprotinin, 1 mM phenylmethanesulfonyl fluoride (PMSF); Sigma-Aldrich). Total protein was extracted by centrifugation at 20,817× *g* at 4 °C for 15 min. The protein concentration of each sample was measured using the Pierce 660 nm Protein Assay reagent (ThermoFisher Scientific) and NanoDrop-2000 Spectrophotometer (ThermoFisher Scientific). A total of 100 μg of total protein was separated on 10% SDS-PAGE at 80 V for 2 h and then transferred to a polyvinylidene fluoride (PVDF) membrane (Merck) for 1 h at 25 V in semi-dry conditions at room temperature. Membranes were blocked overnight with 5% BSA (In Vitro) and then incubated at 4 °C

with primary antibodies mouse anti-PR in dilution 1:300 (Abcam; ab58568) or rabbit anti-α tubulin in dilution 1:1000 (Santa Cruz; sc-5286) for 48 h. Blots were incubated with goat anti-rabbit secondary antibody conjugated to horseradish peroxidase (HRP) in dilution 1:4500 (Santa Cruz; sc-2004) or mouse IgG kappa binding protein (mIgGκ BP) conjugated to HRP in dilution 1:5000 (Santa Cruz; sc516102) at room temperature for 45 min. Immunoreactive species were detected by chemiluminescence exposing blots to Kodak Biomax Light Film (Sigma-Aldrich) after incubation with Super Signal West Femto Maximum Sensitivity Substrate reagent (ThermoFisher Scientific). Blot images were captured with a digital camera (Sony, Tokyo, Japan); the densitometric analysis was performed using the ImageJ software ver. 1.51 (NIH).

2.7. siRNA-Mediated PR-B Silencing

Cultured OPC at 60–80% confluence were subjected to siRNA (small interfering RNA) transfection. The day of transfection, the cell medium was replaced with DMEM/F-12, HEPES phenol-red free without B27, antibiotics, and growth factors. Then, the cells were transfected with a PR-B siRNA duplex (150 nM) or with a control siRNA (150 nM) without any specific mRNA target sequence (Sigma-Aldrich) using the reagent Lipofectamine RNAiMAX (ThermoFisher Scientific) and following the manufacturer's instructions. Then, 24 h later, the transfection medium was exchanged with DMEM/F-12 and HEPES phenol-red free supplemented with B27 and growth factors. PR-B silencing was corroborated 48 h after transfection by RT-qPCR. The sequence of the employed mouse PR-B siRNA duplex was sense 5′-AUGACUGAGCUGCAGGCAA-3′, antisense 5′-UUGCCUGCAGCUCAGUCAU-3′.

2.8. Statistical Analysis

All data were analyzed and plotted with the GraphPad Prism 5.0 software (GraphPad, San Diego, CA, USA). Plotted data are representative of three independent experiments (i.e., from three different and independent cell cultures). Statistical analysis between comparable groups was performed using a one-way ANOVA with a Bonferroni post-test. RT-qPCR, Western blot, and siRNA silencing data were analyzed with a two-tail unpaired Student's *t*-test. Values of $p < 0.05$ were considered statistically significant.

3. Results

3.1. Oligodendrocyte Progenitor Cultures Derived from the Mouse Embryonic Spinal Cord

The cervical segments of the spinal cord of E14.5 mouse embryos (Figure S1A) were isolated to prepare primary neurosphere cultures (Figure 1A), as previously described [47]. The obtained neurospheres were mainly composed of cells positive for the stem cells marker Sox2 (Figure S1B,C). Then, OPC were selectively expanded by disaggregation of the neurospheres and plating the cells in adherent conditions supplemented with the growth factors FGF2 and PDGF (each one at 10 ng/mL); the effectiveness of obtaining cells from the oligodendroglial lineage by following this procedure has been previously demonstrated [48,49]. Highly proliferative cells with bipolar morphology were observed shortly after plating (Figure 1B and Figure S1D), which is the morphology associated with the OPC phenotype [49]. To confirm the oligodendroglial lineage, cells were immunostained with the typical OPC marker NG2 (Figure 1C); as shown, most of the cells were NG2 positive, and the signal was mainly detected in their nuclei and processes. Furthermore, the expression of oligodendroglial lineage genes was detected in OPC by RT-PCR experiments (Figure 1D). To determine whether the cultured OPC responded to well-known differentiation stimuli, cells were cultured without growth factors and treated for 3 days with the thyroid hormone T3 (40 ng/mL). After treatment, morphological changes were observed; additionally, the cells were immunostained positively for O4, a typical marker of differentiated oligodendrocytes. Some MBP (myelin marker)-positive cells were spotted (Figure 1E). Additionally, immunofluorescence to detect MAP2- or GFAP-positive cells after culturing the cells for 3 days without growth factors showed the presence of a low number of neurons or astrocytes, respectively (Figure S1E). With these results, the efficacy to obtain a large amount of highly pure

functional OPC from the spinal cord of E14.5 mouse embryos was demonstrated by following the described procedure.

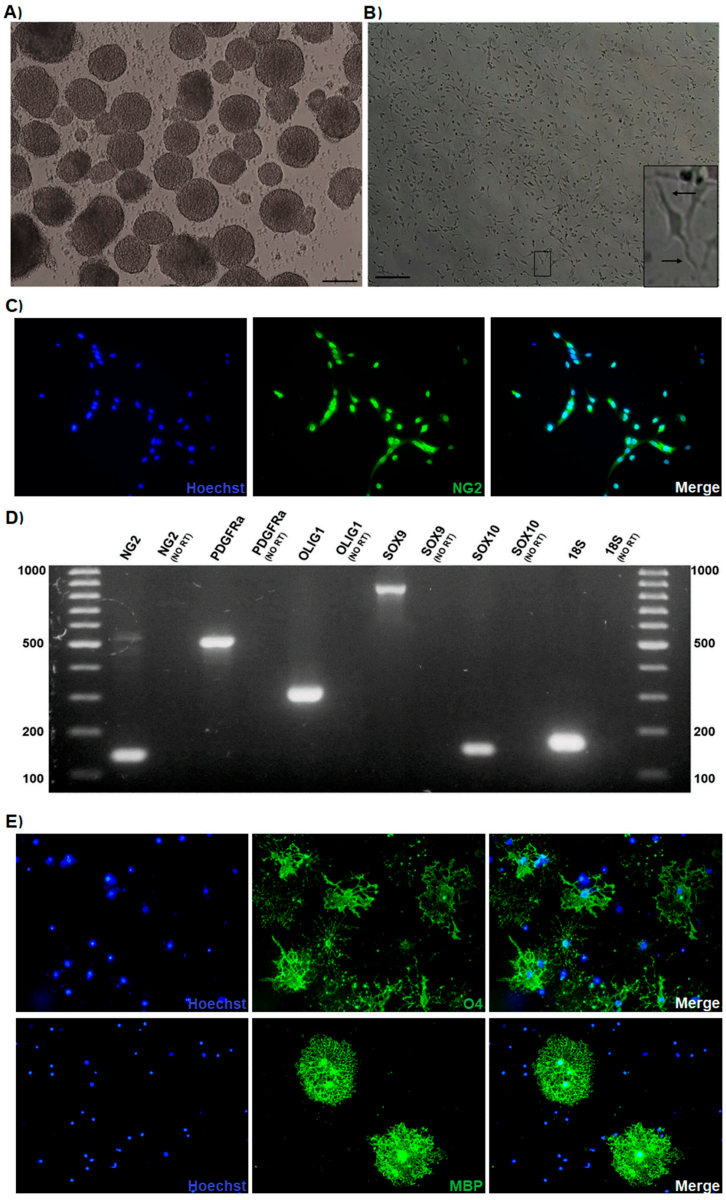

Figure 1. Oligodendroglial progenitor cells (OPC) cultures derived from the spinal cord of E14.5 mouse embryos. (**A**) Primary neurosphere cultures generated from the mouse embryonic spinal cord. (**B**) Selective OPC expansion from the neurospheres. The arrows in the zoomed area shows the bipolar processes. Scale bars: 100 µm. (**C**) Immunodetection of the typical OPC marker NG2 in the cultured cells. Nuclei stained with Hoechst are shown in blue, anti-NG2 primary antibody is shown in green, and merge panel shows the combination of blue and green colors. (**D**) The expression of the oligodendrogial genes NG2 (143 bp), PDGFRa (524 bp), OLIG1 (309 bp), SOX9 (820 bp), and SOX10 (146 bp) was detected in the cultured cells by RT-PCR. (**E**) The OPC were cultured without growth factors and treated for 3 days with T3 hormone (40 ng/mL); differentiation was evaluated by immunodetection of the oligodendrocyte marker O4 and the myelin marker myelin basic protein (MBP). All immunofluorescence images were captured with 400× magnification.

3.2. Progesterone Promotes the Proliferation and Differentiation of Mouse Embryonic OPC and Increases Its Potential of Myelination through the PR

Once the protocol for obtaining OPC from the mouse embryonic cord was established, the effects of progesterone on cell proliferation were evaluated. For this purpose, OPC were cultured with the addition of growth factors (FGF2 and PDGF at 10 ng/mL each one) and treated for 3 days with progesterone (10 nM), the competitive PR antagonist RU486 (1 μM), or progesterone and RU486. As shown in Figure 2, progesterone increased the percentage of Ki67/NG2-positive cells as compared with the vehicle control, whereas the treatment with only RU486 did not induce any change. RU486 blocked progesterone effect, suggesting that progesterone promotes OPC proliferation through its PR. To further confirm this statement, cell proliferation was assessed treating the OPC with the PR agonist R5020 (10 nM), or with the mPRs-specific agonist Org OD 02-0 (100 nM). As observed with progesterone, the agonist R5020 increased the number of proliferating Ki67/NG2 cells, whereas the mPRs agonist did not increase it (Figure S2).

Progesterone also promoted the differentiation of OPC that were cultured without growth factors and treated for 3 days, as seen by a striking increase in the number of O4-positive cells in immunofluorescence preparations (Figure 3A,B). With this approach, it was also observed that progesterone significantly increased the branching area of the differentiated oligodendrocytes (Figure 3C), and all these effects were mediated by the PR because the treatments with RU486 blocked them (Figure 3). Moreover, R5020 induced similar results as compared with progesterone, whereas Org OD 02-0 did not induce any effect (Figure S3).

Regarding the potential of myelination, progesterone increased the expression of the myelin marker MBP in the differentiated OPC, and RU486 blocked this effect (Figure 4). Moreover, the PR agonist R5020 exerted similar effects to those of progesterone. In contrast, Org OD 02-0 did not produce any significant change in MBP expression (Figure S4). These results suggest that progesterone through a genomic mechanism of action regulates the proliferation and differentiation of mouse embryonic OPC, also increasing their myelinating function.

3.3. Progesterone Upregulates the Expression of Oligodendroglial Genes

Considering that progesterone promoted the proliferation and differentiation of the cultured OPC through the specific activation of the PR (i.e., by a genomic mechanism of action), the effects of progesterone on the regulation of the expression of various genes associated with the embryonic oligodendrogenesis were studied. After 24 h of exposure, progesterone upregulated the expression of the transcription factor Nkx 6.1, as well as the expression of the myelin marker Cnp1 in the OPC, whereas after 48 h, the upregulated genes by progesterone were NG2; the transcription factor Sox9; and, as expected, the myelin marker MBP. Although it was not observed that progesterone significantly increased the expression of the genes of PDGFRa, Sox10, and Nkx 6.2, an increasing trend was observed in cells exposed to the hormone (Figure 5). The PR works as a transcription factor that binds to DNA sequences known as PRE, which are usually located in promoter regions of target genes. In order to detect potential PRE sequences in the promoter regions of the progesterone-upregulated genes, an in silico analysis was performed. The promoter sequences of the NG2, Sox9, Nkx 6.1, Cnp1, and MBP genes were obtained from the EPD and confirmed by a BLAST (Basic Local Alignment Search Tool) analysis (https://blast.ncbi.nlm.nih.gov/Blast.cgi). By using the algorithms from the JASPAR, TRANSFAC, and NUBIscan databases, it was identified that all genes have potential PRE in their promoter regions (Figure S5). Based on these results, it was confirmed that the effects of progesterone on embryonic OPC were mediated by a genomic mechanism of action, and that in addition, progesterone can differentially regulate the expression of genes associated with oligodendrogenesis throughout embryogenesis.

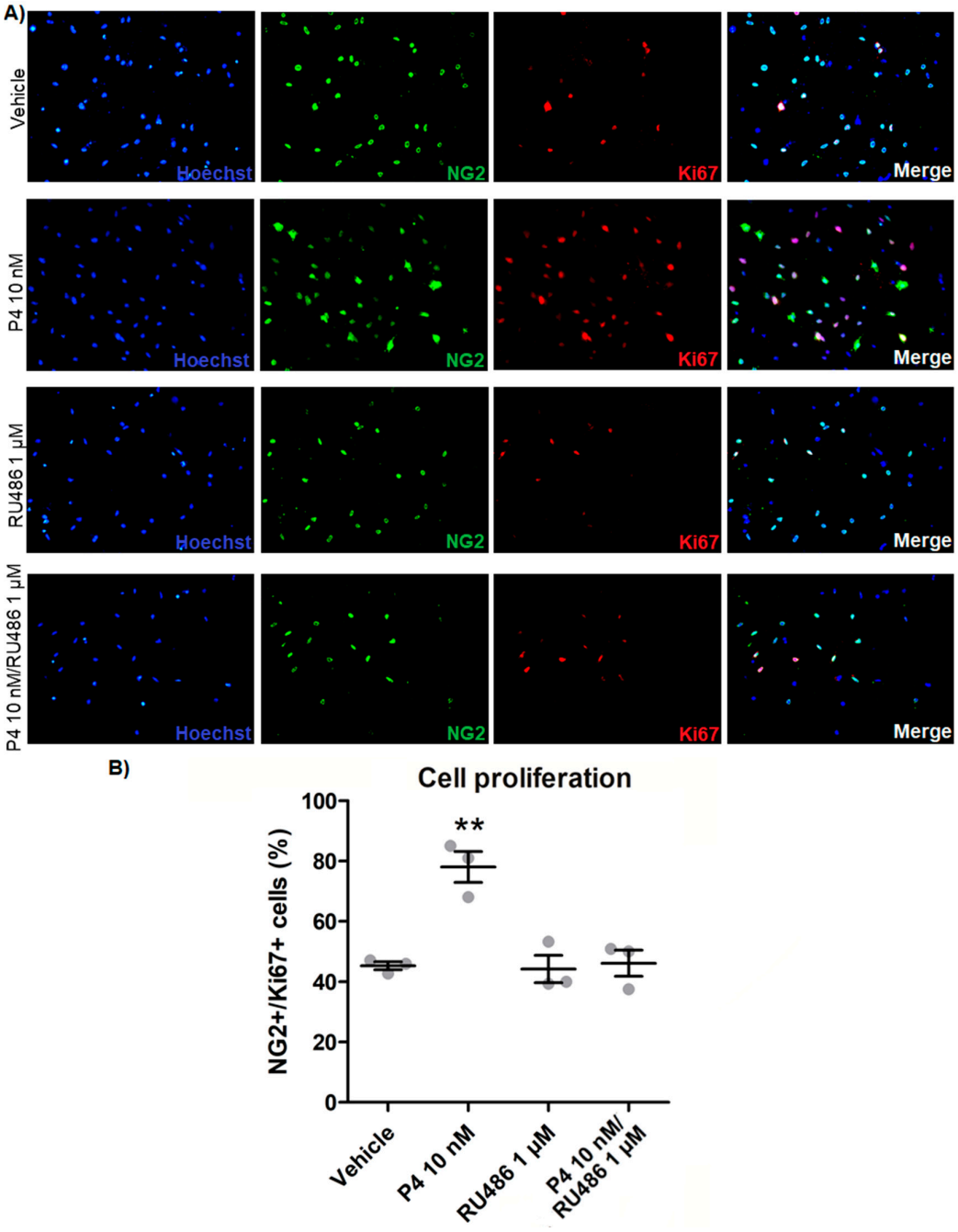

Figure 2. Progesterone increases embryonic OPC proliferation. (**A**) NG2/Ki67 immunostaining in OPC cultured with growth factors and treated with progesterone (P4; 10 nM), RU486 (1 µM), P4 (10 nM) and RU486 (1 µM), and vehicle (DMSO 0.01%), for 3 days. (**B**) Graph derived from the percentage of NG2/Ki67-positive cells observed in the immunofluorescence experiments. The percentage of NG2+/Ki67+ cells was determined as a percentage of the total number of cells stained with Hoechst. Results are expressed as the mean ± standard error of the mean (S.E.M.); $n = 3$; ** $p < 0.01$ vs. the rest of the groups.

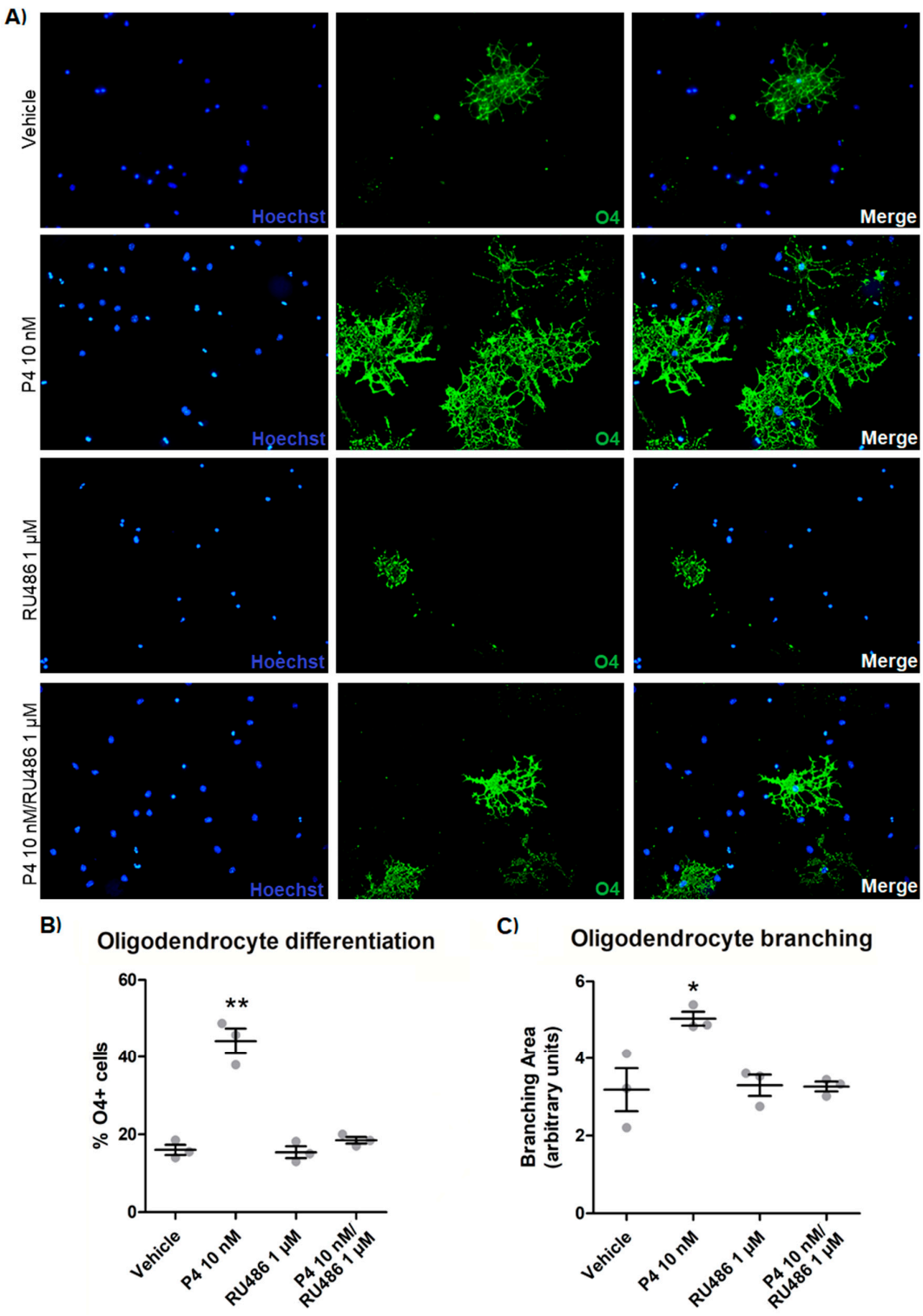

Figure 3. Progesterone promotes oligodendrocyte differentiation. (**A**) O4 immunofluorescence in OPC cultured without growth factors and treated for 3 days with P4 (10 nM), RU486 (1 µM), P4 (10 nM) and RU486 (1 µM), and vehicle (DMSO 0.01%). (**B**) Percentage of O4-positive cells observed in the immunofluorescence experiments. The percentage of O4+ cells was determined as a percentage of the total number of cells stained with Hoechst. (**C**) Cellular branching measured in O4-positive cells. Results are expressed as the mean ± S.E.M. $n = 3$; * $p < 0.05$ and ** $p < 0.01$ vs. the rest of the groups.

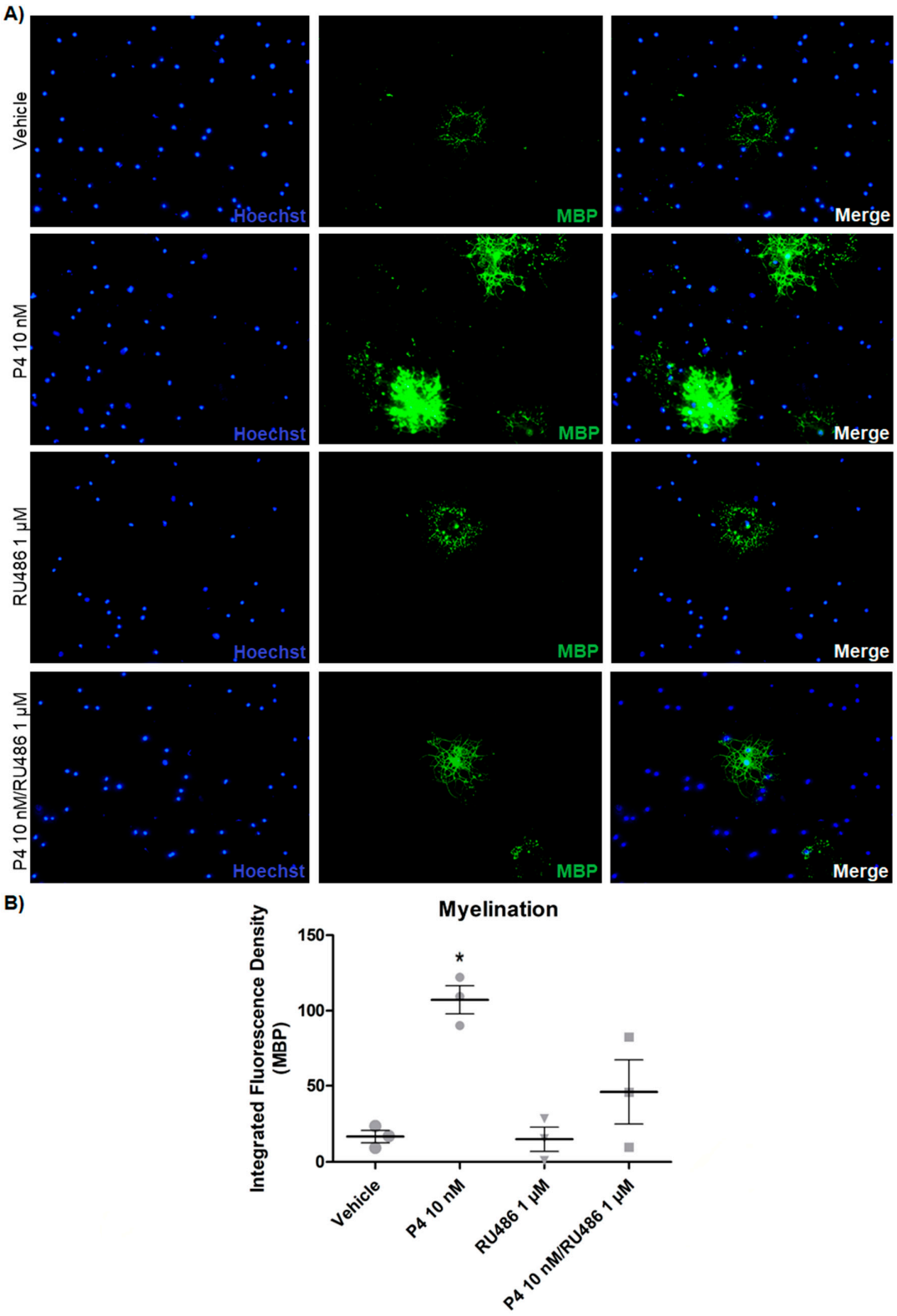

Figure 4. Progesterone increases the potential of myelination of differentiated OPC. (**A**) MBP immunofluorescence in OPC cultured without growth factors and treated for 3 days with P4 (10 nM), RU486 (1 µM), P4 (10 nM) and RU486 (1 µM), and vehicle (DMSO 0.01%). (**B**) MBP expression measured as a fluorescence density. Results are expressed as the mean ± S.E.M. $n = 3$; * $p < 0.05$ vs. vehicle and RU486.

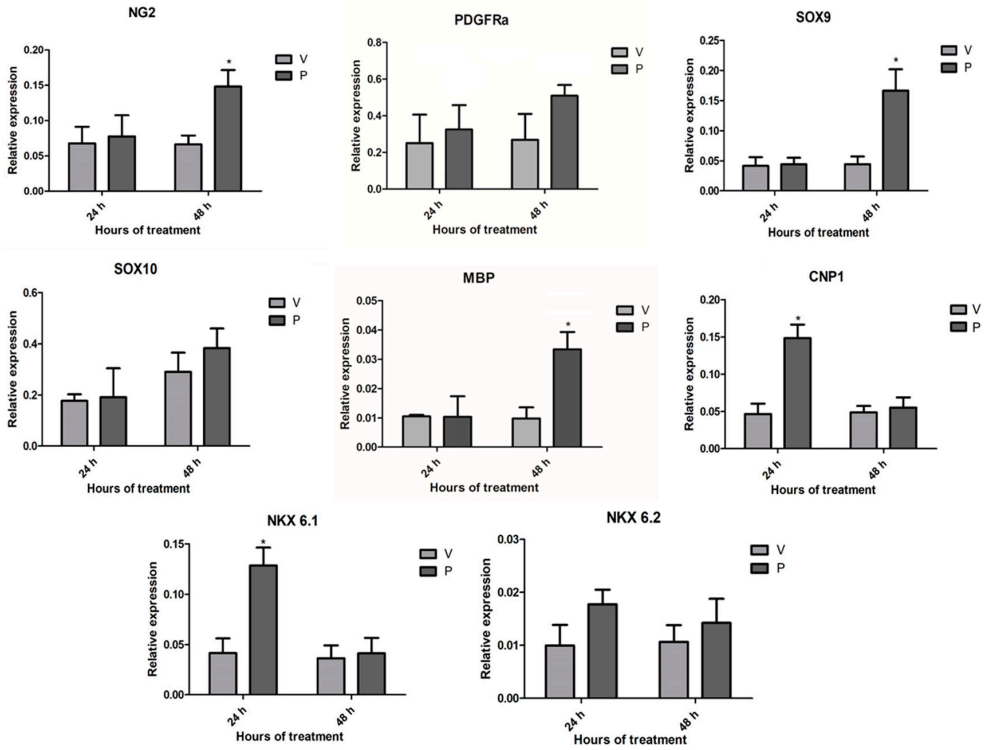

Figure 5. Progesterone upregulates the expression of oligodendroglial genes. The graphs show the relative gene expression (normalized to the 18S gene expression) of the NG2, PDFGR, SOX9, SOX10, MBP, 2′,3′-cyclic-nucleotide 3′-phosphodiesterase (CNP1), NKX 6.1, and NKX 6.2 genes obtained by RT-qPCR after treating OPC with P4 (10 nM) and vehicle (DMSO 0.01%) for 24 and 48 h. Results are expressed as the mean ± S.E.M. $n = 3$; * $p < 0.05$ vs. vehicle.

3.4. The Mouse Embryonic OPC Express the PR-A and PR-B Isoforms and the Oligodendrogenic Actions of Progesterone are Mediated by the PR-B

Because PR expression in embryonic OPC is not yet reported, we first searched in the "Mouse Organogenesis Cell Atlas" (MOCA), using the "Genes" tool (https://oncoscape.v3.sttrcancer.org/atlas.gs.washington.edu.mouse.rna/landin) [50], if PR expression in mouse embryonic oligodendroglial cells was spotted by single-cell RNA sequencing (RNA-seq) during the assembly of this database. According to this database, radial glial cells, OPC, and premature oligodendrocytes from whole mouse embryos between 9.5 and 13.5 days of gestation express the PR; moreover, the expression of the PR increases when radial glial cells are specified towards OPC, and then decreases when they differentiate into oligodendrocytes (Figure 6A), suggesting a particular role of the PR in OPC. We detected the expression of PR-A and PR-B isoforms in the cultured embryonic OPC by Western blot, noticing that PR-B is expressed in a higher proportion than PR-A (Figure 6B). Given that PR-B is a more potent transcription activator than PR-A, and because it was observed that the effects of progesterone in the proliferation and differentiation of the OPC were mediated by a genomic mechanism, the expression of PR-B was silenced by siRNA transfection in order to study the role of this isoform in the mouse OPC. PR-B silencing was corroborated by RT-qPCR, observing that the transfection with the PR-B siRNA diminished PR-B expression by more than 60% as compared with the control siRNA (Figure 6C).

Twenty-four hours after transfection, the OPC were treated for 3 days with progesterone, and then cell proliferation and differentiation were determined by immunofluorescence. We noticed a significant lower percentage of NG2/Ki67 and O4-positive cells in the PR-B siRNA-transfected cells as compared with the control siRNA-transfected cells (Figure 7). This indicates that the oligodendrogenic effects of progesterone are mediated by PR-B.

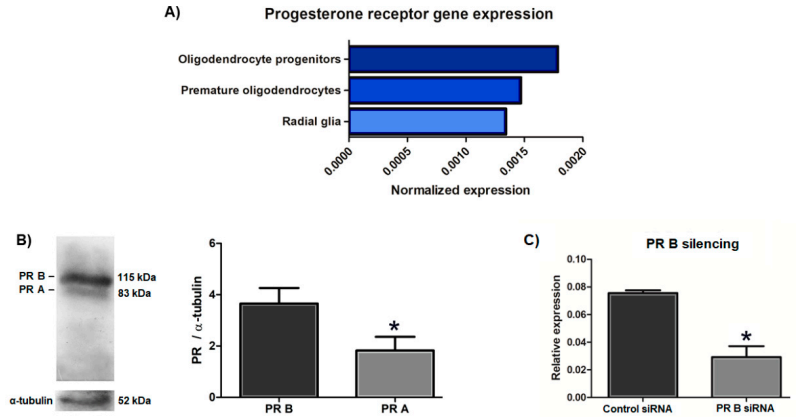

Figure 6. The OPC from the mouse embryonic spinal cord express both progesterone receptor (PR) isoforms. (**A**) PR gene expression analyzed by single cell RNA-seq in radial glial cells, oligodendrocyte progenitors, and premature oligodendrocytes from E9.5-E13.5 whole mouse embryos obtained from the "Mouse Organogenesis Cell Atlas" [50]. (**B**) PR-A and PR-B expression detected by Western blot in the cultured OPC derived from the spinal cord of E14.5 mouse embryos. (**C**) PR-B silencing by siRNA transfection in the cultured OPC corroborated by RT-qPCR. Results are expressed as the mean ± S.E.M. $n = 3$; * $p < 0.05$ vs. PR-B; * $p < 0.05$ vs. control siRNA.

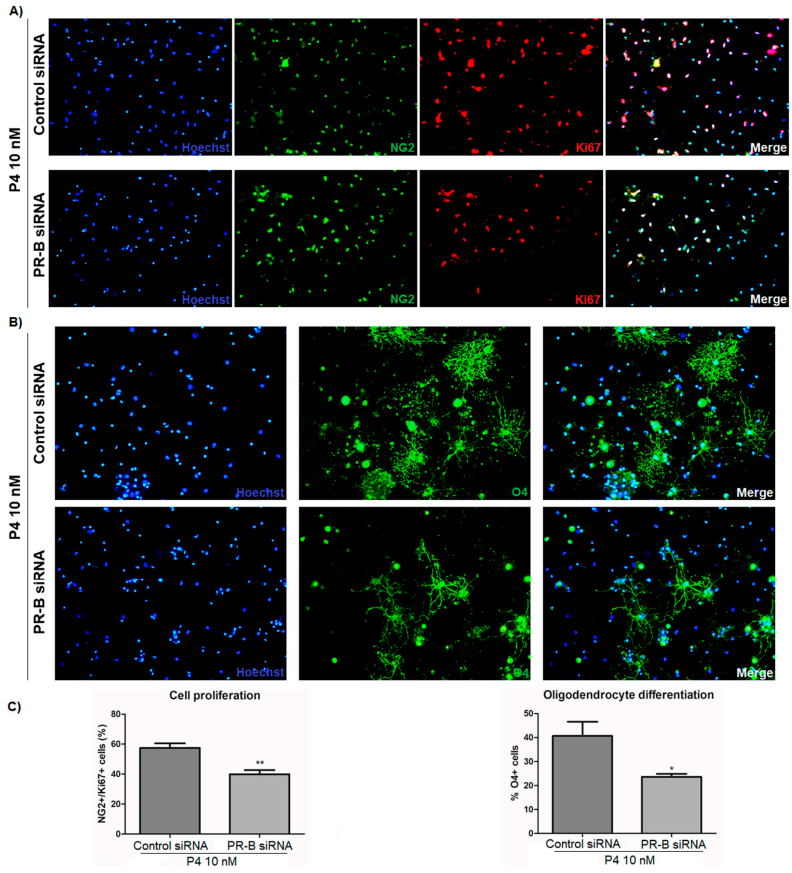

Figure 7. The silencing of PR-B blocks the oligodendrogenic effects of progesterone. (**A**) NG2/Ki67 and (**B**) O4 immunofluorescence in OPC transfected with a control siRNA or with a PR-B siRNA and treated for 3 days with P4 (10 nM). (**C**) Graphs derived from the percentage of NG2/Ki67 and O4-positive cells observed in the immunofluorescence. Results are expressed as the mean ± S.E.M. $n = 3$; * $p < 0.05$ and ** $p < 0.01$ vs. control siRNA.

4. Discussion

Progesterone functions extend beyond the regulation of female reproduction. In fact, because it is synthesized in the CNS of both males and females, it is referred as a neurosteroid and regulates several neural functions including neuroprotection, neuromodulation, neurogenesis, neuronal plasticity, and nerve remyelination [22,23]. Moreover, progesterone also participates in critical development events such as neuronal differentiation, neural circuit organization, brain sex differentiation, and oligodendrogenesis [51].

The effects of progesterone on nerve myelination were first documented in peripheral nerves, where progesterone promotes the remyelination after traumatic injury [52]. These observations were later expanded to the CNS. It has been reported that progesterone has neuroprotective and promyelinating effects on adult individuals with spinal cord injury [42,43], leading to the proposal of the therapeutic use of progesterone for the treatment of demyelinating lesions [43,53]. Regarding the developmental oligodendrogenesis, it is documented that OPC from the brain of newborn rats synthesizes progesterone [41], and that this hormone also promotes, through the activation of its PR, the proliferation and differentiation of the OPC, while also increasing the developmental nerve myelination, as has been observed in the cerebellum of postnatal rodents [39,40]. Nonetheless, it is unknown if progesterone also promotes the proliferation and differentiation of OPC during early oligodendrogenesis in embryonic life, as well as the PR isoform involved in progesterone effects, which is relevant in order to understand the mechanisms that underlie embryonic oligodendrogenesis, and thus develop more efficient therapies to alleviate demyelinating diseases and lesions in postnatal life. Therefore, we studied the effects of progesterone and the role of PR-B isoform in OPC primary cultures derived from the spinal cord of E14.5 mouse embryos.

The developing mouse spinal cord is an accessible embryonic tissue that contains diverse CNS progenitor cells and a reliable study model because the spatial and temporal events underlying the neurogenesis and gliogenesis in this tissue are well defined [54,55]. The specification of the NSC into OPC during mouse neurodevelopment occurs on the embryonic day 12.5 [4]; in addition, it has been reported that NSC isolated from the mouse embryonic spinal cord are more oligogenic than NSC isolated from the developing brain [56]. Thus, we were able to obtain a large amount of highly pure OPC from neurosphere cultures formed primarily of Sox2-positive NSC isolated from the spinal cord of E14.5 mouse embryos. In this study, we showed that progesterone increased the rate of proliferation of the cultured embryonic OPC and promoted its differentiation into oligodendrocytes as previously reported in OPC from the cerebellum of postnatal rodents [39,40]. In addition to this, we observed that progesterone enhanced the potential of myelination of the embryonic OPC, as seen by an increase in MBP protein expression. We were able to observe this latter expression because it has long been known that mouse oligodendrocytes do not need the presence of active neurons to start expressing myelin markers in vitro [57]. The oligodendrogenic effects of progesterone were mediated by the PR because PR agonist R5020 exerted similar effects to those of progesterone, whereas the PR antagonist RU486 blocked them. Likewise, the mPR agonist Org OD 02-0 did not induce any effect. This suggests that progesterone participates in the oligodendrogenesis during prenatal development through a genomic mechanism of action. The genomic effects of progesterone in the OPC were confirmed by evaluating the expression of various genes associated with the specification and maintenance of the oligodendroglial phenotype; specifically, we observed that progesterone increased the expression of Nkx 6.1 and Cnp1 genes 24 h after exposure, whereas the expression of NG2, Sox9, and MBP genes was augmented at 48 h without inducing changes in the expression of Nkx 6.1 and Cnp1, therefore suggesting that progesterone regulates the expression of oligodendroglial genes in a time dependent-manner. Previously, it was reported that progesterone upregulates the expression of the oligodendroglial genes Olig1/2, Nkx 2.2, MBP, myelin proteolipid protein (PLP), and myelin-oligodendrocyte glycoprotein (MOG) in adult rats with complete spinal cord injury, whereas it also increases the number of myelinating oligodendrocytes by promoting the proliferation of the adult remnant OPC and its subsequent differentiation in these same animals [42]. In a similar study, it was also shown that progesterone upregulates the expression of MBP, PLP, Nkx 2.2, and Olig1 in the spinal cord of a murine model of multiple sclerosis. This upregulation

was associated with the observed neuroprotective and remyelinating effects of progesterone in these animals [58]. These studies, together with ours, demonstrate that the role of progesterone in the OPC and myelination process during the development or demyelinating lesions is mediated by the upregulation of key oligodendroglial genes. Furthermore, the fact that OPC from the spinal cord of adult individuals are responsive to progesterone, especially during injury, indicates that these cells retain their sensitivity to this hormone since the prenatal state, and it then expands to adulthood.

Previously, the total expression of the PR has been detected in cultured astrocytes and oligodendrocytes isolated from the brain of newborn rats [59], and additionally the expression of the PR-B has been observed by immunohistochemistry in neurons and glial cells of the rat spinal cord with no significant sex differences [60]. In this work, we were able to detect the expression of both PR isoforms in the embryonic OPC by Western blot, with the particular observation that PR-B expression is higher than that of PR-A. Additionally, we examined in the MOCA database [50] the expression of the PR in oligodendroglial cells directly derived from E9.5-E13.5 whole mouse embryos. According to this database, the expression of the PR increases when radial glial cells are specified towards OPC, and then decreases when they differentiate into oligodendrocytes, indicating that PR plays a key role during the OPC stage. Therefore, we demonstrate that early OPC from the embryonic spinal cord of mouse constitutively express PR. Furthermore, because we noticed that the PR-B is more abundant in the OPC, and it is a more potent transcription activator than PR-A, we silenced its expression. Then, we observed that the effects of progesterone on OPC proliferation, differentiation, and myelination potential were significantly blocked, indicating that PR-B is the active mediator of progesterone and its effects on oligodendroglial cells. Nevertheless, we do not discard the possibility that the oligodendrogenic effects of progesterone could be synergistically mediated by both PR isoforms; for example, as transcriptional repressor, PR-A could inhibit the expression of genes that in turn repress the expression of the oligodendroglial genes regulated by PR-B. Thus, this issue deserves to be addressed in future studies.

Our results suggest that progesterone should participate in prenatal oligodendrogenesis. This is plausible because the expression of PR and the expression and activity of the enzymes required for progesterone synthesis have been found from the early embryo ages of the mammalian development in several regions of the developing CNS [61]. Additionally, pregnancy is characterized by an increase in maternal progesterone levels, and there is evidence that progesterone from the maternal circulation enters the embryo/fetal circulation and binds its PR in the developing rat CNS [62]. Remarkably, the levels of progesterone in fetal circulation and in the brain progressively increases throughout pregnancy, especially during late pregnancy [63], coinciding with the time in which the CNS undergoes critical processes such as neural circuits organization and myelination [64].

As mentioned above, the therapeutic use of progesterone to treat CNS injuries and demyelinating lesions has been proposed [43,53], and clinical studies have already been conducted [65]. However, phase 3 clinical trials in patients with traumatic brain injury have failed to replicate the positive outcomes observed in phase 2 trials and in animal models [66]. It is relevant to mention that these clinical trials, as well those previously performed in animal models, did not contemplate the expression or specific function of PR isoforms. Here, we showed that PR-B is predominantly expressed in the embryonic OPC and that it mediates the oligodendrogenic effects of progesterone. These results suggest that the expression and regulation of PR isoforms should determine the oligodendrogenic and promyelinating actions of progesterone in a tissue and developmentally dependent manner.

Supplementary Materials: The following are available online at http://www.mdpi.com/2073-4409/9/4/960/s1: Figure S1: OPC cultures generated from Sox2-positive neurospheres derived from the spinal cord of E14.5 mouse embryos. Figure S2: Effects of the PR agonist R5020 and the membrane receptors to progesterone (mPR) agonist Org OD 02-0 on OPC proliferation. Figure S3: Effects of the PR agonist R5020 and the mPR agonist Org OD 02-0 on OPC differentiation. Figure S4: Effects of the PR agonist R5020 and the mPR agonist Org OD 02-0 in the potential of myelination. Figure S5: In silico analysis to identify potential progesterone response elements (PRE) sites in the promoter sequences of NG2, SOX9, NKX 6.1, CNP1, and MBP genes.

Author Contributions: J.C.G.-O. and A.D.M.-M. contributed to carrying out the experiments and data analysis. J.C.G.-O. and I.C.-A. conceived and managed all experiments. J.C.G.-O. and I.C.-A. contributed to writing the manuscript. All authors have read and agreed to the published version of the manuscript.

Funding: This work was financially supported by "Programa de Apoyo a Proyectos de Investigación e Innovación Tecnológica" (PAPIIT), project IN213117, DGAPA-UNAM, Mexico.

Acknowledgments: We would like to thank Marisol De La Fuente-Granada and Aliesha González-Arenas (Departamento de Medicina Genómica y Toxicología Ambiental, Instituto de Investigaciones Biomédicas, UNAM, México) for the facilitation of the animals used in this study.

Conflicts of Interest: The authors declare no conflict of interest.

References

1. Kinney, H.C.; Volpe, J.J. *Volpe's Neurology of the Newborn*; Elsevier: Amsterdam, The Netherlands, 2018; pp. 176–188.
2. Downes, N.J.; Mullins, P. The Development of Myelin in the Brain of the Juvenile Rat. *Toxicol. Pathol.* **2013**, *42*, 913–922. [CrossRef]
3. Bergles, D.E.; Richardson, W.D. Oligodendrocyte Development and Plasticity. *Cold Spring Harb. Perspect. Boil.* **2015**, *8*, a020453. [CrossRef] [PubMed]
4. Rowitch, D.H.; Kriegstein, A.R. Developmental genetics of vertebrate glial–cell specification. *Nature* **2010**, *468*, 214–222. [CrossRef] [PubMed]
5. Sim, F.J.; McClain, C.R.; Schanz, S.J.; Protack, T.L.; Windrem, M.S.; A Goldman, S. CD140a identifies a population of highly myelinogenic, migration-competent and efficiently engrafting human oligodendrocyte progenitor cells. *Nat. Biotechnol.* **2011**, *29*, 934–941. [CrossRef] [PubMed]
6. Orentas, D.M.; E Hayes, J.; Dyer, K.L.; Miller, R.H. Sonic hedgehog signaling is required during the appearance of spinal cord oligodendrocyte precursors. *Development* **1999**, *126*, 2419–2429. [PubMed]
7. A Goldman, S.; Kuypers, N.J. How to make an oligodendrocyte. *Development* **2015**, *142*, 3983–3995. [CrossRef]
8. Vallstedt, A.; Klos, J.M.; Ericson, J. Multiple Dorsoventral Origins of Oligodendrocyte Generation in the Spinal Cord and Hindbrain. *Neuron* **2005**, *45*, 55–67. [CrossRef]
9. Finzsch, M.; Stolt, C.C.; Lommes, P.; Wegner, M. Sox9 and Sox10 influence survival and migration of oligodendrocyte precursors in the spinal cord by regulating PDGF receptor α expression. *Development* **2008**, *135*, 637–646. [CrossRef]
10. Reiprich, S.; Cantone, M.; Weider, M.; Baroti, T.; Wittstatt, J.; Schmitt, C.; Küspert, M.; Vera, J.; Wegner, M. Transcription factor Sox10 regulates oligodendroglial Sox9 levels via microRNAs. *Glia* **2017**, *65*, 1089–1102. [CrossRef]
11. Tsai, H.-H.; Niu, J.; Munji, R.; Davalos, D.; Chang, J.; Zhang, J.; Tien, A.-C.; Kuo, C.J.; Chan, J.R.; Daneman, R.; et al. Oligodendrocyte precursors migrate along vasculature in the developing nervous system. *Science* **2016**, *351*, 379–384. [CrossRef]
12. Baron, W.; Metz, B.; Bansal, R.; Hoekstra, D.; De Vries, H. PDGF and FGF-2 Signaling in Oligodendrocyte Progenitor Cells: Regulation of Proliferation and Differentiation by Multiple Intracellular Signaling Pathways. *Mol. Cell. Neurosci.* **2000**, *15*, 314–329. [CrossRef] [PubMed]
13. Sarlième, L.L.; Rodriguez-Pena, A.; Langley, K. Expression of thyroid hormone receptor isoforms in the oligodendrocyte lineage. *Neurochem. Res.* **2004**, *29*, 903–922. [CrossRef] [PubMed]
14. Lee, J.Y.; Petratos, S. Thyroid Hormone Signaling in Oligodendrocytes: From Extracellular Transport to Intracellular Signal. *Mol. Neurobiol.* **2016**, *53*, 6568–6583. [CrossRef] [PubMed]
15. Barres, B.; Burne, J.; Höltmann, B.; Thoenen, H.; Sendtner, M.; Raff, M. Ciliary Neurotrophic Factor Enhances the Rate of Oligodendrocyte Generation. *Mol. Cell. Neurosci.* **1996**, *8*, 146–156. [CrossRef] [PubMed]
16. Buttery, P.C. Laminin-2/integrin interactions enhance myelin membrane formation by oligodendrocytes. *Mol. Cell. Neurosci.* **1999**, *14*, 199–212. [CrossRef] [PubMed]
17. Lourenço, T.M.P.; De Faria, J.P.; Bippes, C.A.; Maia, J.; Da Silva, J.L.; Relvas, J.B.; Grãos, M. Modulation of oligodendrocyte differentiation and maturation by combined biochemical and mechanical cues. *Sci. Rep.* **2016**, *6*, 6. [CrossRef]
18. Snaidero, N.; Simons, M. Myelination at a glance. *J. Cell Sci.* **2014**, *127*, 2999–3004. [CrossRef]

19. Labombarda, F.; Jure, I.; De Nicola, A.F. Progesterone effects on the oligodendrocyte linage: All roads lead to the progesterone receptor. *Neural Regen. Res.* **2019**, *14*, 2029–2034. [CrossRef]
20. Morel, Y.; Roucher, F.; Plotton, I.; Goursaud, C.; Tardy, V.; Mallet, D. Evolution of steroids during pregnancy: Maternal, placental and fetal synthesis. *Ann. d'Endocrinol.* **2016**, *77*, 82–89. [CrossRef]
21. Rego, J.L.D.; Seong, J.Y.; Burel, D.; Leprince, J.; Luu-The, V.; Tsutsui, K.; Tonon, M.-C.; Pelletier, G.; Vaudry, H. Neurosteroid biosynthesis: Enzymatic pathways and neuroendocrine regulation by neurotransmitters and neuropeptides. *Front. Neuroendocr.* **2009**, *30*, 259–301. [CrossRef]
22. Snyder, A.M.; Hull, E.M. Perinatal progesterone affects learning in rats. *Psychoneuroendocrinology* **1980**, *5*, 113–119. [CrossRef]
23. Schumacher, M.; Mattern, C.; Ghoumari, A.; Oudinet, J.; Liere, P.; Labombarda, F.; Sitruk-Ware, R.; De Nicola, A.; Guennoun, R. Revisiting the roles of progesterone and allopregnanolone in the nervous system: Resurgence of the progesterone receptors. *Prog. Neurobiol.* **2014**, *113*, 6–39. [CrossRef] [PubMed]
24. Liu, T.; Ogle, T.F. Signal transducer and activator of transcription 3 is expressed in the decidualized mesometrium of pregnancy and associates with the progesterone receptor through protein-protein interactions. *Boil. Reprod.* **2002**, *67*, 114–118. [CrossRef]
25. Lieberman, B.A.; Bona, B.J.; Edwards, D.P.; Nordeen, S.K. The constitution of a progesterone response element. *Mol. Endocrinol.* **1993**, *7*, 515–527.
26. Valadez-Cosmes, P.; Vázquez-Martínez, E.R.; Cerbón, M.; Camacho-Arroyo, I. Membrane progesterone receptors in reproduction and cancer. *Mol. Cell. Endocrinol.* **2016**, *434*, 166–175. [CrossRef] [PubMed]
27. Boonyaratanakornkit, V.; Bi, Y.; Rudd, M.; Edwards, D. The role and mechanism of progesterone receptor activation of extra-nuclear signaling pathways in regulating gene transcription and cell cycle progression. *Steroids* **2008**, *73*, 922–928. [CrossRef] [PubMed]
28. Jacobsen, B.; Horwitz, K.B. Progesterone receptors, their isoforms and progesterone regulated transcription. *Mol. Cell. Endocrinol.* **2011**, *357*, 18–29. [CrossRef]
29. Kastner, P.; Krust, A.; Turcotte, B.; Stropp, U.; Tora, L.; Gronemeyer, H.; Chambon, P. Two distinct estrogen-regulated promoters generate transcripts encoding the two functionally different human progesterone receptor forms A and B. *EMBO J.* **1990**, *9*, 1603–1614. [CrossRef]
30. Mesiano, S.; Wang, Y.; Norwitz, E.R. Progesterone receptors in the human pregnancy uterus: Do they hold the key to birth timing? *Reprod. Sci.* **2011**, *18*, 6–19. [CrossRef]
31. Labombarda, F.; González, S.L.; Deniselle, M.C.G.; Guennoun, R.; Schumacher, M.; De Nicola, A. Cellular Basis for Progesterone Neuroprotection in the Injured Spinal Cord. *J. Neurotrauma* **2002**, *19*, 343–355. [CrossRef]
32. Guerra-Araiza, C.; Villamar-Cruz, O.; González-Arenas, A.; Chavira, R.; Camacho-Arroyo, I. Changes in progestrone receptor isoforms content in the rat brain during the oestrous cycle and after oestradiol and progesterone treatments. *J. Neuroendocrinol.* **2003**, *15*, 984–990. [CrossRef] [PubMed]
33. Camacho-Arroyo, I.; Hansberg-Pastor, V.; Gutiérrez-Rodríguez, A.; Chávez-Jiménez, J.; González-Morán, M.G. Expression of sex hormone receptors in the brain of male and female newly hatched chicks. *Anim. Reprod. Sci.* **2018**, *188*, 123–129. [CrossRef] [PubMed]
34. Camacho-Arroyo, I.; Guerra-Araiza, C.; Cerbón, M.A. Progesterone receptor isoforms are differentially regulated by sex steroids in the rat forebrain. *NeuroReport* **1998**, *9*, 3993–3996. [CrossRef]
35. Bellance, C.; Khan, J.A.; Meduri, G.; Guiochon-Mantel, A.; Lombès, M.; Loosfelt, H. Progesterone receptor isoforms PRA and PRB differentially contribute to breast cancer cell migration through interaction with focal adhesion kinase complexes. *Mol. Boil. Cell* **2013**, *24*, 1363–1374. [CrossRef] [PubMed]
36. A Lamb, C.; Fabris, V.T.; Jacobsen, B.M.; Molinolo, A.; Lanari, C. Biological and clinical impact of imbalanced progesterone receptor isoform ratios in breast cancer. *Endocr.-Relat. Cancer* **2018**, *25*, R605–R624. [CrossRef] [PubMed]
37. Ilicic, M.; Zakar, T.; Paul, J. Modulation of Progesterone Receptor Isoform Expression in Pregnant Human Myometrium. *BioMed Res. Int.* **2017**, *2017*, 4589214. [CrossRef] [PubMed]
38. Richer, J.K.; Jacobsen, B.; Manning, N.G.; Abel, M.G.; Wolf, D.M.; Horwitz, K.B. Differential Gene Regulation by the Two Progesterone Receptor Isoforms in Human Breast Cancer Cells. *J. Boil. Chem.* **2001**, *277*, 5209–5218. [CrossRef]
39. Ghoumari, A.M.; Baulieu, E.; Schumacher, M. Progesterone increases oligodendroglial cell proliferation in rat cerebellar slice cultures. *Neuroscience* **2005**, *135*, 47–58. [CrossRef]

40. Ghoumari, A.M.; Ibanez, C.; El-Etr, M.; Leclerc, P.; Eychenne, B.; O'Malley, B.W.; Baulieu, E.-E.; Schumacher, M. Progesterone and its metabolites increase myelin basic protein expression in organotypic slice cultures of rat cerebellum. *J. Neurochem.* **2003**, *86*, 848–859. [CrossRef]
41. Gago, N.; Akwa, Y.; Sananès, N.; Guennoun, R.; Baulieu, E.E.; El-Etr, M.; Schumacher, M. Progesterone and the oligodendroglial lineage: Stage-dependent biosynthesis and metabolism. *Glia* **2001**, *36*, 295–308. [CrossRef]
42. Labombarda, F.; González, S.L.; Lima, A.; Roig, P.; Guennoun, R.; Schumacher, M.; De Nicola, A. Effects of progesterone on oligodendrocyte progenitors, oligodendrocyte transcription factors, and myelin proteins following spinal cord injury. *Glia* **2009**, *57*, 884–897. [CrossRef] [PubMed]
43. Jure, I.; De Nicola, A.F.; Labombarda, F. Progesterone effects on oligodendrocyte differentiation in injured spinal cord. *Brain Res.* **2019**, *1708*, 36–46. [CrossRef] [PubMed]
44. Khan, A.; Fornes, O.; Stigliani, A.; Gheorghe, M.; Castro-Mondragon, J.A.; Van Der Lee, R.; Bessy, A.; Chèneby, J.; Kulkarni, S.R.; Tan, G.; et al. JASPAR 2018: Update of the open-access database of transcription factor binding profiles and its web framework. *Nucleic Acids Res.* **2018**, *46*, D1284. [CrossRef] [PubMed]
45. Wingender, E.; Schoeps, T.; Haubrock, M.; Krull, M.; Dönitz, J. TFClass: Expanding the classification of human transcription factors to their mammalian orthologs. *Nucleic Acids Res.* **2017**, *46*, D343–D347. [CrossRef]
46. Podvinec, M.; Kaufmann, M.R.; Handschin, C.; Meyer, U.A. NUBIScan, an in silico approach for prediction of nuclear receptor response elements. *Mol. Endocrinol.* **2002**, *16*, 1269–1279. [CrossRef]
47. Ahlenius, H.; Kokaia, Z. Isolation and Generation of Neurosphere Cultures from Embryonic and Adult Mouse Brain. In *Mouse Cell Culture*; Humana Press: Totowa, NJ, USA, 2010; pp. 241–252.
48. Pedraza, C.E.; Monk, R.; Lei, J.; Hao, Q.; Macklin, W.B. Production, characterization, and efficient transfection of highly pure oligodendrocyte precursor cultures from mouse embryonic neural progenitors. *Glia* **2008**, *56*, 1339–1352. [CrossRef]
49. Pedraza, C.E.; Taylor, C.; Pereira, A.; Seng, M.; Tham, C.-S.; Izrael, M.; Webb, M. Induction of Oligodendrocyte Differentiation and In Vitro Myelination by Inhibition of Rho-Associated Kinase. *ASN Neuro* **2014**, *6*. [CrossRef]
50. Cao, J.; Spielmann, M.; Qiu, X.; Huang, X.; Ibrahim, D.M.; Hill, A.J.; Zhang, F.; Mundlos, S.; Christiansen, L.; Steemers, F.J.; et al. The single-cell transcriptional landscape of mammalian organogenesis. *Nature* **2019**, *566*, 496–502. [CrossRef]
51. González-Orozco, J.C.; Camacho-Arroyo, I. Progesterone Actions During Central Nervous System Development. *Front. Mol. Neurosci.* **2019**, *13*, 503. [CrossRef]
52. Schumacher, M.; Guennoun, R.; Mercier, G.; Désarnaud, F.; Lacor, P.; Benavides, J.; Ferzaz, B.; Robert, F.; Baulieu, E.E. Progesterone synthesis and myelin formation in peripheral nerves. *Brain Res. Rev.* **2001**, *37*, 343–359. [CrossRef]
53. Labombarda, F.; Garcia-Ovejero, D. Give progesterone a chance. *Neural Regen. Res.* **2014**, *9*, 1422–1424. [CrossRef] [PubMed]
54. Tanabe, Y.; Jessell, T.M. Diversity and Pattern in the Developing Spinal Cord. *Science* **1996**, *274*, 1115–1123. [CrossRef] [PubMed]
55. Glasgow, S.M.; Carlson, J.C.; Zhu, W.; Chaboub, L.S.; Kang, P.; Lee, H.K.; Clovis, Y.M.; E Lozzi, B.; McEvilly, R.J.; Rosenfeld, M.G.; et al. Glia-specific enhancers and chromatin structure regulate NFIA expression and glioma tumorigenesis. *Nat. Neurosci.* **2017**, *20*, 1520–1528. [CrossRef] [PubMed]
56. Kelly, T.K.; Karsten, S.L.; Geschwind, D.H.; Kornblum, H. Cell Lineage and Regional Identity of Cultured Spinal Cord Neural Stem Cells and Comparison to Brain-Derived Neural Stem Cells. *PLoS ONE* **2009**, *4*, e4213. [CrossRef]
57. Temple, S.; Raff, M.C. Clonal analysis of oligodendrocyte development in culture: Evidence for a developmental clock that counts cell divisions. *Cell* **1986**, *44*, 773–779. [CrossRef]
58. Garay, L.; Deniselle, M.G.; Brocca, M.E.; Lima, A.; Roig, P.; De Nicola, A. Progesterone down-regulates spinal cord inflammatory mediators and increases myelination in experimental autoimmune encephalomyelitis. *Neuroscience* **2012**, *226*, 40–50. [CrossRef]
59. Jung-Testas, I.; Renoir, J.; Gasc, J.; Baulieu, E. Estrogen-inducible progesterone receptor in primary cultures of rat glial cells. *Exp. Cell Res.* **1991**, *193*, 12–19. [CrossRef]

60. Labombarda, F.; Guennoun, R.; Gonzalez, S.; Roig, P.; Lima, A.; Schumacher, M.; De Nicola, A.F. Immunocytochemical evidence for a progesterone receptor in neurons and glial cells of the rat spinal cord. *Neurosci. Lett.* **2000**, *288*, 29–32. [CrossRef]
61. Compagnone, N.A.; Mellon, S.H. Neurosteroids: Biosynthesis and Function of These Novel Neuromodulators. *Front. Neuroendocr.* **2000**, *21*, 1–56. [CrossRef]
62. Wagner, C.K.; Quadros-Mennella, P. Progesterone from maternal circulation binds to progestin receptors in fetal brain. *Dev. Neurobiol.* **2016**, *77*, 767–774. [CrossRef]
63. Nguyen, P.N.; Billiards, S.S.; Walker, D.W.; Hirst, J.J. Changes in 5α-pregnane steroids and neurosteroidogenic enzyme expression in the perinatal sheep. *Pediatr. Res.* **2003**, *53*, 956–964. [CrossRef] [PubMed]
64. Stiles, J.; Jernigan, T.L. The Basics of Brain Development. *Neuropsychol. Rev.* **2010**, *20*, 327–348. [CrossRef]
65. Shakeri, M.; Boustani, M.R.; Pak, N.; Panahi, F.; Salehpour, F.; Lotfinia, I.; Meshkini, A.; Daghighi, S.; Vahedi, P.; Khani, M.; et al. Effect of progesterone administration on prognosis of patients with diffuse axonal injury due to severe head trauma. *Clin. Neurol. Neurosurg.* **2013**, *115*, 2019–2022. [CrossRef] [PubMed]
66. Schumacher, M.; Denier, C.; Oudinet, J.-P.; Adams, D.; Guennoun, R. Progesterone neuroprotection: The background of clinical trial failure. *J. Steroid Biochem. Mol. Boil.* **2016**, *160*, 53–66. [CrossRef] [PubMed]

© 2020 by the authors. Licensee MDPI, Basel, Switzerland. This article is an open access article distributed under the terms and conditions of the Creative Commons Attribution (CC BY) license (http://creativecommons.org/licenses/by/4.0/).